involve

a journal of mathematics

msp

2019 vol. 12, no. 8

involve

msp.org/involve

INVOLVE YOUR STUDENTS IN RESEARCH

Involve showcases and encourages high-quality mathematical research involving students from all academic levels. The editorial board consists of mathematical scientists committed to nurturing student participation in research. Bridging the gap between the extremes of purely undergraduate research journals and mainstream research journals, *Involve* provides a venue to mathematicians wishing to encourage the creative involvement of students.

See inside back cover or msp.org/involve for submission instructions. The subscription price for 2019 is US $195/year for the electronic version, and $260/year (+$35, if shipping outside the US) for print and electronic. Subscriptions, requests for back issues and changes of subscriber address should be sent to MSP.

Involve (ISSN 1944-4184 electronic, 1944-4176 printed) at Mathematical Sciences Publishers, 798 Evans Hall #3840, c/o University of California, Berkeley, CA 94720-3840, is published continuously online. Periodical rate postage paid at Berkeley, CA 94704, and additional mailing offices.

Involve peer review and production are managed by EditFlow® from Mathematical Sciences Publishers.

PUBLISHED BY

mathematical sciences publishers

nonprofit scientific publishing

http://msp.org/

INVOLVE 12:8 (2019)
dx.doi.org/10.2140/involve.2019.12.1261

On the zero-sum group-magicness of cartesian products

Adam Fong, John Georges, David Mauro, Dylan Spagnuolo, John Wallace, Shufan Wang and Kirsti Wash

(Communicated by Kenneth S. Berenhaut)

Let $G = (V(G), E(G))$ be a graph and let $\mathbb{A} = (A, +)$ be an abelian group with identity 0. Then an $\mathbb{A}$-*magic labeling of* G is a function ϕ from $E(G)$ into $A \setminus \{0\}$ such that for some $a \in A$, $\sum_{e \in E(v)} \phi(e) = a$ for every $v \in V(G)$, where $E(v)$ is the set of edges incident to v. If ϕ exists such that $a = 0$, then G is *zero-sum* $\mathbb{A}$-*magic*. Let G be the cartesian product of two or more graphs. We establish that G is zero-sum $\mathbb{Z}$-magic and we introduce a graph invariant $j^*(G)$ to explore the zero-sum integer-magic spectrum (or null space) of G. For certain G, we establish $\mathcal{A}(G)$, the set of nontrivial abelian groups for which G is zero-sum group-magic. Particular attention is given to $\mathcal{A}(G)$ for regular G, odd/even G, and G isomorphic to a product of paths.

1. Introduction

Let $G = (V(G), E(G))$ be a graph. Let $\mathcal{A}$ be the set all nontrivial abelian groups and let $\mathbb{A} = (A, +) \in \mathcal{A}$, where 0 denotes the identity of $\mathbb{A}$. Then an $\mathbb{A}$-*labeling of* G is a function ϕ from $E(G)$ into $A \setminus \{0\}$. For fixed $e \in E(G)$, $\phi(e)$ is called the *label of* e *under* ϕ, and for fixed $v \in V(G)$, the sum of the labels of the edges incident to v is called the *weight of* v *under* ϕ. The graph G is $\mathbb{A}$-*magic* if and only if there exists an $\mathbb{A}$-labeling ϕ of G such that for some $a \in A$, the weight of every vertex in $V(G)$ under ϕ is a. In such a case, ϕ is called an $\mathbb{A}$-*magic labeling of* G. Additionally, G is *zero-sum* $\mathbb{A}$-*magic* if and only if there is an $\mathbb{A}$-labeling ϕ of G such that the weight of every vertex in $V(G)$ under ϕ is 0. In this case, ϕ is called a *zero-sum* $\mathbb{A}$-*magic labeling of* G. Letting $\mathcal{A}(G)$ denote the set of all $\mathbb{A} \in \mathcal{A}$ such that G is zero-sum $\mathbb{A}$-magic, we observe that if $\mathbb{H}_0 \in \mathcal{A}(G)$ and $\mathbb{H}_0$ is isomorphic to a subgroup of an abelian group $\mathbb{H}$, then $\mathbb{H} \in \mathcal{A}(G)$. Particularly, if $\mathbb{A} \in \mathcal{A}(G)$, then for a positive integer k, we have $\mathbb{A}^k \in \mathcal{A}(G)$. In Figure 1, we

MSC2010: 05C78.
Keywords: cartesian product of graphs, grid graph, magic labeling, group-magic labeling, zero-sum group-magic labeling, zero-sum integer-magic spectrum.

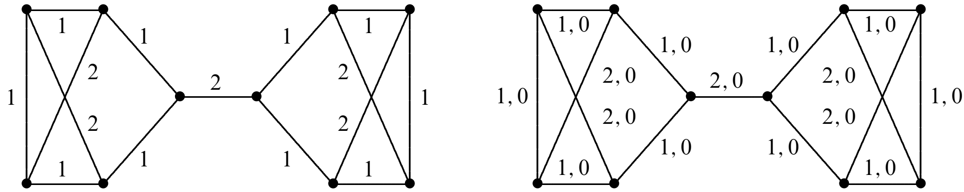

Figure 1. Zero-sum $\mathbb{Z}_4$ and $\mathbb{Z}_4^2$-magic labelings of G.

illustrate a zero-sum $\mathbb{Z}_4$-magic labeling and a zero-sum $\mathbb{Z}_4^2$-magic labeling of a graph G. (The group $\mathbb{Z}_4$ is the cyclic group of integers under addition mod 4. In the specification of elements of Z_4^2, parentheses are omitted.) Note that an alternative zero-sum $\mathbb{Z}_4^2$-magic labeling can be formed by changing each label $(a, 0)$ to (a, a). Other obvious alternatives exist.

The *zero-sum integer-magic spectrum* of a graph G, denoted by $\text{zim}(G)$, is the set of positive integers k such that G is zero-sum $\mathbb{Z}_k$-magic, where $\mathbb{Z}_1$ is the group $\mathbb{Z}$ of integers under addition and, for $k \geq 2$, $\mathbb{Z}_k$ is the cyclic group of integers under addition mod k. Let $\mathcal{N}$ denote the set of positive integers. By the fundamental theorem of finite abelian groups, $\mathcal{N} \setminus \{1\}$ is a subset of $\text{zim}(G)$ if and only if G is zero-sum $\mathbb{A}$-magic for all finite $\mathbb{A}$ in $\mathcal{A}$. Moreover, for any infinite abelian group $\mathbb{A} = (A, +)$ with nonzero $a \in A$, a generates a subgroup of $\mathbb{A}$ that is isomorphic to either $\mathbb{Z}$ or $\mathbb{Z}_k$ for some $k \geq 2$. Thus $\text{zim}(G) = \mathcal{N}$ if and only if $\mathcal{A}(G) = \mathcal{A}$. We note especially that if $\text{zim}(G) = \mathcal{N} \setminus \{2\}$, then $\mathcal{A} \setminus \{\mathbb{Z}_2^k \mid k \in \mathcal{N}\} \subseteq \mathcal{A}(G)$.

Sedláček [1964] first introduced magic labelings, motivated by magic squares in number theory. Stanley [1973] later showed that the study of magic labelings is related to the study of linear homogeneous diophantine equations. It was shown independently in [Low and Lee 2006] and [Shiu et al. 2004] that if G and H are $\mathbb{A}$-magic graphs, then the cartesian product of G and H is also $\mathbb{A}$-magic. More recently, Akbari et al. [2014] proved that every r-regular graph G with $r \geq 3$, $r \neq 5$ has $\text{zim}(G) = \mathcal{N}$ if r is even; otherwise $\text{zim}(G) \supseteq \mathcal{N} \setminus \{2, 4\}$. And, Shiu and Low [2018] have determined the zero-sum integer-magic spectrum of the cartesian product of two trees. For a dynamic survey of results on magic labelings, see [Gallian 2018].

In this paper, we consider the zero-sum $\mathbb{A}$-magicness of cartesian products. In Section 2, we give definitions and preliminary results. In Section 3, we develop our main results, with particular attention given to graph parity and regularity. And in Section 4, we consider the cartesian products of paths, also known as grid graphs.

2. Definitions and preliminary results

Throughout this paper, graphs will be finite, nontrivial, simple, loopless, and connected unless specified otherwise. An *even graph* (resp. *odd graph*) shall refer

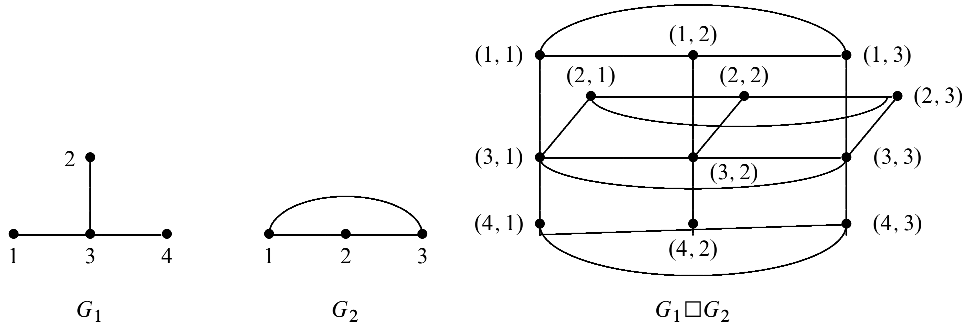

Figure 2. The cartesian product $G_1 \square G_2$.

to a graph G of which each vertex v has even (resp. odd) degree, denoted by $d_G(v)$. Abelian groups shall have identity element 0 and binary operator $+$.

For $i \in \{1, \dots, n\}$, let $G_i = (V(G_i), E(G_i))$ be a graph. The *cartesian product* of $G_1, G_2, \dots, G_n$, denoted by $\square_{i=1}^n G_i$ or $G_1 \square G_2 \square \cdots \square G_n$, is the graph G such that

(1) the vertex set of G is $\prod_{i=1}^n V(G_i)$, and

(2) vertices $(u_1, u_2, \dots, u_n)$ and $(w_1, w_2, \dots, w_n)$ of G are adjacent if and only if $(u_1, u_2, \dots, u_n)$ and $(w_1, w_2, \dots, w_n)$ differ in precisely one component i_0, and u_{i_0} is adjacent to w_{i_0} in G_{i_0}.

The following are well known. Note that the results in (b), (c), and (d) extend to cartesian products of arbitrary finite length by part (a):

(a) As a binary operator on the set of graphs, $\square$ is associative and commutative with respect to isomorphism.

(b) If (u, w) is a vertex of $G_1 \square G_2$, then $d_{G_1 \square G_2}((u, w)) = d_{G_1}(u) + d_{G_2}(w)$.

(c) $G_1 \square G_2$ is regular if and only if each of G_1 and G_2 is regular.

(d) If G_1 and G_2 are graphs with no isolated vertices, then $G_1 \square G_2$ is bridgeless.

In Figure 2, we demonstrate the cartesian product $G_1 \square G_2$ where G_1 is isomorphic to the claw on four vertices and G_2 is isomorphic to the cycle C_3.

Let G be a graph and let h be a positive integer. Then a *factor of* G is a spanning subgraph of G, and an h-factor of G is an h-regular factor of G. (The term *factor* may also refer to a factor of a cartesian product. Its usage will clarify its intended meaning.)

For $n \geq 2$, let G be a cartesian product $\square_{i=1}^n G_i$. For fixed i_0, $1 \leq i_0 \leq n$, suppose that H_{i_0} is an h_{i_0}-factor of G_{i_0}. Then there exists a natural h_{i_0}-factor of G, comprising the union of C disjoint subgraphs of G, each isomorphic to H_{i_0}, where C is the product of the orders of the graphs G_i, $1 \leq i \leq n$, except for $i = i_0$. If, for

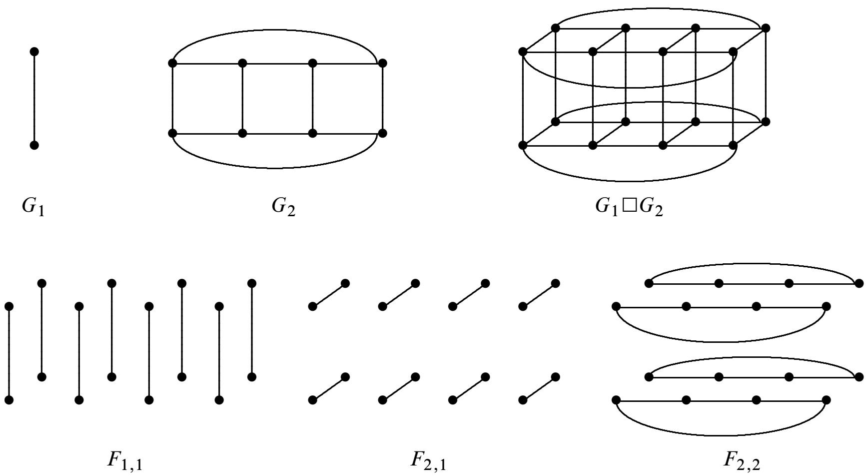

Figure 3. An illustration of regular factors.

each i, $E(G_i)$ is partitioned by the edge sets of regular factors $H_{i,1}, H_{i,2}, \ldots, H_{i,m_i}$ of G_i, then these n partitions of $E(G_1)$, $E(G_2)$, …, and $E(G_n)$ induce a natural partition of $E(G)$ by the edge sets of regular factors $F_{i,j}$, $1 \le i \le n$, $1 \le j \le m_i$, where the regularity of $F_{i,j}$ equals the regularity of $H_{i,j}$. Note that each vertex of G is a vertex of each $F_{i,j}$ as illustrated in Figure 3. Therein, graph $G_1 \cong P_2$ has a 1-factor $H_{1,1} = G_1$ whose edge set trivially partitions $E(G_1)$. And, G_2 has a 1-factor $H_{2,1}$ isomorphic to four vertex-disjoint copies of P_2 and a 2-factor $H_{2,2}$ isomorphic to two vertex-disjoint copies of C_4, where $E(H_{2,1})$ and $E(H_{2,2})$ together partition $E(G_2)$. These regular factors respectively induce $F_{1,1}$, $F_{2,1}$, and $F_{2,2}$, which together partition $E(G_1 \Box G_2)$. (Note that G_2 is itself a cartesian product isomorphic to $P_2 \Box C_4$.)

Let G be a graph that has a zero-sum $\mathbb{Z}$-magic labeling and let $\mathcal{Z}(G)$ represent the (nonempty) set of all zero-sum $\mathbb{Z}$-magic labelings of G. For each $\phi \in \mathcal{Z}(G)$, let $j(\phi)$ equal $\max_{e \in E(G)} |\phi(e)|$. Then $j^*(G)$ shall denote $\min_{\phi \in \mathcal{Z}(G)} j(\phi)$. To illustrate, we note that there exists a zero-sum $\mathbb{Z}$-magic labeling ϕ of K_4 such that $\max_{e \in E(K_4)} |\phi(e)| = 2$. Yet, since K_4 is an odd graph, there is no such labeling ϕ such that $\max_{e \in E(K_4)} |\phi(e)| = 1$. Thus $j^*(K_4) = 2$. On the other hand, some graphs, including C_{2n-1} and P_n for $n \ge 2$, are not zero-sum $\mathbb{Z}$-magic. For such graphs G, $j^*(G)$ does not exist.

Theorem 1. *If G is zero-sum $\mathbb{Z}$-magic, then G is zero-sum $\mathbb{Z}_k$-magic for all $k > j^*(G)$. Additionally, if $j^*(G) = 1$, then $\mathcal{A}(G) = \mathcal{A}$.*

Proof. Let ϕ be any zero-sum $\mathbb{Z}$-magic labeling of G such that $j(\phi) = j^*(G)$, and fix $k > j^*(G)$. We form a zero-sum $\mathbb{Z}_k$-magic labeling of G by assigning $\phi(e) \pmod{k}$

to $e \in E(G)$. Consequently, if $j^*(G) = 1$, then $\text{zim}(G) = \mathcal{N}$, implying that G is zero-sum $\mathbb{A}$-magic for all $\mathbb{A} \in \mathcal{A}$. □

We observe that Georges, Mauro, and Wash [Georges et al. 2017] established necessary and sufficient conditions under which a graph G is zero-sum Z_{2j}^k-magic. In particular, they showed that G has a bridge whose removal results in an isolate or bipartite component if and only if G is not zero-sum Z_{2j}^k-magic for any positive integers j, k. Theorem 1 immediately implies that such G is not zero-sum Z-magic for otherwise G would be zero-sum Z_{2j}-magic for $2j > j^*(G)$.

Theorems 2 through 8, useful in the sequel, can be found in the existing literature.

Theorem 2 [Petersen 1891]. *Let G be a $2t$-regular graph. Then there exist t 2-factors of G that partition $E(G)$.*

Theorem 3 [Ore 1957]. *Let G be a bridgeless regular graph of odd degree k and let h be an even integer, $2 \le h \le \frac{2}{3}k$. Then there exists an h-factor of G.*

Theorem 4 [Georges et al. 2010]. *Let G be a 3-regular graph. Then G is zero-sum $\mathbb{Z}_2^2$-magic if and only if the chromatic index of G is 3.*

Theorem 5 [Georges et al. 2010]. *Let G be a graph with a bridge. Then for each positive integer k, G is not zero-sum $\mathbb{Z}_2^k$-magic.*

Theorem 6 [Choi et al. 2012]. *Let G be a bridgeless graph. Then for each positive integer $k \ge 3$, G is zero-sum $\mathbb{Z}_2^k$-magic.*

Theorem 7 [Low and Lee 2006; Shiu et al. 2004]. *If $G_1, G_2, \dots, G_n$ are zero-sum $\mathbb{A}$-magic graphs, then $\square_{i=1}^n G_i$ is zero-sum $\mathbb{A}$-magic.*

Theorem 8 [Akbari et al. 2014]. *Let G be an r-regular graph, $r \ge 3$, $r \ne 5$. If r is even, then $\text{zim}(G) = \mathcal{N}$. Otherwise, $\mathcal{N} \setminus \{2, 4\} \subseteq \text{zim}(G)$.*

Corollary 9. *Suppose that G is a graph with $j^*(G) \le 2$. Then the following hold:*

(a) *If G is bridgeless, then $\mathcal{A} \setminus \{\mathbb{Z}_2, \mathbb{Z}_2^2\} \subseteq \mathcal{A}(G)$.*

(b) *If G is bridgeless and even, then $\mathcal{A}(G) = \mathcal{A}$.*

(c) *If G is bridgeless with a vertex of odd degree, then*

$$\mathcal{A} \setminus \{\mathbb{Z}_2, \mathbb{Z}_2^2\} \subseteq \mathcal{A}(G) \subseteq \mathcal{A} \setminus \{\mathbb{Z}_2\}.$$

(d) *If G has a bridge, then $\mathcal{A}(G) = \mathcal{A} \setminus \{\mathbb{Z}_2^k \mid k \in \mathcal{N}\}$.*

Proof. (a) We note that $1 \in \text{zim}(G)$ since $j^*(G)$ is assumed to exist. The result follows by Theorems 1 and 6.

(b) Since G is even, G is zero-sum $\mathbb{Z}_2$-magic (assign 1 to each edge of G), and hence zero-sum $\mathbb{Z}_2^2$-magic. The result follows by part (a).

(c) Part (c) follows from part (a) and the fact that any $\mathbb{Z}_2$-labeling of G must assign 1 to each edge; hence, no graph with a vertex of odd degree can be zero-sum $\mathbb{Z}_2$-magic.

(d) We again observe that $1 \in \mathrm{zim}(G)$ and, by Theorem 1, $k \in \mathrm{zim}(G)$ for $k \geq 3$. Thus $\mathcal{N} \setminus \{2\} \subseteq \mathrm{zim}(G)$. The result now follows from Theorem 5. □

We note that $j^*(K_4) = 2$ and, by the upcoming Corollary 10 and Theorem 11, $j^*(K_7) = 2$ as well. Yet $\mathrm{zim}(K_4) = \mathcal{N} \setminus \{2\}$ and, by Theorem 8, $\mathrm{zim}(K_7) = \mathcal{N}$. Moreover, the three graphs K_4, the Petersen graph PG, and the (unique) 3-regular graph G on 10 vertices with one bridge (see Figure 1) are each easily verified to have zero-sum integer-magic spectrum $\mathcal{N} \setminus \{2\}$. Yet, by Theorem 4 and Corollary 9, $\mathcal{A}(K_4) = \mathcal{A} \setminus \{\mathbb{Z}_2\}$, $\mathcal{A}(PG) = \mathcal{A} \setminus \{\mathbb{Z}_2, \mathbb{Z}_2^2\}$, and $\mathcal{A}(G) = \mathcal{A} \setminus \{\mathbb{Z}_2^k \mid k \in \mathcal{N}\}$.

In the following corollary, we utilize $j^*(G)$ to give an alternative proof of Theorem 8 in the case r is even, $r \geq 4$.

Corollary 10. *Let G be an even-regular graph with degree $r = 2t$ such that $t \geq 2$. Then the following hold*:

(a) *If t is even*, *then $j^*(G) = 1$ and $\mathcal{A}(G) = \mathcal{A}$.*

(b) *If t is odd*, *then $j^*(G) \leq 2$ and $\mathcal{A}(G) = \mathcal{A}$.*

Proof. By Theorem 2, $E(G)$ partitions into t 2-factors. If t is even, we construct a zero-sum $\mathbb{Z}$-magic labeling ϕ of G by assigning the label 1 to each edge of precisely $\frac{t}{2}$ 2-factors, and -1 to each edge of the remaining $\frac{t}{2}$ 2-factors. Since $j(\phi) = 1$, we have $j^*(G) = 1$, implying $\mathcal{A}(G) = \mathcal{A}$ by Theorem 1 or (since even graphs are bridgeless) Corollary 9(b). On the other hand, if t is odd, we construct a zero-sum $\mathbb{Z}$-magic labeling ϕ of G by assigning the label 1 to each edge of precisely $\frac{1}{2}(t+1)$ 2-factors, -1 to each edge of precisely $\frac{1}{2}(t-3)$ 2-factors, and -2 to each edge of the one remaining 2-factor. Since $j(\phi) = 2$, we have $j^*(G) \leq 2$, implying $\mathcal{A}(G) = \mathcal{A}$ by Corollary 9(b). □

For illustration, Figure 4 displays vertex α of a 14-regular graph G whose edge set is partitioned by the 2-factors $H_1, H_2, H_3, H_4, H_5, H_6, H_7$. Suppose that for each i, the edge set of H_i includes the edges αu_i and αw_i. Since $t = 7$, we assign the label 1 to the edges of each of four 2-factors H_1, H_2, H_3, and H_4, we assign the label -1 to the edges of each of two 2-factors H_5 and H_6, and we assign the label -2 to the edges of the remaining 2-factor H_7. Since these labels bear upon every vertex, the weight of every vertex is 0.

We observe that the graphs $K_6 \,\square\, P_2$ and K_7 illustrate the case t odd, yet $j^*(K_6 \,\square\, P_2) = 1$ (see Theorem 11), while $j^*(K_7) = 2$.

Theorem 11. *Let G be a* (*connected*) *graph. Then $j^*(G) = 1$ if and only if G is an even graph with even size.*

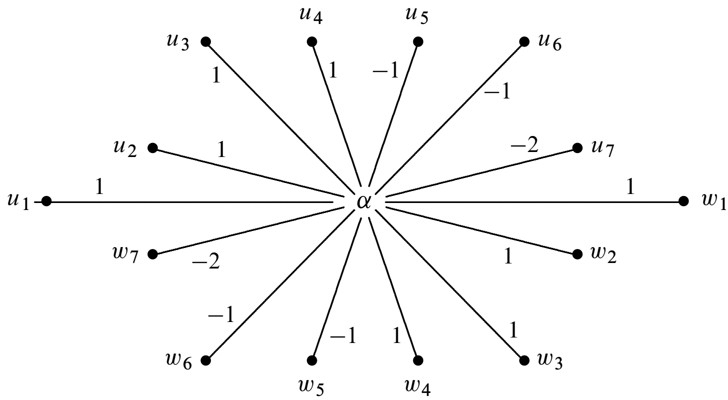

Figure 4. An illustration of Corollary 10.

Proof. Suppose $j^*(G) = 1$. Then it is clear that G is even. To show that G has even size, let ϕ be a zero-sum $\mathbb{Z}$-magic labeling of G with $j(\phi) = 1$. Also let x denote the number of edges of G which receive the label 1 under ϕ, and let y denote the number of edges of G which receive the label -1 under ϕ. Then

$$0 = \sum_{v \in V(G)} w_v(\phi) = 2 \sum_{e \in E(G)} \phi(e) = \sum_{e \in E(G)} \phi(e),$$

implying $x = y$. Thus G has even size.

Now suppose that G is even with even size. Since G is even (and connected), there exists an Eulerian circuit in G with even length. We produce a zero-sum $\mathbb{Z}$-magic labeling ϕ of G with $j(\phi) = 1$ by assigning alternating labels of 1 and -1 to the edges of the circuit. □

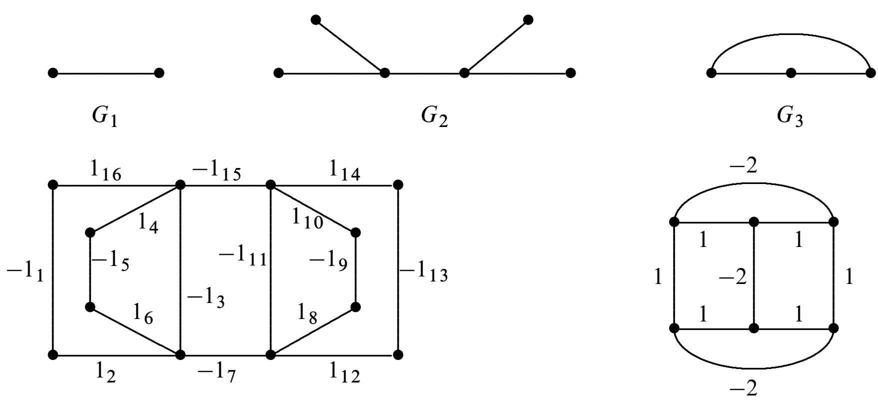

Figure 5. Zero-sum $\mathbb{Z}$-magic labelings of $G_1 \square G_2$ and $G_1 \square G_3$.

Because this paper emphasizes cartesian products, Theorem 11 is illustrated in Figure 5 with an even graph $G_1 \Box G_2$ with even size, and a noneven graph $G_1 \Box G_3$. We exhibit a zero-sum $\mathbb{Z}$-magic labeling ϕ of $G_1 \Box G_2$ with $j(\phi) = 1$ along with indication (via subscripts) of a corresponding Eulerian circuit. And, we show $j^*(G_1 \Box G_3) = 2$ by exhibiting a zero-sum $\mathbb{Z}$-magic labeling of $G_1 \Box G_3$ with maximum absolute label 2.

If M and N are connected odd graphs, then each has even order and $M \Box N$ is an even graph with even size $|V(M)||E(N)| + |V(N)||E(M)|$. As well, if M or N is not connected, then each component of $M \Box N$ is even with even size. Therefore we have the following.

Corollary 12. *Let M and N be odd graphs (not necessarily connected). Then $j^*(M \Box N) = 1$.*

3. Main results

As noted in the preceding section, not all graphs are zero-sum $\mathbb{Z}$-magic. On the other hand, if G is the cartesian product of nontrivial graphs, we have the following result.

Theorem 13. *Let M and N be graphs with $\delta(M), \delta(N) \geq 1$. Then $M \Box N$ is zero-sum $\mathbb{Z}$-magic with $j^*(M \Box N) \leq \max\{\Delta(M), \Delta(N)\}$.*

Proof. Let $V(M) = \{u_1, \ldots, u_m\}$ and $V(N) = \{w_1, \ldots, w_n\}$. For fixed i, $1 \leq i \leq n$, let $M(i)$ be the subgraph of $M \Box N$ induced by the vertices in $\{(u_j, w_i) \mid 1 \leq j \leq m\}$. Similarly, for fixed i, $1 \leq i \leq m$, let $N(i)$ be the subgraph of $M \Box N$ induced by the vertices in $\{(u_i, w_j) \mid 1 \leq j \leq n\}$. Form a $\mathbb{Z}$-labeling of $M \Box N$ as follows: to each edge of $M(\beta)$, assign the label $d_N(w_\beta)$ and to each edge of $N(\alpha)$, assign the label $-d_M(u_\alpha)$. Then the weight of any vertex $(u_\alpha, w_\beta) \in V(M \Box N)$ is $d_M(u_\alpha)d_N(w_\beta) - d_M(u_\alpha)d_N(w_\beta) = 0$. Since the maximum absolute label is $\max\{\Delta(M), \Delta(N)\}$, the result follows. □

It is easy to show the following.

Theorem 14. *Let M and N be zero-sum $\mathbb{Z}$-magic graphs. Then $M \Box N$ is zero-sum $\mathbb{Z}$-magic with $j^*(M \Box N) \leq \max\{j^*(M), j^*(N)\}$.*

Theorem 15. *Let $G = \Box_{i=1}^{n} G_i$ where $n \geq 2$ and $\delta(G_i) \geq 1$ for each i. Then G is zero-sum $\mathbb{Z}$-magic. Moreover, for $\zeta = \max\{\Delta(G_i)\}$ over i, we have $j^*(G) \leq \zeta$ if n is even, and $j^*(G) \leq 2\zeta$ if n is odd.*

Proof. By Theorem 13, G is zero-sum $\mathbb{Z}$-magic.

If $n = 2t$, let $H_i = G_{2i-1} \Box G_{2i}$ for $1 \leq i \leq t$. Then by Theorem 13, each H_i is zero-sum $\mathbb{Z}$-magic with $j^*(H_i) \leq \max\{\Delta(G_{2i-1}), \Delta(G_{2i})\} \leq \zeta$. Since G is isomorphic to $\Box_{i=1}^{t} H_i$, it follows from Theorem 14 that $j^*(G) \leq \max\{j^*(H_i)\} \leq \zeta$.

If $n = 2t+1$, let $H_1 = G_1 \square (G_2 \square G_3)$ and let $H_i = G_{2i} \square G_{2i+1}$ for $2 \le i \le t$. By Theorem 13, each H_i is zero-sum $\mathbb{Z}$-magic. Observing that $\Delta(G_2 \square G_3) = \Delta(G_2) + \Delta(G_3)$, we have from Theorem 13 that $j^*(H_1) \le \max\{\zeta, 2\zeta\} = 2\zeta$. Since $j^*(H_i) \le \zeta$ for $i \ge 2$, we have $j^*(G) \le 2\zeta$ by Theorem 14. □

Lemma 16. *Let G_1, G_2 and G_3 be odd graphs, and let $M = \square_{i=1}^{3} G_i$. Then $j^*(M) = 2$ and $\mathcal{A}(M) = \mathcal{A} \setminus \{\mathbb{Z}_2\}$.*

Proof. Since M is odd, we show $j^*(M) = 2$ by developing a zero-sum $\mathbb{Z}$-magic labeling λ of M with $j(\lambda) = 2$.

Let G_1, G_2, and G_3 have respective vertex sets $\{u_i \mid 1 \le i \le n_1\}$, $\{v_i \mid 1 \le i \le n_2\}$, and $\{w_i \mid 1 \le i \le n_3\}$. Letting $V(P_2) = \{1, 2\}$, we have $j^*(G_i \square P_2) = 1$ by Corollary 12. We thus let ϕ_i'' denote a zero-sum $\mathbb{Z}$-magic labeling of $G_i \square P_2$ such that $j(\phi_i'') = 1$. Let ϕ_i' be the $\mathbb{Z}$-labeling of G_i such that for each edge $\alpha\beta$ of G_i, $\phi_i'(\alpha\beta) = \phi_i''((\alpha, 1)(\beta, 1))$. Note that the weight of each vertex under ϕ_i' is 1 or -1.

Now consider $G_1 \square G_2$. We construct a $\mathbb{Z}$-labeling ψ of $G_1 \square G_2$ as follows. To each edge $(u_x, v)(u_y, v)$ of $G_1 \square G_2$, assign the label $\phi_1'(u_x u_y) w_{\phi_2'}(v)$. And, to each edge $(u, v_x)(u, v_y)$ of $G_1 \square G_2$, assign the label $\phi_2'(v_x v_y) w_{\phi_1'}(u)$. We observe that under ψ, each edge of $G_1 \square G_2$ has label 1 or -1 and each vertex of $G_1 \square G_2$ has weight 2 or -2.

Each edge e in $E(M)$ has one of the following two forms:

- Type I: $e = (z_x, w)(z_y, w)$, where $z_x z_y \in E(G_1 \square G_2)$ and $w \in V(G_3)$.
- Type II: $e = (z, w_x)(z, w_y)$, where $z \in V(G_1 \square G_2)$ and $w_x w_y \in E(G_3)$.

Let λ be a $\mathbb{Z}$-labeling of M such that

$$\lambda(e) = \begin{cases} \psi(z_x z_y) w_{\phi_3'}(w) & \text{if } e \text{ is of type I,} \\ -w_\psi(z)\phi_3'(w_x w_y) & \text{if } e \text{ is of type II.} \end{cases}$$

Since $\psi(z_x z_y) \in \{-1, 1\}$, $w_{\phi_3'}(w) \in \{-1, 1\}$, $w_\psi(z) \in \{-2, 2\}$, and $\phi_3'(w_x w_y) \in \{-1, 1\}$, the edges of type 1 receive ± 1 under λ and edges of type II receive labels of ± 2 under λ. It is easily checked that λ is a zero-sum $\mathbb{Z}$-magic labeling of M and that $j(\lambda) = 2$. Hence $j^*(M) = 2$. (In Figure 6, the evolution of λ is illustrated via edges incident to $(u, v, w) \in V(G_1 \square G_2 \square G_3)$, where each of u, v, and w is assumed to have degree 3 in G_1, G_2, and G_3 respectively. Labels assigned to edges under ϕ_1', ϕ_2', and ϕ_3' are notional, from which labels under ψ and λ follow.)

By Corollary 9(c), it suffices to produce a zero-sum $\mathbb{Z}_2^2$-magic labeling of M. For each edge $e \in E(M)$ of the form $(u_i, v, w)(u_j, v, w)$, let $\rho(e) = (0, 1)$. For each edge e of the form $(u, v_i, w)(u, v_j, w)$, let $\rho(e) = (1, 0)$. And for each edge e of the form $(u, v, w_i)(u, v, w_j)$, let $\rho(e) = (1, 1)$. It follows from the oddness of each G_i that the weight of each vertex under ρ is 0. □

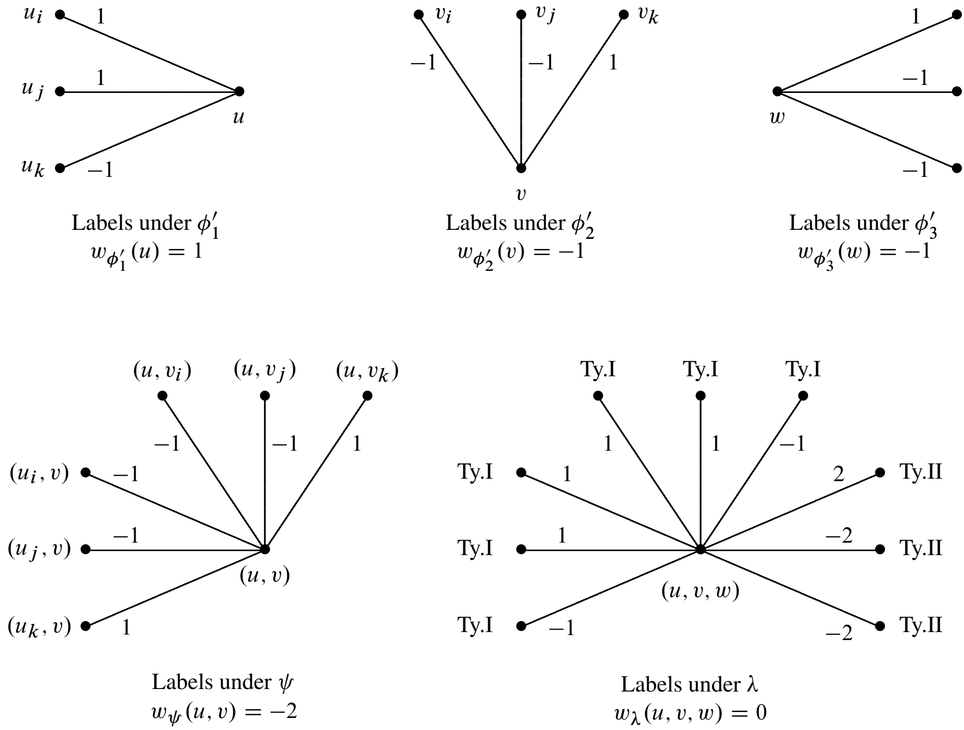

Figure 6. An illustration of the labeling λ of Lemma 16.

Theorem 17. *For $1 \le i \le n$, let G_i be an odd graph, and let $G = \square_{i=1}^n G_i$. Then*

(a) *If n is even, $j^*(G) = 1$ and $\mathcal{A}(G) = \mathcal{A}$.*

(b) *If n is odd, $j^*(G) = 2$ and $\mathcal{A}(G) = \mathcal{A} \setminus \{\mathbb{Z}_2\}$.*

Proof. (a) Let $n = 2t$. Then G is isomorphic to $\square_{i=1}^t H_i$, where $H_i = G_{2i-1} \square G_{2i}$. By Corollary 12, $j^*(H_i) = 1$. The result now follows from Theorems 14 and 1.

(b) Let $n = 2t + 1$, where $t \ge 1$. Let $H_1 = G_1 \square G_2 \square G_3$ and for $2 \le i \le t$, let $H_i = G_{2i} \square G_{2i+1}$. By Lemma 16, $j^*(H_1) = 2$ and $\mathcal{A}(H_1) = \mathcal{A} \setminus \{\mathbb{Z}_2\}$. And, by Corollary 12, $j^*(H_i) = 1$ for $2 \le i \le t$, implying $\mathcal{A}(H_i) = \mathcal{A}$. Thus, by Theorem 7, Theorem 14 and the fact that G is odd, $j^*(G) = 2$ and $\mathcal{A}(G) = \mathcal{A} \setminus \{\mathbb{Z}_2\}$. □

We now consider graphs $G = \square_{i=1}^n G_i$ such that $n \ge 2$, G_i is nontrivial, and G is r-regular. Since the regularity of G coimplies the regularity of each G_i, we assume G_i is r_i-regular, $r_i \ge 1$. Then the degree of G is $r = \sum_{i=1}^n r_i$.

The next theorem follows from Theorem 8 or alternatively Corollary 10 with the 4-cycle handled as a trivial special case.

Theorem 18. *Let $n \ge 2$ and let $G = \square_{i=1}^n G_i$ be an even-regular graph. Then $\mathcal{A}(G) = \mathcal{A}$.*

We turn to the case r is odd. For odd-regular graphs M except 5-regular, Theorem 8 indicates that M is zero-sum $\mathbb{A}$-magic for all $\mathbb{A}$ except possibly $\mathbb{Z}_2^k$, $\mathbb{Z}_4^k$, $k \geq 1$. (Certainly M is not zero-sum $\mathbb{Z}_2$-magic.) However, if M is a cartesian product of at least two factors, then more definitive results can be given for any odd regularity.

Lemma 19. *Let $G = G_1 \square G_2$ be an odd-regular graph, where $\delta(G_i) \geq 1$. Then $\mathcal{A} \setminus \{\mathbb{Z}_2, \mathbb{Z}_2^2\} \subseteq \mathcal{A}(G) \subseteq \mathcal{A} \setminus \{\mathbb{Z}_2\}$. Moreover, if either G_1 or G_2 has degree 1, then $\mathcal{A}(G) = \mathcal{A} \setminus \{\mathbb{Z}_2\}$.*

Proof. Since G is regular if and only if each G_i is regular, we assume without loss of generality G_i is r_i-regular for odd r_1 and even r_2. Let $r_2 = 2t$.

If $r_1 \geq 3$, then by Theorem 3, $E(G_1)$ partitions into a $\frac{1}{2}(r_1+1)$-factor and a $\frac{1}{2}(r_1-1)$-factor. By Petersen's theorem, $E(G_2)$ partitions into t 2-factors. Thus $E(G)$ naturally partitions into t 2-factors $F_1, F_2, \ldots, F_t$, a $\frac{1}{2}(r_1+1)$-factor F', and a $\frac{1}{2}(r_1-1)$-factor F''. We form a zero-sum $\mathbb{Z}$-magic labeling ϕ of G with $j(\phi) = 2$ based on the parity of t.

If $t = 2k+1$,

$$\phi(e) = \begin{cases} 1 & \text{if } e \in F_i,\ 1 \leq i \leq k, \\ -1 & \text{if } e \in F_i,\ k+1 \leq i \leq 2k+1, \\ 2 & \text{if } e \in F', \\ -2 & \text{if } e \in F''. \end{cases}$$

If $t = 2k$,

$$\phi(e) = \begin{cases} 1 & \text{if } e \in F_i,\ 1 \leq i \leq k, \\ -1 & \text{if } e \in F_i,\ k+1 \leq i \leq 2k-1, \\ -2 & \text{if } e \in F_{2k}, \\ 2 & \text{if } e \in F', \\ -2 & \text{if } e \in F''. \end{cases}$$

Since $j(\phi) = 2$ in each case, we have $j^*(G) \leq 2$. The result follows by Corollary 9(c).

Suppose $r_1 = 1$. Then the edge set $E(G)$ partitions naturally into a 1-factor F' (of which there are $|V(G_2)|$ components each isomorphic to P_2) and, by Petersen's theorem, t 2-factors $F_1, F_2, \ldots, F_t$. We form a zero-sum $\mathbb{Z}$-magic labeling ϕ of G with $j(\phi) = 2$ as above, accounting for the vacuous $\frac{1}{2}(r_1-1)$-factor.

If $t = 2k+1$ is odd,

$$\phi(e) = \begin{cases} 1 & \text{if } e \in F_i,\ 1 \leq i \leq k, \\ -1 & \text{if } e \in F_i,\ k+1 \leq 1 \leq 2k+1, \\ 2 & \text{if } e \in F'. \end{cases}$$

If $t = 2k$ is even,

$$\phi(e) = \begin{cases} 1 & \text{if } e \in F_i,\ 1 \le i \le k, \\ -1 & \text{if } e \in F_i,\ k+1 \le i \le 2k-1, \\ -2 & \text{if } e \in F_{2k}, \\ 2 & \text{if } e \in F'. \end{cases}$$

Thus $j^*(G) \le 2$, implying $\mathcal{A} \setminus \{\mathbb{Z}_2, \mathbb{Z}_2^2\} \subseteq \mathcal{A}(G) \subseteq \mathcal{A} \setminus \{\mathbb{Z}_2\}$ by Corollary 9(c). It remains to show that G is zero-sum $\mathbb{Z}_2^2$-magic.

Let H denote a 2-factor of G_2. Then $P_2 \square H$ is a 3-factor of G (not necessarily connected) in which each component is a prism. Since each prism is hamiltonian and hence 3-edge colorable, $P_2 \square H$ is zero-sum $\mathbb{Z}_2^2$-magic by Theorem 4. Letting ϕ' be a zero-sum $\mathbb{Z}_2^2$-magic labeling of $P_2 \square H$, we form a zero-sum $\mathbb{Z}_2^2$-magic labeling ϕ of G as follows:

$$\phi(e) = \begin{cases} \phi'(e) & \text{if } e \in E(P_2 \square H), \\ (1, 1) & \text{if } e \in E(G - (P_2 \square H)). \end{cases}$$ □

Lemma 20. *Suppose $G = G_1 \square G_2 \square G_3$ is odd-regular, where G_i is r_i-regular, $r_i \ge 1$. Suppose also that either $r_i = 1$ for some i or r_i is odd for all i. Then $\mathcal{A}(G) = \mathcal{A} \setminus \{\mathbb{Z}_2\}$.*

Proof. If r_i is odd for all i, then the result follows from Theorem 17. So, with no loss of generality, suppose $r_1 = 1$ and r_2, r_3 are even. Since G is isomorphic to $G_1 \square H$, where $H = G_2 \square G_3$, the result follows from Lemma 19. □

Theorem 21. *Suppose $G = \square_{i=1}^n G_i$ is odd-regular, where $n \ge 3$ and G_i is r_i-regular, $r_i \ge 1$. Let ω denote the number of odd-regular G_i. Then the following hold:*

(a) *If $\omega \ge 3$, then $\mathcal{A}(G) = \mathcal{A} \setminus \{\mathbb{Z}_2\}$.*

(b) *If $\omega = 1$, then $\mathcal{A} \setminus \{\mathbb{Z}_2, \mathbb{Z}_2^2\} \subseteq \mathcal{A}(G) \subseteq \mathcal{A} \setminus \{\mathbb{Z}_2\}$. Moreover, if the sole odd-regular G_i has degree 1, then $\mathcal{A}(G) = \mathcal{A} \setminus \{\mathbb{Z}_2\}$.*

Proof. We observe that ω must be odd since G is odd-regular with degree equal to $\sum_{i=1}^n r_i$.

(a) With no loss of generality, let G_1 and G_2 be odd-regular. Then $\square_{i=3}^n G_i$ is odd regular as well, which implies that G is isomorphic to the cartesian product of three odd-regular graphs G_1, G_2, and $\square_{i=3}^n G_i$. The result follows by Lemma 20.

(b) With no loss of generality, let G_1 be odd-regular. Then $\square_{i=2}^n G_i$ is even-regular, which implies that G is isomorphic to the cartesian product of one odd-regular graph G_1 and one even-regular graph $\square_{i=2}^n G_i$. The result follows by Lemma 19. □

4. Grid graphs

In this section we consider the cartesian product of paths $G = \square_{i=1}^{n} P_{a_i}$, where $n \geq 2$ and $a_i \geq 2$. We denote the vertex set of P_m by $\{1, 2, 3, 4, \ldots, m\}$, where x is adjacent to y if and only if $|x - y| = 1$. We note that if α is the number of a_i's equal to 2, then $\Delta(G) = 2n - \alpha$, $\delta(G) = n$, and for all integers j, $n \leq j \leq 2n - \alpha$, there exists a vertex of G with degree j. We also note that G is regular (in particular, n-regular) if and only if $a_i = 2$ for all i.

Lemma 22. *Let M be a graph such that $j^*(M) \leq 2$ and $j^*(M \,\square\, P_2) \leq 2$. Then $j^*(M \,\square\, P_n) \leq 2$ for $n \geq 3$.*

Proof. Let H' denote the subgraph of $M \,\square\, P_n$ induced by the vertices in $\{(v, 1) \mid v \in V(M)\}$ and let H'' denote the subgraph of $M \,\square\, P_n$ induced by the vertices in $\{(v, i) \mid v \in V(M), i = 1, 2\}$. Since H' and H'' are respectively isomorphic to M and $M \,\square\, P_2$, we can find zero-sum $\mathbb{Z}$-magic labelings ϕ' of H' and ϕ'' of H'' such that $j(\phi')$ and $j(\phi'')$ are each at most 2. As follows, we construct a zero-sum $\mathbb{Z}$-magic labeling ϕ of $M \,\square\, P_n$ that draws its labels from the images of ϕ' and ϕ'' (this labeling is illustrated in Figure 7 with $n = 5$ and a graph M that is seen by inspection to satisfy the hypotheses of the lemma):

$$\phi(e) = \begin{cases} \phi''(e) & \text{if } e = (u, 1)(w, 1), \\ \phi'((u, 1)(w, 1)) & \text{if } e = (u, i)(w, i),\ 2 \leq i \leq n-1, \\ \phi''((u, 1)(u, 2)) & \text{if } e = (u, i)(u, i+1),\ 1 \leq i \leq n-1,\ i \text{ odd}, \\ -\phi''((u, 1)(u, 2)) & \text{if } e = (u, i)(u, i+1),\ 1 \leq i \leq n-1, i \text{ even}, \\ -\phi''((u, 1)(w, 1)) & \text{if } e = (u, n)(w, n), n \text{ odd}, \\ \phi''((u, 1)(w, 1)) & \text{if } e = (u, n)(w, n), n \text{ even}. \end{cases}$$

Thus $j(\phi) \leq 2$, giving the result. □

Lemma 23. *Let M be a graph and let $\mathbb{A} \in \mathcal{A}$ such that both M and $M \,\square\, P_2$ are zero-sum $\mathbb{A}$-magic. Then $M \,\square\, P_n$ is zero-sum $\mathbb{A}$-magic for $n \geq 3$.*

Proof. Let H' and H'' denote the subgraphs of $M \,\square\, P_n$ given in the proof of Lemma 22, and let ϕ' and ϕ'' be zero-sum $\mathbb{A}$-magic labelings of H' and H'', respectively. Then the labeling ϕ of that proof is a zero-sum $\mathbb{A}$-magic labeling of $M \,\square\, P_n$. □

Theorem 24. *Suppose $G = \square_{i=1}^{n} P_{a_i}$, where $n \geq 2$. If n is even and $a_i = 2$ for all i, then $\mathcal{A}(G) = \mathcal{A}$. Otherwise, $\mathcal{A}(G) = \mathcal{A} \setminus \{\mathbb{Z}_2\}$.*

Proof. If n is even and $a_i = 2$ for all i, the result follows from Theorem 18. If n is odd and $a_i = 2$ for all i, the result follows from Lemma 19 and the observation that G is isomorphic to $H_1 \,\square\, H_2$, where $H_1 = P_2$ and $H_2 = \square_{i=2}^{n} P_2$. We thus assume $a_i \geq 3$ for some i, which implies that G has a vertex of odd degree.

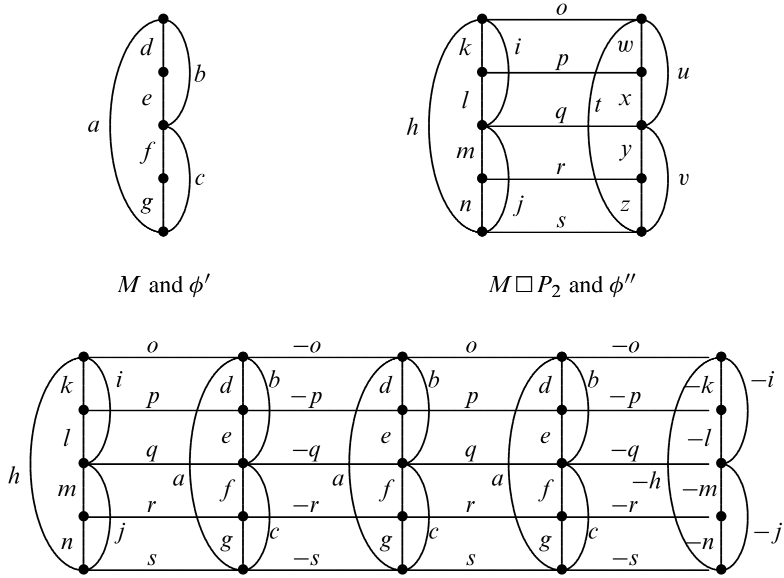

Figure 7. An illustration of the labeling ϕ of Lemma 22.

Express G as follows:

- If $n = 2k$, then $G = \square_{i=1}^{k} H_i$, where $H_i = P_{a_{2i-1}} \square P_{a_{2i}}$.
- If $n = 2k+1$, then $G = \square_{i=1}^{k} H_i$, where $H_1 = P_{a_1} \square P_{a_2} \square P_{a_3}$ and $H_i = P_{a_{2i}} \square P_{a_{2i+1}}$ for $2 \le i \le k$.

Each H_i must be isomorphic to one of the following:

- Class 1: $P_2 \square P_2$.
- Class 2: $P_r \square P_s,\ r \ge 2,\ s > 2$.
- Class 3: $P_2 \square P_2 \square P_2$.
- Class 4: $P_2 \square P_2 \square P_s,\ s \ge 3$.
- Class 5: $P_2 \square P_s \square P_t,\ s, t \ge 3$.
- Class 6: $P_s \square P_t \square P_r,\ s, t, r \ge 3$.

We first show that for each H_i, we have $j^*(H_i) \le 2$.

By Theorem 15, the graphs H_i of classes 1, 2, and 3 have $j^*(H_i) \le 2$.

Consider graphs of class 4. Since $j^*(P_2 \square P_2) \le 2$ and $j^*((P_2 \square P_2) \square P_2) \le 2$, graphs H_i of class 4 have $j^*(H_i) \le 2$ by Lemma 22.

Consider graphs of class 5. Since $j^*(P_2 \square P_s) \le 2$ and $j^*((P_2 \square P_s) \square P_2) \le 2$, graphs H_i of class 5 have $j^*(H_i) \le 2$ by Lemma 22.

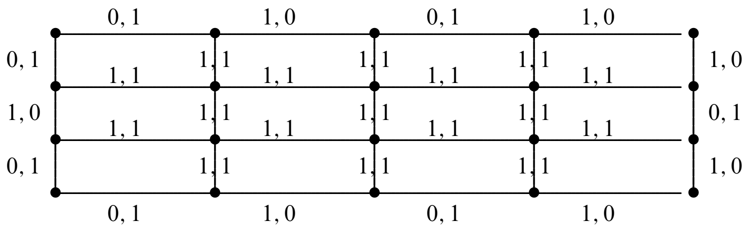

Figure 8. A zero-sum $\mathbb{Z}_2^2$-magic labeling of $P_4 \square P_5$.

Consider graphs of class 6. Since $j^*(P_s \square P_t) \leq 2$ and $j^*((P_s \square P_t) \square P_2) \leq 2$, graphs H_i of class 6 have $j^*(H_i) \leq 2$ by Lemma 22.

Thus, by Theorem 14, $j^*(G) \leq 2$, which implies by Corollary 9(c) that

$$\mathcal{A} \setminus \{\mathbb{Z}_2, \mathbb{Z}_2^2\} \subseteq \mathcal{A}(G) \subseteq \mathcal{A} \setminus \{\mathbb{Z}_2\}.$$

It now suffices to show that G is zero-sum $\mathbb{Z}_2^2$-magic. To that end, we next show that each H_i is zero-sum $\mathbb{Z}_2^2$-magic.

By inspection, the graph H_i of class 1 has $\mathcal{A}(H_i) = \mathcal{A}$.

By Corollary 9(c), the graphs H_i of class 2 are zero-sum $\mathbb{A}$-magic for all $\mathbb{A}$ except $\mathbb{Z}_2$ and possibly $\mathbb{Z}_2^2$. But it is an easy matter to construct a zero-sum $\mathbb{Z}_2^2$-magic labeling of H_i, thereby establishing that $\mathcal{A}(H_i) = \mathcal{A} \setminus \{Z_2\}$. Particularly, consider the following sequence of vertices that specifies a cycle:

$$(1, 1), \ldots, (1, s), (2, s), \ldots, (r, s), (r, s-1), \ldots, (r, 1), (r-1, 1), \ldots, (1, 1).$$

Moving around the cycle, assign each edge a label from $\{(0, 1), (1, 0)\}$ according to the following algorithm and as illustrated in Figure 8 (where parentheses are omitted): assign $(0, 1)$ to the edge $(1, 1)(1, 2)$. For every two distinct edges e' and e'' of the cycle, assign distinct labels if e' and e'' are incident to a common vertex of degree 3 in G; otherwise, assign equal labels if e' and e'' are incident to a common vertex of degree 2 in G. To each other edge of G, assign $(1, 1)$.

By Theorem 21(a), the graph H_i of class 3 has $\mathcal{A}(H_i) = \mathcal{A} \setminus \{\mathbb{Z}_2\}$.

Consider graphs of class 4. Since $P_2 \square P_2$ is of class 1, it is zero-sum $\mathbb{A}$-magic for all $\mathbb{A}$. And since $(P_2 \square P_2) \square P_2$ is of class 3, it is zero-sum $\mathbb{A}$-magic for all $\mathbb{A}$ except Z_2. Thus, by Lemma 23 and the fact that graphs H_i of class 4 have vertices of odd degree, $\mathcal{A}(H_i) = \mathcal{A} \setminus \{\mathbb{Z}_2\}$.

Consider graphs of class 5. Since $P_2 \square P_s$ is of class 2, it is zero-sum $\mathbb{A}$-magic for all $\mathbb{A}$ except $\mathbb{Z}_2$. And since $(P_2 \square P_s) \square P_2$ is of class 4, it is zero-sum $\mathbb{A}$-magic for all $\mathbb{A}$ except Z_2. Thus, by Lemma 23 and the fact that graphs H_i of class 5 have vertices of odd degree, $\mathcal{A}(H_i) = \mathcal{A} \setminus \{\mathbb{Z}_2\}$.

Consider graphs of class 6. Since $P_s \square P_t$ is of class 2, it is zero-sum $\mathbb{A}$-magic for all $\mathbb{A}$ except $\mathbb{Z}_2$. And since $(P_s \square P_t) \square P_2$ is of class 5, it is zero-sum $\mathbb{A}$-magic for all $\mathbb{A}$ except Z_2. Thus, by Lemma 23 and the fact that graphs H_i of class 6 have vertices of odd degree, $\mathcal{A}(H_i) = \mathcal{A} \setminus \{\mathbb{Z}_2\}$.

We therefore see by Theorem 7 that $\mathcal{A} \setminus \{\mathbb{Z}_2\} \subseteq \mathcal{A}(G)$. But since G has a vertex of odd degree, G is not zero-sum $\mathbb{Z}_2$-magic. Thus $\mathcal{A}(G) = \mathcal{A} \setminus \{\mathbb{Z}_2\}$. □

We close this section with a theorem that utilizes Corollary 12.

Theorem 25. *Let $n \geq 3$ and let G be an odd graph. Then $\mathcal{A}(G \,\square\, P_n) = \mathcal{A} \setminus \{\mathbb{Z}_2\}$.*

Proof. Let H' be the subgraph of $G \,\square\, P_n$ induced by $\{(v, i) \mid v \in V(G),\ i = 1, 2\}$. Since H' is isomorphic to $G \,\square\, P_2$, Corollary 12 implies the existence of a zero-sum $\mathbb{Z}$-magic labeling ϕ' of H' such that $j(\phi') = 1$. We establish a zero-sum $\mathbb{Z}$-magic labeling ϕ of $G \,\square\, P_n$ with $j(\phi) = 2$, thereby establishing $j^*(G \,\square\, P_n) \leq 2$:

$$\phi(e) = \begin{cases} \phi'((u,1)(w,1)) & \text{if } e = (u,1)(w,1) \text{ or } (u,n)(w,n), \\ 2\phi'((u,1)(w,1)) & \text{if } e = (u,i)(w,i),\ 2 \leq i \leq n-1, \\ \phi'((u,1)(u,2)) & \text{if } e = (u,i)(u,i+1),\ 1 \leq i \leq n-1. \end{cases}$$

By Corollary 9(c), it now suffices to establish a zero-sum $\mathbb{Z}_2^2$-magic labeling ϕ of $G \,\square\, P_n$:

$$\phi(e) = \begin{cases} (0,1) & \text{if } e = (u,1)(w,1), \\ (1,1) & \text{if } e = (u,i)(w,i),\ 2 \leq i \leq n-1, \\ (0,1) & \text{if } e = (u,n)(w,n),\ n \text{ even}, \\ (1,0) & \text{if } e = (u,n)(w,n),\ n \text{ odd}, \\ (0,1) & \text{if } e = (u,i)(u,i+1),\ i \text{ odd}, \\ (1,0) & \text{if } e = (u,i)(u,i+1),\ i \text{ even}. \end{cases}$$ □

5. Closing remarks

We close this paper with suggestions for further study.

If G is the cartesian product of two odd graphs, then $j^*(G) = 1$. What can be said of $j^*(G)$ if one or each factor is even?

If $T_1, T_2, \ldots, T_n$ is a collection of nontrivial trees and $G = \square_{i=1}^{n} T_i$, we are able to show that $j^*(G) \leq 4$. Is this a sharp upper bound?

What can be said of $j^*(G)$ if G is an odd cartesian product?

We have seen that the graphs G under study have $j^*(G) \leq 2$, with $j^*(G) = 1$ if and only if G is an even graph with even size. We have also seen that $j^*(G) = 1$ is a sufficient but not necessary condition for $\mathcal{A}(G) = \mathcal{A}$. Are there cartesian products G such that $j^*(G) \geq 3$? Are there necessary and sufficient conditions for $j^*(G) = 2$?

Acknowledgments

This paper reflects the efforts of the participants of an undergraduate research seminar in graph theory at Trinity College. The authors, including students A. Fong,

D. Spagnuolo, J. Wallace, and S. Wang, gratefully acknowledge the support and sponsorship of Dr. T. Savage. We also express our gratitude to the referee for thoughtful and constructive direction.

References

[Akbari et al. 2014] S. Akbari, F. Rahmati, and S. Zare, "Zero-sum magic labelings and null sets of regular graphs", *Electron. J. Combin.* **21**:2 (2014), Paper 2.17. MR Zbl

[Choi et al. 2012] J. O. Choi, J. P. Georges, and D. Mauro, "Relating edge-coverings to the classification of $\mathbb{Z}_2^k$-magic graphs", *Discrete Math.* **312**:19 (2012), 2938–2945. MR Zbl

[Gallian 2018] J. A. Gallian, "A dynamic survey of graph labeling", *Electron. J. Combin.* **5** (2018), Dynamic Survey 6. Zbl

[Georges et al. 2010] J. P. Georges, D. W. Mauro, and Y. Wang, "On the structures of V_4-magic and $\mathbb{Z}_4$-magic graphs", *J. Combin. Math. Combin. Comput.* **75** (2010), 137–152. MR Zbl

[Georges et al. 2017] J. P. Georges, D. Mauro, and K. Wash, "On zero-sum $\mathbb{Z}_{2^j}^k$-magic graphs", *J. Comb. Optim.* **34**:1 (2017), 94–113. MR Zbl

[Low and Lee 2006] R. M. Low and S.-M. Lee, "On the products of group-magic graphs", *Australas. J. Combin.* **34** (2006), 41–48. MR Zbl

[Ore 1957] O. Ore, "Graphs and subgraphs", *Trans. Amer. Math. Soc.* **84** (1957), 109–136. MR Zbl

[Petersen 1891] J. Petersen, "Die Theorie der regulären graphs", *Acta Math.* **15**:1 (1891), 193–220. MR Zbl

[Sedláček 1964] J. Sedláček, "Problem 27", pp. 163–167 in *Theory of graphs and its applications* (Smolenice, 1963), edited by M. Fiedler, Publ. House Czechoslovak Acad. Sciences, Prague, 1964.

[Shiu and Low 2018] W. C. Shiu and R. M. Low, "The integer-magic spectra and null sets of the Cartesian product of trees", *Australas. J. Combin.* **70** (2018), 157–167. MR Zbl

[Shiu et al. 2004] W. C. Shiu, P. C. B. Lam, and P. K. Sun, "Construction of group-magic graphs and some A-magic graphs with A of even order", pp. 97–107 in *Proceedings of the Thirty-Fifth Southeastern International Conference on Combinatorics, Graph Theory and Computing* (Boca Raton, FL), Congressus Numerantium **167**, Utilitas Math., Winnipeg, MB, 2004. MR Zbl

[Stanley 1973] R. P. Stanley, "Linear homogeneous Diophantine equations and magic labelings of graphs", *Duke Math. J.* **40** (1973), 607–632. MR Zbl

Received: 2018-03-14 Revised: 2019-08-27 Accepted: 2019-09-20

adam.y.w.fong@gmail.com Department of Mathematics, Trinity College, Hartford, CT, United States

john.georges@trincoll.edu Department of Mathematics, Trinity College, Hartford, CT, United States

david.mauro@trincoll.edu Department of Mathematics, Trinity College, Hartford, CT, United States

dylanspag@gmail.com Department of Mathematics, Trinity College, Hartford, CT, United States

jackwallacemv@gmail.com Department of Mathematics, Trinity College, Hartford, CT, United States shufan.wang.2018@trincoll.edu *Department of Mathematics, Trinity College, Hartford, CT, United States*

kwashmath@gmail.com *Department of Mathematics, Trinity College, Hartford, CT, United States*

INVOLVE 12:8 (2019)
dx.doi.org/10.2140/involve.2019.12.1279

The variable exponent Bernoulli differential equation

Karen R. Ríos-Soto, Carlos E. Seda-Damiani
and Alejandro Vélez-Santiago

(Communicated by Toka Diagana)

We investigate the realization of a Bernoulli-type first-order differential equation with a variable exponent. Using substitution methods, we show the existence of an implicit solution to the Bernoulli problem. Numerical simulations applied to several examples are also provided.

1. Introduction

The aim of this paper is to investigate a Bernoulli-type first-order ordinary differential equation with a variable exponent, formally written as

$$\frac{dy}{dx}+a(x)y=b(x)y^{p(x)}. \tag{1-1}$$

Here $a(x)$, $b(x)$ are continuous functions and $p(x)$ is a function of class C^1 in a bounded interval $[\alpha,\beta]$, with $p(x)\neq 1$ for all x.

Equation (1-1) is well known and standard in the case when $p(x)=p$, a constant; e.g., see [Boyce and DiPrima 2012; Edwards and Penney 2008; Zill and Cullen 2012]. However, when the exponent is variable, to the best of our knowledge, this problem has not been investigated up to the present time. The focus of this work is to provide a first attempt to solve the generalized Bernoulli-type problem (1-1) for particular functions $p(x)$. Unfortunately, even for simple types of functions $p(x)$, the solution of problem (1-1) cannot be given explicitly, and its formulation is in most cases quite complicated. At the end, for the main examples, we will provide numerical simulations for the solutions of ODEs of the type presented in this paper, and we will analyze and compare them with the analytical solutions.

Problem (1-1) for p a constant, known as the Bernoulli ODE, was proposed by James Bernoulli in 1695. A year later, Leibniz solved the equation by making

MSC2010: 34A34, 34A09, 34B15, 65L06.
Keywords: variable exponent differential equations, Bernoulli differential equation, implicit solutions, numerical simulations.

substitutions and simplifying to a linear equation, similar to the method employed in this work. This type of ODE can be viewed as a generalization of the frictional forces equation. Furthermore, modern physics uses Bernoulli differential equations for modeling the dynamics behind certain circuit elements, known as Bernoulli memristors (for more details, we refer to [O'Neil 2012], among others). The Bernoulli differential equation also shows up in some economic utility maximization problems; see, e.g., [Merton 1969]. As mentioned above, all these models consider p to be constant, and there is no literature known for the case when $p = p(x)$ is nonconstant.

Over the recent years, various mathematical problems with variable exponent have attracted the attention of many authors. Interest in variational problems and differential equations with nonstandard growth conditions has grown, highly motivated by various applications, such as elastic mechanics, electrorheological fluids, fluid dynamics, and image restoration; see [Acerbi and Mingione 2002; Bollt et al. 2009; Chen et al. 2006; Cruz-Uribe and Fiorenza 2013; Diening et al. 2011; Diening and Růžička 2003], among others. However, to the best of our knowledge, there is no work done on variable exponent ordinary differential equations.

The paper is organized as follows. In Section 2 we work with (1-1) in all its generality. By making proper substitutions, we transform (1-1) into an exponential-type first-order ODE with variable coefficients, which depends on the variable exponent function $p(x)$. We show that under appropriate conditions on $p(x)$, the corresponding initial value problem of type (1-1) is well-posed. Section 3 is devoted entirely to the solvability of problem (1-1) in the case when the coefficients a, b are constant. However, up to the present time, there are no known appropriate tools that could allow us to solve the problem (1-1) in a general form. Consequently, in this section we focus on the realization of problem (1-1) under particular choices of the function $p(x)$. Even under such restrictions, the solution of problem (1-1) turns out to be of a very complicated structure, and in almost all cases only implicit solutions are achieved. Under some additional restrictions, we are able to provide a concrete formula for the solution of problem (1-1) (under the assumptions of Section 3), which is given as an elaborated convergent infinite series which involves complicated expressions, such as exponential integral functions. In Section 4, we consider a particular case when the coefficients are variable with a specific structure directly related with the exponent $p(x)$. Several examples will be illustrated, whose structure will coincide with the structure outlined at Section 2. Consequently, solutions can only be given implicitly, as argued in the previous section. Finally, in Section 5, some numerical methods are performed over the solutions of particular examples of ODEs of types given by problem (1-1). When possible, we will discuss the relationship between the behavior shown by the solution deduced through numerical methods, in comparison with the analytic solution.

2. Reformulation of the problem

In this section, simple calculations to transform the original Bernoulli equation (1-1) into a simple differential equation will be employed.

Let us start by performing the substitution

$$v = y^{1-p(x)}. \tag{2-1}$$

Then one has

$$\begin{aligned} y &= v^{1/(1-p(x))}, \\ y' &= \frac{d}{dx}(v^{1/(1-p(x))}) = v^{1/(1-p(x))}\left(\frac{p'(x)}{(1-p(x))^2}\ln v + \frac{1}{(1-p(x))}\frac{v'}{v}\right). \end{aligned} \tag{2-2}$$

Substituting (2-2) and (2-1) into (1-1), and multiplying both sides by v we obtain

$$v^{1/(1-p(x))}\left(\frac{p'(x)}{(1-p(x))^2}v\ln v + \frac{1}{(1-p(x))}v' + a(x)v\right) = b(x)v^{1/(1-p(x))},$$

where we recall that $p = p(x)$. Dividing both sides of the equality above by $v^{1/(1-p(x))}$, we arrive at

$$\frac{p'(x)}{(1-p(x))^2}v\ln v + \frac{1}{(1-p(x))}v' + a(x)v = b(x). \tag{2-3}$$

Performing the substitution $w = \ln v$ in (2-3), we have the nonlinear ODE

$$\frac{p'(x)}{(1-p(x))^2}e^w w + \frac{1}{(1-p(x))}e^w w' + a(x)e^w = b(x),$$

which, in turn, can be further simplified into the ODE

$$w' = b(x)e^{-w}(1-p) - a(x)(1-p) - \frac{p'}{1-p}w. \tag{2-4}$$

Note that (2-4) is fully nonlinear, and cannot be linearized, and consequently its solvability is quite nontrivial (as we will see in the subsequent section, even for particular cases). However, the following result asserts that the ODE (2-4) can be solved under certain conditions.

Theorem 2.1 (see [Edwards and Penney 2008]). *Assume that both $f(x, y)$ and its partial derivative $\partial_y f(x, y)$ are continuous over a rectangular region R in the xy-plane that contains the point (a, b) in its interior. Then, there exists some open interval I containing the point a such that the initial value problem*

$$\frac{dy}{dx} = f(x, y), \quad y(a) = b,$$

is uniquely solvable over I.

For our case of interest, namely, the solution of (2-4), under suitable conditions on the functions $a(x)$, $b(x)$ and $p(x)$, we have

$$f(x,w) = b(x)e^{-w}(1-p) - a(x)(1-p) - \frac{p'}{1-p}w,$$

$$\partial_w f(x,w) = -e^{-w}b(x)(1-p) - \frac{p'}{1-p}.$$

Hence we can easily find a rectangle in $\mathbb{R}^2$ in which both $f(x,w)$ and $\partial_w f(x,w)$ are continuous. Consequently, we can apply Theorem 2.1 to obtain that (2-4) is solvable over some interval $I = (\alpha, \beta)$.

3. Solvability of problem (1-1): constant coefficients case

The following section will be devoted in finding tools to solve the problem (1-1). Because of the generality and difficulty of the original problem (1-1), we will investigate the solvability for particular constant coefficient cases. It is shown that even in very simple cases the problem will be highly nontrivial, as will its solution, and basically impossible to be solved explicitly.

3A. ***The case: $a = 0$ and $b = 1$.*** Consider the situation when $a(x) = 0$ and $b(x) = 1$. Then (1-1), using the substitution argument in (2-4), becomes the simplified differential equation

$$w' = e^{-w}(1-p) - \frac{p'}{1-p}w. \tag{3-1}$$

We seek an even more simplified version of the problem (3-1). In fact, below we present some particular cases when the problem (3-1) can be solved implicitly (under suitable conditions that will be explained in more detail).

3A1. *A separable case.* We consider the case when the exponent $p = p(x)$ satisfies the ordinary differential equation

$$\frac{p'}{(1-p)} = \lambda(1-p), \tag{3-2}$$

where $\lambda \in \mathbb{R}\setminus\{0\}$ is a fixed constant. Then (3-2) becomes

$$\frac{1}{(1-p)^2}\,dp = \lambda\,dx, \tag{3-3}$$

which is clearly separable. The function $p(x) = 1 - 1/(\lambda x)$ is a particular solution to the problem (3-3). For this particular case, substituting the function $p(x)$ in (3-1) yields

$$\frac{dw}{dx} = \frac{1}{\lambda x}(e^{-w} - \lambda w), \tag{3-4}$$

which is also a separable first-order ODE. Hence solving (3-4), we get the implicit equation

$$\int \frac{1}{e^{-w} - \lambda w}\, dw = \frac{\ln|x|}{\lambda} + C, \tag{3-5}$$

where the integral on the left-hand side cannot be computed explicitly. We then examine the case when

$$\left| \frac{e^{-w}}{\lambda w} \right| < 1. \tag{3-6}$$

This condition guarantees the uniform convergence of the series in the right-hand side of (3-5) in the function $h(w)$, defined by

$$h(w) = \frac{1}{e^{-w} - \lambda w} = -\frac{1}{\lambda w}\left(\frac{1}{1 - e^{-w}/(\lambda w)}\right) = -\sum_{k=0}^{\infty} \frac{1}{(\lambda w)^{k+1} e^{kw}}. \tag{3-7}$$

The uniform convergence of the series in $h(w)$ allows us to perform term by term integration, arriving at

$$\int h(w)\, dw = -\sum_{k=0}^{\infty} \int \frac{1}{(\lambda w)^{k+1} e^{kw}}\, dw = \frac{1}{\lambda} \sum_{k=0}^{\infty} (\lambda w)^{-k} E_{k+1}(kw), \tag{3-8}$$

where $E_n(x)$ is the so called *n-th exponential integral function*, defined by

$$E_n(x) = \int_1^{\infty} \frac{e^{-xt}}{t^n}\, dt \quad (n \in \mathbb{N}). \tag{3-9}$$

Thus in view of (3-5) and (3-8) (under the special assumption (3-6)), the implicit solution to (3-4) with $a(x) = 0,\ b(x) = 1$ and $p(x) = 1 - 1/(\lambda x)$ is given by

$$\sum_{k=0}^{\infty} (\lambda w)^{-k} E_{k+1}(kw) - \ln|x| = C. \tag{3-10}$$

Performing backward substitutions on w and using the explicit formula for the variable exponent $p(x)$, the solution for (3-1) becomes

$$G(x, y) = C$$

for

$$G(x, y) := \sum_{k=0}^{\infty} \left(\frac{x}{\ln y}\right)^k E_{k+1}(k(\lambda x)^{-1} \ln y) - \ln|x|, \tag{3-11}$$

whenever

$$0 < y < \left(\frac{|\ln y|}{\lambda x}\right)^{\lambda x}.$$

A further analysis on the solution (3-11) together with the condition above shows that the solution $y = y(x)$ fulfills $y(x) \geq e^x$, with $y \approx e^x$ as x is large enough. In particular, the solution blows up as x tend to infinity.

3A2. *The exact method.* The previous case can be worked with an exact ODE by taking (3-4) and rewriting it such that

$$(e^{-w} - \lambda w)\, dx - \lambda x\, dw = 0, \tag{3-12}$$

where $M(x, w) = e^{-w} - \lambda w$ and $N(x, w) = -\lambda x$, and looking over the partial derivatives M_w and N_x it is clear that (3-12) is not exact; see, e.g., [Boyce and DiPrima 2012]. Thus, suppose that an integration factor $\mu(x, w) = \mu(w)$ exists such that

$$\mu(w)(e^{-w} - \lambda w)\, dx - \mu(w)\lambda x\, dw = 0 \tag{3-13}$$

is an exact differential equation. Then $\widetilde{M}_w = \widetilde{N}_x$, where $\widetilde{M}(x, w) = \mu(w)(e^{-w} - \lambda w)$ and $\widetilde{N}(x, w) = -\mu(w)\lambda x$, from which we obtain

$$\mu(w) = \exp\biggl(\int \frac{1}{1 - \lambda w e^w}\, dw\biggr). \tag{3-14}$$

Now let

$$\Phi(w) = \frac{1}{1 - \lambda w e^w} = \sum_{k=0}^{\infty} \lambda^k w^k e^{kw}$$

for $|\lambda w e^w| < 1$, and where the integration of this series is

$$\int \Phi(w)\, dw = 1 + \sum_{k=1}^{\infty} \int \lambda^k w^k e^{kw}\, dw = 1 + \sum_{k=1}^{\infty} -w(\lambda w)^k E_{-k}(-kw). \tag{3-15}$$

Substitution of (3-15) into (3-14) yields

$$\mu(w) = \exp\biggl(1 + \sum_{k=1}^{\infty} -w(\lambda w)^k E_{-k}(-kw)\biggr). \tag{3-16}$$

With this function we are now able to perform partial integration over (3-13) and obtain an expression for the implicit solution of problem (3-1) for $a = 0$, $b = 1$ and $p(x) = 1 - 1/(\lambda x)$:

$$F(x, w) = \mu(w)(e^{-w} - \lambda w)x = C, \tag{3-17}$$

where $\mu(w)$ is as shown in (3-14).

3B. ***The case $a = b = 1$.*** In this subsection we take a quick look into the case when $a \neq 0$; for simplicity we take $a = 1$. In fact, setting $a(x) = b(x) = 1$, (1-1) and (2-4) become

$$\frac{dy}{dx} + y = y^{p(x)}, \tag{3-18}$$

$$w' = (e^{-w} - 1)(1 - p) - \frac{p'}{1 - p} w, \tag{3-19}$$

respectively. Then as in the previous subsection, we concentrate on the separable case for (3-19).

In fact, to have separability, as before we require that the function $p(x)$ fulfill (3-2) (here for simplicity we take $\lambda = 1$). Proceeding as in Section 3A1, we have that $p(x) = 1 - 1/x$ is the required function. Inserting this function into (3-19), we get

$$\frac{dw}{dx} = \frac{1}{x}(e^{-w} - w - 1), \tag{3-20}$$

a clearly separable ODE whose integral equation is given by

$$\int \frac{dw}{e^{-w} - w - 1} = \ln|x| + C. \tag{3-21}$$

Now let

$$h(w) = \frac{1}{e^{-w} - w - 1} = -\frac{1}{1+w}\left(\frac{1}{1 - e^{-w}/(1+w)}\right) = -\sum_{k=0}^{\infty} \frac{e^{-kw}}{(1+w)^{k+1}}, \tag{3-22}$$

where we are requiring that

$$\left|\frac{e^{-w}}{1+w}\right| < 1. \tag{3-23}$$

Then under such restriction, the series appearing in (3-22) converges absolutely, and consequently, we have

$$\int h(w)\,dw = -\sum_{k=0}^{\infty} \int \frac{e^{-kw}}{(1+w)^{k+1}}\,dw = \sum_{k=0}^{\infty} e^{-k}(w+1)^{-k} E_{k+1}(k(w+1)). \tag{3-24}$$

In view of (3-23) and (3-24), the solution of the ODE (3-18) is given implicitly by $H(x, y) = C$ for

$$H(x, y) := \sum_{k=0}^{\infty} e^{-k}\left(\frac{\ln y}{x} + 1\right)^{-k} E_{k+1}\left(\frac{k \ln y}{x} + k\right) - \ln|x|, \tag{3-25}$$

whenever (3-23) holds for $w = \ln v = (\ln y)/x$. A careful examination of this condition shows that (3-23) is valid if and only if $w > 0$, or equivalently, if and only if $(\ln y)/x > 0$. Going over the solution (3-25) over the given interval of convergence shows that the solution y satisfies $y = y(x) \geq 1$ when $x > 0$, with $y \approx 1$ as x tends to infinity.

3C. ***Method of differences.*** In this subsection we consider another approach to solve (3-1) (and consequently (1-1)) in the case when $a(x) = a$ and $b(x) = b$ are constant coefficients. For simplicity, we take $a = b = 1$.

We begin by considering the ODE

$$\gamma' + \frac{p'}{1-p}\gamma = (1-p)[e^{-w} - 1], \tag{3-26}$$

where $\gamma := \gamma(x)$ and $w = w(x)$ is the solution of problem (3-1). One sees that (3-26) is a linear first-order ODE, and thus the solution $\gamma(x)$ of problem (3-26) is given by

$$\gamma(x) = (1-p(x)) \int (e^{-w} - 1)\, dx = (1-p(x))\left[-x + \int e^{-w}\, dx\right]. \tag{3-27}$$

On the other hand, since w solves the ODE (3-19), we have

$$w' + \frac{p'}{1-p} w = (1-p)[e^{-w} - 1]. \tag{3-28}$$

Substituting the solution (3-27) into (3-26), and then taking the difference of (3-26) and (3-28), we obtain

$$\frac{d\phi}{dx} = \frac{p'}{1-p}\phi, \tag{3-29}$$

where $\phi(x) := \gamma(x) - w(x)$. Equation (3-29) is separable, and its solution is given by

$$\phi(x) = \frac{E}{1-p(x)} \tag{3-30}$$

for $E = e^D$ some arbitrary constant. Using the definition of ϕ, we arrive at the integral equation

$$w(x) = (1-p(x))\left[-x + \int e^{-w}\, dx\right] - \frac{E}{1-p(x)}. \tag{3-31}$$

Substituting back into the original variable $y = y(x)$, solution (3-31) becomes the exponential integral equation

$$y(x) = \exp\left(-x + \int [y(x)]^{p(x)-1}\, dx - \frac{E}{(1-p(x))^2}\right). \tag{3-32}$$

4. Solvability of problem (1-1): variable coefficients case

In this section, we will look into problem (1-1) for particular cases of the (variable) coefficients $a(x)$, $b(x)$. A careful examination of (2-4) shows that the cases where such problem can be solved (with the standard tools) are very few. In particular, one can deduce that a requirement is that $a(x) = b(x)$, and this may equal a particular function depending on the exponent function $p(x)$, as we show below.

In view of the above paragraph, we let

$$a(x) = b(x) = \frac{p'(x)}{(1-p(x))^2}. \tag{4-1}$$

Then, substituting these choices into (2-4) gives the ODE

$$w' = \frac{p'}{1-p}(e^{-w} - 1 - w). \tag{4-2}$$

Equation (4-2) is clearly a separable differential equation, and consequently, its solution is given by the integral equation

$$\int \frac{dw}{e^{-w} - 1 - w} = -\ln|p(x) - 1| + C, \tag{4-3}$$

where the solution to the left-hand side of (4-3) is given by solution (3-24) (under the assumption (3-23)). The following examples illustrate in a more concrete way the above formulations.

Example 4.1. Consider the differential equation

$$y' - e^x y = -e^x y^{1+e^{-x}}. \tag{4-4}$$

Here $a(x) = b(x) = -e^x$ and $p(x) = 1 + e^{-x}$. Observe that $a,\ b,\ p \in C^\infty(\mathbb{R})$ with $p(x) > 1$ for all $x \in \mathbb{R}$. Furthermore, one clearly sees that (4-1) holds, and consequently applying (4-3), recalling (3-24) and proceeding as in the derivation of (3-25), the solution of the differential equation (4-4) is given by

$$\sum_{k=0}^{\infty} e^{-k}\left(\frac{\ln y}{x} + 1\right)^{-k} E_{k+1}\left(\frac{k\ln y}{x} + k\right) - x = C, \tag{4-5}$$

provided that the condition $(\ln y)/x > 0$ is valid.

Example 4.2. Consider the differential equation

$$y' + 2\tan x \sec^2 x y = 2\tan x \sec^2 x y^{\sin^2 x} \tag{4-6}$$

for $x \in \left(-\frac{\pi}{2}, \frac{\pi}{2}\right)$. Then $a(x) = b(x) = 2\tan x \sec^2 x \in C^\infty\left(-\frac{\pi}{2}, \frac{\pi}{2}\right)$ and $p(x) = \sin^2 x \in C^\infty\left(\left[-\frac{\pi}{2}, \frac{\pi}{2}\right]\right)$ with $|p| < 1$ over $\left(-\frac{\pi}{2}, \frac{\pi}{2}\right)$. Again, (4-1) holds, and thus proceeding as in the previous example, one gets that the solution of ODE (4-6) is given implicitly by

$$\sum_{k=0}^{\infty} e^{-k}\left(\frac{\ln y}{x} + 1\right)^{-k} E_{k+1}\left(\frac{k\ln y}{x} + k\right) - 2\ln(\cos x) = D, \tag{4-7}$$

whenever the inequality $(\ln y)/x > 0$ holds.

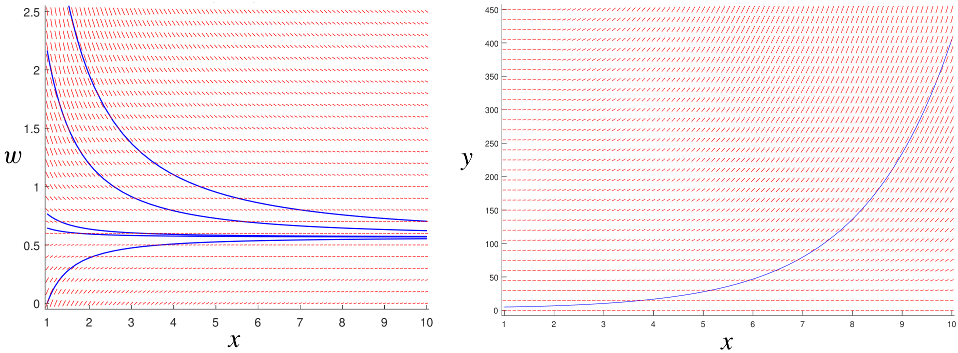

Figure 1. Solutions of $dw/dx = (1/x)(e^{-w} - w)$ with different initial conditions (left) and the solution of $dy/dx = y^{1-1/x}$ with initial condition $y(1) = 5$ (right).

5. Numerical simulations: some examples

In this section, we look at numerical solutions the problems (1-1) and (3-4) (for a, b constant). Several examples are examined for particular choices of the function $p = p(x)$. With MATLAB software we tested numerical convergence to a solution using the Runge–Kutta solution method through the built in function ode45. In each of the examples provided, the plot on the left represents the solution of the substitution problem given by (2-4) (under the specific assumptions for each example) with five initial conditions taken randomly at $x_0 = 1$. The plot on the right shows a solution with initial condition $y(1) = 5$ for the original Bernoulli-type equation (1-1), under the same assumptions as the plot on the left. All solutions are plotted over their respective vector fields.

5A. ***The separable case.*** As shown in Section 3, the separable case of the problem (2-4) (for a, b constants, $b \neq 0$) is given when $p(x) = 1 - 1/(\lambda x)$ (for $\lambda \neq 0$ an arbitrary fixed constant).

Example 5.1. We take the constants $a = 0$ and $b = \lambda = 1$ and $p(x) = 1 - 1/x$. The solutions produced are given in Figure 1. Notice that, as described in Section 3A1 solutions blow up as x tends to infinity.

Observe that Figure 1(left) illustrates that as x tends to infinity, the numerical solution converges, whereas the graph of the solution of the original equation, Figure 1 (right) seems to blow-up as x goes to infinity. These facts agree with the analysis performed over (3-11).

Example 5.2. We consider now the case where the constants satisfy $a = b = \lambda = 1$, and $p(x) = 1 - 1/x$. The simulations produced are given in Figure 2.

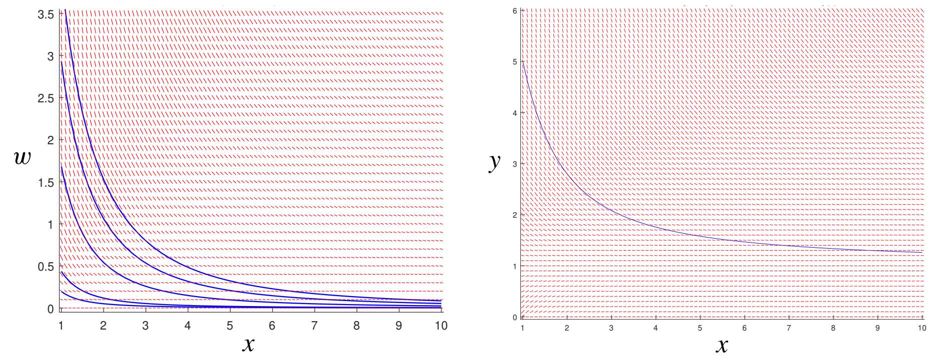

Figure 2. Solutions of $dw/dx = (1/x)(e^{-w} - w - 1)$ with different initial conditions (left) and the solution of $dy/dx = y^{1-1/x} - y$ with initial condition $y(1) = 5$ (right).

Notice, again, we have numerical convergence in Figure 2 (left) and Figure 2 (right) shows convergence to $y = 1$; this agrees with the analysis done over (3-25).

5B. ***Other examples.*** In this section, we examine numerical solutions to the (non-separable) problem (2-4) and the original equation, by exploring other choices for the function $p(x)$, but over the same domain and conditions used in the previous simulations. Unlike the previous cases, we will be unable to provide a more rigorous examination of the solution for these examples, since in these cases both (1-1) and (2-4) become unsolvable with any of the known methods for ODEs. For simplicity, we will assume that $a(x) = 0$ and $b(x) = 1$ in the following examples.

Example 5.3. Let $p(x) = 1 - e^x$. The resulting simulations are given in Figure 3.

Example 5.4. Let $p(x) = 1 - e^{-x}$. The resulting simulations are given in Figure 4.

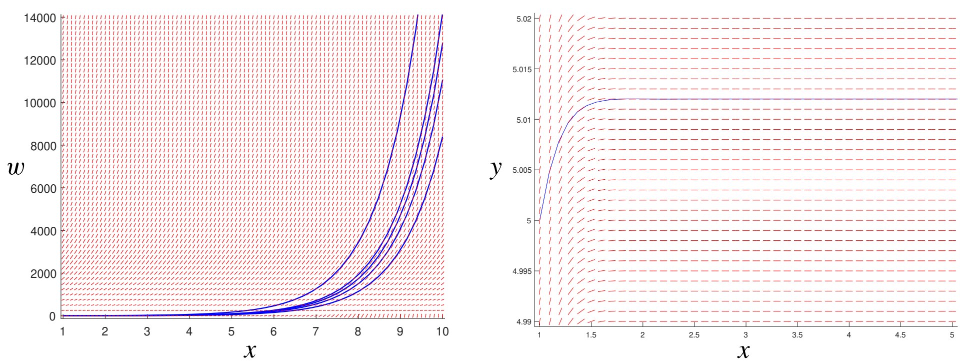

Figure 3. Solutions of $dw/dx = e^{x-w} + w$ with different initial conditions (left) and the solution of $dy/dx = y^{1-e^x}$ with initial condition $y(1) = 5$ (right).

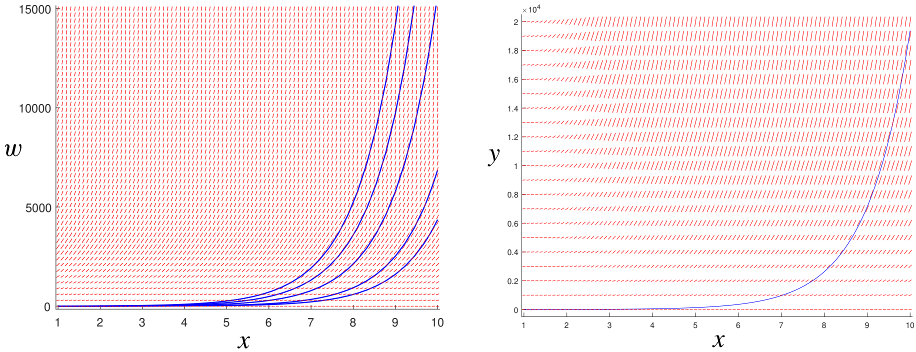

Figure 4. Solutions of $dw/dx = e^{-(x+w)} + w$ with different initial conditions (left) and the solution of $dy/dx = y^{1-e^{-x}}$ with initial condition $y(1) = 5$ (right).

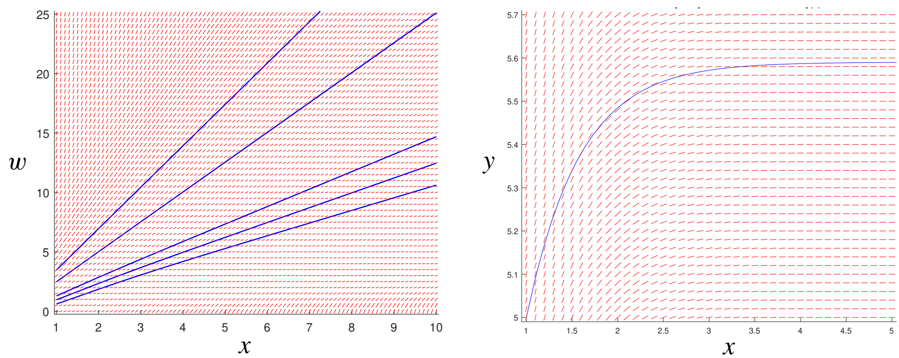

Figure 5. Solutions of $dw/dx = xe^{-w} + w/x$ with different initial conditions (left) and the solution of $dy/dx = y^{1-x}$ with initial condition $y(1) = 5$ (right).

Example 5.5. Let $p(x) = 1 - x$. The resulting simulations are given in Figure 5.

In the examples above of nonseparable ODEs, one can notice that the corresponding solutions to problem (2-4) are unbounded as x becomes large enough. Nevertheless, their corresponding solutions to the original equation (1-1) can be bounded, as Examples 5.3 and 5.5 show. Since for these particular examples, there is no method available to allow a more rigorous and deep analysis on the solutions of problems (1-1) and (2-4), further details concerning these last examples cannot be provided.

References

[Acerbi and Mingione 2002] E. Acerbi and G. Mingione, "Regularity results for stationary electrorheological fluids", *Arch. Ration. Mech. Anal.* **164**:3 (2002), 213–259. MR Zbl

[Bollt et al. 2009] E. M. Bollt, R. Chartrand, S. Esedoḡlu, P. Schultz, and K. R. Vixie, "Graduated adaptive image denoising: local compromise between total variation and isotropic diffusion", *Adv. Comput. Math.* **31**:1-3 (2009), 61–85. MR Zbl

[Boyce and DiPrima 2012] W. E. Boyce and R. C. DiPrima, *Elementary differential equations and boundary value problems*, 10th ed., Wiley, Hoboken, NJ, 2012.

[Chen et al. 2006] Y. Chen, S. Levine, and M. Rao, "Variable exponent, linear growth functionals in image restoration", *SIAM J. Appl. Math.* **66**:4 (2006), 1383–1406. MR Zbl

[Cruz-Uribe and Fiorenza 2013] D. V. Cruz-Uribe and A. Fiorenza, *Variable Lebesgue spaces: foundations and harmonic analysis*, Springer, 2013. MR Zbl

[Diening and Růžička 2003] L. Diening and M. Růžička, "Calderón–Zygmund operators on generalized Lebesgue spaces $L^{p(\cdot)}$ and problems related to fluid dynamics", *J. Reine Angew. Math.* **563** (2003), 197–220. MR Zbl

[Diening et al. 2011] L. Diening, P. Harjulehto, P. Hästö, and M. Růžička, *Lebesgue and Sobolev spaces with variable exponents*, Lecture Notes in Mathematics **2017**, Springer, 2011. MR Zbl

[Edwards and Penney 2008] C. H. Edwards and D. E. Penney, *Elementary differential equations*, 6th ed., Prentice Hall, Upper Saddle River, NJ, 2008.

[Merton 1969] R. C. Merton, "Lifetime portfolio selection under uncertainty: the continuous-time case", *Rev. Econ. Stat.* **51**:3 (1969), 247–252.

[O'Neil 2012] P. V. O'Neil, *Advanced engineering mathematics*, 7th ed., Cengage, Boston, MA, 2012.

[Zill and Cullen 2012] D. G. Zill and M. R. Cullen, *Differential equations with boundary-value problems*, 8th revised ed., Cengage, Boston, MA, 2012.

Received: 2018-06-06 Revised: 2019-06-18 Accepted: 2019-08-31

karen.rios3@upr.edu — *Department of Mathematical Sciences, University of Puerto Rico at Mayagüez, Mayagüez, Puerto Rico*

carlos.seda1@upr.edu — *Department of Mathematical Sciences, University of Puerto Rico at Mayagüez, Mayagüez, Puerto Rico*

alejandro.velez2@upr.edu — *Department of Mathematical Sciences, University of Puerto Rico at Mayagüez, Mayagüez, Puerto Rico*

INVOLVE 12:8 (2019)
dx.doi.org/10.2140/involve.2019.12.1293

The supersingularity of Hurwitz curves

Erin Dawson, Henry Frauenhoff, Michael Lynch, Amethyst Price, Seamus Somerstep, Eric Work, Dean Bisogno and Rachel Pries

(Communicated by Ken Ono)

We study when Hurwitz curves are supersingular. Specifically, we show that the curve $H_{n,\ell} : X^nY^\ell + Y^nZ^\ell + Z^nX^\ell = 0$, with n and ℓ relatively prime, is supersingular over the finite field $\mathbb{F}_p$ if and only if there exists an integer i such that $p^i \equiv -1 \bmod (n^2 - n\ell + \ell^2)$. If this holds, we prove that it is also true that the curve is maximal over $\mathbb{F}_{p^{2i}}$. Further, we provide a complete table of supersingular Hurwitz curves of genus less than 5 for characteristic less than 37.

1. Introduction

In 1941, Deuring defined the basic theory of supersingular elliptic curves. Supersingular curves are useful in error-correcting codes called Goppa codes. They also have potential applications to quantum resistant cryptosystems.

In this paper we determine a condition for supersingularity of Hurwitz curves $H_{n,\ell}$ when n and ℓ are relatively prime. In particular we show that every supersingular Hurwitz curve $H_{n,\ell}$ is maximal over some finite field. We also provide a classification of supersingular Hurwitz curves with genus less than 5 over fields with characteristic less than 37 and find some restrictions on the genera of Hurwitz curves.

2. Background information

We first define the Hurwitz curve and the Fermat curve. Next we define the zeta function of a curve. From the zeta function we compute the normalized Weil numbers which we use to study supersingularity. We must also state the Hasse–Weil bound in order to define maximality and minimality.

2A. ***The Hurwitz curve and the Fermat curve.*** Let n, ℓ, and d be positive integers. Let F be a field.

MSC2010: primary 11G20, 11M38, 14H37, 14H45, 11E81; secondary 11G10, 14H40, 14K15.
Keywords: Hurwitz curve, Hasse–Weil bound, maximal curve, minimal curve, Fermat curve, supersingular curve.

Definition 2.1 (Hurwitz curve $H_{n,\ell}$). The *Hurwitz curve* $H_{n,\ell}$ over F is given by the projective equation

$$H_{n,\ell} : X^n Y^\ell + Y^n Z^\ell + Z^n X^\ell = 0.$$

Throughout this paper, set $m = n^2 - n\ell + \ell^2$. The Hurwitz curve $H_{n,\ell}$ has genus

$$g = \frac{m + 2 - 3\gcd(n, \ell)}{2}$$

and is smooth when the characteristic p of F is relatively prime to m.

Definition 2.2 (Fermat curve $\mathcal{F}_d$). The *Fermat curve* of degree d over F is given by the projective equation

$$\mathcal{F}_d : U^d + V^d + W^d = 0.$$

The Fermat curve $\mathcal{F}_d$ has genus $\frac{1}{2}(d-1)(d-2)$ and is smooth when the characteristic p of F does not divide d. Note that the Hurwitz curve $H_{n,\ell}$ is covered by the Fermat curve of degree $m = n^2 - n\ell + \ell^2$; see Section 3B for more details.

2B. ***Zeta function.*** Let $\mathbb{F}_q$ be a finite field of cardinality q, where q is a power of a prime p. For a curve C defined over $\mathbb{F}_q$, denote the number of points on C by $\#C(\mathbb{F}_q)$. For extensions of $\mathbb{F}_q$, define $N_s = \#C(\mathbb{F}_{q^s})$.

Definition 2.3 (zeta function). The *zeta function* of a curve $C/\mathbb{F}_q$ is the series

$$Z(C/\mathbb{F}_q, T) = \exp\left(\sum_{s=1}^{\infty} \frac{N_s T^s}{s}\right). \tag{1}$$

Rationality of the zeta function for curves was proven by Weil [1948a; 1949]. In particular, Weil showed that the zeta function can be written as

$$Z(C/\mathbb{F}_q, T) = \frac{L(C/\mathbb{F}_q, T)}{(1-T)(1-qT)}. \tag{2}$$

The L-polynomial, $L(C/\mathbb{F}_q, T) \in \mathbb{Z}[T]$, has degree $2g$ [Ireland and Rosen 1990, p. 152]:

$$L(C/\mathbb{F}_q, T) = 1 + C_1 T + \cdots + C_{2g} T^{2g}. \tag{3}$$

The L-polynomial of a curve C over $\mathbb{F}_q$ with genus g factors in $\mathbb{C}[T]$ as

$$L(C/\mathbb{F}_q, T) = \prod_{i=1}^{2g} (1 - \alpha_i T).$$

Furthermore, $|\alpha_i| = \sqrt{q}$ for each $1 \le i \le 2g$ [Ireland and Rosen 1990, p. 155]. The normalized Weil numbers (NWNs) are the normalized reciprocal roots of the L-polynomial.

Definition 2.4 (normalized Weil numbers). The *Weil numbers* of $C/\mathbb{F}_q$ are the reciprocal roots α_i of $L(C/\mathbb{F}_q, T)$ for $1 \leq i \leq 2g$. The *normalized Weil numbers* are the values $\alpha_i/\sqrt{q}$ for $1 \leq i \leq 2g$.

Remark 2.5. If $\{\alpha_1, \ldots, \alpha_{2g}\}$ are the normalized Weil numbers over $\mathbb{F}_q$, then $\{\alpha_1^i, \ldots, \alpha_{2g}^i\}$ are the normalized Weil numbers over $\mathbb{F}_{q^i}$.

The coefficients of $L(C/\mathbb{F}_q, T)$ follow a pattern. For $k \in \mathbb{N}$, we denote the set of partitions of k by $\operatorname{par}(k)$ and the length of a partition γ by $\operatorname{len}(\gamma)$.

Lemma 2.6. *In (3) for $0 \leq k \leq 2g$, the coefficient C_k has the form*

$$C_k = \sum_{\gamma \in \operatorname{par}(k)} \frac{\prod_{j \in \gamma} N_j/j}{\operatorname{len}(\gamma)!} - \sum_{i=0}^{k-1} \Big(C_i \sum_{\mu=0}^{k-i} q^{\mu} \Big).$$

Proof. Equation (1) can be expanded using the Taylor series of the exponential function

$$Z(C/\mathbb{F}_q, T) = \sum_{i=0}^{\infty} \frac{(N_1 T + (N_2/2)T^2 + \cdots + (N_{2g}/(2g))T^{2g})^i}{i!}.$$

Collecting terms up through T^3 gives a pattern to follow:

$$Z(C/\mathbb{F}_q, T) = 1 + (N_1)T + \left(\frac{N_2}{2} + \frac{N_1^2}{2}\right)T^2 + \left(\frac{N_3}{3} + \frac{N_1 N_2}{2} + \frac{N_1^3}{6}\right)T^3 + \cdots. \quad (4)$$

The key step is to recognize that the subscripts on the N_j are the partitions of k. The coefficient on T^k can be written as

$$\sum_{\gamma \in \operatorname{par}(k)} \frac{\prod_{j \in \gamma} N_j/j}{\operatorname{len}(\gamma)!}.$$

Equation (2) gives a simplified version of $Z(C/\mathbb{F}_q, T)$. Using the Taylor series for each of the denominator terms as well as (3) yields the expansion

$$Z(C/\mathbb{F}_q, T) = (1 + C_1 T + \cdots + C_{2g} T^{2g})(1 + T + T^2 + \cdots)(1 + qT + q^2T^2 + \cdots). \quad (5)$$

Expanding and collecting terms, the coefficients on T^k are given by

$$\sum_{i=0}^{k-1} \Big(C_i \sum_{j=0}^{k-i} q^j \Big) + C_k.$$

Setting (4) and (5) equal and comparing coefficients gives a linear system allowing one to solve for C_k in terms of the values of N_s. □

2C. ***The Newton polygon and supersingularity.*** Fix a curve $C/\mathbb{F}_q$ with associated L-polynomial $L(C/\mathbb{F}_q, T)$.

Definition 2.7 (supersingularity). The curve C is *supersingular* if all its normalized Weil numbers are roots of unity.

Another way to check if C is supersingular is with its Newton polygon.

Definition 2.8 (normalized valuation on $\mathbb{F}_{p^r}$). Let $n = p^l k$ be an integer with $p \nmid k$. We denote the normalized $\mathbb{F}_{p^r}$-valuation of n by $\mathrm{val}_{p^r}(n) = l/r$ and the prime-to-p part of n by $n_p = k$. If $n = 0$, we say $\mathrm{val}_{p^r}(0) = \infty$.

Definition 2.9 (Newton polygon). Fix a curve $C/\mathbb{F}_{p^r}$ with L-polynomial in the form of (3). The *Newton polygon* of $C/\mathbb{F}_{p^r}$ is the lower convex hull of the points $\{(i, \mathrm{val}_{p^r}(C_i)) \mid 0 \le i \le 2g\}$.

Remark 2.10. Because $C_0 = 1$ for every curve $C/\mathbb{F}_{p^r}$, the Newton polygon will always have initial point $(0, 0)$. Likewise the final coefficient of $L(C/\mathbb{F}_{p^r}, T)$ is always $C_{2g} = p^{rg}$. For this reason the Newton polygon always has terminal point $(2g, g)$.

From Remark 2.10, we can see that the Newton polygon of a curve C over $\mathbb{F}_{p^r}$ is always a union of line segments on or below the line $y = \frac{1}{2}x$ with increasing slopes.

Remark 2.11. A curve $C/\mathbb{F}_q$ is supersingular if and only if its Newton polygon is a line segment with slope $\frac{1}{2}$.

2D. ***Minimality and maximality.*** As a consequence of the Weil conjectures, the number of points on a curve $C/\mathbb{F}_q$ is controlled by the Hasse–Weil bound:

$$1 + q - 2g\sqrt{q} \le \#C(\mathbb{F}_q) \le 1 + q + 2g\sqrt{q}.$$

The Hasse–Weil bound for curves was proven by Weil [1948a].

Definition 2.12 (minimal). A curve $C/\mathbb{F}_q$ is *minimal* if

$$\#C(\mathbb{F}_q) = 1 + q - 2g\sqrt{q}.$$

Definition 2.13 (maximal). A curve $C/\mathbb{F}_q$ is *maximal* if

$$\#C(\mathbb{F}_q) = 1 + q + 2g\sqrt{q}.$$

Remark 2.14 [Weil 1948a, p. 22; 1948b, p. 69]. The curve C is maximal over $\mathbb{F}_q$ if and only if all its normalized Weil numbers are -1 over $\mathbb{F}_q$, and it is minimal over $\mathbb{F}_q$ if and only if all its normalized Weil numbers are 1 over $\mathbb{F}_q$.

In the following remark, we use the notation that ζ_k is the primitive k-th root of unity $e^{2\pi i/k}$. Notice that there is a power s such that $\zeta_k^s = -1$ if and only if k is even.

Lemma 2.15. *Let C be a supersingular curve over $\mathbb{F}_q$. Suppose the normalized Weil numbers of $C/\mathbb{F}_q$ are of the form $\zeta_{k_1}^{t_1}, \dots, \zeta_{k_{2g}}^{t_{2g}}$. Assume* $\gcd(k_i, t_i) = 1$. *The curve C is maximal over $\mathbb{F}_{q^r}$ if and only if*

- *there exists $s \geq 1$ and b_i odd such that $k_i = 2^s(b_i)$,*
- *and r is an odd multiple of $2^{s-1}\operatorname{lcm}(b_1, \dots, b_n)$.*

Proof. Assume C is maximal over $\mathbb{F}_{q^r}$. By Remark 2.14, the curve C is maximal over $\mathbb{F}_{q^r}$ if and only if $\zeta_{k_i}^{rt_i} = -1$ for all i. Consequently, k_i is even for all i. Thus $k_i = 2^{s_i} b_i$ for some positive integer s_i and odd integer b_i. The condition $\zeta_{k_i}^{rt_i} = -1$ for all i implies that there exists an s such that $s = s_i$ for all i and r is an odd multiple of $2^{s-1}\operatorname{lcm}(b_1, \dots, b_n)$.

For the converse, the conditions imply that the normalized Weil numbers of C over $\mathbb{F}_{q^r}$ are all -1. □

3. Curve maps and covers

3A. ***Aoki's curve.*** Let $\alpha = (a, b, c) \in \mathbb{N}^3$ with $a + b + c = m$. Note that S_3, the symmetric group on three letters, acts on α by permuting the coordinates. For $\sigma \in S_3$ we denote the action by α^σ. We say two triples $\alpha = (a_1, a_2, a_3)$ and $\beta = (b_1, b_2, b_3)$ are equivalent, denoted by $\alpha \approx \beta$, if there exist elements $t \in (\mathbb{Z}/m)^*$ and $\sigma \in S_3$ such that

$$(a_1, a_2, a_3) \equiv (tb_{\sigma(1)}, tb_{\sigma(2)}, tb_{\sigma(3)}) \bmod m.$$

Aoki [2008a; 2008b] studied curves of the form

$$D_\alpha : v^m = (-1)^c u^a (1-u)^b.$$

He provides the following conditions for when D_α is supersingular.

Theorem 3.1 [Aoki 2008b, Theorem 1.1]. *The curve D_α is supersingular over $\mathbb{F}_{p^r}$ if and only if at least one of the following conditions holds*:

- $p^i \equiv -1 \bmod m$ *for some i.*
- $\alpha = (a, b, c) \approx (1, -p^i, p^i - 1)$ *for some integer i such that* $d = \gcd(p^i - 1, m) > 1$ *and* $p^j \equiv -1 \bmod (m/d)$ *for some integer j.*

3B. ***Covers of $H_{n,\ell}$ by $\mathcal{F}_m$.*** In Section 2A, we noted that the Hurwitz curve $H_{n,\ell}$ is covered by the Fermat curve $\mathcal{F}_m$, where $m = n^2 - n\ell + \ell^2$. On an affine patch the Fermat and Hurwitz curves are given by the equations

$$\mathcal{F}_m : u^m + v^m + 1 = 0,$$
$$H_{n,l} : x^n y^\ell + y^n + x^\ell = 0.$$

Then the following covering map is provided by [Aguglia et al. 2001, Lemma 4.1]:

$$\phi : \mathcal{F}_m \to H_{n,\ell}, \quad (u, v) \mapsto (u^n v^{-l}, u^l v^{n-l}).$$

Furthermore, it is known that $\mathcal{F}_m$ is supersingular over $\mathbb{F}_p$ if and only if $p^i \equiv -1 \bmod m$ for some integer i [Shioda and Katsura 1979, Proposition 3.10]. See also [Yui 1980, Theorem 3.5]. In [Tafazolian 2010, Theorem 5] it is shown that $\mathcal{F}_m$ is maximal over $\mathbb{F}_{p^{2i}}$ if and only if $p^i \equiv -1 \bmod m$.

Remark 3.2. If $X \to Y$ is a covering of curves defined over $\mathbb{F}_{p^r}$, then the normalized Weil numbers of $Y/\mathbb{F}_{p^r}$ are a subset of the normalized Weil numbers of $X/\mathbb{F}_{p^r}$; see [Serre 1985].

Thus when a covering curve is supersingular (or maximal or minimal) the curve it covers is as well.

3C. ***A birational transformations.*** Bennama and Carbonne [1997] show that $H_{n,\ell}$ is isomorphic to a curve with affine equation

$$y'^m = x'^\lambda (x' - 1) \tag{6}$$

via the following variable change. Suppose $1 \leq \ell < n$ and $\gcd(n, \ell) = 1$. Then there exist integers θ and δ such that $1 \leq \theta \leq \ell$, $1 \leq \delta \leq n-1$, and $n\theta - \delta\ell = 1$. Let $\lambda = \delta n - \theta(n - \ell)$ and $m = n^2 - n\ell + \ell^2$. The birational transformation is

$$\begin{cases} x = (-x')^{-\delta}((-1)^\lambda y')^n, \\ y = (-x')^{-\theta}((-1)^\lambda y')^\ell \end{cases} \quad \text{and} \quad \begin{cases} x' = -x^\ell y^{-n}, \\ y' = (-1)^\lambda x^\theta y^{-\delta}. \end{cases}$$

Equation (6) is very similar to the equation for D_α that Aoki studied but there are small differences. The following argument shows that these can be reconciled. Consequently, this variable change can be used to apply Aoki's results to Hurwitz curves.

Notice that (6) is divisible by $(x' - 1)$ while Aoki studied curves whose equation contains a $(1 - x')$ factor. Aoki requires that $a + b + c = m$ so the exponent on the negative sign is important. Inspecting (6) we see that m will always be odd since $(n, \ell) = 1$. Consequently, this negative sign is not an issue. Since m is always odd we can replace v with $-v$. This choice allows us to pick $c = m - a - b$. Then $b = 1$ and $a = \lambda$.

4. Supersingular Hurwitz curves

We arrive at explicit conditions on supersingularity for $H_{n,\ell}$ when n and ℓ are relatively prime. We use results from [Bennama and Carbonne 1997; Aoki 2008a] to accomplish this. We will be using affine equations for the Hurwitz curve in this section.

Lemma 4.1. *If n and ℓ are relatively prime then $x^n y^\ell + y^n + x^\ell = 0$ is supersingular over $\mathbb{F}_p$ if and only if at least one of the following conditions holds*:

(1) *There exists $i \in \mathbb{Z}_{>0}$ such that $p^i \equiv -1 \bmod m$. (In this case the Fermat curve covering the Hurwitz curve is maximal over $\mathbb{F}_{p^{2i}}$.)*

(2) *There exists $i \in \mathbb{Z}_{>0}$ with $d = (p^i - 1, m) > 1$ such that*

$$(\delta(n-\ell) + \ell\theta - 1, 1, -(\delta(n-\ell) + \ell\theta)) \approx (1, -p^i, p^i - 1)$$

and $p^j \equiv -1 \bmod (m/d)$ for some integer j.

Proof. We use the variable substitution from [Bennama and Carbonne 1997] to apply Aoki's results to Hurwitz curves. We use the substitutions

$$m = n^2 - n\ell + \ell^2, \quad a = \lambda = \delta(n-\ell) + \ell\theta - 1, \quad b = 1, \quad c = m - (\delta(n-\ell) + \ell\theta). \tag{7}$$

Combining these with Aoki's results completes the proof. □

Remark 4.2. If n and ℓ are relatively prime, then n and ℓ are relatively prime to $n^2 - n\ell + \ell^2$.

Theorem 4.3. *Suppose n and ℓ are relatively prime and $m = n^2 - n\ell + \ell^2$. Then $H_{n,\ell}$ is supersingular over $\mathbb{F}_p$ if and only if $p^i \equiv -1 \bmod m$ for some positive integer i.*

Proof. If $p^i \equiv -1 \bmod m$ for some positive integer i, then $\mathcal{F}_m$ is supersingular over $\mathbb{F}_p$ by [Shioda and Katsura 1979, Proposition 3.10]. Recall from Section 3B that $\mathcal{F}_m$ covers $H_{n,\ell}$. Thus $H_{n,\ell}$ is supersingular over $\mathbb{F}_p$ by Remark 3.2.

Suppose $H_{n,\ell}$ is supersingular over $\mathbb{F}_p$. By Lemma 4.1 it is enough to show condition (2) in Lemma 4.1 cannot happen. We begin by simplifying it using the substitution $\theta = (1 + \ell\delta)/n$ and reducing modulo m to show that condition (2) is equivalent to $(\ell/n - 1, 1, -\ell/n) \approx (1, -p^i, p^i - 1)$ for some i such that $d = (p^i - 1, m) > 1$ and $p^j \equiv -1 \bmod (m/d)$ for some integer j. Recall that $\alpha \approx \alpha'$ if $\alpha = t\alpha'^{\sigma}$ for some $t \in (\mathbb{Z}/m)^*$ and $\sigma \in S_3$. We will show that $p^i - 1$ and m are relatively prime. We label the three coordinates of $(\ell/n - 1, 1, -\ell/n)$ as (a, b, c) and the three coordinates of $(1, -p^i, p^i - 1)$ as (A, B, C).

The proof will address six cases accounting for the orbit of (A, B, C) under the action of S_3. In each case we will show that $\gcd(p^i - 1, m) = 1$. Specifically, we show $d = 1$ by taking these congruences modulo d. By Remark 4.2 we know that n^{-1} exists modulo m and modulo d. Finally, note that ℓ/n is relatively prime to d.

- $(a, b, c) \equiv t(A, B, C) \bmod m$: Comparing c and tC yields

$$-\frac{\ell}{n} \equiv t(p^i - 1) \bmod m.$$

Consequently, $\ell/n \equiv 0 \bmod d$. Therefore, $d = 1$.

- $(a,b,c) \equiv t(B,A,C) \bmod m$: Comparing a with tB and b with tA yields

$$\frac{\ell}{n} - 1 \equiv -tp^i \bmod m, \quad 1 \equiv t \bmod m.$$

Substituting we have $\ell/n \equiv p^i - 1 \bmod m$. Reducing modulo d produces $\ell/n \equiv 0 \bmod d$, thus $d = 1$.

- $(a,b,c) \equiv t(A,C,B) \bmod m$: Comparing b and tC yields

$$-\frac{\ell}{n} \equiv t(p^i - 1) \bmod m.$$

This is identical to the first case.

- $(a,b,c) \equiv t(C,B,A) \bmod m$: Comparing a and tC yields

$$\frac{\ell}{n} - 1 \equiv t(p^i - 1) \bmod m.$$

Thus $\ell/n - 1 \equiv 0 \bmod d$. Recall by the definition of m and selection of d, we have $d \mid (n^2 - n\ell + \ell^2)$. Hence, d divides $1 - \ell/n + (\ell/n)^2$. We conclude $d \mid (\ell/n)$; thus $d = 1$.

- $(a,b,c) \equiv t(C,A,B) \bmod m$: Comparing b with tA and c with tB yields

$$1 \equiv t \bmod m, \quad \frac{\ell}{n} \equiv tp^i \bmod m.$$

This case is completed as in the previous case.

- $(a,b,c) \equiv t(B,C,A) \bmod m$: Comparing b with tC yields

$$1 \equiv t(p^i - 1) \bmod m.$$

Modulo d this reduces to $1 \equiv 0 \bmod d$. Therefore, $d = 1$. □

Remark 4.4. There is a family of Hurwitz-type curves with affine equations $\mathcal{C}_{a_1,a_2,n_1,n_2} : x^{n_1} y^{a_1} + y^{n_2} + x^{a_2} = 0$. Set $\delta = a_1 a_2 - a_2 n_2 + n_1 n_2$. When $q = p^r$ is coprime to δ, the curve C_{a_1,a_2,n_1,n_2} is $\mathbb{F}_q$-covered by the Fermat curve $\mathcal{F}_\delta$ of degree δ. Tafazolian and Torres [2017, Theorem 2.9] showed that under certain numerical conditions the statements

- the Fermat curve $\mathcal{F}_\delta$ is maximal over $\mathbb{F}_{q^2}$,
- the Hurwitz-type curve $\mathcal{C}_{1,a_2,n_1,n_2}$ is maximal over $\mathbb{F}_{q^2}$,
- and $q + 1 \equiv 0 \mod \delta$

are all equivalent.

The Hurwitz-type curve $\mathcal{C}_{\ell,\ell,n,n}$ is the Hurwitz curve $H_{n,\ell}$. Thus in the case that $\ell = a_1 = a_2$ and $n = n_1 = n_2$, Theorem 4.3 generalizes [Tafazolian and Torres 2017, Theorem 2.9].

Remark 4.5. Consider the family of curves with affine equations

$$N_{a_1,a_2,n_1,n_2} : x^{n_1} y^{a_1} + k_1 y^{n_2} + k_2 x^{a_2} = 0$$

over $\mathbb{F}_{p^r}$ with $k_1, k_2 \in (\mathbb{F}_q)^*$, $n_1 \geq a_1$, $n_1 + a_1 > a_2$, $n_1 + a_1 > n_2$, if $n_1 = a_1$ then $n_2 \geq a_2$, and $p \nmid \gcd(a_1, a_2, n_1, n_2)$. Set $d = \gcd(a_1, a_2, n_1, n_2)$ and δ as in Remark 4.4. Recall the definition of n_p in Definition 2.8. With these assumptions [Nie 2016, Theorem 4.12] shows that if $(\delta/d)_p$ divides $q+1$ then N_{a_1,a_2,n_1,n_2} is maximal over $\mathbb{F}_q$ and if N_{a_1,a_2,n_1,n_2} is maximal over $\mathbb{F}_{q^2}$ then $(\delta/d)_p$ divides q^2+1.

Note $N_{\ell,\ell,n,n} = H_{n,\ell}$. Thus Theorem 4.3 generalizes [Nie 2016, Theorem 4.12] when $a_1 = a_2 = \ell$ and $n_1 = n_2 = n$.

Corollary 4.6. *If n and ℓ are relatively prime and $H_{n,\ell}$ is supersingular over $\mathbb{F}_p$, then it will be maximal over $\mathbb{F}_{p^{2i}}$, where i is the same as in Theorem 4.3.*

Proof. By Theorem 4.3, if $H_{n,\ell}$ is supersingular over $\mathbb{F}_p$, then $p^i \equiv -1 \bmod m$ for some i. By [Tafazolian 2010], this implies $\mathcal{F}_m$ will be maximal over $\mathbb{F}_{p^{2i}}$. Since $\mathcal{F}_m$ covers $H_{n,\ell}$, this implies $H_{n,\ell}$ will also be maximal over $\mathbb{F}_{p^{2i}}$. □

A priori, if $H_{n,\ell}$ is supersingular (or maximal or minimal) over $\mathbb{F}_p$ then $\mathcal{F}_m$ may not be because it has more normalized Weil numbers.

Corollary 4.7. *If n and ℓ are relatively prime and $H_{n,\ell}$ is supersingular over $\mathbb{F}_p$, then $\mathcal{F}_m$ is supersingular over $\mathbb{F}_p$.*

Proof. If $H_{n,\ell}$ supersingular over $\mathbb{F}_p$ and $\gcd(n,\ell) = 1$, Theorem 4.3 shows the existence of positive integer i such that $p^i \equiv -1 \bmod m$. Then by [Shioda and Katsura 1979, Proposition 3.10], $\mathcal{F}_m$ is supersingular over $\mathbb{F}_p$. □

Partial results are known for when a Hurwitz curve is maximal.

Theorem 4.8 [Aguglia et al. 2001, Theorem 3.1]. *Let $\ell = 1$. The curve $H_{n,1}$ is maximal over $\mathbb{F}_{q^{2j}}$ if and only if $p^j \equiv -1 \bmod m$ for some positive integer j.*

Theorem 4.9 [Aguglia et al. 2001, Theorem 4.5]. *Assume that $\gcd(n,\ell) = 1$ and m is prime. Then $H_{n,\ell}$ is maximal over $\mathbb{F}_{p^{2j}}$ if and only if $p^j \equiv -1 \bmod m$ for some positive integer j.*

Note that the key property used in [Aguglia et al. 2001] is the existence of some positive integer j such that

$$p^j \equiv -1 \bmod m. \tag{8}$$

Remark 4.10. Under the requirements $\ell = 1$, or $\gcd(n,\ell) = 1$ and m prime, the results in [Aguglia et al. 2001] and [Tafazolian 2010, Theorem 5] show that $\mathcal{F}_m$ is maximal over $\mathbb{F}_{q^2}$ if and only if $H_{n,\ell}$ is maximal over $\mathbb{F}_{q^2}$.

We consider the case when $H_{n,\ell}$ and $\mathcal{F}_m$ are minimal.

Corollary 4.11. *If $\ell = 1$, or n and ℓ are relatively prime and m is prime, $H_{n,\ell}$ is minimal over $\mathbb{F}_{p^{4i}}$ if and only if $\mathcal{F}_m$ is minimal over $\mathbb{F}_{p^{4i}}$.*

Proof. First suppose $\mathcal{F}_m$ is minimal over $\mathbb{F}_{p^{4i}}$ with set N of normalized Weil numbers. Then the normalized Weil numbers of $H_{n,\ell}$ are a subset of N. Thus $H_{n,\ell}$ will also be minimal over $\mathbb{F}_{p^{4i}}$.

Now assume $H_{n,\ell}$ is minimal over $\mathbb{F}_{p^{4i}}$. Minimality implies supersingularity, thus $H_{n,\ell}$ must also be supersingular. By Theorem 4.3 supersingularity of $H_{n,\ell}$ over $\mathbb{F}_p$ implies $p^j \equiv -1 \bmod m$ for some positive integer j. Choose a minimal such j. Then Corollary 4.6 shows $H_{n,\ell}$ is maximal over $\mathbb{F}_{p^{2j}}$ and thus minimal over $\mathbb{F}_{p^{4j}}$. Minimality of j implies that $\mathbb{F}_{p^{4j}}$ is a subfield of $\mathbb{F}_{p^{4i}}$. Consequently, $j \mid i$.

Now, by [Aguglia et al. 2001] $p^j \equiv -1 \bmod m$ implies that $\mathcal{F}_m$ is maximal over $\mathbb{F}_{p^{2j}}$. Hence, $\mathcal{F}_m$ is minimal over $\mathbb{F}_{p^{4j}}$. Because $j \mid i$, we have $\mathcal{F}_m$ is minimal over $\mathcal{F}_{p^{4i}}$. □

Remark 4.12. The curve $H_{3,3}$ is maximal over $\mathbb{F}_{5^2}$ but $\mathcal{F}_9$ is not. The theorems above show a supersingular Hurwitz curve and its covering Fermat curve will both be maximal over $\mathbb{F}_{p^{2i}}$. This does not imply that the Fermat curve will always be maximal over the same field extension that the Hurwitz curve is. The Hurwitz curve could also be maximal over $\mathbb{F}_{p^{2j}}$, where $j \mid i$ with i/j odd. In this case the Fermat curve may not be maximal over this field because it has a higher genus. Unfortunately our example of this does not have n and ℓ being relatively prime. It is difficult to find an example with n and ℓ relatively prime, as the genera of Hurwitz curves grow quickly causing the point counts to become computationally expensive.

Figure 1 illustrates how the current theory fits together. The straight, dotted arrows are under the conditions $\ell = 1$, or $\gcd(n, \ell) = 1$ and m prime. The notation

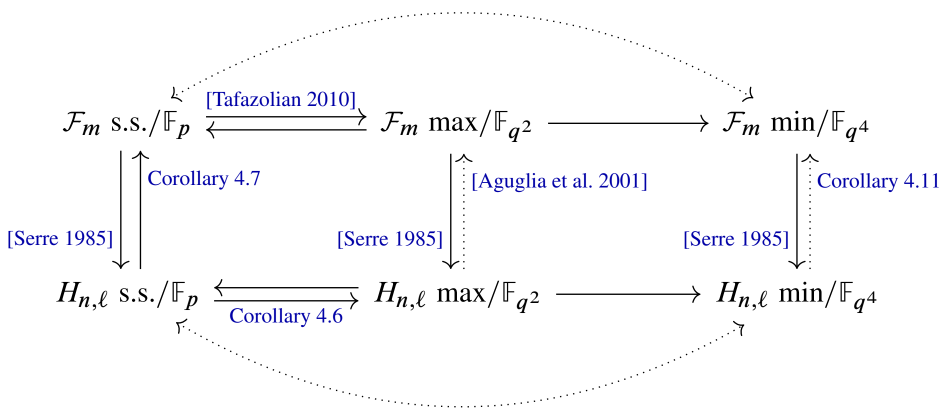

Figure 1. Current results regarding supersingularity, minimality, and maximality of Hurwitz and Fermat curves.

max/$\mathbb{F}_{q^2}$ means, for some power q of p, the curve is maximal over $\mathbb{F}_{q^2}$. If a curve is maximal over $\mathbb{F}_{q^2}$ then it is minimal over $\mathbb{F}_{q^4}$. The curved arrows show that under appropriate conditions a Hurwitz or Fermat curve is supersingular if and only if it is minimal over some field extension. Corollaries 4.6 and 4.7 are under the condition that $\gcd(n,\ell)=1$, while [Aguglia et al. 2001] and Corollary 4.11 are under the condition that $\ell=1$, or $\gcd(n,\ell)=1$ and m is prime.

5. Genera of Hurwitz curves and additional data

Here we provide information about which genera occur for Hurwitz curves and provide a classification of supersingular Hurwitz curves having genus less than 5, defined over $\mathbb{F}_p$ when $p<37$.

Recall that the genus of the Hurwitz curve $H_{n,\ell}$ is

$$g=\frac{n^2-n\ell+\ell^2-3\gcd(n,\ell)+2}{2}.$$

From this, it can be seen that the genus is determined by the quadratic form $q(x,y)=x^2-xy+y^2$ and $\gcd(x,y)$. In this section, we provide information about which genera can appear as a result of these equations.

Theorem 5.1 [Fermat 1999, Volume II, pp. 310–314]. *The equation $m=x^2-xy+y^2$ has solutions $x,y\in\mathbb{Z}$ if and only if for every prime p in the prime decomposition of m, either $p\equiv 0,1 \bmod 3$ or p is raised to an even power.*

There is no restriction in Theorem 5.1 on what the values x and y are. However, for Hurwitz curves we require n and ℓ to be positive. The question remains as to when the equation $m=q(x,y)$ has solutions in the positive integers. To solve this we study the following automorphisms of $q(x,y)=m$:

$$\begin{aligned} f&:\mathbb{Z}^2\to\mathbb{Z}^2, & f(x,y)&\mapsto(y,x),\\ g&:\mathbb{Z}^2\to\mathbb{Z}^2, & g(x,y)&\mapsto(-x,-y),\\ \varphi&:\mathbb{Z}^2\to\mathbb{Z}^2, & \varphi(x,y)&\mapsto(x,x-y),\\ I&:\mathbb{Z}^2\to\mathbb{Z}^2, & I(x,y)&\mapsto(x,y).\end{aligned}$$

To see that $\varphi(x,y)$ is an automorphism, we compute

$$\begin{aligned} q\circ\varphi(x,y)&=x^2-x(x-y)+(x-y)^2\\ &=x^2-x^2+xy+x^2-2xy+y^2\\ &=x^2-xy+y^2\\ &=q(x,y).\end{aligned}$$

Corollary 5.2. *If the equation $m=q(x,y)$ has a solution $(x,y)\in\mathbb{Z}^2$ then there is a solution with $(x',y')\in\mathbb{N}^2$.*

n	l	p	g	L-polynomial	NWNs (multiplicity)
2	1	5	1	$5T^2+1$	i, -i
2	1	11	1	$11T^2+1$	i, -i
2	1	17	1	$17T^2+1$	i, -i
2	1	23	1	$23T^2+1$	i, -i
2	1	29	1	$29T^2+1$	i, -i
3	3	5	1	$5T^2+1$	i, -i
3	3	11	1	$11T^2+1$	i, -i
3	3	17	1	$17T^2+1$	i, -i
3	3	23	1	$23T^2+1$	i, -i
3	3	29	1	$29T^2+1$	i, -i
3	1	3	3	$27T^6+1$	i,-i, $\zeta_{12}, \zeta_{12}^5, \zeta_{12}^7, \zeta_{12}^{11}$
3	1	5	3	$125T^6+1$	i,-i, $\zeta_{12}, \zeta_{12}^5, \zeta_{12}^7, \zeta_{12}^{11}$
3	1	13	3	$2197T^6+507T^4+39T^2+1$	i(3), -i(3)
3	1	17	3	$4913T^6+1$	i, -i, $\zeta_{12}, \zeta_{12}^5, \zeta_{12}^7, \zeta_{12}^{11}$
3	1	19	3	$6859T^6+1$	i, -i, $\zeta_{12}, \zeta_{12}^5, \zeta_{12}^7, \zeta_{12}^{11}$
3	1	31	3	$29791T^6+1$	i, -i, $\zeta_{12}, \zeta_{12}^5, \zeta_{12}^7, \zeta_{12}^{11}$
3	2	3	3	$27T^6+1$	i,-i, $\zeta_{12}, \zeta_{12}^5, \zeta_{12}^7, \zeta_{12}^{11}$
3	2	5	3	$125T^6+1$	i,-i, $\zeta_{12}, \zeta_{12}^5, \zeta_{12}^7, \zeta_{12}^{11}$
3	2	13	3	$2197T^6+507T^4+39T^2+1$	i(3), -i(3)
3	2	17	3	$4913T^6+1$	i, -i, $\zeta_{12}, \zeta_{12}^5, \zeta_{12}^7, \zeta_{12}^{11}$
3	2	19	3	$6859T^6+1$	i, -i, $\zeta_{12}, \zeta_{12}^5, \zeta_{12}^7, \zeta_{12}^{11}$
3	2	31	3	$29791T^6+1$	i, -i, $\zeta_{12}, \zeta_{12}^5, \zeta_{12}^7, \zeta_{12}^{11}$
4	2	5	4	$625T^8+500T^6+150T^4+20T^2+1$	i(4), -i(4)
4	2	17	4	$83521T^8+19652T^6+1734T^4+68T^2+1$	i(4), -i(4)
4	2	29	4	$707281T^8+97556T^6+5046T^4+116T^2+1$	i(4), -i(4)
4	1	5	6	$15625T^{12}+1875T^8+75T^4+1$	$\zeta_8(3), \zeta_8^3(3), \zeta_8^5(3), \zeta_8^7(3)$
4	3	5	6	$15625T^{12}+1875T^8+75T^4+1$	$\zeta_8(3), \zeta_8^3(3), \zeta_8^5(3), \zeta_8^7(3)$
5	5	3	6	$729T^{12}+243T^8+27T^4+1$	$\zeta_8(3), \zeta_8^3(3), \zeta_8^5(3), \zeta_8^7(3)$
5	5	7	6	$117649T^{12}+7203T^8+147T^4+1$	$\zeta_8(3), \zeta_8^3(3), \zeta_8^5(3), \zeta_8^7(3)$
5	5	13	6	$4826809T^{12}+85683T^8+507T^4+1$	$\zeta_8(3), \zeta_8^3(3), \zeta_8^5(3), \zeta_8^7(3)$

Table 1. Supersingular Hurwitz curves in characteristic $p < 37$ with genus < 5.

Proof. We separate into cases, depending on the values of x and y:

(1) If both x and y are negative, then $g(x, y) = (-x, -y) \in \mathbb{N}^2$.

(2) If y is negative and x is positive, then $\varphi(x, y) = (x, x - y) \in \mathbb{N}^2$.

(3) If x is negative and y is positive, then $\varphi(f(x, y)) = (y, y - x) \in \mathbb{N}^2$.

(4) If x is 0, then $\varphi \circ f(0, y) = (y, y)$ and if y is 0, then $\varphi(y, 0) = (y, y)$. □

By counting points and using Lemma 2.6 we computed, using CoCalc, the L-polynomials and normalized Weil numbers of many supersingular Hurwitz curves over $\mathbb{F}_p$. When n and ℓ are not relatively prime, it is possible that certain points of the equation for $H_{n,\ell}$ are singular. Resolving these singularities requires taking a field extension of $\mathbb{F}_p$. To adjust for this we check if $q \equiv 1 \bmod \gcd(n, \ell)$ and count the multiplicities of singular points. This gives the correct point counts to compute the L-polynomial of the normalization of the equation. Table 1 has all supersingular Hurwitz curves $H_{n,\ell}$ of genus less than 5 for primes less than 37. Table 1 also includes some curves of genus 6.

Acknowledgements

We would like to thank Dr. Rachel Pries for proposing this question and guiding us through our research process. We would also like to thank Dr. Özlem Ejder for all of her help and the referee for helpful comments. Finally, we would like to thank the College of Natural Sciences, the CSU Department of Mathematics, and the National Science Foundation for the REU supplement to DMS-15-02227. Pries was partially supported by NSF grant DMS-15-02227. This project would not be possible without all of you.

References

[Aguglia et al. 2001] A. Aguglia, G. Korchmáros, and F. Torres, "Plane maximal curves", *Acta Arith.* **98**:2 (2001), 165–179. MR Zbl

[Aoki 2008a] N. Aoki, "On supersingular cyclic quotients of Fermat curves", *Comment. Math. Univ. St. Pauli* **57**:1 (2008), 65–90. MR Zbl

[Aoki 2008b] N. Aoki, "On the zeta function of some cyclic quotients of Fermat curves", *Comment. Math. Univ. St. Pauli* **57**:2 (2008), 163–185. MR Zbl

[Bennama and Carbonne 1997] H. Bennama and P. Carbonne, "Courbes $X^mY^n+Y^mZ^n+Z^mX^n=0$ et décomposition de la jacobienne", *J. Algebra* **188**:2 (1997), 409–417. MR Zbl

[Fermat 1999] P. Fermat, *Œuvres de Pierre Fermat, I: La théorie des nombres*, Librairie Scientifique et Technique Albert Blanchard, Paris, 1999. MR Zbl

[Ireland and Rosen 1990] K. Ireland and M. Rosen, *A classical introduction to modern number theory*, 2nd ed., Graduate Texts in Mathematics **84**, Springer, 1990. MR Zbl

[Nie 2016] M. Nie, "Zeta functions of trinomial curves and maximal curves", *Finite Fields Appl.* **39** (2016), 52–82. MR Zbl

[Serre 1985] J. P. Serre, "Rational points on curves over finite fields", handwritten notes by F. Q. Gouvêa of lectures given at Harvard University, 1985.

[Shioda and Katsura 1979] T. Shioda and T. Katsura, "On Fermat varieties", *Tohoku Math. J.* (2) **31**:1 (1979), 97–115. MR Zbl

[Tafazolian 2010] S. Tafazolian, "A characterization of maximal and minimal Fermat curves", *Finite Fields Appl.* **16**:1 (2010), 1–3. MR Zbl

[Tafazolian and Torres 2017] S. Tafazolian and F. Torres, "A note on certain maximal curves", *Comm. Algebra* **45**:2 (2017), 764–773. MR Zbl

[Weil 1948a] A. Weil, *Sur les courbes algébriques et les variétés qui s'en déduisent*, Actualités Sci. Ind. **1041**, Hermann et Cie., Paris, 1948. MR Zbl

[Weil 1948b] A. Weil, *Variétés abéliennes et courbes algébriques*, Actualités Sci. Ind. **1064**, Hermann et Cie., Paris, 1948. MR Zbl

[Weil 1949] A. Weil, "Numbers of solutions of equations in finite fields", *Bull. Amer. Math. Soc.* **55** (1949), 497–508. MR Zbl

[Yui 1980] N. Yui, "On the Jacobian variety of the Fermat curve", *J. Algebra* **65**:1 (1980), 1–35. MR Zbl

Received: 2018-11-15 Revised: 2019-06-24 Accepted: 2019-07-06

erinrdawson@gmail.com *Colorado State University, Fort Collins, CO, United States*

hwy027@gmail.com *Colorado State University, Fort Collins, CO, United States*

keylynch@rams.colostate.edu *Colorado State University, Fort Collins, CO, United States*

ameprice@rams.colostate.edu *Colorado State University, Fort Collins, CO, United States*

smstep@rams.colostate.edu *Colorado State University, Fort Collins, CO, United States*

ewewok75@gmail.com *Colorado State University, Fort Collins, CO, United States*

dean.bisogno@gmail.com *Colorado State University, Fort Collins, CO, United States*

pries@math.colostate.edu *Colorado State University, Fort Collins, CO, United States*

INVOLVE 12:8 (2019)
dx.doi.org/10.2140/involve.2019.12.1307

Multicast triangular semilattice network

Angelina Grosso, Felice Manganiello, Shiwani Varal and Emily Zhu

(Communicated by Nigel Boston)

We investigate the structure of the code graph of a multicast network that has a characteristic shape of an inverted equilateral triangle. We provide a criterion that determines the validity of a receiver placement within the code graph, present invariance properties of the determinants corresponding to receiver placements under symmetries, and provide a complete study of these networks' receivers and required field sizes up to a network of four sources. We also improve on various definitions related to code graphs.

1. Introduction

A communication network is a collection of directed links connecting transmitters, switches, and receivers, whose underlying structure can be mathematically represented by a directed graph $\mathcal{G} = (\mathcal{V}, \mathcal{E})$ as introduced in [Ahlswede et al. 2000]. Koetter and Médard [2003] studied the network code design as an algebraic problem that depends on the structure of the underlying graph. They made a connection between a given network information flow problem and an algebraic variety over the closure of a finite field.

In particular, a multicast network is an error-free network with unit-capacity channels represented by a directed acyclic graph and with the communication requirement that every receiver demands the message sent by every source. Treating the messages as elements of some large enough finite field $\mathbb{F}_q$, it is known that linear network coding suffices to transmit the maximal number of messages.

Code graphs condense the information in a choice of edge-disjoint paths of a multicast network based on the coding points, i.e., edges which are “bottlenecks” where messages are combined in linear network coding. Under this framework, linear network coding is reduced to assigning vectors to vertices in the code graph with independence conditions based on receivers. The triangular semilattice networks are then a family of code graphs embedded in the integer lattice restricted to

MSC2010: primary 68P30, 68R10; secondary 11T06.
Keywords: multicast network, triangular semilattice, determinantal condition, finite field, multivariate polynomial, linear network coding, multicast communication, code graph.

nonnegative coordinates of some maximum 1-norm with edges between adjacent lattice points directed towards the origin.

This paper is organized as follows. In Section 2, we refer briefly to and improve upon coding points, code graphs, and $\mathbb{F}_q$-labelings of code graphs; these are discussed in detail in [Anderson et al. 2017]. We then present a result with regards to determinants in the $\mathbb{F}_q$-labeling. In Section 3, we introduce a type of code graph called the triangular semilattice network. We discuss receiver placements and invariance of the minors corresponding to receiver placements under symmetries. From this general study, we shift to a complete study of triangular semilattice networks with up to four sources in Section 4.

2. Coding points and code graphs

In this work, we represent a multicast network by a directed acyclic graph $\mathcal{G} = (\mathcal{V}, \mathcal{E})$ with a set $\mathcal{S} \subset \mathcal{V}$ of sources, i.e., vertices without incoming edges, and a set $\mathcal{R} \subset \mathcal{V}$ of receivers, i.e., vertices without outgoing edges. Each directed edge is a unit capacity noise-free communication channel over a finite field $\mathbb{F}_q$. We further assume that the edge mincut between each source and each receiver is at least 1 and the overall mincut between the set of sources and each receiver is at least the number of sources. Together with the assumption of coordination at source level and with the requirement that every receiver $R \in \mathcal{R}$ gets the message from every source $S \in \mathcal{S}$, the network is equivalent to a multicast network as defined in [Ahlswede et al. 2000].

If $\mathcal{R}$ consists of a single receiver, the communication requirement is satisfied by a routing solution if and only if $|\mathcal{S}| \leq \text{mincut}(\mathcal{S}, R)$ as a result of Menger's theorem, which states that the edge $\text{mincut}(\mathcal{S}, R)$ is equal to the maximum number of edge-disjoint paths between the source set $\mathcal{S}$ and the receiver R [Anderson et al. 2017]. In the case of multiple receivers where $|\mathcal{S}| \leq \min_{R \in \mathcal{R}} \text{mincut}(\mathcal{S}, R)$, Ahlswede et al. [2000] first showed that a network coding solution exists; later it was found that a linear network coding solution over a finite field $\mathbb{F}_q$ exists when q is sufficiently large [Li et al. 2003]; in particular, $q \geq |\mathcal{R}|$ was found to be sufficient [Jaggi et al. 2005]. Interested readers may also refer to [Médard and Sprintson 2011] for a complete algebraic proof showing that $q > |\mathcal{R}|$ is sufficient.

To condense the information about these receiver requirements, we consider the corresponding code graph of a multicast network. Anderson et al. [2017] explain coding points of a network as the bottlenecks of the network where the linear combinations occur. More formally:

Definition 2.1. Let $\mathcal{G}$ be the underlying directed acyclic graph of a multicast network and for each $R \in \mathcal{R}$ let $\mathcal{P}_R = \{P_{S,R} \mid S \in \mathcal{S}\}$ be a set of edge-disjoint paths, where $P_{S,R}$ denotes a path from S to R. A coding point of $\mathcal{G}$ is an edge $e = (v, v') \in \mathcal{E}$ such that:

- There are distinct sources $S, S' \in \mathcal{S}$ and distinct receivers $R, R' \in \mathcal{R}$ such that e appears in both $P_{S,R} \in \mathcal{P}_R$ and $P_{S',R'} \in \mathcal{P}_{R'}$.
- The parents of v in $P_{S,R}$ and $P_{S',R'}$ are distinct.

Definition 2.2. A coding-direct path in $\mathcal{G}$ from $v_1 \in \mathcal{V}$ to $v_2 \in \mathcal{V}$ is a path from v_1 to v_2 that does not pass through any coding point in $\mathcal{G}$, except possibly in the first edge.

Note that coding points are dependent on the choices of edge-disjoint paths to each receiver. With $\mathcal{G} = (\mathcal{V}, \mathcal{E}, \mathcal{S}, \mathcal{R}, \{\mathcal{P}_R \mid R \in \mathcal{R}\})$ we denote a multicast network with chosen sets of edge-disjoint paths from the sources to each receiver. For a given multicast network, Anderson et al. [2017] define the code graph as a directed graph with labeled vertices that preserves the essential information of the network:

Definition 2.3. Let $\mathcal{G} = (\mathcal{V}, \mathcal{E}, \mathcal{S}, \mathcal{R}, \{\mathcal{P}_R \mid R \in \mathcal{R}\})$ be a multicast network and let $\mathcal{Q}$ be its set of coding points. Let the code graph $\Gamma = \Gamma(\mathcal{G})$ be the vertex-labeled directed acyclic graph constructed as follows:

- The vertex set of Γ is $\mathcal{S} \cup \mathcal{Q}$. Given a vertex v of Γ, the corresponding source or coding point in $\mathcal{G}$ is called the $\mathcal{G}$-object of v.
- The edge set of Γ is the set of all ordered pairs of vertices of Γ such that there is a coding-direct path in $\mathcal{G}$ between the corresponding $\mathcal{G}$-objects.
- Each vertex v of Γ is labeled with a subset $L_v \subseteq \mathcal{R}$. A receiver $R \in \mathcal{R}$ is in L_v if and only if there is a coding-direct path in $\mathcal{G}$ from the $\mathcal{G}$-object of v to R.

In general, Anderson et al. [2017] present the following proposition that attempts to outline the properties of a code graph:

Proposition 2.4. *For any code graph* $\Gamma = \Gamma(\mathcal{G})$, *we have that*:

- Γ *is an acyclic graph.*
- *Every vertex in* Γ *either has in-degree* 0, *in which case its* $\mathcal{G}$*-object is a source*, *or it has in-degree at least* 2, *in which case its* $\mathcal{G}$*-object is a coding point.*
- *For each* $R \in \mathcal{R}$, *the set of vertices* $V_R = \{v \in V \mid R \in L_v\}$ *has cardinality* $|\mathcal{S}|$, *and there are* $|\mathcal{S}|$ *vertex-disjoint paths from the sources to this set corresponding to the original* $|\mathcal{S}|$ *edge-disjoint paths.*

The networks we consider in this work will satisfy these properties. Nonetheless, the condition on the in-degree of a coding point seems to require additional constraints. In Figure 1, the code graph construction only produces one edge to the bottom coding point.

Figure 2 represents a slight modification of this construction and shows that taking a set of paths with the minimum number of coding points is insufficient to guarantee that the in-degree of every coding point is at least 2. For simplicity, edges between sources and receivers are omitted.

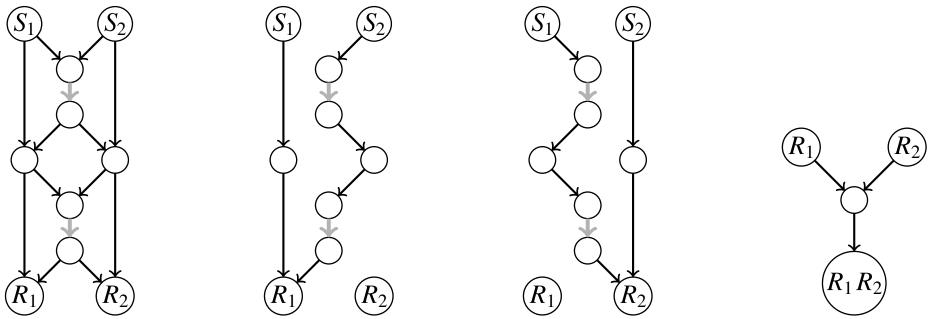

(a) The network. (b) Paths to R_1. (c) Paths to R_2. (d) Code graph.

Figure 1. Convoluted choice of paths.

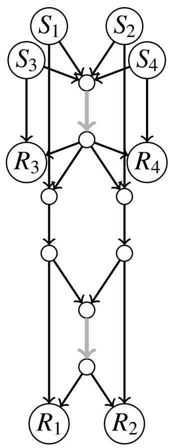

Figure 2. Bottom coding point has in-degree 1 when taking paths analogous to the above.

Anderson et al. [2017] also provide a criterion to determine when a labeled network is a code graph:

Proposition 2.5. *Let $\Gamma = (V, E)$ be a vertex-labeled, directed acyclic graph where each vertex v is labeled with a finite set L_v. Let $\mathcal{S} := \{v \in V \mid v \text{ has in-degree } 0\}$, $\mathcal{Q} := V \backslash \mathcal{S}$, and $\mathcal{R} = \bigcup_{v \in V} L_v$. Suppose*:

- *The in-degree of every vertex in $\mathcal{Q}$ is at least* 2.
- *For each $R \in \mathcal{R}$, the set $V_R = \{v \in V : R \in L_v\}$ has $|\mathcal{S}|$ vertices.*
- *For each $R \in \mathcal{R}$ there is a set $\Pi_R = \{\pi_{S,R} \mid S \in \mathcal{S}\}$ of vertex-disjoint paths where every vertex and edge of Γ is contained in some $\pi_{S,R}$.*

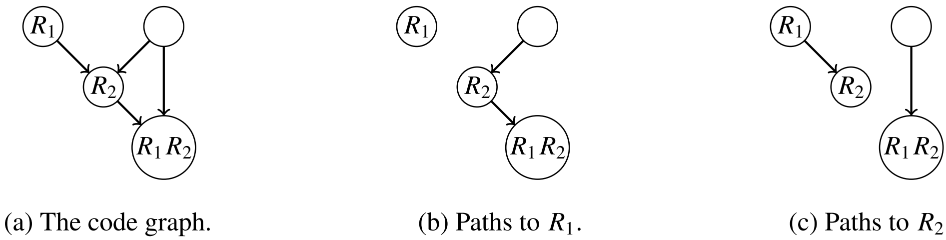

Figure 3. Insufficiency of modification of Proposition 2.5.

Then Γ *is the code graph for a reduced multicast network whose sources, coding points, and receivers are in one-to-one correspondence with the elements of* $\mathcal{S}$, $\mathcal{Q}$, *and* $\mathcal{R}$, *respectively.*

In Figure 3, we find that the condition that a single choice of vertex-disjoint paths using all edges and vertices may be insufficient to guarantee that a graph is a code graph of some multicast network. In this case, the bottom node cannot act as a coding point as the two paths to it originate from the same source. One can note that the edge between the coding points can be avoided completely when instead taking the path directly from the second source to the bottom coding point as the path to R_1.

Note that it is still insufficient to require that all choices of vertex-disjoint paths $\{\Pi_R\}_{R\in\mathcal{R}}$ use all edges/vertices. Consider Figure 4 below, which has only the shown vertex-disjoint paths but for which the bottom vertex cannot be a coding point. Further in this paper, we will require various receiver placements which will ensure that the formed labeled directed acyclic graphs are code graphs.

There exists extensive literature, e.g., [Koetter and Médard 2003; Médard and Sprintson 2011; Sun et al. 2015], that follows the approach of assigning edge transfer coefficients or vertex transfer matrices directly to the multicast network. Fragouli and Soljanin [2006] introduced (as coding vectors) and Anderson et al. [2017] expanded on the concept of $\mathbb{F}_q$-labelings of code graphs, which allow us to focus on the linear dependence and independence conditions of a single matrix.

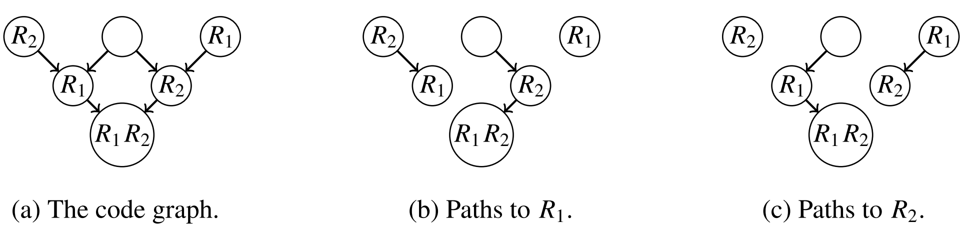

Figure 4. Only one choice of paths (but not a code graph).

Definition 2.6. Let $\mathcal{G} = (\mathcal{V}, \mathcal{E}, \mathcal{S}, \mathcal{R}, \{\mathcal{P}_R \mid R \in \mathcal{R}\})$ be a multicast network and $\Gamma = (V, E)$ be its corresponding code graph. Each $v \in V$ is labeled with a set of receivers $L_v \subseteq \mathcal{R}$. Let $V_R = \{v \in V \mid R \in L_v\}$. An $\mathbb{F}_q$-labeling of Γ is an assignment of elements of $\mathbb{F}_q^{|\mathcal{S}|}$ to the vertices of Γ satisfying:

- The vectors assigned to the source nodes of the code graph are linearly independent and without loss of generality they can be chosen to be the standard basis.
- The vectors assigned to vertices labeled with a common receiver are linearly independent.
- The vector assigned to a coding point $Q \in V$ is in the span of vectors assigned to the tails of the directed edges terminating at Q.

We call the $|\mathcal{S}| \times |V|$ matrix consisting of the vectors of the $\mathbb{F}_q$-labeling, an $\mathbb{F}_q$-labeling matrix of Γ.

Anderson et al. [2017] note that the capacity of $\mathcal{G}$ is achievable over $\mathbb{F}_q$ if and only if there exists an $\mathbb{F}_q$-labeling of Γ. With this, it suffices to examine properties of code graphs as opposed to complete networks. In this paper, we study the solvability of a multicast network over various finite fields upon the addition of receiver placements.

Definition 2.7. Let $\mathcal{G} = (\mathcal{V}, \mathcal{E}, \mathcal{S}, \mathcal{R}, \{\mathcal{P}_R \mid R \in \mathcal{R}\})$ be a multicast network and $\Gamma = (V, E)$ be its corresponding code graph and $R \in \mathcal{R}$. We call the set $V_R = \{v \in V \mid R \in L_v\}$ a receiver placement of R and a vertex $v \in V_R$ a label of R or more generally, a receiver label. The determinant of a receiver placement of R is the maximal minor of the $\mathbb{F}_q$-labeling matrix of Γ with columns corresponding to its labels.

Since a set of vectors forming a square matrix is linearly independent if and only if the matrix's determinant is nonzero, we examine the structure of the determinants of receiver placements. In particular, to assist in determining if such an $\mathbb{F}_q$-labeling matrix exists, we will consider the matrix over $\mathbb{F}_q[\alpha_{(u,v)} : (u, v) \in E]$ formed by assigning the standard basis to the sources and variable linear combinations of the parents' vectors; i.e., if N_u is the vector in the $\mathbb{F}_q$-labeling matrix corresponding to a vertex $u \in V$, for some $v \in \mathcal{Q}$, we would consider the vector $\sum_{u:(u,v)\in E} \alpha_{(u,v)} \cdot N_u$.

Definition 2.8. Let $\mathcal{S} = \{S_1, \dots, S_n\}$ and V_R be a receiver placement, i.e., $V_R = \{R^{(1)}, \dots, R^{(n)}\} \subset V$. We introduce the following notation:

- $\pi_{i,j}$ denotes a path from S_i to $R^{(j)}$.
- $\Pi_{R,\sigma} = \{\pi_{i,\sigma(i)} \mid i \in [n]\}$ for some $\sigma \in \mathcal{S}_n$, where $[n] = \{i\}_{i=1}^n$ and $\mathcal{S}_n$ is the symmetric group of degree n, is a set of paths matching the sources to the receiver-labeled vertices

- $\Psi_R = \{\Pi^{(j)}_{R,\sigma} \mid \sigma \in \mathcal{S}_n,\ j \in [m_\sigma]\}$, where m_σ is the number of paths, possibly 0, for this given matching of sources to receiver-labeled vertices, consists of all sets of paths from the sources to the receiver-labeled vertices.
- $\Phi_R = \{\Pi_{R,\sigma} = \Pi^{(j)}_{R,\sigma} \in \Psi_R \mid j \in [m_\sigma], \pi_{i,\sigma(i)}$ are vertex-disjoint$\}$ consists of all sets of vertex-disjoint paths from the sources to the receiver-labeled vertices.

Note that the σ corresponding to $\Pi_{R,\sigma}$ is well-defined and unique as we have n sources and n labels, but for a given σ, the set $\Pi_{R,\sigma}$ is not necessarily unique — it may not even exist. In a slight abuse of notation, we will also write $(u, v) \in \Pi_{R,\sigma}$ to denote that $(u, v) \in \pi_{i,\sigma(i)}$ for some $\pi_{i,\sigma(i)} \in \Pi_{R,\sigma}$.

Proposition 2.9. *Let $S_1, \dots, S_n$ denote the sources in a code graph with the $\mathbb{F}_q$-labeling matrix denoted by N. Given a receiver placement of R, i.e., $V_R = \{R^{(1)}, \dots, R^{(n)}\}$, we have*

$$\det(N_R) = \sum_{\Pi_{R,\sigma} \in \Phi_R} \operatorname{sign}(\sigma) \prod_{(u,v) \in \Pi_{R,\sigma}} \alpha_{(u,v)} \in \mathbb{F}_q[\alpha_{(u,v)} : (u, v) \in E],$$

where N_R is the submatrix of N corresponding to $R^{(1)}, \dots, R^{(n)}$ and $\alpha_{(u,v)}$ is the transfer coefficient, also called channel gain, corresponding to the edge (u, v) and $\mathbb{F}_q[\alpha_{(u,v)} : (u, v) \in E]$ is the multivariate polynomial ring where variables correspond to the transfer coefficients.

This proposition says that the minor corresponding to a receiver placement in an $\mathbb{F}_q$-labeling matrix can be calculated by the sum over the sets of vertex-disjoint paths to the receiver-labeled vertices of the product of the transfer coefficients corresponding to the edges in any of those paths. In other words, sets including vertex-intersecting paths do not affect the minor.

We first show the following property about the set $\Psi_R \backslash \Phi_R$ of sets of paths with vertex-intersecting paths.

Lemma 2.10. *There is a matching of $\Psi_R \backslash \Phi_R$ without fixed points, meaning a bijective map $\mu : \Psi_R \backslash \Phi_R \to \Psi_R \backslash \Phi_R$ with $\mu \circ \mu = \mathrm{id}$ and $\mu(\Pi_{R,\sigma}) \neq \Pi_{R,\sigma}$ for all $\Pi_R \in \Psi_R \backslash \Phi_R$ such that for $\mu(\Pi_{R,\sigma}) = \Pi'_{R,\sigma'}$*

$$\operatorname{sign}(\sigma) = -\operatorname{sign}(\sigma') \quad \textit{and} \quad \prod_{(u,v) \in \Pi_{R,\sigma}} \alpha_{(u,v)} = \prod_{(u,v) \in \mu(\Pi_{R,\sigma})} \alpha_{(u,v)}.$$

Proof. Let $\Pi_{R,\sigma} \in \Psi_R \backslash \Phi_R$ be arbitrary and let sources S_i, S_j be the minimum (i, j) (under lexicographic ordering) such that $\pi_{i,\sigma(i)}$ and $\pi_{j,\sigma(j)}$ intersect at some vertex. Let x be the first vertex at which these paths intersect. Furthermore, let $\pi_{l,x} \subseteq \pi_{l,\sigma(l)}$ denote the subset of the path $\pi_{l,\sigma(l)}$ going from S_l to x and $\pi_{x,\sigma(l)} \subseteq \pi_{l,\sigma(l)}$ denote the subset of the path $\pi_{l,\sigma(l)}$ going from x to $R^{(\sigma(l))}$ for $l = i, j$.

We define $\mu(\Pi_{R,\sigma}) = \{\pi'_{k,\sigma'(k)} : k \in [n]\}$, where

$$\sigma'(k) = \begin{cases} \sigma(k) & \text{if } k \neq i, j, \\ \sigma(j) & \text{if } k = i, \\ \sigma(i) & \text{if } k = j \end{cases} \quad \text{and} \quad \pi'_{k,\sigma'(k)} = \begin{cases} \pi_{k,\sigma(k)} & \text{if } k \neq i, j, \\ \pi_{i,x} \cup \pi_{x,\sigma(j)} & \text{if } k = i, \\ \pi_{j,x} \cup \pi_{x,\sigma(i)} & \text{if } k = j. \end{cases}$$

Note that this μ satisfies the desired properties:

- Clearly there is no $\mu(\Pi_{R,\sigma}) = \Pi_{R,\sigma}$ since necessarily distinct portions of the paths from two sources are swapped to get $\mu(\Pi_{R,\sigma})$.
- $\mu \circ \mu(\Pi_{R,\sigma}) = \Pi_{R,\sigma}$ as the minimum (i, j) and first vertex of intersection are the same for $\Pi_{R,\sigma}$ and $\mu(\Pi_{R,\sigma})$, so applying μ again simply swaps the swapped portion back to the original paths, returning $\mu(\mu(\Pi_{R,\sigma}))$ to $\Pi_{R,\sigma}$.
- This is bijective since by the above, μ is its own inverse.
- We have that $\text{sign}(\sigma) = -\text{sign}(\sigma')$ as $\sigma' = \tau_{i,j} \circ \sigma$ (where $\tau_{i,j}$ denotes the transposition of i, j, which fixes all other elements).
- $\prod_{(u,v)\in\Pi_{R,\sigma}} \alpha_{(u,v)} = \prod_{(u,v)\in\mu(\Pi_{R,\sigma})} \alpha_{(u,v)}$ as both sets of paths use exactly the same edges with the same multiplicity by definition. □

We now turn to the proof of the proposition:

Proof of Proposition 2.9. Note that by the definition of determinant

$$\det(N_R) = \sum_{\rho\in\mathcal{S}_n} \text{sign}(\rho) \prod_{i=1}^{n} (N_R)_{i,\rho(i)},$$

where we note that $\rho(i)$ determines at which receiver a path ends and i determines from which source a path originates. As such, based on the line graph (like in Kschischang's argument in Appendix C [Médard and Sprintson 2011]), we see that an entry of the matrix is the sum over the paths from S_i to $R^{(\rho(i))}$ of the product over the edges of the transfer coefficients, so

$$(N_R)_{i,\rho(i)} = \sum_{\pi_{i,\rho(i)} \text{ a path}} \; \prod_{(u,v)\in\pi_{i,\rho(i)}} \alpha_{(u,v)},$$

where $\pi_{i,\rho(i)}$ is any path from S_i to $R^{(\rho(i))}$. Now expanding $\prod_{i=1}^{n}(N_R)_{i,\rho(i)}$, which is the product over the sources of the sums over different paths from that source to the desired receiver and thus the sum over the different sets of paths from the sources to the receivers of the product over those paths, we get

$$\prod_{i=1}^{n}(N_R)_{i,\rho(i)} = \prod_{i=1}^{n}\Bigg(\sum_{\pi_{i,\rho(i)} \text{ a path}} \Bigg(\prod_{(u,v)\in\pi_{i,\rho(i)}} \alpha_{(u,v)} \Bigg)\Bigg) = \sum_{\Pi_{R,\sigma}\in\Psi_R : \sigma=\rho} \Bigg(\prod_{(u,v)\in\Pi_{R,\sigma}} \alpha_{(u,v)} \Bigg),$$

so by the uniqueness of σ for a given $\Pi_{R,\sigma}$, we have

$$\det(N_R) = \sum_{\rho \in \mathcal{S}_n} \operatorname{sign}(\rho) \sum_{\Pi_{R,\sigma} \in \Psi_R : \sigma = \rho} \left(\prod_{(u,v) \in \Pi_{R,\sigma}} \alpha_{(u,v)} \right)$$
$$= \sum_{\Pi_{R,\sigma} \in \Psi_R} \operatorname{sign}(\sigma) \prod_{(u,v) \in \Pi_{R,\sigma}} \alpha_{(u,v)}$$

Now the only difference between our current expression for $\det(N_R)$ and the desired expression is that the set of paths $\Pi_{R,\sigma}$ for the determinant might not be vertex-disjoint. But as a result of the matching in Lemma 2.10, we have

$$\sum_{\Pi_{R,\sigma} \in \Psi_R \setminus \Phi_R} \operatorname{sign}(\sigma) \prod_{(u,v) \in \Pi_{R,\sigma}} \alpha_{(u,v)} = \sum_{\{\Pi_{R,\sigma}, \mu(\Pi_{R,\sigma})\} \subseteq \Psi_R \setminus \Phi_R} 0 = 0,$$

making

$$\det(N_R) = \sum_{\Pi_{R,\sigma} \in \Phi_R} \operatorname{sign}(\sigma) \prod_{(u,v) \in \Pi_{R,\sigma}} \alpha_{(u,v)}$$

as desired. □

Corollary 2.11. *The number of terms in* $\det(N_R)$ *is the number of sets of vertex-disjoint paths from* $S_1, \ldots, S_n$ *to* $R^{(1)}, \ldots, R^{(n)}$.

This follows from Proposition 2.9.

Corollary 2.12. *For a receiver placement* V_R, *the* $\alpha_{(u,v)}$*-degree of* $\det(N_R)$ *has degree at most* 1.

This follows by noting that since the paths are vertex-disjoint, any edge can be traversed at most once among a set of paths. Therefore the corresponding variable can only appear once in a monomial corresponding to some path.

3. Triangular semilattice network

We now introduce and discuss properties of the triangular semilattice network, a code graph with a structure that visually resembles an inverted equilateral triangle. We then seek to add receiver placements to require a greater minimum field size.

Definition 3.1. Let a triangular semilattice code graph ∇_n of length n for $n \in \mathbb{N} \setminus \{0\}$ be a code graph with underlying directed acyclic graph given by the vertex and edge sets

$$V = \{(x, y) \in \mathbb{Z}^2 \mid x, y \geq 0, \; x+y < n\},$$
$$E = \{((x+1, y), (x, y)) \mid 0 \leq x+y < n-1\} \cup \{((x, y+1), (x, y)) \mid 0 \leq x+y < n-1\}.$$

For $1 \leq i \leq n$, we call the set of vertices $\{(a, b) \mid a+b = n-i\}$ the i-th level, where the first level is called the top level and the n-th level is called the bottom

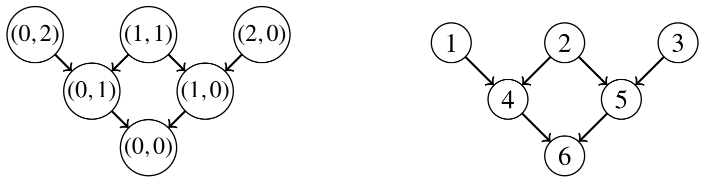

(a) Definition of $\bigtriangledown_3$. (b) Enumeration of the vertices.

Figure 5. Representation of a triangular semilattice code graph $\bigtriangledown_3$ with vertex enumeration.

level. We enumerate the vertices in increasing order of level and then increasing order of the x-coordinate within the level.

We may refer to the triangular semilattice network of length n as any network with associated code graph $\bigtriangledown_n$.

Figure 5 shows $\bigtriangledown_3$ without receiver labels but with the enumeration of the vertices. Later in this work, we will often identify vertices with the value in this enumeration.

Definition 3.2. Let the left-side refer to the n vertices in the $\bigtriangledown_n$ with x-coordinate equal to 0. Similarly the right-side refers to the n vertices with y-coordinate equal to 0. We collectively refer to these as the sides.

Note that embedding $\bigtriangledown_n$ as above, the left side corresponds with vertices without left children and the right side corresponds with vertices without right children.

Valid receiver placements. We introduce some more definitions and lemmas to help us prove the characterization of valid receiver placements, meaning labeled vertices distributed such that there is a choice of disjoint paths between sources and labeled vertices.

Definition 3.3. A k-triangle in a triangular semilattice network $\bigtriangledown_n$ is a subgraph isomorphic as a directed graph to a triangular semilattice network $\bigtriangledown_k$. We call k the length of a k-triangle.

We will drop k if the length of the triangle is clear from the context. Note that length can also be defined via the length of the longest path between any two vertices in the triangle (also considering number of vertices for length) or the number of vertices along the top of the triangle.

Definition 3.4. Given a receiver placement of R, a k-triangle is overcrowded if there are at least $k+1$ labels among its vertices. It is crowded if there are exactly k labels. A k-triangle is distributed if no triangle contained in it is overcrowded.

Definition 3.5. The extension of a k-triangle is the $(k+1)$-triangle containing the original k-triangle and all parents of the vertices in the k-triangle.

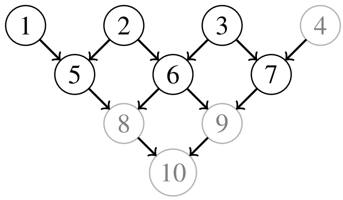

Figure 6. A graph with no overcrowded 3-triangles but an overcrowded 2-triangle.

Remark 3.6. It is insufficient to just consider $(n-1)$-triangles for the distributed property. Consider the network in Figure 6, where the receiver-labeled vertices are shown in gray. Note that there are three labels in a 2-triangle, making it not distributed but there are not four labels in a 3-triangle.

Definition 3.7. We say that two vertices a and b are consecutive if they share a child. A sequence $a_1, \dots, a_k$ of distinct vertices has consecutive vertices if a_i and a_{i+1} are consecutive for every $i = 1, \dots, k-1$. A vertex c is between a and b if there is a sequence of consecutive vertices with extremals a and b containing c.

Intuitively, consecutive vertices are "next to" each other on the same level of the network.

Definition 3.8. For two distinct vertices a, b on the same level, we say that a is to the left of b (equivalently that b is to the right of a) if its value in the enumeration is less than (greater than) that of b.

Definition 3.9. For a vertex a to the left of some vertex b on some i-th level, we say some vertex c is trapped between a and b if the vertex is in the level $i+1$ and it is between a's right child and b's left child; see Figure 7.

Lemma 3.10. *Let $\triangledown_n$ be a distributed triangular semilattice network with a sequence of consecutive vertices where each vertex is contained in a crowded triangle. Then, there is a crowded triangle containing all vertices in this sequence.*

Proof. We induct on the length of the sequence. If there is just one such vertex, we are done.

On two consecutive vertices x and y, we have a crowded k-triangle corresponding to x which may intersect a crowded l-triangle corresponding to y (where k, l are

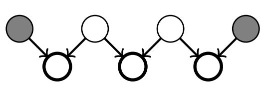

Figure 7. The thickly outlined vertices are trapped between the two filled-in vertices.

some lengths). Note that if the intersection has length $i \geq 0$, it has at most i labels or we have a contradiction. In that case, consider the triangle of length $k+l-i$ containing the two crowded triangles; note that it contains at least the labels in the k-triangle and l-triangle, which by inclusion/exclusion have at least $k+l-i$ labels combined. By assumption, a $(k+l-i)$-triangle must have at most $k+l-i$ labels, so we have equality, thus forming a crowded triangle.

Now for our inductive step, assume the result for $m \geq 2$ and consider $m+1$ consecutive vertices contained in crowded triangles. By the inductive hypothesis, we have some crowded l-triangle containing the first m vertices. We can then apply the case for two vertices to the m-th vertex (with the crowded l-triangle) and the $(m+1)$-th vertex (with some crowded k-triangle) to get some crowded j-triangle containing all $m+1$ vertices (where j, k, l are some lengths). □

Lemma 3.11. *Let ∇_n be an distributed triangular semilattice network with $t > 1$ labels in the top level. Then, there are $t-1$ unlabeled vertices in the second level such that upon labeling them, the bottom $(n-1)$-triangle is distributed.*

Proof. Let L be the leftmost labeled vertex in the top level. Note that it suffices to show that iteratively, for every top-level labeled vertex $v \neq L$, we can label a previously unlabeled vertex trapped by u, the rightmost labeled vertex to the left of v, and v such that the bottom $(n-1)$-triangle is distributed.

We prove the claim by contraposition: Assume that at some point, there exists a labeled vertex $v \neq L$ in the top level such that we create an overcrowded triangle in the bottom $(n-1)$-triangle for every such labeling. Then, we show that there was originally an overcrowded triangle in the network. In particular, we claim that if every labeling creates an overcrowded triangle, every vertex trapped by v and the previous labeled vertex u is in some crowded triangle. Each of the labeled trapped vertices forms a crowded 1-triangle. Moreover, by assumption, upon labeling each of the unlabeled trapped vertices, it is in a k-triangle with at least $k+1$ labeled vertices. Without that added label, we thus have at least k labeled vertices in a k-triangle. If we have more than k labels in this k-triangle, we arrive at a contradiction; otherwise, we have a crowded triangle. We can then apply Lemma 3.10 to get a crowded l-triangle containing all of the trapped vertices. From there, we can extend the triangle to the first level to include u and v as in Definition 3.5, getting $l+2$ labels in an $(l+1)$-triangle in the original graph. □

Theorem 3.12. *Given a triangular semilattice network ∇_n, a labeling V_R of n vertices corresponding to some receiver R is valid, meaning that there are vertex-disjoint paths to the vertices labeled by V_R from the sources if and only if the network is distributed.*

Proof. We first show the forward direction. Fix a valid receiver placement and a triangle of length k. Consider the set S_k of the vertices corresponding to the labels in the triangle. Note that the mincut from the sources to the set S_k is at most k, since the top level of the triangle is a cut of size k. As such, by Menger's theorem, there are at most k vertex-disjoint paths to the set S_k, and thus, at most k labels in the triangle.

We now show the other direction by induction on n. The base cases of $n = 1, 2$ are trivial. Now assume the result for $n \geq 2$. Consider a triangular semilattice network $\bigtriangledown_{n+1}$ and a receiver placement satisfying the desired property. As there are at most n labels in the bottom triangle of length n, there must be at least one label in the top level. We call the leftmost label L and match the remaining n vertices in the top level with the next level as follows.

If there is only one label in the top level, we can iteratively match/biject all vertices in the first level, from left to right, to the leftmost unmatched vertex in the next level — in particular, we match the vertices to the left of L with their right child and those to the right of L with their left child. Applying the inductive hypothesis to the bottom n-triangle, we can extend the n vertex-disjoint paths from the second level to the receivers to begin at the sources via the matching. With $\{L\}$, we then have our $n + 1$ vertex-disjoint paths to the labels.

Otherwise there are at least two labels in the top level. By Lemma 3.11, we have a matching of the labeled vertices in the top level to some trapped vertices in the next level. Note that if we enumerate the top level's vertices as $a_1, \ldots, a_{n+1}$ and the second level's vertices as $b_1, \ldots, b_n$, a vertex a_i has children b_{i-1}, b_i if $i - 1, i \in [n]$. Now, we match each remaining unlabeled vertex in the top level with an unmatched child as follows:

- We can match any consecutive vertices $a_1, \ldots, a_m$ up to L (exclusive) by matching a_i with b_i for $i = 1, \ldots, m$. None of those b_i have been matched as they are not trapped by any two labeled vertices.
- We can match any consecutive vertices $a_t, \ldots, a_{n+1}$ after the rightmost labeled vertex in the top level by matching a_{i+1} with b_i for $i = t - 1, \ldots, n$. Again we note that none of these b_i are trapped by any two labeled vertices.
- For the unlabeled vertices $a_r, \ldots, a_s$ between two labeled vertices u and v in the top level, we match these to $\{b_{r-1}, \ldots, b_s\} \backslash \{b_p\}$, where b_p is the vertex matched to v. For $1 < r \leq i \leq p$, we match a_i with b_{i-1} and for $p < i \leq s$, we match a_i with b_i.

Note that this process creates a bijection between vertices. Within a section (between the trapped vertices or at the ends), the process is clearly injective. Across the consecutive sections, we reach a label at position a_j where the furthest right vertex the left section matches to is b_{j-1} (and sections further left match to vertices further left) and the furthest left vertex the right section matches to is b_j.

Finally, by our inductive hypothesis, we have vertex-disjoint paths from the sources/top level of the bottom n-triangle to the labels originally there and those added by Lemma 3.11. The set of vertex-disjoint paths in the original $(n+1)$-triangle is then as follows. Every label in the top level is just a path with a single vertex. For every other label in a lower level, we extend the path found in the bottom n-triangle via the matching with the unlabeled sources that we just found. This is vertex-disjoint as there are no intersections in the top level and the paths when restricted to the bottom n-triangle are either empty or are as found in the inductive hypothesis. □

We can further locate some receiver placements with well-understood determinants. Previously we denoted transfer coefficients using $\alpha_{(u,v)}$, where $(u, v) \in E$. Henceforth we use $\alpha_j^{(i)}$ for the transfer coefficients of the triangular semilattice network $\triangledown_n$ for $i \in [|\triangledown_{n-1}|]$, where $|\triangledown_{n-1}|$ is the number of vertices in $\triangledown_{n-1}$ and thus the bottom $(n-1)$-triangle of $\triangledown_n$, and $j \in [2]$. Here, $\alpha_1^{(i)}$ is the transfer coefficient of the edge between vertex $i+n$ and its left parent and $\alpha_2^{(i)}$ is the one between $i+n$ and its right parent.

Proposition 3.13. *Let V_R be a receiver placement in a triangular semilattice network $\triangledown_n$ consisting of exactly one label per level, where each label is along the sides of the network, and let $V_{R'}$ be the reflected receiver placement, meaning that its labels are the remaining side labels together with the bottom one. Then*

$$\det(N_R)\det(N_{R'}) = \pm \prod_{i\in[|\triangledown_{n-1}|],\, j\in[2]} \alpha_j^{(i)}.$$

Proof. We prove this by induction on the length n of the triangular semilattice network $\triangledown_n$. This is trivial in the case of $\triangledown_1$, as there are no variables. In the case of $\triangledown_2$, we either take the right source and the bottom vertex — for a determinant of $\alpha_2^{(1)}$ — or the left source and the bottom vertex — for a determinant of $\alpha_1^{(1)}$, and we have the product is then $\alpha_1^{(1)}\alpha_2^{(1)}$, as desired.

Now consider the triangular semilattice network $\triangledown_{n+1}$ for $n \in \mathbb{N}$, $n \geq 2$, where we fix a receiver placement such that we have a label in each level along the sides. Let N_R be the submatrix corresponding to this receiver placement. Consider

$$L = \begin{pmatrix} 1 & \alpha_1^{(1)} & 0 & \cdots & 0 \\ 0 & \alpha_2^{(1)} & \alpha_1^{(2)} & \cdots & 0 \\ \vdots & \vdots & \ddots & \vdots & \\ 0 & 0 & 0 & \cdots & \alpha_2^{(n)} \end{pmatrix} \quad \text{or} \quad L_{i,j} = \begin{cases} 1 & \text{if } i=j=1, \\ \alpha_1^{(j-1)} & \text{if } i+1=j\geq 2, \\ \alpha_2^{(j)} & \text{if } i=j\geq 2 \\ 0 & \text{otherwise,} \end{cases}$$

$$T = \begin{pmatrix} 0 & \alpha_1^{(1)} & 0 & \cdots & 0 \\ 0 & \alpha_2^{(1)} & \alpha_1^{(2)} & \cdots & 0 \\ \vdots & \vdots & \ddots & \vdots & \\ 1 & 0 & 0 & \cdots & \alpha_2^{(n)} \end{pmatrix} \quad \text{or} \quad T_{i,j} = \begin{cases} 1 & \text{if } i=n \text{ and } j=1, \\ \alpha_1^{(j-1)} & \text{if } i+1=j\geq 2, \\ \alpha_2^{(j)} & \text{if } i=j\geq 2 \\ 0 & \text{otherwise.} \end{cases}$$

Extending to the field of fractions $\mathbb{F}_q(\alpha_j^{(i)} \mid i \in [|\nabla_n|], j \in [2])$, note that L^{-1} corresponds to the basis change taking the leftmost label and the second level and T^{-1} corresponds to the basis change taking the rightmost label and the second level. Further note that $\det(L) = \prod_{i=1}^{n} \alpha_2^{(i)}$ and $\det(T) = \pm \prod_{i=1}^{n} \alpha_1^{(i)}$. To calculate $\det(N_R)$, it suffices to calculate $\det(LL^{-1}N_R) = \det(L)\det(L^{-1}N_R)$ or $\det(TT^{-1}N_R) = \det(T)\det(T^{-1}N_R)$. Now after the basis change (using L if we picked the top left label and T if we picked the top right label), the label's structure of the bottom n-triangle is identical to that of a triangular semilattice network ∇_n.

Further note that the basis-changed matrix $\overline{N}_R = L^{-1}N_R$ or $T^{-1}N_R$ is in the block matrix form

$$\overline{N}_R = \begin{pmatrix} 1 & 0 \\ 0 & \overline{N}'_R \end{pmatrix},$$

where $\overline{N}'_R$ is the matrix corresponding to the bottom n labels in ∇_n. Expanding by minors, we have $\det(\overline{N}_R) = \det(\overline{N}'_R)$. By inductive hypothesis we have that $\det(\overline{N}'_R)$ is a monomial where the product of this determinant and that corresponding to the reflection of the bottom n labels is a monomial with all transfer coefficients in ∇_n. As switching between the leftmost top label and the rightmost top label swaps between L and T, combining this with the bottom n-triangle for the original determinants, we get the desired result. □

As a consequence we obtain that a receiver placement V_R for a triangular semilattice network ∇_n defined as in Proposition 3.13 is a valid receiver placement for any choice of triangular semilattice network of length n and there exists an $\mathbb{F}_q$-labeling with nonzero transfer coefficients for any finite field $\mathbb{F}_q$. As such, for the rest of the paper we consider the triangular semilattice network ∇_n to be equipped with two receivers: the left-side and the right-side receivers, meaning the receivers with placements $\{(0, n-1), \dots, (0, 0)\}$ and $\{(n-1, 0), \dots, (0, 0)\}$ respectively as defined in Definition 3.2.

Invariance under symmetries of receiver placements. In this section we study properties of minors of $\mathbb{F}_q$-labelings from receiver placements. We will show that the property of having an $\mathbb{F}_q$-labeling for a receiver placement implies the existence of an $\mathbb{F}_q$-labeling for any receiver placement that is obtained from the original from either rotation or reflection with respect to the underlining graph of the network.

Definition 3.14. Let ∇_n be defined as in Definition 3.1. Then, the map $\rho : V \to V$ defined as $\rho(x, y) = (n - 1 - x - y, x)$ and the map $\sigma : V \to V$ defined as $\sigma(x, y) = (y, x)$ are bijections of the set of vertices with $\rho^3 = \mathrm{id}$ and $\sigma^2 = \mathrm{id}$ respectively.

Roughly speaking, ρ represents a counterclockwise rotation of the vertices, whereas σ represents a reflection. These two maps can be naturally extended

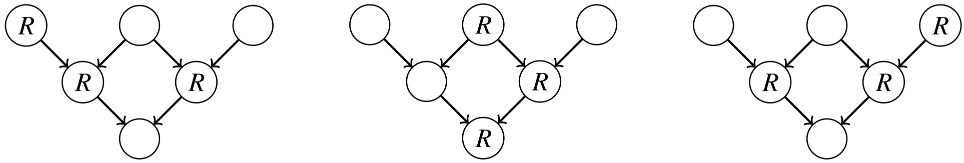

(a) V_R receiver placement. (b) $V_{\rho(R)}$ receiver placement. (c) $V_{\sigma(R)}$ receiver placement.

Figure 8. Receiver placements of the 3-semilattice.

to subsets of vertices. We are going to use these maps prevalently on receiver placements, meaning that the directed structure of the network is not going to change. Let $V_R = \{v \in V \mid R \in L_v\}$ be a receiver placement; then $V_{\rho(R)} := \{\rho(v) \in V \mid R \in L_v\}$ and $V_{\sigma(R)} := \{\sigma(v) \in V \mid R \in L_v\}$ are two others receiver placements. Figure 8 provide examples for the 3-semilattice network.

Theorem 3.15. *Let V_R be a receiver placement for a triangular semilattice network $\triangledown_n$. The following hold*:

(1) *$V_{\rho(R)}$ and $V_{\sigma(R)}$ are valid if and only if V_R is valid.*

(2) *If $\triangledown_n$ is equipped with the side receivers, there exists an $\mathbb{F}_q$-labeling for $\triangledown_n$ with valid receiver placements $V_{\rho(R)}$ or $V_{\sigma(R)}$ if and only if there exists an $\mathbb{F}_q$-labeling for $\triangledown_n$ with the valid receiver placement V_R.*

Proof. By Theorem 3.12, the receiver placement V_R is valid if the triangular semilattice network $\triangledown_n$ with the labels in V_R is distributed. It is evident that being distributed is a property of the labeled network which is preserved by rotation or reflection of the labels. So it holds that $V_{\rho(R)}$ and $V_{\sigma(R)}$ are valid if and only if V_R is valid.

Let N be an $\mathbb{F}_q$-labeling of the triangular semilattice network $\triangledown_n$ with side receivers. Let $V_{\mathcal{S}}$, V_ℓ and V_r in V refer to the placements of the sources, the left receiver and the right receiver respectively. It holds that

$$V_{\rho(\ell)} = V_r \quad \text{and} \quad V_{\rho(r)} = V_{\mathcal{S}}, \tag{1}$$

$$V_{\sigma(\ell)} = V_r \quad \text{and} \quad V_{\sigma(\mathcal{S})} = V_{\mathcal{S}}. \tag{2}$$

Let V_R be a valid receiver placement and let N be an $\mathbb{F}_q$-labeling. Let N_v denote the column of N corresponding to vector $v \in V$ and N_T denote the submatrix of N with columns indexed by $T \subseteq V$. Let N^ρ be the matrix defined by the relation $N^\rho_v := N_{\rho^{-1}(v)}$. Up to a multiplication of an invertible $|\mathcal{S}| \times |\mathcal{S}|$ matrix, N^ρ is an $\mathbb{F}_q$-labeling of $\triangledown_n$ with side receivers and receiver placement $V_{\rho(R)}$. In fact, by (1), $N^\rho_{\mathcal{S}}$, N^ρ_ℓ, N^ρ_r and $N^\rho_{V_{\rho(R)}}$ are invertible since, up to reordering of the columns, they correspond to matrices N_r, $N_{\mathcal{S}}$, N_ℓ and N_{V_R}. Similar reasoning works for the reflection map σ. $\square$

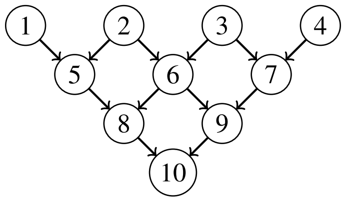

Figure 9. The triangular semilattice network $\triangledown_4$.

4. Complete study of triangular semilattice network up to four sources

We now will demonstrate various properties relating to the receiver placements and minimum field sizes required to solve the $\mathbb{F}_q$-labeling conditions for the triangle semilattice network on small lengths.

The triangular semilattice networks $\triangledown_2$ ***and*** $\triangledown_3$. The 2-semilattice has three different valid receiver placements and is trivially solvable over $\mathbb{F}_2$. Note that it is the code graph for the butterfly network.

The 3-semilattice has 17 different valid receiver placements. Excluding the receiver placement corresponding to the three corner nodes, all valid receiver placements have one term in their associated minors. Therefore, any choice of receiver placements that does not include the receiver placement corresponding to the three corner nodes is solvable over $\mathbb{F}_2$ by assigning all of the variables a value of 1. When receiver placements are chosen to include those receiver placements along the left-side, along the right-side, and corresponding to the three corner nodes, $\mathbb{F}_2$ will cause one associated minor to equal zero, so the minimum field size over which the network is solvable is $\mathbb{F}_3$.

The triangular semilattice network $\triangledown_4$. The triangular semilattice network $\triangledown_4$, see Figure 9, has 150 possible receiver placements. Through exhaustion, we know that $\mathbb{F}_5$ is sufficient for $\triangledown_4$ to be solvable when all 150 receiver placements are considered. We consider $\triangledown_4$ together with the side receivers and we find the solvability of the network by increasing its receivers.

Proposition 4.1. *The semilattice network* $\triangledown_4$ *together with any two receivers is solvable over* $\mathbb{F}_q$ *for* $q \leq 3$.

Proof. First recall that having $\{1, 5, 8, 10\}$ and $\{4, 7, 9, 10\}$ as receiver placements forces every transfer coefficient of $\triangledown_4$ to be nonzero as shown in Proposition 3.13. Moreover, let V_R be a receiver placement; then, from Corollary 2.11, $\det(N_R) \in \mathbb{F}_q[\alpha_j^{(i)} \mid i \in [6],\ j \in [2]]$ is a multivariate polynomial with at most three terms.

Let $[i, j]$ for $1 \leq i \leq j \leq 3$ represents the number of terms of the minors corresponding to the two further receivers, where we assume $i \leq j$ without loss of generality. We are going to prove the theorem by working through the different cases.

Case 1: [1, 1], [1, 3], [3, 3]: The minors all have odd numbers of terms and by setting all variables to 1 over $\mathbb{F}_2$, the value of every minor is then 1.

Case 2: [1, 2], [2, 2]: Setting all variables to 1 over $\mathbb{F}_3$, the value of the 1-term minor would be 1 and the value of the 2-term minor(s) would be 2.

Case 3: [2, 3]: This case is not solvable over $\mathbb{F}_2$ since then the 2-term minor is 0. We prove that this case is solvable over $\mathbb{F}_3$ by contradiction; assume that for every evaluation point $\mathsf{a} = (\mathsf{a}_j^{(i)} \mid i \in [6],\ j \in [2]) \in \mathbb{F}_3^{12}$ without zero entries at least one of the minors is zero.

Since all transfer coefficients must be nonzero, without loss of generality we can denote the minors as $A + B$ and $C + D + E$, where A, B and C, D, E are terms with no common factor respectively. In the following, swapping a nonzero value $a \in \mathbb{F}_3$ corresponds to taking the value $2a \in \mathbb{F}_3$.

(i) Let $\mathsf{a} \in \mathbb{F}_3^{12}$ be such that $(A+B)(\mathsf{a}) = (C+D+E)(\mathsf{a}) = 0$ and $\alpha_j^{(i)}$ be a variable in $C + D + E$. Define $\mathsf{a}' \in \mathbb{F}_3^{12}$ to be equal to a except for $\mathsf{a}_j^{(i)}$, which is swapped; then $(C + D + E)(\mathsf{a}') \neq 0$. If the same $\alpha_j^{(i)}$ appears in $A + B$ as well, we have $(A + B)(\mathsf{a}') \neq 0$, a contradiction. If no variable in $C + D + E$ appears in $A + B$, instead define $\mathsf{a}' \in \mathbb{F}_3^{12}$ from a by swapping two values of it corresponding to some variable in $A + B$ and to some variable in $C + D + E$ independently to again get $(C + D + E)(\mathsf{a}') \neq 0,\ (A + B)(\mathsf{a}') \neq 0$, a contradiction.

(ii) Let instead for all $\mathsf{a} \in \mathbb{F}_3^{12}$ exactly one of $(A + B)(\mathsf{a})$ and $(C + D + E)(\mathsf{a})$ be 0.

Note that all variables in $A + B$ must appear in $C + D + E$; assume for the sake of contradiction that there is some variable $\alpha_j^{(i)}$ which appears in $A+B$ which does not appear in $C + D + E$. Then, if $(A + B)(\mathsf{a}) = 0$ and $(C + D + E)(\mathsf{a}) \neq 0$, the evaluation point $\mathsf{a}' \in \mathbb{F}_3^{12}$ defined from a by swapping the value of $\mathsf{a}_j^{(i)}$ produces $(A+B)(\mathsf{a}') \neq 0$ and $(C + D + E)(\mathsf{a}') \neq 0$, a contradiction. If $(C + D + E)(\mathsf{a}) = 0$, $(A + B)(\mathsf{a}) \neq 0$, then taking $\mathsf{a}' \in \mathbb{F}_3^{12}$ defined from a by swapping the value of $\mathsf{a}_j^{(i)}$ produces $(A + B)(\mathsf{a}') = 0,\ (C + D + E)(\mathsf{a}') = 0$, again a contradiction of item (i). This proves that all variables in $A + B$ must appear in $C + D + E$.

Let $\mathsf{a} \in \mathbb{F}_3^{12}$ be such that $(A + B)(\mathsf{a}) = 0$ and $(C + D + E)(\mathsf{a}) \neq 0$. Then if a' is obtained by a by swapping one of the values corresponding to a variable contained in $A + B$, then $(A + B)(\mathsf{a}') \neq 0$ and $(C + D + E)(\mathsf{a}') = 0$.

Without loss of generality we can focus on the case where $\mathsf{a} \in \mathbb{F}_3^{12}$ is such that $(A + B)(\mathsf{a}) \neq 0$ and $(C + D + E)(\mathsf{a}) = 0$.

- Consider now the case where there exists a variable $\alpha_j^{(i)}$ which appears in $C+D+E$ but not in $A + B$ and define $\mathsf{a}' \in \mathbb{F}_3^{12}$ from a by swapping the value of $\mathsf{a}_j^{(i)}$. Then, $(A + B)(\mathsf{a}') \neq 0$ and $(C + D + E)(\mathsf{a}') \neq 0$, a contradiction.

- Consider instead the case where $A + B$ and $C + D + E$ share the same set of variables. Let $\mathsf{a} \in \mathbb{F}_3^{12}$ be a root of $C + D + E$. As each swap changes whether $A + B$

is nonzero, if $\mathsf{a}' \in \mathbb{F}_3^{12}$ is obtained from a by swapping the values of two distinct variables $\alpha_{j_1}^{(i_1)}, \alpha_{j_2}^{(i_2)}$ contained in $C+D+E$, we get back to $(C+D+E)(\mathsf{a}') = 0$. Indeed, either the distinct variables appear in the same terms or they partition the terms. Note that two such variables $\alpha_{j_1}^{(i_1)}, \alpha_{j_2}^{(i_2)}$ partitioning the terms exist since we cannot have everything sharing the same terms by assumption. Then, we are able to partition all variables as to whether they share a term with $\alpha_{j_1}^{(i_1)}$ or $\alpha_{j_2}^{(i_2)}$, so we can represent our sum in the form of $C+C+E$. This is impossible as the minor is formed by a sum of the product of transfer coefficients over different sets of paths, while the repetition of C corresponds to a repeated set of paths. □

We can also characterize some sets of receivers in the 4-semilattice which require a larger field size.

Proposition 4.2. *There exists a choice of three receivers of the semilattice network ∇_4 which is not solvable over $\mathbb{F}_q$ for $q \le 3$ but it is over $\mathbb{F}_4$.*

Proof. We prove that there is no evaluation point $\mathsf{a} \in \mathbb{F}_q^{12}$ without zero entries for $q = 2, 3$ such that the minors related to receiver placements $\{2, 5, 7, 10\}$, $\{2, 4, 9, 10\}$, $\{1, 4, 5, 10\}$ are simultaneously nonzero. It holds that

$$\begin{aligned}
\det(N_{\{2,5,7,10\}}) &= \alpha_1^{(1)}\alpha_2^{(2)}\alpha_2^{(3)}\alpha_2^{(4)}\alpha_1^{(6)} + \alpha_1^{(1)}\alpha_2^{(2)}\alpha_2^{(3)}\alpha_1^{(5)}\alpha_2^{(6)} = A+B,\\
\det(N_{\{2,4,9,10\}}) &= \alpha_1^{(1)}\alpha_2^{(2)}\alpha_1^{(4)}\alpha_1^{(5)}\alpha_1^{(6)} + \alpha_1^{(1)}\alpha_1^{(3)}\alpha_1^{(4)}\alpha_2^{(5)}\alpha_1^{(6)} = C+D,\\
\det(N_{\{1,4,5,10\}}) &= \alpha_2^{(1)}\alpha_2^{(2)}\alpha_2^{(4)}\alpha_1^{(6)} + \alpha_2^{(1)}\alpha_2^{(2)}\alpha_1^{(5)}\alpha_2^{(6)} + \alpha_2^{(1)}\alpha_1^{(3)}\alpha_2^{(5)}\alpha_2^{(6)}\\
&= \alpha_2^{(1)} \frac{(A+B)(C+D) - AD}{(\alpha_1^{(1)})^2\alpha_2^{(2)}\alpha_2^{(3)}\alpha_1^{(4)}\alpha_1^{(5)}\alpha_1^{(6)}}.
\end{aligned}$$

It is enough to show at least one of the three polynomials of the forms $A+B$, $C+D$ and $(A+B)(C+D)-AD$ evaluate to zero. Over $\mathbb{F}_2$, note that $(A+B)(\mathsf{a}) = 1+1 = 0$. Over $\mathbb{F}_3$, if either $(A+B)(\mathsf{a}) = 0$ or $(C+D)(\mathsf{a}) = 0$, we are done. Otherwise, if there exists $\mathsf{a} \in \mathbb{F}_3^{12}$ such that $(A+B)(\mathsf{a}) \ne 0$ and $(C+D)(\mathsf{a}) \ne 0$, then $A(\mathsf{a}) = B(\mathsf{a})$ and $C(\mathsf{a}) = D(\mathsf{a})$. It follows that

$$((A+B)(C+D) - AD)(\mathsf{a}) = ((2A)(2D))(\mathsf{a}) - (AD)(\mathsf{a}) = (AD - AD)(\mathsf{a}) = 0.$$

A solution over $\mathbb{F}_4 = \mathbb{F}_2/(a^2+a+1)$ for ∇_4 with receiver placements $\{2, 5, 7, 10\}$, $\{2, 4, 9, 10\}$ and $\{1, 4, 5, 10\}$ is

$$\mathsf{a} = (1, a+1, a+1, a+1, a, a, a+1, a+1, a, 1, a, a) \in \mathbb{F}_4^{12}. \qquad \square$$

By exhaustive search, there exist 324 choices of three receiver placements (fixing the sides) that require a minimum field size of $\mathbb{F}_4$ to be solved. Also through exhaustive search, we know that any selection of up to five receiver placements is solvable over $\mathbb{F}_4$ or a smaller finite field.

Proposition 4.3. *There exists a choice of six receivers of the semilattice network* ∇_4 *which is not solvable over* $\mathbb{F}_q$ *for* $q \leq 4$ *but it is over* $\mathbb{F}_5$.

Proof. We prove that there is no evaluation point $\mathsf{a} \in \mathbb{F}_q^{12}$ without zero entries for $q \leq 4$ such that the minors related to receiver placements

$$\{1,2,4,9\},\quad \{1,3,4,8\},\quad \{2,5,7,10\},\quad \{1,4,8,9\},\quad \{1,4,5,10\},\quad \{1,3,4,10\}$$

are simultaneously nonzero. It holds that

$$\begin{aligned}
\det(N_{\{1,2,4,9\}}) &= \alpha_2^{(2)}\alpha_1^{(5)} + \alpha_1^{(3)}\alpha_2^{(5)} = A + B,\\
\det(N_{\{1,3,4,8\}}) &= \alpha_2^{(1)}\alpha_1^{(4)} + \alpha_1^{(2)}\alpha_2^{(4)} = C + D,\\
\det(N_{\{2,5,7,10\}}) &= \alpha_1^{(1)}\alpha_2^{(2)}\alpha_2^{(3)}\alpha_2^{(4)}\alpha_1^{(6)} + \alpha_1^{(1)}\alpha_2^{(2)}\alpha_2^{(3)}\alpha_1^{(5)}\alpha_2^{(6)} = E + F,\\
\det(N_{\{1,4,8,9\}}) &= \alpha_2^{(1)}\alpha_2^{(2)}\alpha_1^{(4)}\alpha_1^{(5)} + \alpha_2^{(1)}\alpha_1^{(3)}\alpha_1^{(4)}\alpha_2^{(5)} + \alpha_1^{(2)}\alpha_1^{(3)}\alpha_2^{(4)}\alpha_2^{(5)}\\
&= (A+B)(C+D) - AD,\\
\det(N_{\{1,4,5,10\}}) &= \alpha_2^{(1)}\alpha_2^{(2)}\alpha_2^{(4)}\alpha_1^{(6)} + \alpha_2^{(1)}\alpha_2^{(2)}\alpha_1^{(5)}\alpha_2^{(6)} + \alpha_2^{(1)}\alpha_1^{(3)}\alpha_2^{(5)}\alpha_2^{(6)}\\
&= \alpha_2^{(1)}\frac{(A+B)(E+F) - BE}{\alpha_1^{(1)}\alpha_2^{(2)}\alpha_2^{(3)}\alpha_1^{(5)}},\\
\det(N_{\{1,3,4,10\}}) &= \alpha_2^{(1)}\alpha_1^{(4)}\alpha_1^{(6)} + \alpha_1^{(2)}\alpha_2^{(4)}\alpha_1^{(6)} + \alpha_1^{(2)}\alpha_1^{(5)}\alpha_2^{(6)}\\
&= \frac{(C+D)(E+F) - CF}{\alpha_1^{(1)}\alpha_2^{(2)}\alpha_2^{(3)}\alpha_2^{(4)}}.
\end{aligned}$$

The cases of $q = 2, 3$ follow from Proposition 4.2 by just considering $A+B$, $C+D$, $(A+B)(C+D) - AD$. Let $\mathbb{F}_4 = \mathbb{F}_2/(a^2+a+1)$ and $\mathsf{a} \in \mathbb{F}_4^{12}$ be such that $(A+B)(\mathsf{a}) \neq 0$, $(C+D)(\mathsf{a}) \neq 0$ and $(D+E)(\mathsf{a}) \neq 0$. Since a is not a zero of A, C, E, we can normalize the sums

$$\begin{aligned}
(A+B)(\mathsf{a}) &= A(\mathsf{a})(1+b'),\\
(C+D)(\mathsf{a}) &= C(\mathsf{a})(1+d'),\\
(E+F)(\mathsf{a}) &= E(\mathsf{a})(1+f'),
\end{aligned}$$

where $b', d', f' \in \mathbb{F}_4^*$. It also holds that

$$\begin{aligned}
\frac{((A+B)(C+D) - AD)(\mathsf{a})}{(AC)(\mathsf{a})} &= (1+b')(1+d') - d' = 1 + b' + b'd',\\
\frac{((A+B)(E+F) - BE)(\mathsf{a})}{(AE)(\mathsf{a})} &= (1+b')(1+f') - b' = 1 + f' + b'f',\\
\frac{((C+D)(E+F) - CF)(\mathsf{a})}{(CE)(\mathsf{a})} &= (1+d')(1+f') - f' = 1 + d' + d'f'.
\end{aligned}$$

If any of $1+b'$, $1+d'$, $1+f'$ are 0, then we are done. Otherwise if all of $1+b'$, $1+d'$, $1+f'$ are nonzero, then $b', d', f' \in \{a, a+1\}$, and by the pigeonhole principle we have that two of them are equal. Without loss of generality, let $b'=d'$; then note that

$$1+b'+b'd' = 1+b'+(b')^2 = 0$$

by the field equation, which implies

$$((A+B)(C+D)-AD)(\mathsf{a}) = 0.$$

A solution over $\mathbb{F}_5$ for $\triangledown_4$ with receiver placements $\{1,2,4,9\}$, $\{1,3,4,8\}$, $\{2,5,7,10\}$, $\{1,4,8,9\}$, $\{1,4,5,10\}$ and $\{1,3,4,10\}$ is

$$\mathsf{a} = (1,4,3,1,1,4,4,1,4,3,3,2) \in \mathbb{F}_5^{12}. \qquad \square$$

We have also found that there exist 8748 choices of six receiver placements that are solvable over minimum field size of $\mathbb{F}_5$.

Valid receiver placements and field sizes' implementations. Valid receiver placements for triangular semilattice networks $\triangledown_n$ for n up to 9 were calculated based on Theorem 3.12 using Python and SML (see Table 1).

To calculate whether a set of receiver placements is solvable for a given field size, we first calculate the minors corresponding to the receiver placements and multiply them together to get a polynomial f. As in the proof of the linear network coding theorem in [Médard and Sprintson 2011], we have a nonzero solution for all of these minors if and only if f has a nonzero root. This is also true if and only if the remainder of f modulo $(x_i^q - x_i \mid i \in [n])$ in $\mathbb{F}_q$ is nonzero [Geil et al. 2008, Proposition 2]. The largest possible minimum field size required for any set of receiver placements for $\triangledown_4$ and $\triangledown_5$ has been computed implementing this method on MAGMA [Bosma et al. 1997].

length	valid	invalid	total
1	1	0	1
2	3	0	3
3	17	3	20
4	150	60	210
5	1848	1155	3003
6	29636	24628	54264
7	589362	594678	1184040
8	14032452	16227888	30260340
9	389622192	496540943	886163135

Table 1. Number of valid receiver placements.

Acknowledgments

The authors are grateful to Clemson University for hosting the REU at which this work was completed. The REU was made possible by an NSF Research Training Group (RTG) grant (DMS #1547399) promoting coding theory, cryptography, and number theory at Clemson.

References

[Ahlswede et al. 2000] R. Ahlswede, N. Cai, S.-Y. R. Li, and R. W. Yeung, "Network information flow", *IEEE Trans. Inform. Theory* **46**:4 (2000), 1204–1216. MR Zbl

[Anderson et al. 2017] S. E. Anderson, W. Halbawi, N. Kaplan, H. H. López, F. Manganiello, E. Soljanin, and J. L. Walker, "Representations of the multicast network problem", pp. 1–23 in *Algebraic geometry for coding theory and cryptography*, edited by E. W. Howe et al., Assoc. Women Math. Ser. **9**, Springer, 2017. MR Zbl

[Bosma et al. 1997] W. Bosma, J. Cannon, and C. Playoust, "The Magma algebra system, I: The user language", *J. Symbolic Comput.* **24**:3-4 (1997), 235–265. MR Zbl

[Fragouli and Soljanin 2006] C. Fragouli and E. Soljanin, "Information flow decomposition for network coding", *IEEE Trans. Inform. Theory* **52**:3 (2006), 829–848. MR Zbl

[Geil et al. 2008] O. Geil, R. Matsumoto, and C. Thomsen, "On field size and success probability in network coding", pp. 157–173 in *Arithmetic of finite fields*, edited by J. von zur Gathen et al., Lecture Notes in Comput. Sci. **5130**, Springer, 2008. MR Zbl

[Jaggi et al. 2005] S. Jaggi, P. Sanders, P. A. Chou, M. Effros, S. Egner, K. Jain, and L. M. G. M. Tolhuizen, "Polynomial time algorithms for multicast network code construction", *IEEE Trans. Inform. Theory* **51**:6 (2005), 1973–1982. MR

[Koetter and Médard 2003] R. Koetter and M. Médard, "An algebraic approach to network coding", *IEEE/ACM Trans. Networking* **11**:5 (2003), 782–795.

[Li et al. 2003] S.-Y. R. Li, R. W. Yeung, and N. Cai, "Linear network coding", *IEEE Trans. Inform. Theory* **49**:2 (2003), 371–381. MR Zbl

[Médard and Sprintson 2011] M. Médard and A. Sprintson, *Network coding: fundamentals and applications*, Academic, Amsterdam, 2011.

[Sun et al. 2015] Q. T. Sun, X. Yin, Z. Li, and K. Long, "Multicast network coding and field sizes", *IEEE Trans. Inform. Theory* **61**:11 (2015), 6182–6191. MR Zbl

Received: 2019-01-14 Revised: 2019-07-03 Accepted: 2019-08-31

angelina_grosso@brown.edu — *Division of Applied Mathematics, Brown University, Providence, RI, United States*

manganm@clemson.edu — *School of Mathematical and Statistical Sciences, Clemson University, Clemson, SC, United States*

varal.shiwani@gmail.com — *Faculty of Business, Law and Politics, University of Hull, Hull, United Kingdom*

e9zhu@ucsd.edu — *Department of Mathematics, University of California at San Diego, La Jolla, CA, United States*

INVOLVE 12:8 (2019)
dx.doi.org/10.2140/involve.2019.12.1329

Edge-transitive graphs and combinatorial designs

Heather A. Newman, Hector Miranda,
Adam Gregory and Darren A. Narayan

(Communicated by Anant Godbole)

A graph is said to be edge-transitive if its automorphism group acts transitively on its edges. It is known that edge-transitive graphs are either vertex-transitive or bipartite. We present a complete classification of all connected edge-transitive graphs on less than or equal to 20 vertices. We investigate biregular bipartite edge-transitive graphs and present connections to combinatorial designs, and we show that the Cartesian products of complements of complete graphs give an additional family of edge-transitive graphs.

1. Introduction

A graph is vertex-transitive (edge-transitive) if its automorphism group acts transitively on its vertex (edge) set. We note the alternative definition given in [Andersen et al. 1992].

Theorem 1 (Andersen, Ding, Sabidussi, and Vestergaard). *A finite simple graph G is edge-transitive if and only if $G - e_1 \cong G - e_2$ for all pairs of edges e_1 and e_2.*

We also mention the following well-known result, which appears as Proposition 15.1 in [Biggs 1974].

Proposition 2. *If G is an edge-transitive graph, then G is either vertex-transitive or bipartite; in the latter case, vertices in a given part belong to the same orbit of the automorphism group of G on vertices.*

Given a graph G we will denote its vertex set by $V(G)$ and edge set by $E(G)$. We will use K_n to denote the complete graph with n vertices, and $K_{m,n}$ to denote the complete bipartite graph with m vertices in one part and n in the other. The path on n vertices will be denoted by P_n and the cycle on n vertices by C_n. The disjoint union of t copies of a graph H will be denoted by tH. The cube on n vertices will be denoted by Q_n. The complement of a graph G will be denoted by $\overline{G}$. For any undefined notation, please see [West 2001].

MSC2010: 05C25.
Keywords: edge-transitive, combinatorial designs.

Definition 3. A graph is regular if all of its vertices have the same degree. A bipartite graph is said to be biregular if all vertices on the same side of the bipartition have the same degree. Particularly, we refer to a bipartite graph with parts of size m and n as an (r, s)-biregular subgraph of $K_{m,n}$ if the m vertices in the same part each have degree r and the n vertices in the same part each have degree s.

It follows from Proposition 2 that bipartite edge-transitive graphs are biregular.

Definition 4. Given a group G and generating set S, the Cayley graph $\Gamma(G, S)$ is a graph with vertex set $V(\Gamma)$ and edge set

$$E(\Gamma) = \{\{x, y\} \mid x, y \in V(\Gamma), \text{there exists an integer } s \text{ in } S \text{ such that } y = xs\}.$$

It is known that all Cayley graphs are vertex-transitive. Next we recall a specialized class of Cayley graphs known as circulant graphs.

Definition 5. A circulant graph $C_n(L)$ is a graph on vertices $v_1, v_2, \ldots, v_n$ where each v_i is adjacent to $v_{(i+j) \pmod n}$ and $v_{(i-j) \pmod n}$ for each j in a list L. Algebraically, circulant graphs are Cayley graphs of finite cyclic groups. For a list L containing m items, we refer to $C_n(L)$ as an m-circulant. We say an edge e is a chord of length k when $e = v_i v_j$, $|i - j| \equiv k \pmod n$.

In our next definition we present another family of vertex-transitive graphs.

Definition 6. A wreath graph, denoted by $W(n, k)$, has n sets of k vertices each, arranged in a circle where every vertex in set i is adjacent to every vertex in bunches $i+1$ and $i-1$. More precisely, its vertex set is $\mathbb{Z}_n \times \mathbb{Z}_k$ and its edge set consists of all pairs of the form $\{(i, r), (i+1, s)\}$.

It was proved in [Onkey 1995] that all wreath graphs are edge-transitive. We next recall the definition of the line graph which we use later to show that certain graph families are edge-transitive.

Definition 7. Given a graph G, the line graph $L(G)$ is a graph where $V(L(G)) = E(G)$ and two vertices in $V(L(G))$ are adjacent in $L(G)$ if and only if their corresponding edges are incident in G.

Finally we recall the operation of the Cartesian product of graphs.

Definition 8. Given two graphs H and K, with vertex sets $V(H)$ and $V(K)$, the Cartesian product $G = H \times K$ is a graph where

$$V(G) = \{(u_i, v_j) \mid u_i \in V(H) \text{ and } v_j \in V(K)\}$$

and $\{(u_i, v_j), (u_k, v_l)\} \in E(G)$ if and only if $i = k$ and v_j and v_l are adjacent in K or $j = l$ and u_i and u_k are adjacent in H.

The properties vertex-transitive and edge-transitive are distinct. This is clear with the following examples:

- K_n, $n \geq 2$, is both vertex-transitive and edge-transitive.
- $C_n(1, 2)$, $n \geq 6$, is vertex-transitive, but not edge-transitive.
- $K_{1,n-1}$ is not vertex-transitive, but is edge-transitive.
- P_n, $n \geq 4$, is neither vertex-transitive nor edge-transitive.

However the two properties are linked, as is evident from the following proposition, which is a consequence of results of [Whitney 1932; Sabidussi 1961].

Proposition 9. *A connected graph is edge-transitive if and only if its line graph is vertex-transitive.*

Note, however, that a graph may not be the line graph of some original graph. For example, $K_{1,3} \times C_4$ is vertex-transitive, but it follows by a theorem of [Beineke 1968] that this graph is not the line graph of some graph.

We used the databases from Brendan McKay[1] to obtain all connected edge-transitive graphs on 20 vertices or less. We then reported the number of edge-transitive graphs up to 20 vertices to the Online Encyclopedia of Integer Sequences, and they are listed under sequence #A095424. The full classification of these graphs is given in the online supplement. We can extrapolate much from this data and these results are presented in this paper. It was recently brought to our attention that Marston Conder and Gabriel Verret independently determined the edge-sets of the connected edge-transitive bipartite graphs on up to 63 vertices[2] using the Magma system, and a complete list of all connected edge-transitive graphs on up to 47 vertices[3] with their edge sets.[4] In our paper we provide additional details about these graphs, allowing us to generalize some cases to infinite families of graphs.

We note the following graph families are edge-transitive: K_n, $n \geq 2$; C_n, $n \geq 3$; $K_{n,n}$ minus a perfect matching; K_{2n} minus a perfect matching; and all complete bipartite graphs $K_{t,n-t}$, $1 \leq t \leq \lfloor \frac{n}{2} \rfloor$. Wreaths [Onkey 1995] and Kneser graphs [Godsil and Royle 2001, pp. 135–161] are also edge-transitive. Besides these predictable and apparent cases, we can identify other infinite families of edge-transitive graphs, using the data up through 20 vertices.

We say that H is an (r, s)-biregular subgraph of $K_{m,n}$ if H is bipartite graph with degrees r and s. In Section 2 of this paper we begin by exploring the problem of

[1] http://users.cecs.anu.edu.au/∼bdm/data/graphs.html
[2] https://www.math.auckland.ac.nz/∼conder/AllSmallETBgraphs-upto63-summary.txt
[3] https://www.math.auckland.ac.nz/∼conder/AllSmallETgraphs-upto47-summary.txt
[4] https://www.math.auckland.ac.nz/∼conder/AllSmallETgraphs-upto47-full.txt

determining which values of m, n, r, s, where $mr = ns$, result in a (connected) (r, s)-biregular subgraph of $K_{m,n}$ that is edge-transitive. In Section 2.1, we investigate bipartite edge-transitive graphs where one of the two vertex degrees in G is 2.

Connections between balanced incomplete block designs and graphs are well-known. For some recent papers, see [Abueida and Pike 2013; Mamut et al. 2004; McKay and Pike 2007]. In Section 2.2, we investigate connections between edge-transitive graphs and balanced incomplete block designs.

2. Connected bipartite graphs

Given positive integers m and n, we first describe which values of r and s are possible for an (r, s)-biregular subgraph of $K_{m,n}$. Note that if $\gcd(m, n) = 1$, the only biregular subgraph of $K_{m,n}$ is $K_{m,n}$.

Proposition 10. *An (r, s)-biregular subgraph of $K_{m,n}$ satisfies*

$$mr = ns,$$
$$r = \frac{n}{\gcd(m,n)}k, \quad k = 1, 2, \ldots, \gcd(m, n).$$

Proof. We know

$$s = \frac{mr}{n} = \frac{m/\gcd(m,n)}{n/\gcd(m,n)}r,$$

and since

$$\gcd\left(\frac{m}{\gcd(m,n)}, \frac{n}{\gcd(m,n)}\right) = 1,$$

r is a multiple of $n/\gcd(m, n)$ (and is less than or equal to n). □

Corollary 11. *If $\gcd(m, n) = 2$, there are only two possible pairs (r, s), namely, $(r, s) = \left(\frac{n}{2}, \frac{m}{2}\right)$ and $(r, s) = (n, m)$. The latter case is the complete bipartite graph $K_{m,n}$.*

We now introduce a construction for generating nontrivial edge-transitive (connected) bipartite subgraphs of $K_{m,n}$ for $\gcd(m, n) > 2$. This construction involves a process of extending a nontrivial edge-transitive (connected) bipartite graph to a larger one, which we describe in the following lemma.

Lemma 12. *Let G be an edge-transitive (connected) (r, s)-biregular subgraph of $K_{m,n}$. Then, for any positive integers a, b, and r, the subgraph G can be extended to an edge-transitive (connected) (ra, sb)-biregular subgraph of $K_{mb,na}$.*

Proof. It suffices to show that, by letting G be a (connected) edge-transitive (r, s)-biregular subgraph of $K_{m,n}$, we can build a (connected) edge-transitive graph H that is an $(r, 2s)$-biregular subgraph of $K_{2m,n}$. Let G consist of partite sets A, B,

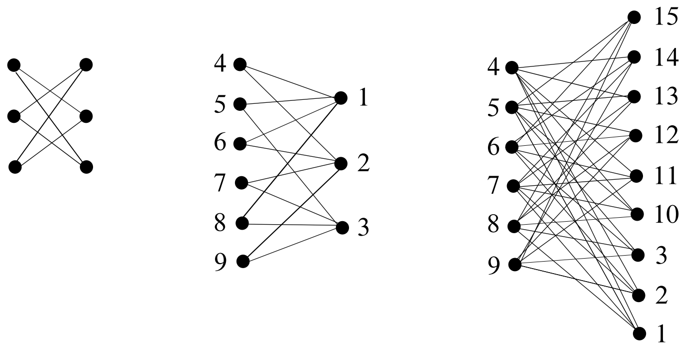

Figure 1. An example of the construction in the theorem, with vertices drawn in the same color being vertices that are connected to the graph in the same way.

where $A = \{a_1, a_2, \ldots, a_m\}$ and $B = \{b_1, b_2, \ldots, b_n\}$. Now create the set $A' = \{a_1, a_2, \ldots, a_m, a'_1, a'_2, \ldots, a'_m\}$ and create a graph H with partite sets A' and B as follows. For each a_i, let $N_H(a_i) = N_G(a_i)$. For each a'_i, let $N_H(a'_i) = N_G(a_i)$. Then by construction, H is a (connected) $(r, 2s)$-biregular subgraph of $K_{2m,n}$. Since G is edge-transitive, H is edge-transitive by construction. □

It turns out we can use the results above to state the following general theorem.

Theorem 13. *Let* $\gcd(m,n) > 2$. *Then there exists a noncomplete edge-transitive* (*connected*) *subgraph of* $K_{m,n}$.

Proof. We appeal to the construction in the preceding lemma, and consider the following two cases. It may be helpful to refer to Figure 1.

Case 1: $m \mid n$. Then $n = mk$ for some positive integer k. Let G be the graph that results from removing a perfect matching from $K_{m,m}$. Then G is connected, biregular, and edge-transitive but not complete. Repeating the construction in the lemma $k-1$ times, we obtain a subgraph of $K_{m,mk} = K_{m,n}$ that is connected, biregular, edge-transitive, and not complete.

Case 2: $m \nmid n$. Let $l = \gcd(m,n)$ and $m = k_1 l$, $n = k_2 l$. Let G be the graph that results from removing a perfect matching from $K_{l,l}$. Then G is connected, biregular, and edge-transitive but not complete. Following the construction in the lemma, increase the left partite set by l vertices $k_1 - 1$ times and the right partite set by l vertices $k_2 - 1$ times. The resulting graph will be a connected, biregular, and edge-transitive subgraph of $K_{k_1 l, k_2 l} = K_{m,n}$ but not complete. □

Remark 14. Theorem 13 gives rise to the following observations/questions:

- When $\gcd(m,n) = 1$, the only possible (connected) biregular subgraph is the complete graph $K_{m,n}$.

• When $\gcd(m,n) = 2$, the method fails because the only connected, biregular subgraph of $K_{2,2}$ is $K_{2,2}$, and we seek a noncomplete bipartite graph.

• When $\gcd(m,n) = 2$, under what additional conditions does the theorem still hold?

2.1. ***Edge-transitive (connected) $(r,2)$-biregular subgraphs of $K_{m,n}$.*** We now investigate bipartite edge-transitive graphs where one of the two vertex degrees in G is 2. We will provide a construction for some graphs in this family. As pointed out by a referee, such a graph G can be obtained by subdividing every edge of another multigraph F. Here F is formed by taking a complete graph on m vertices and "cloning" each of its edges a fixed number of times. Let F be the graph with m vertices and t edges between each pair of distinct vertices. This forms a multigraph with m vertices and $s = t\binom{m}{2}$ edges. Subdividing each edge yields a bipartite subgraph of $K_{m,s}$ with degrees $(t(m-1), 2)$. We could also create F by taking other arc-transitive graphs and cloning each of the edges a fixed number of times.

Using this construction, in general G is edge-transitive if and only if F is arc-transitive. In these arc-transitive multigraphs, every edge must have the same multiplicity, hence reducing this case to the study of arc-transitive graphs. We formalize these ideas in the following theorem.

Theorem 15. *G is an edge-transitive connected $(r,2)$-biregular subgraph of $K_{m,n}$ if and only if there exists an arc-transitive graph F such that F is obtained by contracting every edge of G.*

Proof. Let G is an edge-transitive connected $(r,2)$-biregular subgraph of $K_{m,n}$. Then any two edges e_1 and e_2 incident to the same vertex in the part of size n are indistinguishable. Then contracting the P_3 with edges e_1 and e_2 results in an edge between vertices in F that is indistinguishable in either direction. Hence F is arc-transitive. For the other direction, using reasoning similar to the above, note that subdividing edges of an arc-transitive graph results in a graph that is edge-transitive. □

We use this theorem for small cases of $|V(G)|$. We first consider the case where $m = 4$. Assume that G is an $(r,2)$-biregular subgraph of $K_{4,n}$. Then F is an arc-transitive multigraph of order 4 with degrees equal to r. Since the only arc-transitive graphs of order 4 are K_4, C_4, and $2P_2$, we know F must be one of these three graphs with each edge cloned a fixed number of times. This will give a complete classification for G. This method can be generalized for cases where all of the arc-transitive graphs of a given order are known.

We next use the same procedure on graphs of up to nine vertices. A list of all of the arc-transitive graphs for small orders (with a minor correction) is found on MathWorld [Weisstein]:

- $|V(G)| = 2$:
  - P_2 with edges cloned $t \geq 2$ times gives a $(t,2)$-biregular subgraph of $K_{2,t}$.
- $|V(G)| = 3$:
  - C_3 with edges cloned $t \geq 2$ times gives a $(2t,2)$-biregular subgraph of $K_{3,3t}$.
- $|V(G)| = 4$:
  - K_4 with edges cloned $t \geq 2$ times gives a $(3t,2)$-biregular subgraph of $K_{4,6t}$.
  - C_4 with edges cloned $t \geq 2$ times gives a $(2t,2)$-biregular subgraph of $K_{4,4t}$.
- $|V(G)| = 5$:
  - K_5 with edges cloned $t \geq 2$ times gives a $(4t,2)$-biregular subgraph of $K_{5,10t}$.
  - C_5 with edges cloned $t \geq 2$ times gives a $(2t,2)$-biregular subgraph of $K_{5,5t}$.
- $|V(G)| = 6$:
  - K_6 with edges cloned $t \geq 2$ times gives a $(5t,2)$-biregular subgraph of $K_{6,15t}$.
  - C_6 with edges cloned $t \geq 2$ times gives a $(2t,2)$-biregular subgraph of $K_{6,6t}$.
  - $C_6(1,2)$ with edges cloned $t \geq 2$ times gives a $(4t,2)$-biregular subgraph of $K_{6,12t}$.
  - $K_{3,3}$ with edges cloned $t \geq 2$ times gives a $(3t,2)$-biregular subgraph of $K_{9,9t}$.
- $|V(G)| = 7$:
  - K_7 with edges cloned $t \geq 2$ times gives a $(6t,2)$-biregular subgraph of $K_{7,21t}$.
  - C_7 with edges cloned $t \geq 2$ times gives a $(4,2)$-biregular subgraph of $K_{7,7t}$.
- $|V(G)| = 8$:
  - K_8 with edges cloned $t \geq 2$ times gives a $(7t,2)$-biregular subgraph of $K_{8,28t}$.
  - C_8 with edges cloned $t \geq 2$ times gives a $(4,2)$-biregular subgraph of $K_{8,8t}$.
  - $C_8(2,4)$ with edges cloned $t \geq 2$ times gives a $(4t,2)$-biregular subgraph of $K_{8,16t}$.
  - $C_8(1,2,3)$ with edges cloned $t \geq 2$ times gives a $(6t,2)$-biregular subgraph of $K_{8,24t}$.
  - Q_8 doubled gives a $(3t,2)$-biregular subgraph of $K_{8,12t}$.
  - $K_{4,4}$ doubled gives a $(4t,2)$-biregular subgraph of $K_{8,16t}$.
- $|V(G)| = 9$:
  - K_9 with edges cloned $t \geq 2$ times gives a $(8t,2)$-biregular subgraph of $K_{9,36t}$.
  - C_9 with edges cloned $t \geq 2$ times gives a $(4,2)$-biregular subgraph of $K_{9,9t}$.
  - $C_3 \times C_3$ doubled gives a $(4t,2)$-biregular subgraph of $K_{9,18t}$.
  - $K_{3,3,3}$ doubled gives a $(8,2t)$-biregular subgraph of $K_{9,36t}$.

We can also state a result of a general nature. For every positive integer n, K_n and C_n are arc-transitive graphs. As a result, we can double K_n to obtain an $(n-1,2)$-biregular subgraph of K_{n,n^2-n} and double C_n to obtain a $(4,2)$-biregular subgraph of $K_{n,2n}$. For even n we can double $K_{\frac{n}{2},\frac{n}{2}}$ to obtain an $(n,2)$-biregular subgraph of $K_{n,2n^2}$. Other graphs will depend on the prime factorization of n.

2.2. *Edge-transitive graphs and combinatorial designs.* We now explore regular and biregular edge-transitive bipartite graphs, where the valences can be larger than 2. In fact we will provide constructions of edge-transitive bipartite graphs where the valences can be made arbitrarily large. We investigate connections between biregular bipartite edge-transitive graphs and combinatorial designs. Here the edge incidences arise directly from the combinatorial structure. We begin by recalling the definition of a balanced incomplete block design (BIBD).

Definition 16. A (v, b, r, k, λ)-BIBD is an arrangement of v objects (varieties) into b blocks such that

(i) each object appears in exactly r blocks,

(ii) each block contains exactly k $(k < v)$ objects, and

(iii) each pair of distinct objects appear together in exactly λ blocks.

A *partially balanced incomplete block design* is a design where λ is not fixed.

A BIBD is called symmetric if $v = b$. Connections are known between the existence of symmetric BIBDs and edge-transitive graphs [Levi 1942; Yang et al. 2016]. A symmetric BIBD is defined for any block design (P, B), where P is the set of points and B is the set of blocks with every edge representing an incident point-block pair (p, B). We note that a projective plane of order n is equivalent to a bipartite graph with two parts each of size $n^2 + n + 1$, where every vertex has degree $n+1$, and every two vertices in the same part have a unique common neighbor. The edge-transitive Levi graphs are incidence graphs of the projective plane. Yang, W. Liu, H. Liu, and Feng [Yang et al. 2016] proved a relationship between incidence graphs and BIBDs. These showed a connection between edge-transitive regular bipartite graphs and flag transitive symmetric block designs.

We note here that connections also exist between nonsymmetric (v, b, r, k, λ)-balanced incomplete block designs and edge-transitive graphs.

Example 17. Consider the $(4, 6, 3, 2, 1)$-block design with blocks

$$\{y_1, y_2\}, \quad \{y_1, y_3\}, \quad \{y_1, y_4\}, \quad \{y_2, y_3\}, \quad \{y_2, y_4\}, \quad \{y_3, y_4\}.$$

This corresponds to the graph in Figure 2 where the edges connect vertices corresponding to the different points in P and different elements of the blocks.

The edge-transitivity of this graph follows from the symmetry as the neighborhoods of the vertices on the left side are the $\binom{4}{2}$ different pairs of the vertices y_1, y_2, y_3, and y_4. As a result the $(4, 6, 3, 2, 1)$-block design corresponds to an edge-transitive $(2, 3)$-biregular subgraph of the complete bipartite graph $K_{6,4}$.

Example 18. Consider the $(5, 10, 4, 2, 1)$-block design with blocks

$$\{y_1, y_2\}, \quad \{y_1, y_3\}, \quad \{y_1, y_4\}, \quad \{y_1, y_5\}, \quad \{y_2, y_3\},$$
$$\{y_2, y_4\}, \quad \{y_2, y_5\}, \quad \{y_3, y_4\}, \quad \{y_3, y_5\}, \quad \{y_4, y_5\}.$$

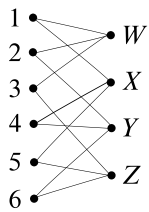

Figure 2. The bipartite graph from Example 17.

This corresponds to an edge-transitive $(2,4)$-biregular subgraph of the complete bipartite graph $K_{10,5}$.

We can generalize the past two examples in the following theorem, where we consider the different subsets of size k from the set $\{y_1, y_2, \dots, y_t\}$.

Theorem 19. *For any $k \in \mathbb{Z}^+$, a $\left(t, \binom{t}{k}, r, k, 1\right)$-balanced incomplete block design forms the incidences of an edge-transitive $K_{\binom{t}{k},t}$ graph.*

Proof. The edge-transitivity of the graph follows from the fact that neighbors of the vertices on the left are the different subsets of k vertices on the right. □

Theorem 19 can be further generalized by replacing each y_i with multiple elements.

Example 20. Using the design from Example 17, we replace each y_i with the elements $y_{i,1}$ and $y_{i,2}$. This creates the design

$$\begin{aligned}
&\big\{\{y_{1,1}, y_{1,2}\}, \{y_{2,1}, y_{2,2}\}\big\}, \quad \big\{\{y_{1,1}, y_{1,2}\}, \{y_{3,1}, y_{3,2}\}\big\},\\
&\big\{\{y_{1,1}, y_{1,2}\}, \{y_{4,1}, y_{4,2}\}\big\}, \quad \big\{\{y_{2,1}, y_{2,2}\}, \{y_{3,1}, y_{3,2}\}\big\},\\
&\big\{\{y_{2,1}, y_{2,2}\}, \{y_{4,1}, y_{4,2}\}\big\}, \quad \big\{\{y_{3,1}, y_{3,2}\}, \{y_{4,1}, y_{4,2}\}\big\}.
\end{aligned}$$

This will correspond to a $\left(2t, \binom{t}{k}, \frac{(t-1)!}{(k-1)!\,(t-k)!}, 2k, \lambda\right)$-partially balanced incomplete block design which forms the incidences of an edge-transitive $K_{\binom{t}{k},2t}$ graph.

In general we can replace each y_i with the elements $y_{i,1}, y_{i,2}, \dots, y_{i,s}$ to form a larger class of edge-transitive graphs.

Theorem 21. *For integers $k \geq 1$ and $s \geq 0$ a $\left(st, \binom{t}{k}, \frac{(t-1)!}{(k-1)!\,(t-k)!}, sk, \lambda\right)$-partially balanced incomplete block design forms the incidences of an edge-transitive $K_{\binom{t}{s},kt}$ graph.*

In Example 18 we provided an example of a $(2,4)$-biregular subgraph of the complete bipartite graph $K_{10,5}$ that corresponded a $(5,10,4,2,1)$-block design. We can form a second $(2,4)$-biregular subgraph of the complete bipartite graph $K_{10,5}$ (nonisomorphic to the first) by starting with a different block design. Let the blocks of this design be

$$B_1=\{y_1,y_3\},\quad B_3=\{y_1,y_5\},\quad B_5=\{y_2,y_3\},\quad B_7=\{y_2,y_4\},\quad B_9=\{y_4,y_5\},$$
$$B_2=\{y_1,y_3\},\quad B_4=\{y_1,y_5\},\quad B_6=\{y_2,y_3\},\quad B_8=\{y_2,y_4\},\quad B_{10}=\{y_4,y_5\}.$$

This is a $(5,10,4,2,\lambda)$-block design whose structure represents the incidences of the Folkman graph.

For designs where there is an initial block and other blocks can be obtained by a linear transformation, it is straightforward to show that the resulting graph is edge-transitive. However if this is not the case, the graph may not be edge-transitive as shown below.

Consider a $(9,18,8,4,3)$-BIBD whose incidences form a biregular bipartite graph, but the resulting graph is not edge-transitive. Consider the design

$$\begin{array}{lll}
(0,1,2,4), & (6,7,8,1), & (3,6,7,1),\\
(1,2,3,5), & (7,8,0,2), & (4,7,8,2),\\
(2,3,4,6), & (8,0,1,3), & (5,8,0,3),\\
(3,4,5,7), & (0,3,4,7), & (6,0,1,4),\\
(4,5,6,8), & (1,4,5,8), & (7,1,2,5),\\
(5,6,7,0), & (2,5,6,0), & (8,2,3,6)
\end{array}$$

[Bose 1939]. This corresponds to a $(4,8)$-biregular subgraph of $K_{18,9}$ with the incidences

$$\begin{array}{lll}
x_1: y_0,y_1,y_2,y_4, & x_7: y_6,y_7,y_8,y_1, & x_{13}: y_3,y_6,y_7,y_1,\\
x_2: y_1,y_2,y_3,y_5, & x_8: y_7,y_8,y_0,y_2, & x_{14}: y_4,y_7,y_8,y_2,\\
x_3: y_2,y_3,y_4,y_6, & x_9: y_8,y_0,y_1,y_3, & x_{15}: y_5,y_8,y_0,y_3,\\
x_4: y_3,y_4,y_5,y_7, & x_{10}: y_0,y_3,y_4,y_7, & x_{16}: y_6,y_0,y_1,y_4,\\
x_5: y_4,y_5,y_6,y_8, & x_{11}: y_1,y_4,y_5,y_8, & x_{17}: y_7,y_1,y_2,y_5,\\
x_6: y_5,y_6,y_7,y_0, & x_{12}: y_2,y_5,y_6,y_0, & x_{18}: y_8,y_2,y_3,y_6,
\end{array}$$

However, the graph G is not edge-transitive, as $G-x_1y_1$ is not isomorphic to $G-x_{18}y_6$. Verification of this fact is far from trivial. Using Mathematica we found that $G-x_1y_1$ has 172924 cycles of length 10 and $G-x_{18}y_6$ has 172926 cycles of length 10. Hence by Theorem 1, G is not edge-transitive.

We also note that there can exist an edge-transitive (r,k)-biregular subgraph of the complete bipartite graph $K_{v,b}$ where the incidences are not a (v,b,r,k,λ)-BIBD design.

For example, consider the blocks

$$B_1=\{y_1,y_2,y_7,y_8\},\quad B_3=\{y_5,y_6,y_7,y_8\},\quad B_5=\{y_1,y_3,y_5,y_7\},$$
$$B_2=\{y_3,y_4,y_5,y_6\},\quad B_4=\{y_1,y_2,y_3,y_4\},\quad B_6=\{y_2,y_4,y_6,y_8\}.$$

This is not a design as the pair $\{y_1, y_5\}$ does not appear in any block. However the incidences give rise to an edge-transitive $(4, 3)$-biregular subgraph of the complete bipartite graph $K_{6,8}$. We used Mathematica to show that this graph is edge-transitive and is nonisomorphic to the graph in Example 17. Both graphs are noted in the online supplement.

3. Complements of Cartesian products

Recall that some previously known infinite families of vertex-transitive graphs are wreath graphs and Kneser graphs. We identify an additional infinite family of edge-transitive graphs that are vertex-transitive, stated in terms of Cartesian products.

Theorem 22. *The graph $\overline{K_m \times K_n}$ is edge-transitive.*

Proof. It may be helpful to refer to Figure 3. The graph $\overline{K_m \times K_n}$ is precisely the graph $\overline{L(K_{m,n})}$, that is, the complement of the line graph of $K_{m,n}$ [Weisstein and Wagon]. First, we observe the structure of $L(K_{m,n})$. Let the partite sets of $K_{m,n}$ be $A = \{a_1, a_2, \dots, a_m\}$ and $B = \{b_1, b_2, \dots, b_n\}$. The graph $L(K_{m,n})$ consists of m sets of n vertices, which we denote by $V_1, V_2, \dots, V_m$. The n vertices in each V_i correspond to the edges incident to a_i in the graph of $K_{m,n}$. Specifically, $V_i = \{v_{i,1}, v_{i,2}, \dots, v_{i,n}\}$, where $v_{i,k}$ corresponds to the edge $a_i b_k$ in the graph $K_{m,n}$. By construction, all of the vertices in a given set V_i are adjacent to each other, since these vertices correspond to all edges incident to a_i in $K_{m,n}$. Additionally, each $v_{i,k}$ is adjacent to $v_{j,k}$ for all $j \neq i$, since these vertices correspond to all edges incident to b_k in $K_{m,n}$. This completes the construction of $L(K_{m,n})$. To construct $\overline{L(K_{m,n})}$, we retain the vertex sets $V_1, \dots, V_m$. However, now we have an m-partite graph, since none of the edges in V_i are connected to each other in $\overline{L(K_{m,n})}$. Each $v_{i,k}$ is connected to $v_{j,l}$ for all $j \neq i$ and all $l \neq k$. In other words, all possible edges of the m-partite graph exist except for edges of the form $v_{i,k} v_{j,k}$. It is clear from this description that $\overline{L(K_{m,n})}$ is edge-transitive. This follows from

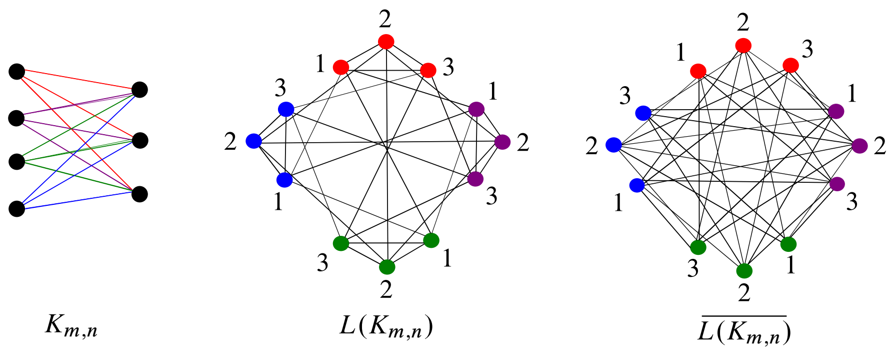

Figure 3. An example of the construction in the proof of Theorem 22 for $m = 4,\ n = 3$.

the fact every vertex in a given partite set is indistinguishable from every other vertex in that set, and the fact that each partite set is indistinguishable from every other partite set. Hence $\overline{K_m \times K_n} = \overline{L(K_{m,n})}$. □

4. Conclusion

In Section 2.2 we explored $(r, 2)$-bipartite subgraphs of $K_{m,n}$. More results of this type can be obtained by determining all arc-transitive graphs of order larger than 9. It would be an interesting but challenging problem to explore the family of (r, k) and determine which graphs are edge-transitive and determine the number of nonisomorphic graphs of this form.

Acknowledgements

We would like to thank Stanisław Radziszowski for useful discussion and for processing graph data on edge-transitive graphs up to 20 vertices. Research was supported by National Science Foundation Research Experiences for Undergraduates Site Award #1659075.

References

[Abueida and Pike 2013] A. A. Abueida and D. A. Pike, "Cycle extensions of BIBD block-intersection graphs", *J. Combin. Des.* **21**:7 (2013), 303–310. MR Zbl

[Andersen et al. 1992] L. D. Andersen, S. K. Ding, G. Sabidussi, and P. D. Vestergaard, "Edge orbits and edge-deleted subgraphs", *Graphs Combin.* **8**:1 (1992), 31–44. MR Zbl

[Beineke 1968] L. W. Beineke, "On derived graphs and digraphs", pp. 17–23 in *Beiträge zur Graphentheorie* (Manebach, East Germany, 1967), edited by H. Sachs et al., B. G. Teubner, Leipzig, 1968. Zbl

[Biggs 1974] N. Biggs, *Algebraic graph theory*, Cambridge Tracts in Mathematics **67**, Cambridge University Press, 1974. MR Zbl

[Bose 1939] R. C. Bose, "On the construction of balanced incomplete block designs", *Ann. Eugenics* **9** (1939), 353–399. MR Zbl

[Godsil and Royle 2001] C. Godsil and G. Royle, *Algebraic graph theory*, Graduate Texts in Mathematics **207**, Springer, 2001. MR Zbl

[Levi 1942] F. W. Levi, *Finite geometrical systems*, University of Calcutta, 1942. MR Zbl

[Mamut et al. 2004] A. Mamut, D. A. Pike, and M. E. Raines, "Pancyclic BIBD block-intersection graphs", *Discrete Math.* **284**:1-3 (2004), 205–208. MR Zbl

[McKay and Pike 2007] N. A. McKay and D. A. Pike, "Existentially closed BIBD block-intersection graphs", *Electron. J. Combin.* **14**:1 (2007), Research Paper 70. MR Zbl

[Onkey 1995] R. Onkey, "On the edge-transitivity of circulant graphs", preprint, 1995, http://jan.ucc.nau.edu/~ns46/student/1995/Richard_Onkey.pdf.

[Sabidussi 1961] G. Sabidussi, "Graph derivatives", *Math. Z.* **76** (1961), 385–401. MR Zbl

[Weisstein] E. Weisstein, "Arc-transitive graph", from MathWorld, http://mathworld.wolfram.com/Arc-TransitiveGraph.html.

[Weisstein and Wagon] E. Weisstein and S. Wagon, "Rook graph", from MathWorld, http://mathworld.wolfram.com/RookGraph.html.

[West 2001] D. B. West, *Introduction to graph theory*, 2nd ed., Prentice Hall, Upper Saddle River, NJ, 2001. Zbl

[Whitney 1932] H. Whitney, "Congruent graphs and the connectivity of graphs", *Amer. J. Math.* **54**:1 (1932), 150–168. MR Zbl

[Yang et al. 2016] X. Yang, W. Liu, H. Liu, and L. Feng, "Incidence graphs constructed from t-designs", *Appl. Anal. Discrete Math.* **10**:2 (2016), 457–478. MR Zbl

Received: 2019-01-28 Revised: 2019-05-15 Accepted: 2019-06-10

hnewman@alumni.princeton.edu *Department of Mathematics, Princeton University, Princeton, NJ, United States*

hectormirandaalvarez@gmail.com *Department of Mathematics, Lehigh University, Bethlehem, PA, United States*

adamgregory@ufl.edu *Department of Mathematics, University of Florida, Gainesville, FL, United States*

dansma@rit.edu *School of Mathematical Sciences, Rochester Institute of Technology, Rochester, NY, United States*

INVOLVE 12:8 (2019)
dx.doi.org/10.2140/involve.2019.12.1343

A logistic two-sex model with mate-finding Allee effect

Elizabeth Anderson, Daniel Maxin, Jared Ott and Gwyneth Terrett

(Communicated by Kenneth S. Berenhaut)

We analyze a logistic two-sex model with mate-finding Allee effects assuming distinct sex-related parameters. We compute the threshold of the Allee-effect strength that separates population extinction from persistence and prove that a bistability regimen appears whereby the total population either goes extinct or stabilizes at a positive level depending on the initial demographic conditions. We show that this effect is the only possible outcome as far as the population limiting behavior is concerned. In addition, we compute the optimal female-sex probability at birth that maximizes this threshold.

1. Introduction

Mathematical population models are a compromise between realism and mathematical tractability. It is obvious that no model can fully resemble the complexity of population interactions (both human or from the animal world). On the other hand, the simplest possible models are not acceptable for long-term predictions. The classical example is given by the exponential model, which appears whenever the vital rates such as birth and death are constant:

$$\frac{dP}{dt} = rP,$$

where P is the total population at time t and r is the difference between a constant birth and death rate. Such a model will always predict an exponentially increasing population as long as births exceeds deaths. This results in completely unrealistic population sizes as t increases.

The most well-known improvement on this model is the logistic equation:

$$\frac{dP}{dt} = r\left(1 - \frac{P}{K}\right)P. \tag{1}$$

MSC2010: 92D25, 92D50.
Keywords: two-sex models, mate-finding Allee effect, bistability.

This model takes into account the fact that there are always factors present that limit the growth rate as the total population increases. Indeed the population cannot grow if it surpasses K in the equation above (also known as *carrying capacity*). Typically, these logistic effects are modeled by considering the mortality rate as an increasing function of the total population size. What that means in real life varies depending on the context. In the ecological models the logistic effect can mean the effect of finite resources such as food. In the human populations the same effect can mean anything which affects the population negatively in overcrowding situations (i.e., infectious diseases, competition for resources, conflicts and other limiting effects). Altogether, logistic effects are examples of a negative correlation between population growth rate and the total population size: the bigger the population size the lower the growth rate.

While logistic effects make perfect sense whenever the population reaches high levels, they should not have any effect when the population density is low. For example, in many models, the logistic mortality is modeled as an increasingly linear function in P:

$$\text{logistic mortality} = \mu + bP,$$

where μ denotes the natural mortality (without population-dependent limiting factors) and $b > 0$ is a technical term that controls how fast the mortality increases with P. It is important to always assume that b is a very small coefficient. Otherwise, the mortality will increase too fast for relatively small increases in P. Indeed, at low population values, in many situations, an opposite effect happens: the growth rate should increase with P. This is the core assumption of the Allee effect, which, by definition, means that the population growth rate is *positively* correlated with the total population size if this size is low. One typical explanation for this effect is geographical dispersal: if the density is low the opportunity for reproduction is rare and it increases if the population density increases.

To summarize, a logistic effect assumes that the population cannot grow past a certain maximum level (the logistic threshold) and the Allee effect *requires* a minimum population level for the growth to occur (the Allee threshold). Most researchers agree that in many ecosystems both assumptions should be present for a more realistic model. A simple modification of the logistic equation (1) is the following one found in [Courchamp et al. 2008], among many other proposed functional forms:

$$\frac{dP}{dt} = r\left(\frac{P}{A} - 1\right)\left(1 - \frac{P}{K}\right).$$

Notice that the population can only grow if $A < P(t) < K$. Should the population size drop below the Allee threshold A, the total population goes extinct. This phenomenon is called a *strong Allee effect* to separate it from the *weak Allee effect* in which low population values cause an exceedingly lower growth rate but without causing extinction. For a more detailed description of various types of Allee effects in ecology see [Courchamp et al. 2008].

One particular type of Allee effect, which is the focus of this paper, is the *mate-finding Allee effect*. This effect is considered in two-sex population models. It assumes that, whenever an individual of one sex is actively looking for a mating partner, the scarcity of the population of the opposite sex induces a strong Allee effect. In other words, the reproduction is hindered by the low population level of the opposite sex. Consider a two-sex population where F and M denote the total population of females and males at time t. Assuming that the female is the mate-searching sex, the mating probability of a given female will be a function of the total male population $p(M)$ with the properties

$$p(0)=0, \qquad \lim_{M\to\infty} p(M)=1, \qquad \text{and} \qquad p \text{ increasing in } M.$$

These assumptions reflect that, if M is small, the reproduction chance is also small, whereas, if M is large, the reproduction probability approaches 1. It is important to point out that the actual reproduction term also depends on other factors. The total male population $p(M)$ is only the mate-finding Allee effect as part of the mating term. There are many explicit forms for $p(M)$ considered in the literature; see again [Courchamp et al. 2008]. Here we focus on the form

$$p(M)=\frac{M}{M+\theta}.$$

Other possible forms, with the properties listed above, are

$$1-e^{-M/\theta} \qquad \text{and} \qquad \frac{M^d}{M^d+\theta} \quad \text{with } d>1.$$

The constant term $\theta>0$ is a measure of the Allee-effect strength and it describes how low the male population should be in order to notice a significant drop in the mating probability. In other words, if θ is very small, the male population should be very small as well in order for $p(M)$ to significantly drop below 1. A large θ indicates that the mating probability decreases faster as M decreases. As we will show in this paper, there exists a threshold θ^* above which the population always goes extinct.

A model containing this type of mate-finding Allee effect has been analyzed in [Berec et al. 2018] under the assumptions that the sex ratio at birth is even and that the background mortality rates of females and males are equal. In reality, these parameters are sometimes different. One example, discussed later in this article, is provided by some mosquito populations. Seasonal conditions exert an influence in the hatching stimuli for the eggs of mosquitoes (as shown in [Lounibos and Escher

2008]) which leads to uneven sex ratios. Variation in the sex birth ratios is observed in other species as well, including birds and mammals; see [Mondard et al. 1997; Weimerskirch et al. 2005].

In this article we improve the result from [Berec et al. 2018] by keeping all sex-related parameters distinct. The paper is structured as follows: in Section 2 we introduce the two-sex model with mate-finding Allee effect and provide its full stability analysis. We also compute the threshold of the Allee-effect strength θ that separates population persistence from extinction. In Section 3 we consider θ as a function of the female-sex probability at birth and compute its optimal value that maximizes it. We conclude the paper with some interpretations of these results in Section 4 and thoughts on possible avenues for future research in Section 5.

2. A two-sex model with mate-finding Allee effect

The logistic two-sex population model with mate-finding Allee effect that we consider is

$$\begin{cases} \dfrac{dF}{dt} = \beta\gamma_f \dfrac{FM}{M+\theta} - \bar{\mu}_f F, \\ \dfrac{dM}{dt} = \beta\gamma_m \dfrac{FM}{M+\theta} - \bar{\mu}_m M, \end{cases} \tag{2}$$

where:

- F and M are the female and male population sizes at time t.
- β is the per capita female birth rate when there is no mate-finding Allee effect (i.e., when M is large).
- γ_f and γ_m are the probabilities that a newborn is a female or male respectively. Hence, $\gamma_f + \gamma_m = 1$.
- θ is the strength of the mate-finding Allee effect.
- μ_f and μ_m are the background female and male mortality rates respectively, in the absence of logistic effects.
- $\bar{\mu}_f := \mu_f + b(F+M)$ and $\bar{\mu}_m := \mu_m + b(F+M)$ are the female and male logistic mortality rates as linear functions of the total population; $b > 0$ represents the strength of the logistic effect.

Remark. While model (2) assumes that the female is the mate-searching sex, the result we establish in this paper holds if the roles are reversed; i.e., the male being the mate-searching sex while the mate-finding Allee effect would be $F/(F+\theta)$. It is not necessary to analyze this scenario separately: one would simply interchange the subscripts f and m throughout the paper.

Consider also the following additional notation (which will be justified in the proof of the main result):

$$\theta^* := \frac{\gamma_m}{b}\left[\beta\gamma_f - \mu_f + 2(\gamma_f\mu_m + \gamma_m\mu_f) - 2\sqrt{\gamma_f(\gamma_f\mu_m + \gamma_m\mu_f)(\beta - \mu_f + \mu_m)}\right], \quad (3)$$

and

$$\mathcal{R}_f := \frac{\beta\gamma_f}{\mu_f}.$$

Since $1/\mu_f$ is the expected female lifetime without the logistic effects, $\mathcal{R}_f$ can be interpreted as the maximum net female reproductive number (the expected female offspring per reproductive female during her lifetime).

We now state our main result:

Theorem 2.1. If $\mathcal{R}_f < 1$ or $\theta > \theta^*$ then the population goes extinct due to either low female reproductive ability or too high a mate-finding Allee effect. If $\mathcal{R}_f > 1$ and $\theta < \theta^*$ then there exist two positive equilibria: one unstable and the other one locally asymptotically stable. The total population either goes extinct if it drops to low levels or it approaches the stable equilibrium.

Proof. The Jacobian of model (2) is

$$J(F, M) = \begin{bmatrix} \frac{\beta\gamma_f M}{M+\theta} - \bar{\mu}_f - bF & \frac{\beta\gamma_f F}{M+\theta} - \frac{\beta\gamma_f FM}{(M+\theta)^2} - bF \\ \frac{\beta\gamma_m M}{M+\theta} - bM & \frac{\beta\gamma_m F}{M+\theta} - \frac{\beta\gamma_m FM}{(M+\theta)^2} - \bar{\mu}_m - bM \end{bmatrix}.$$

The model always admits an extinction equilibrium (0, 0) which is always locally stable since

$$J(0, 0) = \begin{bmatrix} -\mu_f & 0 \\ 0 & -\mu_m \end{bmatrix}$$

with two negative eigenvalues $-\mu_f$ and $-\mu_m$.

Consider now a positive equilibrium (F^*, M^*) with $P^* := F^* + M^*$. Notice that any positive equilibrium must satisfy

$$\frac{\beta\gamma_f M^*}{M^* + \theta} = \mu_f + bP^* \quad \text{and} \quad \frac{\beta\gamma_m F^*}{M^* + \theta} = \mu_m + bP^*.$$

Using these identities, the Jacobian evaluated at this steady state becomes

$$J(F^*, M^*) = \begin{bmatrix} -bF^* & \frac{\beta\gamma_f F^*}{M^*+\theta} - \frac{\beta\gamma_f F^* M^*}{(M^*+\theta)^2} - bF^* \\ \frac{\beta\gamma_m M^*}{M^*+\theta} - bM^* & -\frac{\beta\gamma_m F^* M^*}{(M^*+\theta)^2} - bM^* \end{bmatrix}.$$

In a system of two differential equations, the necessary and sufficient condition for the local stability of a steady state is $\mathrm{Trace}(J(F^*, M^*)) < 0$ and $\det(J(F^*, M^*)) > 0$.

It is easy to see that the trace of this matrix is always negative and its determinant is

$$\det(J(F^*, M^*)) = \frac{\beta F^* M^*}{(M^*+\theta)^3}[b(M^*+\theta)(\theta+\gamma_m P^*) - \beta\gamma_f\gamma_m\theta].$$

Hence the stability condition for any biologically feasible (positive) steady state is

$$b(M^*+\theta)(\theta+\gamma_m P^*) - \beta\gamma_f\gamma_m\theta > 0. \tag{4}$$

Concerning the existence of a positive steady state, first, notice that

$$F^* = \frac{\gamma_f\theta(\mu_m + bP^*)}{\gamma_m(\beta\gamma_f - \mu_f - bP^*)} \quad \text{and} \quad M^* = \frac{\theta(\mu_f + bP^*)}{\beta\gamma_f - \mu_f - bP^*}.$$

Hence, to ensure they are positive, any feasible value for P^* must satisfy

$$P^* < \frac{\beta\gamma_f - \mu_f}{b}. \tag{5}$$

However this requires $\beta\gamma_f - \mu_f > 0$, which is equivalent to $\mathcal{R}_f > 1$. Thus, if the opposite holds, i.e., $\mathcal{R}_f < 1$, then $(0, 0)$ is the only equilibrium point.

From here on we assume $\mathcal{R}_f > 1$, i.e.,

$$\beta\gamma_f > \mu_f.$$

From

$$P^* = F^* + M^* = \frac{\gamma_f\theta(\mu_m + bP^*)}{\gamma_m(\beta\gamma_f - \mu_f - bP^*)} + \frac{\theta(\mu_f + bP^*)}{\beta\gamma_f - \mu_f - bP^*}$$

it follows, after some computations, that P^* must be a positive root of

$$f(P) := b\gamma_m P^2 + [b\theta - \gamma_m(\beta\gamma_f - \mu_f)]P + \theta(\gamma_f\mu_m + \gamma_m\mu_f)$$

and P^* must satisfy (5). Furthermore, the stability condition (4) can be rewritten in terms of P^* as

$$P^* > P_v := \frac{\gamma_m(\beta\gamma_f - \mu_f) - b\theta}{2b\gamma_m}. \tag{6}$$

Notice also that P_v is the P-coordinate vertex of the parabola $f(P)$.

Consider now the discriminant of $f(P)$ as a function of θ:

$$g(\theta) := b^2\theta^2 - 2b\gamma_m[\beta\gamma_f - \mu_f + 2(\gamma_f\mu_m + \gamma_m\mu_f)]\theta + (\beta\gamma_f - \mu_f)^2(\gamma_m)^2.$$

The discriminant of $g(\theta)$ is

$$16b^2\gamma_f(\gamma_m)^2(\gamma_f\mu_m + \gamma_m\mu_f)(\beta - \mu_f + \mu_m).$$

Under our current assumptions, this is positive since

$$\beta > \beta\gamma_f > \mu_f.$$

Taking into account the signs of the coefficients of $g(\theta)$ we conclude that $g(\theta)$ has two positive roots θ_1 and θ_2:

$$\theta_1 = \frac{\gamma_m}{b}\big[\beta\gamma_f - \mu_f + 2(\gamma_f\mu_m + \gamma_m\mu_f) - 2\sqrt{\gamma_f(\gamma_f\mu_m + \gamma_m\mu_f)(\beta - \mu_f + \mu_m)}\big],$$
$$\theta_2 = \frac{\gamma_m}{b}\big[\beta\gamma_f - \mu_f + 2(\gamma_f\mu_m + \gamma_m\mu_f) + 2\sqrt{\gamma_f(\gamma_f\mu_m + \gamma_m\mu_f)(\beta - \mu_f + \mu_m)}\big].$$

Hence, $g(\theta)$ is positive whenever $0 < \theta < \theta_1$ and $\theta_2 < \theta < \infty$. From the sign of the coefficients of $f(P)$ it is clear that, if $f(P)$ has real roots, they are either both negative or both positive. They are positive provided that

$$\theta < \frac{\gamma_m}{b}(\beta\gamma_f - \mu_f).$$

However a straightforward computation shows that

$$g\left(\frac{\gamma_m}{b}(\beta\gamma_f - \mu_f)\right) = -4(\gamma_m)^2(\beta\gamma_f - \mu_f)(\gamma_f\mu_m + \gamma_m\mu_f) < 0,$$

which means

$$\theta_1 < \frac{\gamma_m}{b}(\beta\gamma_f - \mu_f) < \theta_2.$$

This shows that the model (2) admits two positive equilibrium points (F_1, M_1) and (F_2, M_2) corresponding to the two positive roots $P_1 < P_2$ if and only if the mate-finding Allee-effect strength θ is less than the threshold

$$\theta^* := \theta_1 = \frac{\gamma_m}{b}\big[\beta\gamma_f - \mu_f + 2(\gamma_f\mu_m + \gamma_m\mu_f) - 2\sqrt{\gamma_f(\gamma_f\mu_m + \gamma_m\mu_f)(\beta - \mu_f + \mu_m)}\big]. \quad (7)$$

If $\theta > \theta^*$ then the extinction equilibrium $(0, 0)$ would be the only steady state. Notice also that P_1 and P_2, when they exist and are positive, both satisfy the feasibility condition $P^* < (\beta\gamma_f - \mu_f)/b$ since

$$f\left(\frac{\beta\gamma_f - \mu_f}{b}\right) = \theta\gamma_f(\beta - \mu_f + \mu_m) > 0,$$
$$f'\left(\frac{\beta\gamma_f - \mu_f}{b}\right) = \gamma_m(\beta\gamma_f - \mu_f) + b\theta > 0,$$

which means $P_1 < P_2 < (\beta\gamma_f - \mu_f)/b$.

Furthermore, $P_1 < P_v < P_2$, which means (F_1, M_1) is unstable and (F_2, M_2) is locally asymptotically stable. Thus we have bistability between the extinction and the positive steady state (F_2, M_2).

It remains now to show that the asymptotic behavior established in this proof holds in the global sense and not just within an unspecified basin of attraction of each locally stable steady state. In other words, we want to show that, regardless of the initial population size, the population converges to either $(0, 0)$ or (F_2, M_2). In the case of a planar system, the only other possible limiting behavior is that of a limit cycle or, more generally, a finite number of equilibria cyclically chained. We show that this is not possible for our model (2).

First notice that it is not possible to have the extinction equilibrium (0, 0) as part of a group of equilibrium points that are cyclically chained. This is because (0, 0) is a sink (i.e., both eigenvalues are real and negative). Any other possible cycle would be entirely contained in a compact subset of the positive quadrant. We rule out also this possibility using the Dulac criterion [Perko 1991]. It states that if

$$\frac{\partial}{\partial F}(\varphi(F, M)F') + \frac{\partial}{\partial M}(\varphi(F, M)M')$$

has a constant sign on that compact subset for some differentiable function $\varphi(F, M)$ then the system (2) does not have any periodic solutions or limit cycles. A typical choice for the Dulac function is $\varphi(F, M) = 1/(FM)$. Indeed, in our case, this leads to

$$\frac{\partial}{\partial F}\left(\frac{1}{FM}F'\right) + \frac{\partial}{\partial M}\left(\frac{1}{FM}M'\right) = -\frac{1}{FM}\left[\frac{\beta\gamma_m FM}{(M+\theta)^2} + b(F+M)\right] < 0. \quad \square$$

3. Maximization of the Allee-effect strength

As mentioned earlier, the model (2) has been analyzed in [Berec et al. 2018] using equal sex-related parameters. In this section we illustrate the advantage of keeping these parameters distinct whenever the biological question under study is specific to one sex only. To this end, we can see that the threshold θ^* can be analyzed further for various optimal scenarios. For example, if population persistence is a desired objective, then a natural question to ask is what combinations of parameters will maximize θ^*. Based on our results, a larger threshold θ^* means that the population may persist for relatively stronger Allee effects. One will still have bistability between extinction and persistence but, as long as $\theta < \theta^*$ and the population size is not too low to begin with, the long-term outcome is persistence. For example, it is easy to see that whenever μ_f approaches zero then, unsurprisingly, the threshold θ^* is maximized. When we analyze other parameters, the optimal combination that maximizes θ^* is less obvious. As an example, we compute in this section the female-sex probability at birth (γ_f) that maximizes θ^* for a numerical case. We will provide a more general result for a simplified version of θ^*.

Theorem 3.1. If $\mathcal{R}_f > 1$ there exists an optimal female-sex probability at birth, γ_f, that maximizes θ^*.

In the case of equal mortality rates $\mu_f = \mu_m := \mu$, this optimal value is

$$\frac{1}{16}\left(\sqrt{\frac{\mu}{\beta}} + \sqrt{\frac{\mu}{\beta} + 8}\right)^2.$$

Proof. Consider the threshold θ^* written in a more compact form:

$$\theta^* = \frac{\gamma_m}{b}\left[\sqrt{\gamma_f(\beta-\mu_f+\mu_m)} - \sqrt{\gamma_f\mu_m+\gamma_m\mu_f}\,\right]^2.$$

Substituting $\gamma_f := x$ and $\gamma_m := 1-x$ we can see that maximizing θ^* under the assumption $\mathcal{R}_f > 1$ is equivalent to maximizing the following function in x for $\mu_f/\beta \le x \le 1$:

$$h(x) := \frac{1}{b}(1-x)\left[\sqrt{x(\beta-\mu_f+\mu_m)} - \sqrt{x\mu_m+(1-x)\mu_f}\,\right]^2.$$

It is easy to see that $h(1)=0$ and also, after some simplifications, that $h(\mu_f/\beta)=0$. This is expected since $x=1$ means no male births and $x=\mu_f/\beta$ means there is no net gain in the female reproduction. Since $h(x)$ is positive, continuous and differentiable on $\mu_f/\beta < x < 1$, it will have an absolute maximum $x = x^*$. Its exact value is difficult to obtain in general but it is relatively easy under the assumption of equal mortality rates, $\mu_f = \mu_m := \mu$, while still keeping $\gamma_f \neq \gamma_m$. Setting $R := \beta/\mu > 1,\ h(x)$ becomes

$$h(x) := \frac{1}{R}(1-x)(\sqrt{Rx}-1)^2, \quad \frac{1}{R} \le x \le 1.$$

We now show that $h(x)$ has a unique critical value in its domain. Its first derivative is

$$h'(x) = \frac{1}{R}\left(R - \sqrt{\frac{R}{x}}\right)\left(-2x + \frac{\sqrt{x}}{\sqrt{R}} + 1\right).$$

The expression in the second set of parentheses can be viewed as a quadratic in $\sqrt{x}$. We make the change of variable $y := \sqrt{x}$ with $1/\sqrt{R} \le y \le 1$ and the expression becomes

$$k(y) = -2y^2 + \frac{y}{\sqrt{R}} + 1.$$

Notice that $k(y)$ has two real roots, one positive and one negative. The positive root is

$$y^* = \frac{1}{4}\left(\sqrt{\frac{1}{R}} + \sqrt{\frac{1}{R}+8}\right).$$

Furthermore

$$k(1) = -1 + \frac{1}{\sqrt{R}} < 0 \quad \text{and} \quad k\left(\frac{1}{\sqrt{R}}\right) = -\frac{1}{R} + 1 > 0,$$

since we are under the assumption $R > 1$. Hence y^* is in the domain $1/\sqrt{R} < y < 1$.

Thus $h(x)$ has a unique critical value

$$x^* = (y^*)^2 = \frac{1}{16}\left(\sqrt{\frac{1}{R}} + \sqrt{\frac{1}{R}+8}\right)^2.$$

Since $h(x)$ is positive and vanishes at the end points of its domain, it follows that $x = x^*$ maximizes the threshold θ^*. $\square$

Remark. Notice that if $R \to \infty$ then $x^* \to \frac{1}{2}$ and if $R \to 1$ then $x^* \to 1$. If we think of R as the overall net reproductive number, these limits suggest that if the net-gain rate in the population is unbounded then the optimal sex ratio is even since there will be plenty of individuals of the mate-searching sex (the females) with plenty choices for mating (the males). On the other hand, as the net gain is close to zero, the optimal sex ratio is more and more biased toward the mate-searching sex. These results make intuitive sense and confirm the validity of the optimal female-sex probability at birth as a function of the net reproductive number.

4. Example

We illustrate this result with a numerical example applied to a generic population of mosquitoes. In [Xue et al. 2017] the authors analyze a two-sex population model of mosquitoes deliberately infected by *Wolbachia* bacteria, which is known to reduce the ability of mosquitoes to transmit viral infections such as *Zika* or dengue fever. While the authors do not include Allee effects in their model, they do use different sex probabilities at birth. In [Lounibos and Escher 2008], the authors observed variations in the sex ratio at birth of mosquitoes. We argue here that the inclusion of Allee effects in such models and the computation of the threshold θ^* may be helpful in predicting whether the population of mosquitoes will persist or go extinct.

It is important to point out that persistence happens only if the initial population size is large enough as the Allee effect always causes the extinction equilibrium to be locally asymptotically stable. With larger Allee-effect values, naturally, the

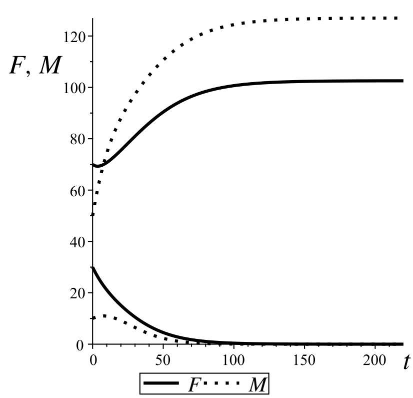

Figure 1. $\theta^* = 81.2$ with suboptimal female-sex probability at birth $\gamma_f = 0.4$. Allee-effect strength used in the example is $\theta = 70$, which leads to population persistence.

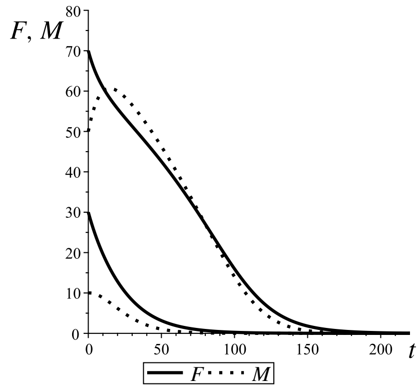

Figure 2. $\theta^* = 81.2$ with suboptimal female-sex probability at birth $\gamma_f = 0.4$. Allee-effect strength used in the example is $\theta = 90$, which leads to extinction.

initial population needs to be larger to escape the basin of attraction of the extinction steady state. Therefore, θ^* indicates a threshold beyond which the Allee effect is strong enough to drive the population to extinction regardless of initial conditions.

In our example below we will use numerical values for the vital parameters from the ranges provided in [Xue et al. 2017] for the mosquito population except θ and the logistic effect b. The θ-values are chosen by us to illustrate the result in this section. The logistic effect b only affects the overall population size and not the threshold θ^* or any other stability condition. We chose a value for it that provides a clearer figure. In all three figures, these values are $\beta = 0.55$, $\mu_f = 0.05$, $\mu_m = 0.08$ and $b = 0.0004$.

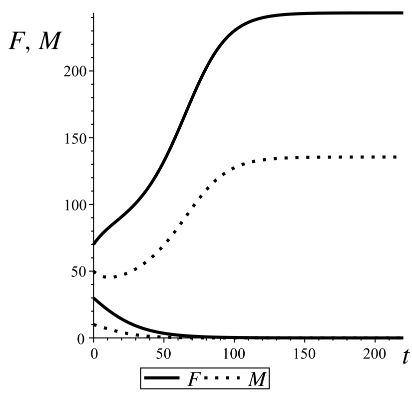

Figure 3. $\theta^* = 108.4$ with optimal female-sex probability at birth $\gamma_f = 0.61$. Allee-effect strength used in the example is $\theta = 90$, which, unlike the suboptimal scenario, now leads to population persistence.

With these values, $h(x)$ becomes

$$h(x) = 2500(1-x)(0.762\sqrt{x} - \sqrt{0.03x + 0.05})^2$$

and, using a computer algebra system, it is straightforward to see that it is maximized, in its domain, for $x^* = 0.61$ and its maximum value is $\theta^* = 108.4$.

First, we use a suboptimal female-sex probability at birth $\gamma_f = 0.4$. Its corresponding threshold is $\theta^* = 81.2$. In Figures 1 and 2 we show an example where the population may persist if $\theta < \theta^*$, while it goes extinct if $\theta > \theta^*$. We chose $\theta = 70$ in the first case and $\theta = 90$ in the second case. Finally, in Figure 3, we use the same Allee effect $\theta = 90$ that caused extinction in the previous case and show that, using the optimal value $\gamma_f = 0.61$, the population now may persist.

5. Conclusions

We analyzed a planar two-sex model with mate-finding Allee effect assuming sex-specific vital parameters: sex ratio at birth and mortality rate. We proved that the total population either goes extinct or exhibits a bistability regimen between a positive steady state and the extinction equilibrium. The specific outcome depends on the strength of the Allee effect. This confirms an earlier result proved under the assumption of equal female and male populations. We further illustrate, with an example, a possible avenue of inquiry which requires maintaining a sex-specific assumption on the model parameters.

There are several limitations of our result that also suggest avenues of future research. First, a planar system for two-sex modeling is not suitable for populations that form long-lasting pairs in order to reproduce. Modeling in this case requires at least three state variables: single females, males and couples. Such behavior is seen in many species and, obviously, is also prevalent in human populations. A next step is then to replicate this analysis for a two-sex model with pair-formation in which F and M will denote the single female and male populations, while a third state variable C will be introduced to model couples. Births will then be a function either exclusively of couples or a mixed system in which births from single individuals are considered as well. The pair-formation term will then contain the mate-finding Allee effect. Since, at the very least, such models will have three equations, the stability analysis will be considerably more difficult.

Another important generalization is to use a different form for the mate-finding Allee effect, possibly one that allows both sexes to play the "mate-searching" role to a various degree. Finally, a generalization that does not even assume a specific Allee-effect form might be desirable since there are already various forms proposed in the literature and a model containing an unspecified one might have a unifying value for this concept. We plan to address some of these questions in the near future.

Acknowledgment

This research was partially supported by NSF Grant DMS-1559912.

References

[Berec et al. 2018] L. Berec, V. Bernhauerová, and B. Boldin, "Evolution of mate-finding Allee effect in prey", *J. Theoret. Biol.* **441** (2018), 9–18. MR Zbl

[Courchamp et al. 2008] F. Courchamp, L. Berec, and J. Gascoigne, *Allee effects in ecology and conservation*, Oxford Univ. Press, 2008.

[Lounibos and Escher 2008] L. P. Lounibos and R. L. Escher, "Sex ratios of mosquitoes from long-term censuses of Florida tree holes", *J. Amer. Mosquito Control Assoc.* **24**:1 (2008), 11–15.

[Mondard et al. 1997] A.-M. Mondard, P. Duncan, H. Fritz, and C. Feh, "Variations in the birth sex ratio and neonatal mortality in a natural herd of horses", *Behav. Ecol. Sociobiol.* **41**:4 (1997), 243–249.

[Perko 1991] L. Perko, *Differential equations and dynamical systems*, Texts in Appl. Math. **7**, Springer, 1991. MR Zbl

[Weimerskirch et al. 2005] H. Weimerskirch, J. Lallemand, and J. Martin, "Population sex ratio variation in a monogamous long-lived bird, the wandering albatross", *J. Animal Ecol.* **74**:2 (2005), 285–291.

[Xue et al. 2017] L. Xue, C. A. Manore, P. Thongsripong, and J. M. Hyman, "Two-sex mosquito model for the persistence of *Wolbachia*", *J. Biol. Dyn.* **11**:suppl. 1 (2017), 216–237. MR

Received: 2019-02-01 Revised: 2019-07-07 Accepted: 2019-07-07

eander35@villanova.edu — *Department of Mathematics and Statistics, Villanova University, Villanova, PA, United States*

daniel.maxin@valpo.edu — *Department of Mathematics and Statistics, Valparaiso University, Valparaiso, IN, United States*

jared.ott@huskers.unl.edu — *Department of Mathematics, University of Nebraska, Lincoln, NE, United States*

gwyneth.terrett@gmail.com — *Mathematics Department, Taylor University, Upland, IN, United States*

INVOLVE 12:8 (2019)
dx.doi.org/10.2140/involve.2019.12.1357

Unoriented links and the Jones polynomial

Sandy Ganzell, Janet Huffman, Leslie Mavrakis,
Kaitlin Tademy and Griffin Walker

(Communicated by Joel Foisy)

The Jones polynomial is an invariant of oriented links with $n \geq 1$ components. When $n = 1$, the choice of orientation does not affect the polynomial, but for $n > 1$, changing orientations of some (but not all) components can change the polynomial. Here we define a version of the Jones polynomial that is an invariant of *unoriented* links; i.e., changing orientation of any sublink does not affect the polynomial. This invariant shares some, but not all, of the properties of the Jones polynomial.

The construction of this invariant also reveals new information about the original Jones polynomial. Specifically, we show that the Jones polynomial of a knot is never the product of a nontrivial monomial with another Jones polynomial.

1. Introduction

Jones' original construction [1985] of the polynomial $V_L = V_L(t) \in \mathbb{Z}[t^{1/2}, t^{-1/2}]$ was through the skein relation

$$t^{-1} V_{L_-} - t V_{L_+} = (t^{1/2} - t^{-1/2}) V_{L_0},$$

where L_+, L_- and L_0 are three oriented links that are identical except inside a ball that contains respectively, a positive crossing, a negative crossing, and two uncrossed strands. It is easy to see that when L is a knot (i.e., a link of one component), the polynomial $V_L(t)$ is unchanged by reversing the orientation on L, since crossing signs are preserved by such a change in orientation.

For links of more than one component, however, the Jones polynomial may change depending on the choice of orientation for each component. The Hopf link is the simplest example. The oriented Hopf link with linking number $+1$ has Jones polynomial $-t^{1/2} - t^{5/2}$, but reversing the orientation of one component gives us $-t^{-5/2} - t^{-1/2}$. A complete list of oriented links up to nine crossings, together with their polynomials can be found in [Doll and Hoste 1991].

MSC2010: 57M25, 57M27.
Keywords: Jones polynomial, unoriented link.
Supported by NSF grant DMS-1560301.

Based on the skein-relation definition, it is a surprising result that a change in orientation of some components of L simply multiplies V_L by a power of t. Let $L = M \cup N$ be an oriented link with components $M_1, \dots, M_r, N_1, \dots, N_s$, and write $L_N = M \cup -N$ for the link formed by reversing the orientations on $N_1, \dots, N_s$. Morton [1986] proved that

$$V_L(t) = t^{3\lambda} V_{L_N}(t),$$

where λ is the linking number of M with N, defined as

$$\lambda = \mathrm{lk}(M, N) = \sum_{i,j} \mathrm{lk}(M_i, N_j).$$

A much simpler proof using Kauffman's bracket polynomial construction of the Jones polynomial appears below.

Recall [Kauffman 1988] the bracket polynomial $\langle L \rangle \in \mathbb{Z}[A, A^{-1}]$ is defined recursively:

$$\begin{aligned} \langle \times \rangle &= A\langle \asymp \rangle + A^{-1}\langle)(\rangle, \\ \langle \bigcirc L \rangle &= (-A^2 - A^{-2})\langle L \rangle, \\ \langle \bigcirc \rangle &= 1. \end{aligned}$$

The bracket polynomial is invariant under Reidemeister moves R2 and R3, but not under move R1. Define $X_L(A) = (-A^3)^{-w}\langle L \rangle$, where $w = w(L)$ is the writhe (sum of all crossing signs) of L, to obtain a link invariant. Under the change of variables $A = t^{-1/4}$, we have $X_L(A) = V_L(t)$. We will often write $d = -A^2 - A^{-2}$; thus $\langle \bigcirc L \rangle = d\langle L \rangle$.

Now it is clear that changing the orientations of some components of L multiplies the Jones polynomial by a power of t, since only the writhe (but not the bracket polynomial) is affected by such a change. Using the notation above, if $L = M \cup N$, then the crossing signs that change to produce L_N are the ones that involve some crossing of component M_i with component N_j. Since the linking number of M with N involves precisely the same crossings, we have

$$\begin{aligned} w(L_N) &= w(L) - 2\sum(\text{crossing signs of } M_i \text{ with } N_j) \\ &= w(L) - 4 \cdot \mathrm{lk}(M, N). \end{aligned}$$

Thus

$$\begin{aligned} V_L(t) = X_L(A) &= (-A^3)^{-w(L)}\langle L \rangle \\ &= (-A^3)^{-4\cdot\mathrm{lk}(M,N) - w(L_N)}\langle L \rangle \\ &= (-A)^{-12\cdot\mathrm{lk}(M,N)}(-A^3)^{-w(L_N)}\langle L \rangle \\ &= (A^4)^{-3\lambda} X_{L_N}(A) = t^{3\lambda} V_{L_N}(t), \end{aligned}$$

confirming Morton's result.

Given an unoriented link of n components, there may be up to 2^{n-1} associated Jones polynomials for the links obtained by choosing an orientation for each component. (Note: it is not up to 2^n, since changing *all* orientations does not affect the Jones polynomial.) None of these is a natural choice to be the Jones polynomial of the unoriented link since there is no preferred orientation. In the next section we define a version of the Jones polynomial that is an invariant of unoriented links.

2. The Jones polynomial for unoriented links

We begin by defining the *self-writhe* of a link diagram.

Definition 1. For a link diagram L with components $K_1, \dots, K_n$, we define the self-writhe of L, denoted by $\psi(L)$, to be the sum of the writhes of each component of L, ignoring the other components when computing each writhe. That is,

$$\psi(L) = \sum_{j=1}^{n} w(K_j).$$

Equivalently, the self-writhe can be defined as the sum of the signs of those crossings of L for which both the under and over strands are from the same component.

Reidemeister moves affect the self-writhe exactly as they do the writhe. Both are invariant under moves R2 and R3. This is because the two crossings involved in move R2 are of opposite sign regardless of orientation, and the crossing signs ε_i are unchanged by R3 moves regardless of orientations and components. See Figure 1. Under move R1, both the writhe and self-writhe change by ± 1, since move R1 always involves a single component of the link. See Figure 2.

Unlike the writhe, however, the self-writhe of a link L is independent of the choice of orientations of the components of L. This is because changing the orientation of a component K of L does not affect the writhe of K, and hence does not affect $\psi(L)$.

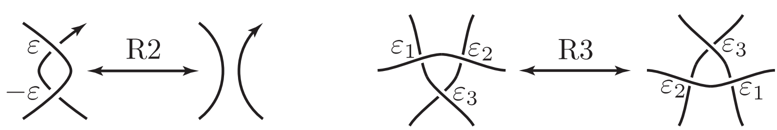

Figure 1. Crossing signs and Reidemeister moves.

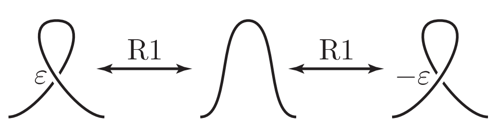

Figure 2. Crossing signs and move R1.

Thus we can define $U_L(A) = (-A^3)^{-\psi}\langle L\rangle$. This modified Jones polynomial is an invariant for the same reason that $X_L(A)$ is: both $\langle L\rangle$ and $\psi(L)$ are invariant under moves R2 and R3, and $\langle L\rangle$ changes by a factor of $(-A^3)^{\pm 1}$ with each R1 move.

But since $\psi(L)$ is unaffected by changing orientations of any components of L, the polynomial $U_L(A)$ is also unaffected by such changes. We can thus make the same change of variables $A = t^{-1/4}$ to obtain $W_L(t) \in \mathbb{Z}[t^{1/2}, t^{-1/2}]$, noting that $W_L(t) = U_L(A)$.

Definition 2. Let L be an unoriented link with self-writhe ψ. The Laurent polynomial $U_L(A) = (-A^3)^{-\psi}\langle L\rangle$ (or equivalently $W_L(t)$) for any choice of orientation of components of L is the unoriented Jones polynomial of L. We will refer to $U_L(A)$ as the U-polynomial of L.

3. Properties of the unoriented Jones polynomial

For knots we have $W_K(t) = V_K(t)$ since $w(K) = \psi(K)$. Thus we will examine the properties of the unoriented Jones polynomial for links of at least two components. Jones [1985] established that if the link L has an odd number of components, then $V_L(t)$ is a Laurent polynomial over the integers; if the number of components of L is even then $V_L(t)$ is $\sqrt{t}$ times a Laurent polynomial. $W_L(t)$ does not share these properties. For example, if L is the Hopf link, then $W_L(t) = -t^{-1} - t$, since $\langle \bigcirc\!\!\!\bigcirc \rangle = -A^4 - A^{-4}$, and $\psi(\bigcirc\!\!\!\bigcirc) = 0$.

On the other hand, if L is link 5^2_1 (Figure 3), then $\psi(L) = w(L) = -1$, regardless of orientation. Therefore,

$$W_L(t) = V_L(t) = t^{-7/2} - 2t^{-5/2} + t^{-3/2} - 2t^{-1/2} + t^{1/2} - t^{3/2}.$$

There are two different oriented links corresponding to 7^3_1 (Figure 3), both of which have integral exponents for the original Jones polynomials, but the unoriented Jones polynomial is

$$t^{-5/2} - t^{-3/2} + 4t^{-1/2} - 3t^{1/2} + 4t^{3/2} - 3t^{5/2} + 3t^{7/2} - t^{9/2}.$$

For the remainder of this paper we use A as the indeterminate. This is simply to avoid fractional exponents.

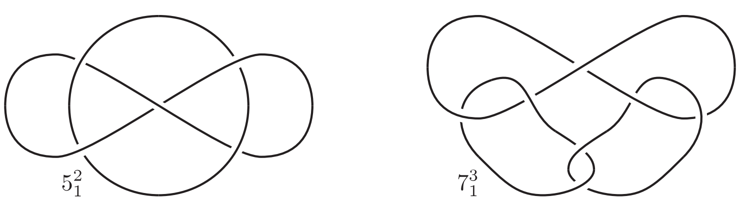

Figure 3. Links 5^2_1 and 7^3_1.

Figure 4. $L\#M$.

Some properties of the Jones polynomial do carry over to $U_L(A)$. Let L^* denote the mirror image of L.

Proposition 3. $$U_{L^*}(A) = U_L(A^{-1}).$$

Proof. This follows immediately from Definition 2, since $\psi(L) = -\psi(L^*)$. □

Theorem 4. *If L and M are links, then $U_{L\#M} = U_L U_M$.*

Proof. Observe that for diagrams L and M, the self-writhe of $L\#M$ is just $\psi(L) + \psi(M)$. Now take diagrams for L, M and $L\#M$ as in Figure 4. Let

where p_1, p_2, q_1 and q_2 are polynomials in A. Then we have $\langle L\rangle = p_1 + p_2 d$, and $\langle M\rangle = q_1 + q_2 d$. Moreover,

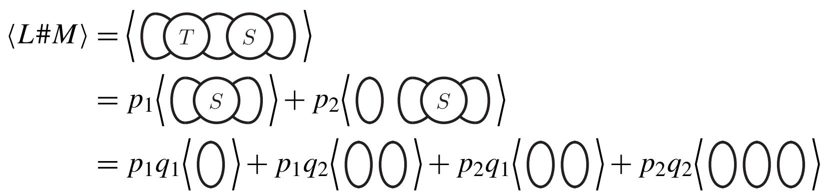

$$= p_1q_1 + p_1q_2d + p_2q_1d + p_2q_2d^2.$$

Thus,

$$\begin{aligned} U_{L\#M}(A) &= (-A^3)^{-\psi(L\#M)}(p_1q_1 + p_1q_2d + p_2q_1d + p_2q_2d^2) \\ &= (-A^3)^{-\psi(L)}(-A^3)^{-\psi(M)}(p_1 + p_2d)(q_1 + q_2d) \\ &= U_L(A)U_M(A). \end{aligned}$$ □

When two links have the same number of components, their U-polynomials are related algebraically. Specifically, if L and L' are both n-component links, then $U(L) - U(L')$ is divisible by a certain fixed polynomial $C(A)$, independent of L, L' and n. Equivalently, we may say $U(L)$ and $U(L')$ are equal in the quotient ring $\mathbb{Z}[A, A^{-1}]/\langle C(A)\rangle$. For convenience, we will write $U(L) \equiv U(L') \pmod{C(A)}$.

Theorem 5. *Let L and L' be two links with the same number of components. Then $U_L(A) \equiv U_{L'}(A) \pmod{A^6 - 1}$.*

Proof. Suppose L and L' are two links that differ by a crossing change. We will show that $U_L(A) - U_{L'}(A)$ is divisible by $A^6 - 1$. Since any link can be transformed

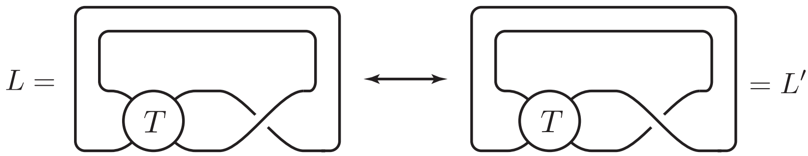

Figure 5. Two links that differ by a crossing change.

by crossing changes to any other link with the same number of components, the theorem follows.

Draw L and L' as the numerator closures of tangles that differ by a crossing as in Figure 5. Take the self-writhes of L and L' to be ψ and ψ' respectively. Therefore ψ' will equal ψ, $\psi+2$, or $\psi-2$, depending on the orientation of the strands in the crossing change, and whether they are from the same component. We compute $U_L(A) - U_{L'}(A)$. Write

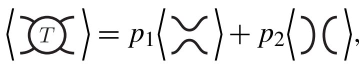

where p_1 and p_2 are polynomials in A. Then

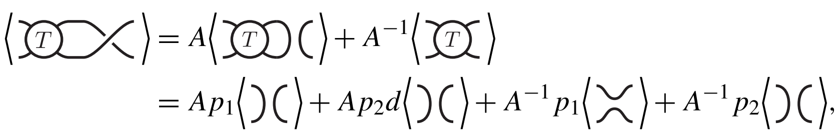

$$\begin{aligned}\langle L\rangle &= Ap_1 + Ap_2 d + A^{-1}p_1 d + A^{-1}p_2\\ &= p_1(A + A^{-1}d) + p_2(Ad + A^{-1})\\ &= p_1(-A^{-3}) + p_2(-A^3),\\ U_L(A) &= (-A^3)^{-\psi}[p_1(-A^{-3}) + p_2(-A^3)].\end{aligned}$$

Similarly,

$$\begin{aligned}\langle L'\rangle &= p_1(-A^3) + p_2(-A^{-3}),\\ U_{L'}(A) &= (-A^3)^{-\psi'}[p_1(-A^3) + p_2(-A^{-3})].\end{aligned}$$

Since $\psi' \in \{\psi, \psi+2, \psi-2\}$, either

$$\begin{aligned}U_L(A) - U_{L'}(A) &= (-A^3)^{-\psi}[p_1(-A^{-3} + A^3) - p_2(A^3 - A^{-3})]\\ &= (-1)^{-\psi}(A^3)^{-\psi-1}(p_1 - p_2)(A^6 - 1),\end{aligned}$$

or

$$\begin{aligned}U_L(A) - U_{L'}(A) &= (-A^3)^{-\psi}p_2(-A^3 + A^{-9})\\ &= (-A^3)^{-\psi-3}p_2(A^6+1)(A^6-1),\end{aligned}$$

or

$$U_L(A) - U_{L'}(A) = (-A^3)^{-\psi} p_1(-A^{-3} + A^9)$$
$$= (-A^3)^{-\psi-1} p_1(A^6+1)(A^6-1). \qquad \square$$

Corollary 6. *Let L be a link with n components. Then $U_L(1) = (-2)^{n-1}$.*

Proof. Let $\bigcirc^n$ be the unlink of n components. Then

$$U_{\bigcirc^n}(A) = d^{n-1} = (-A^2 - A^{-2})^{n-1}.$$

Therefore by Theorem 5, we can write $U_L(A) = (A^6-1)q(A) + (-A^2 - A^{-2})^{n-1}$, where q is some polynomial in A. Thus $U_L(1) = (-2)^{n-1}$. $\square$

Theorem 5 establishes that A^6-1 divides the difference of any two U-polynomials of links with the same number of components. However, A^6-1 does not appear to be the highest-degree such polynomial. In all examples known to the authors, the difference is a multiple of $A^8 - A^6 - A^2 + 1$, which equals $(A^6-1)(A^2-1)$. We conjecture this is always the case.

Conjecture 7. Let L and L' be two links with the same number of components. Then $U_L(A) \equiv U_{L'}(A) \pmod{A^8 - A^6 - A^2 + 1}$.

We prove Conjecture 7 for links of three or fewer components.

Theorem 8. *Let L and L' be two n-component links, where $n \le 3$. Then $U_L(A) \equiv U_{L'}(A) \pmod{A^8 - A^6 - A^2 + 1}$.*

Proof. It is shown in [Ganzell 2014] that when L is a knot (i.e., $n = 1$), then $X_L(A) - X_{L'}(A)$ (and hence $U_L(A) - U_{L'}(A)$) is always divisible by $A^{16} - A^{12} - A^4 + 1$, which equals $(A^8 - A^6 - A^2 + 1)(A^8 + A^6 + A^2 + 1)$.

For $n = 2$, we proceed as follows. It is proved in [Murakami and Nakanishi 1989] that the link L can be transformed into the link L' by Δ-moves (Figure 6) if and only if L and L' have the same number of components and the pairwise linking numbers of the components of L equal those of L'. That is, if $L = K_1 \cup \cdots \cup K_n$ and $L' = K'_1 \cup \cdots \cup K'_{n'}$, then L can be transformed into L' by Δ-moves if and only if $n = n'$ and $\mathrm{lk}(K_i, K_j) = \mathrm{lk}(K'_i, K'_j)$ for $1 \le i < j \le n$. In this case we say L and L' are Δ-move equivalent. Thus every 2-component link is Δ-move equivalent to a link of the form in Figure 7, where $k \in \mathbb{Z}$ is the linking number.

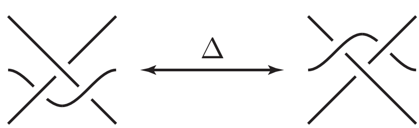

Figure 6. Δ-move.

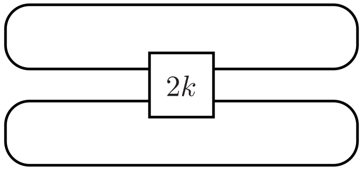

Figure 7. L_{2k}, a 2-component link with linking number k.

It is shown in [Ganzell 2014] that two links that differ by a sequence of Δ-moves have bracket polynomials that are congruent mod $A^8 - A^6 - A^2 + 1$ (in fact mod $A^{16} - A^{12} - A^4 + 1$). Since Δ-moves do not affect the self-writhe, the U-polynomials are also congruent mod $A^8 - A^6 - A^2 + 1$. Now, let L_{2k} be the link in Figure 7. We will show that $\langle L_{2k}\rangle - \langle \bigcirc\bigcirc\rangle$ is also a multiple of $A^8 - A^6 - A^2 + 1$. Thus every 2-component link has bracket polynomial congruent to $\langle \bigcirc\bigcirc\rangle \pmod{A^8 - A^6 - A^2 + 1}$. Since L_{2k} has self-writhe equal to 0, this will complete the proof.

We first compute $\langle L_{2k}\rangle$. We have

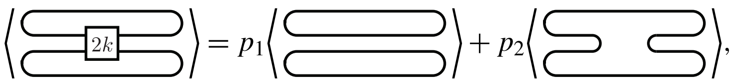

where $p_1 = A^{2k}$ and $p_2 = \sum_{m=1}^{2k} \binom{2k}{m} A^{2k-2m} d^{m-1}$. Now observe that

$$\sum_{m=0}^{2k} \binom{2k}{m} A^{2k-2m} d^m = \sum_{m=0}^{2k} \binom{2k}{m} A^{2k-2m} (-A^2 - A^{-2})^m$$
$$= \sum_{m=0}^{2k} \binom{2k}{m} A^{2k-m} (-A - A^{-3})^m = [(-A - A^{-3}) + A]^{2k}$$

by the binomial theorem. The last expression simplifies to A^{-6k}. Therefore $p_2 = (A^{-6k} - A^{2k})/d$, and

$$\langle L_{2k}\rangle = A^{2k} d + \frac{A^{-6k} - A^{2k}}{d}$$
$$= \frac{A^{2k}(A^4 + 2 + A^{-4}) + A^{-6k} - A^{2k}}{-A^2 - A^{-2}}$$
$$= \frac{-A^{2k+6} - A^{2k+2} - A^{2k-2} - A^{-6k+2}}{A^4 + 1}.$$

Thus,

$$\langle L_{2k}\rangle - \langle \bigcirc\bigcirc\rangle = \frac{-A^{2k+6} - A^{2k+2} - A^{2k-2} - A^{-6k+2}}{A^4 + 1} + A^2 + A^{-2}$$
$$= \frac{A^{8k+4} + A^{8k} + A^{8k-4} - A^{6k+4} - 2A^{6k} - A^{6k-4} + 1}{-A^{6k-2}(A^4 + 1)}. \qquad (1)$$

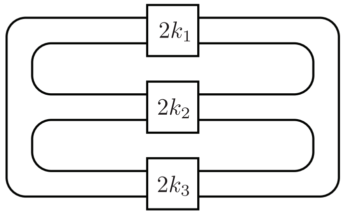

Figure 8. A 3-component link with linking numbers k_1, k_2, k_3.

Let $N(A)$ be the numerator of (1). Since

$$A^8 - A^6 - A^2 + 1 = (A+1)^2(A-1)^2(A^2+A+1)(A^2-A+1),$$

we must show that $N(A)$ has these factors. (Actually, we only need to prove that 1 and -1 are double roots, since we have already established Theorem 5. But it is not hard to show directly.) Rewrite $N(A)$ in the form

$$N(A) = (A^{8k+4} + A^{8k} + A^{8k-4}) - (A^{6k+4} + A^{6k} + A^{6k-4}) - (A^{6k} - 1).$$

Observe that

$$A^{8k+4} + A^{8k} + A^{8k-4} = A^{8k-4}(A^4 - A^2 + 1)(A^2+A+1)(A^2-A+1),$$
$$A^{6k+4} + A^{6k} + A^{6k-4} = A^{6k-4}(A^4 - A^2 + 1)(A^2+A+1)(A^2-A+1),$$

and

$$A^{6k} - 1 = (A^2+A+1)(A^2-A+1)\sum_{m=0}^{6k-6}(A^{m+2} - A^m).$$

It remains to show that $(A+1)^2$ and $(A-1)^2$ are factors of $N(A)$. It is straightforward to verify that 1 and -1 are both roots of $N(A)$ and of the derivative $N'(A)$, completing the proof for 2-component links.[1]

The proof for $n = 3$ is similar. Observe that every 3-component link is Δ-move equivalent to a link of the form in Figure 8. Define

$$q(k) = \sum_{m=1}^{k} \binom{k}{m} A^{k-2m} d^{m-1},$$

so that

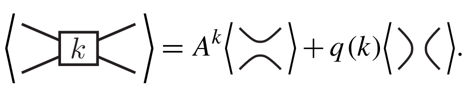

[1]Note that $N(A)$ must also be divisible by A^4+1, since bracket polynomials are Laurent polynomials. We can see this directly by writing $N(A) = (A^{8k} + A^{8k-4}) - (A^{6k+4} + A^{6k}) - (A^{6k} + A^{6k-4}) + (A^{8k+4} + 1)$. The first three binomials are multiples of A^4+1, and $A^{8k+4}+1 = (A^4+1)(A^{8k} - A^{8k-4} + A^{8k-8} - \cdots + 1)$.

Then if L is the link in Figure 8, we have

$$\begin{aligned}\langle L\rangle = A^{2k_1+2k_2+2k_3}d^2 \\ + A^{2k_1+2k_2}q(2k_3)d + A^{2k_1+2k_3}q(2k_2)d + A^{2k_2+2k_3}q(2k_1)d \\ + A^{2k_1}q(2k_2)q(2k_3) + A^{2k_2}q(2k_1)q(2k_3) + A^{2k_3}q(2k_1)q(2k_2) \\ + q(2k_1)q(2k_2)q(2k_3)d,\end{aligned}$$

and we must verify that $\langle L\rangle - \langle \bigcirc\bigcirc\bigcirc\rangle$ is divisible by $A^8 - A^6 - A^2 + 1$. The proof is tedious but elementary, and follows the same outline as for 2-component links. □

Corollary 9. *For n-component links L, L' with $n \leq 3$, the U-polynomial of L can never be a nontrivial monomial times the U-polynomial of L'. That is, if $U_{L'}(A) = rA^kU_L(A)$, then $r = 1$ and $k = 0$.*

Proof. Let $p(A) = A^8 - A^6 - A^2 + 1$, so that $U_L(A) - U_{L'}(A) = p(A)g(A)$ for some Laurent polynomial g. Now suppose $U_{L'}(A) = rA^kU_L(A)$. Then

$$U_L(A) - rA^kU_L(A) = p(A)g(A). \tag{2}$$

Setting $A = 1$, we obtain

$$(-2)^{n-1} - r(-2)^{n-1} = 0$$

from Corollary 6. Thus $r = 1$.

Differentiating (2) with respect to A and setting $r = 1$, we obtain

$$(1 - A^k)U_L'(A) - kA^{k-1}U_L(A) = p'(A)g(A) + p(A)g'(A).$$

Again, setting $A = 1$ produces

$$kU_L(A) = 0.$$

Thus $k = 0$. □

Corollary 9 does not hold for the original Jones polynomial. Example 10 below, shows a pair of 2-component links whose Jones polynomials do not satisfy the conclusion of the corollary. However, since the U-polynomial for a *knot* is identical to the original Jones polynomial, Corollary 9 does apply. Hence, the Jones polynomial of a knot cannot be the product of a nontrivial monomial with another Jones polynomial.

Example 10. In [Eliahou et al. 2003], examples are given of n-component links (for $n \geq 2$) that have the same Jones polynomial as $\bigcirc^n$. The link in Figure 9 (left) is the first of an infinite family of such links. Those examples all have $w = \psi = 0$, and therefore satisfy $U_L = U_{\bigcirc^n}$. Other examples are given in that paper of links

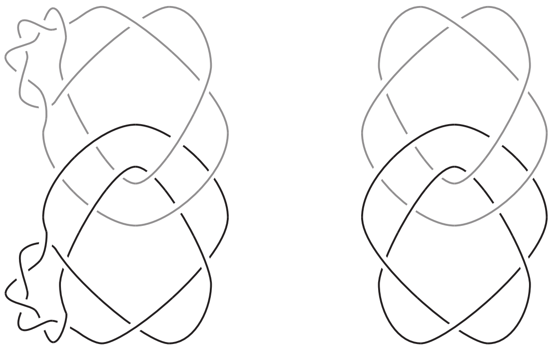

Figure 9. Links with $U_L = U_{\bigcirc^n}$.

whose Jones polynomial has the form $t^k d^{n-1}$, as in Figure 9 (right). These links have $\psi = 0$, and as a result, $U(A) = d^{n-1}$.

References

[Doll and Hoste 1991] H. Doll and J. Hoste, "A tabulation of oriented links", *Math. Comp.* **57**:196 (1991), 747–761. MR Zbl

[Eliahou et al. 2003] S. Eliahou, L. H. Kauffman, and M. B. Thistlethwaite, "Infinite families of links with trivial Jones polynomial", *Topology* **42**:1 (2003), 155–169. MR Zbl

[Ganzell 2014] S. Ganzell, "Local moves and restrictions on the Jones polynomial", *J. Knot Theory Ramifications* **23**:2 (2014), art. id. 1450011. MR Zbl

[Jones 1985] V. F. R. Jones, "A polynomial invariant for knots via von Neumann algebras", *Bull. Amer. Math. Soc.* (*N.S.*) **12**:1 (1985), 103–111. MR Zbl

[Kauffman 1988] L. H. Kauffman, "New invariants in the theory of knots", *Amer. Math. Monthly* **95**:3 (1988), 195–242. MR Zbl

[Morton 1986] H. R. Morton, "The Jones polynomial for unoriented links", *Quart. J. Math. Oxford Ser.* (2) **37**:145 (1986), 55–60. MR Zbl

[Murakami and Nakanishi 1989] H. Murakami and Y. Nakanishi, "On a certain move generating link-homology", *Math. Ann.* **284**:1 (1989), 75–89. MR Zbl

Received: 2019-04-10 Revised: 2019-06-19 Accepted: 2019-07-06

sganzell@smcm.edu — *Department of Mathematics and Computer Science, St. Mary's College of Maryland, St. Mary's City, MD, United States*

janet.huffman@uky.edu — *University of Kentucky, Lexington, KY, United States*

lmavrakis@math.ucsb.edu — *University of California, Santa Barbara, CA, United States*

kaitlin.tademy@huskers.unl.edu — *University of Nebraska, Lincoln, NE, United States*

griffin.ea.walker@gmail.com — *Wheaton College, Wheaton, IL, United States*

INVOLVE 12:8 (2019)
dx.doi.org/10.2140/involve.2019.12.1369

Nonsplit module extensions over the one-sided inverse of $k[x]$

Zheping Lu, Linhong Wang and Xingting Wang

(Communicated by Scott T. Chapman)

Let R be the associative k-algebra generated by two elements x and y with defining relation $yx = 1$. A complete description of simple modules over R is obtained by using the results of Irving and Gerritzen. We examine the short exact sequence $0 \to U \to E \to V \to 0$, where U and V are simple R-modules. It shows that nonsplit extension only occurs when both U and V are one-dimensional, or, under certain condition, U is infinite-dimensional and V is one-dimensional.

1. Introduction

In this short note, we study nonsplit extensions of simple modules over the associative algebra $R = k\{x, y\}/\langle yx - 1\rangle$ over a base field k of characteristic 0. The algebra R is also known as the one-sided inverse of the polynomial algebra $k[x]$ and appeared in [Bavula 2010; Gerritzen 2000; Jacobson 1950; Irving 1979]. Note that

$$y(1 - xy) = (1 - xy)x = 0.$$

The algebra R is not a domain, and $Z(R) = k$. As a k-vector space R has basis

$$\{x^i y^j \mid i, j = 0, 1, 2, \ldots\}.$$

Moreover, R admits the involution $\eta : x \mapsto y$ and $y \mapsto x$. Hence, the left and right algebraic properties of R are the same.

Jacobson [1950] gave a faithful irreducible representation of R as follows. Let S be the infinite-dimensional k-vector space with the basis $\{e_1, e_2, \ldots\}$ and let R act on S by assigning

$$\begin{aligned} xe_n &= e_{n+1}, \quad n > 0, \\ ye_n &= e_{n-1}, \quad n > 1, \\ ye_1 &= 0. \end{aligned}$$

It was proved by Bavula [2010] and Gerritzen [2000] that there is only one isomorphic class of infinite-dimensional simple R-modules. Note that there is an

MSC2010: primary 16D60; secondary 16G99.
Keywords: simple modules, representations, module extensions.

algebra monomorphism $R \to \mathrm{End}_k(k[x])$ such that $x \mapsto x$ and $y \mapsto H^{-1}\frac{d}{dx}$, where $H \in \mathrm{End}_k(k[x])$ is given by $H(f) = \frac{d}{dx}(xf)$ for any $f \in k[x]$. In particular,

$$\bigoplus_{i\geq 0} kx^i(1-xy) \cong k[x]$$

is a simple and faithful left R-module, where the left R-module structure on $k[x]$ is via the algebra map $R \to \mathrm{End}_k(k[x])$ discussed above. Following [Bavula 2010], R contains a subring which is canonically isomorphic to the ring (without identity) of infinite-dimensional matrices. Let

$$F = \bigoplus_{i,j\geq 0} kM_{ij} \cong M_\infty(k),$$

where $M_{ij} = x^i(1-xy)y^j$ can be identical to the matrix units of $M_\infty(k)$. In particular, we have

$$x \sim \begin{pmatrix} 0 & & & \\ 1 & 0 & & \\ & 1 & 0 & \\ & & \ddots & \ddots \end{pmatrix}, \quad y \sim \begin{pmatrix} 0 & 1 & & \\ & 0 & 1 & \\ & & 0 & \ddots \\ & & & \ddots \end{pmatrix}. \tag{1}$$

As a left R-module,

$$F = \bigoplus_{i,j\geq 0} kx^i(1-xy)y^j \cong \bigoplus_{i\geq 0}\Big(\bigoplus_{t\geq 0} kx^t x^i(1-xy)y^i\Big) \cong \bigoplus_{i\geq 0} k[x]$$

is a direct sum of infinitely many simple R-modules. Hence R is neither left nor right noetherian. Similarly, we see that there is an ascending chain of left annihilators in R which is not stable. Then R is neither left nor right Goldie. Moreover, F is equal to the ideal of R generated by $\langle 1-xy\rangle$. Since $F^2 = F$, $\mathrm{lann}(F)$ and $\mathrm{rann}(F)$ are both zero, we have F is an essential left and right ideal of R, which equals the socle of left and right R-module R. Hence F is contained in any nonzero ideal of R and it follows that the set of proper (two-sided) ideals of R is

$$\{0, \langle 1-xy\rangle, \langle 1-xy, f(x)\rangle\},$$

where $f(x)$ is a monic polynomial in $k[x]$ which is not a monomial. In particular, the ideals of R satisfy the ascending chain condition.

It follows from [Bavula 2010; Gerritzen 2000; Irving 1979] that the prime ideals are given by

$$\mathrm{Spec}(R) = \{0, \langle 1-xy\rangle, \langle 1-xy, f(x)\rangle\},$$

where $f(x)$ is a monic irreducible polynomial in $k[x]$ which is not a monomial. In particular, $\langle 1-xy, f(x)\rangle$ are the maximal ideals of R. Therefore simple R-modules are isomorphic to $k[x]$ or $k[x^{\pm 1}]/\langle f(x)\rangle$. When k is algebraically closed, the simple R-modules are either one-dimensional or infinite-dimensional.

A discussion of how Jategaonkar's main lemma and a theorem of Stafford apply to this nonnoetherian R is given in Section 3.

2. Nonsplit extensions of simple R-modules

Throughout k is an algebraically closed field with $\operatorname{char}(k) = 0$. All modules are left modules. Then simple R-modules are isomorphic to $k[x]$ or $k[x^{\pm 1}]/\langle x - \lambda\rangle$ for $\lambda \in k^\times$. When a simple module is one-dimensional, i.e., isomorphic to k as a vector space, the x-action is multiplication by a scalar λ, and the y-action is multiplication by its inverse λ^{-1}. We denote such a simple R-module by k_λ. It is clear that $k_{\lambda_1} \cong k_{\lambda_2}$ as simple R-modules for any $\lambda_1, \lambda_2 \in k^\times$ if and only if $\lambda_1 = \lambda_2$.

We consider the R-module extension E with the short exact sequence (s.e.s.)

$$0 \to U \to E \to V \to 0 \tag{2}$$

of R-modules U and V. It is clear that E is isomorphic to $U \oplus V$, as k-vector spaces. The R-action on E is then given by the ring homomorphism

$$\rho_\delta : r \mapsto \begin{pmatrix} \alpha(r) & \delta(r) \\ 0 & \beta(r) \end{pmatrix},$$

where

$$\alpha : R \to \operatorname{End}_k(U) \quad \text{and} \quad \beta : R \to \operatorname{End}_k(V)$$

are ring homomorphisms, and $\delta(r)$ is a k-linear map in $\operatorname{Hom}_k(V, U)$ such that

$$\delta(r_1 r_2) = \alpha(r_1)\delta(r_2) + \delta(r_1)\beta(r_2)$$

for any $r_1, r_2 \in R$. In particular,

$$\alpha(y)\delta(x) + \delta(y)\beta(x) = \delta(yx) = \delta(1).$$

Since $\rho_\delta(1)$ must be the identity matrix, we have $\delta(1) = 0$. Therefore,

$$\alpha(y)\delta(x) + \delta(y)\beta(x) = 0. \tag{3}$$

That is, given α and β, the map δ is uniquely determined by the pair of k-linear maps $\delta(x), \delta(y) \in \operatorname{Hom}_k(V, U)$ satisfying the compatibility condition (3). If δ is the zero mapping, then $E \cong U \oplus V$. Let E_δ and $E_{\delta'}$ be two module extensions of U by V, equipped with ring homomorphisms ρ_δ and $\rho_{\delta'}$. Then $E_\delta \cong E_{\delta'}$ if and only if there is a k-vector space isomorphism $f : E_\delta \to E_{\delta'}$ such that $f \circ \rho_\delta(r) = \rho_{\delta'}(r) \circ f$. Note that R has the k-basis $\{x^i y^j \mid i, j = 0, 1, 2, \ldots\}$. Therefore, it is sufficient to verify $\rho_\delta(x) = f^{-1} \circ \rho_{\delta'}(x) \circ f$ and $\rho_\delta(y) = f^{-1} \circ \rho_{\delta'}(y) \circ f$.

Now consider another R-module extension E' with the s.e.s.

$$0 \to U' \to E' \to V' \to 0 \tag{4}$$

of R-modules U' and V'. We say that the two s.e.s. (2) and (4) are *equivalent* if there is an R-module isomorphism $f : E \to E'$ such that the restriction of f on U yields an isomorphism from U to U'.

We focus on the R-module extension E of a simple R-module U by another simple R-module V. We start with the case when V is infinite-dimensional. It is shown in the following lemma that the s.e.s in this case is always split. This result can be directly derived from Bavula's proof that the infinite-dimensional simple R-module $k[x]$ is projective. We include an alternative proof without using projectivity.

Lemma 2.1. *Suppose* $0 \to U \to E_\delta \to V \to 0$ *is an s.e.s., where U and V are simple R-modules and* $\dim_k(V) = \infty$. *Then the s.e.s. is always split.*

Proof. Let $\{b_0, b_1, b_2, \ldots\}$ be a basis of V such that y and x are left and right shift operators, respectively. As vector spaces, $E_\delta \cong U \oplus V$. Consider the element

$$a := b_0 - x\delta(y)b_0$$

of E_δ. It is clear that $a \in E_\delta \setminus U$. Then the left cyclic submodule Ra of E_δ is distinct from 0 and U. For any element $r \in R$, we have

$$ra = \delta(r)b_0 + \beta(r)b_0 - rx\delta(y)b_0.$$

Hence $ra \in R_a \cap U$ only if $\beta(r)b_0 = 0$, that is, $r = sy$ for some $s \in R$. But

$$ya = yb_0 - yx\delta(y)b_0 = \delta(y)b_0 + \beta(y)b_0 - \delta(y)b_0 = 0.$$

That is, $R_a \cap U = 0$. Then $R_a \oplus U = E_\delta$ since $E_\delta/U \cong V$ is simple. Therefore $E_\delta \cong U \oplus V$ as left R-modules. □

The next case deals with the module extension when U is infinite-dimensional and V is one-dimensional.

Lemma 2.2. *Let U and U' be two infinite-dimensional simple R-modules, k_λ and $k_{\lambda'}$ be two one-dimensional R-modules for nonzero scalars λ and λ'. Suppose E_δ and $E_{\delta'}$ are two R-module extensions with the respective s.e.s.*

$$0 \to U \to E_\delta \to k_\lambda \to 0 \quad \text{and} \quad 0 \to U' \to E_{\delta'} \to k_{\lambda'} \to 0.$$

Then $E_\delta \cong E_{\delta'}$ if and only if $\lambda = \lambda'$ and $\delta'(x) = c\delta(x)$ for some nonzero $c \in k$. In this case the two s.e.s. are equivalent if and only if $E_\delta \cong E_{\delta'}$. As a consequence, E_δ (resp. $E_{\delta'}$) is nonsplit if and only if $\delta \neq 0$ (resp. $\delta' \neq 0$).

Proof. We will fix a basis $\{e_0, e_1, e_2, \dots, d\}$ for both E_δ and $E_{\delta'}$ as k-vector spaces, where $\{e_0, e_1, e_2, \dots\}$ is a basis of U (and U') such that y and x are left and right shift operators, respectively. For any $r \in R$, we can identify the map $\delta(r)$, under the fixed basis, with an infinite-dimensional vector

$$\langle \delta(r)_0, \delta(r)_1, \delta(r)_2, \dots \rangle$$

with only finitely many nonzero components. Note that $\alpha(y)\delta(x) + \delta(y)\beta(x) = 0$, where $\beta(x) = \lambda$ and y is the upper diagonal line matrix given in (1). It follows that

$$\delta(y)_i = \lambda^{-1}\delta(x)_{i+1} \quad \text{for } i \geq 1. \tag{5}$$

A similar result for $\delta'(x)$ and $\delta'(y)$ holds. Suppose that m is the smallest integer such that $\delta(y)_i = \delta'(y)_i = 0$ for any $i > m$. Consequently, $\delta(x)_i = \delta'(x)_i = 0$ for any $i > m+1$.

Suppose that f is an R-module isomorphism $E_{\delta'} \to E_\delta$; that is, f is a k-vector space isomorphism such that both $\rho_\delta(x)f = f\rho_{\delta'}(x)$ and $\rho_\delta(y)f = f\rho_{\delta'}(y)$. We will obtain necessary conditions on f through its images on the basis elements of the selected basis. Let

$$f(e_0) = ae_0 + a_1e_1 + a_2e_2 + \dots + a'd$$

for some $a', a_i \in k$, $i = 1, 2, \dots$, where only finitely many a_i's are nonzero. First,

$$f \circ \rho_{\delta'}(y)(e_0) = 0,$$
$$\rho_\delta(y) \circ f(e_0) = \sum_{i \geq 0}(a_{i+1} + a'\delta(y)_i)e_i + \frac{1}{\lambda}a'd.$$

Hence, $a' = a_i = 0$ for all $i = 1, 2, \dots$, and so $f(e_0) = ae_0$. Moreover,

$$f(e_1) = f(xe_0) = xf(e_0) = x(ae_0) = ae_1$$

implies $f(e_1) = ae_1$. Inductively, $f(e_i) = ae_i$ for some $a \neq 0$ and all $i \geq 0$. Next, suppose that

$$f(d) = b_0e_0 + b_1e_1 + b_2e_2 + \dots + bd,$$

where $b \neq 0$, $b_i \in k$ for $i \geq 0$, and only finitely many b_i's are nonzero. Then

$$\rho_\delta(y) \circ f(d) = \sum_{i \geq 0} b_{i+1}e_i + \sum_{i \geq 0} b\delta(y)_ie_i + \lambda^{-1}bd,$$
$$f \circ \rho_{\delta'}(y)(d) = \sum_{i \geq 0}\left(a\delta'(y)_i + \frac{1}{\lambda'}b_i\right)e_i + \frac{1}{\lambda'}bd.$$

Thus, we have

$$\lambda = \lambda', \quad b_{i+1} + b\delta(y)_i = a\delta'(y)_i + \lambda^{-1}b_i \quad \text{for } i \geq 0.$$

Since $\delta(y)_i = \delta'(y)_i = 0$ for any $i > m$, we have $b_{i+1} = \lambda^{-1} b_i$ for any $i > m$. But only finitely many b_i's are nonzero; it then follows inductively that

$$b_{m+1} = b_{m+2} = \cdots = 0.$$

Hence, we have the $m+1$ relations

$$\begin{aligned} b\delta(y)_m &= a\delta'(y)_m + \lambda^{-1} b_m, \\ b_{i+1} + b\delta(y)_i &= a\delta'(y)_i + \lambda^{-1} b_i \quad \text{for } i = 0, 1, \ldots, m-1. \end{aligned} \tag{6}$$

Similarly, we have

$$\begin{aligned} \rho_\delta(x) \circ f(d) &= \sum_{i \geq 1} b_{i-1} e_i + \sum_{i \geq 0} b\delta(x)_i e_i + \lambda bd, \\ f \circ \rho_{\delta'}(x)(d) &= \sum_{i \geq 0} (a\delta'(x)_i + \lambda' b_i) e_i + \lambda' bd. \end{aligned}$$

Note that $\delta(x)_j = \delta'(x)_j = 0$ for any $j > m+1$. It then follows that

$$\begin{aligned} b\delta(x)_0 &= a\delta'(x)_0 + \lambda b_0, \\ b_m + b\delta(x)_{m+1} &= a\delta'(x)_{m+1}, \\ b_{i-1} + b\delta(x)_i &= a\delta'(x)_i + \lambda b_i \quad \text{for } i = 1, 2, \ldots, m. \end{aligned} \tag{7}$$

Combining the relations (5) and (7), we have

$$\begin{aligned} b\delta(y)_m - a\delta'(y)_m &= -\lambda^{-1} b_m, \\ b\delta(y)_i - a\delta'(y)_i &= b_{i+1} - \lambda^{-1} b_i \quad \text{for } i = 0, 1, \ldots, m-1. \end{aligned}$$

From (6), we have

$$\begin{aligned} b\delta(y)_m - a\delta'(y)_m &= \lambda^{-1} b_m, \\ b\delta(y)_i - a\delta'(y)_i &= \lambda^{-1} b_i - b_{i+1} \quad \text{for } i = 0, 1, \ldots, m-1. \end{aligned}$$

Hence, $b_i = \lambda b_{i+1}$ for $0 \leq i \leq m-1$ and $b_m = 0$. Thus, $b_0 = b_1 = \cdots = b_m = 0$.

Therefore, $f(e_i) = ae_i$ and $f(d) = bd$ for some nonzero scalars $a, b \in k$ and all $i \geq 0$. Such a k-vector space isomorphism is an R-module isomorphism if and only if $\delta'(x) = \frac{b}{a}\delta(x)$ for the nonzero scalars $a, b \in k$ or equivalently, $\delta'(r) = \frac{b}{a}\delta(r)$ for any $r \in R$.

Therefore, any module extension E_δ such that $E_\delta / U \cong k_\lambda$ is nonsplit if and only if $\delta(x) \neq 0$. Let E_δ and $E_{\delta'}$ be nonsplit extensions such that

$$0 \to U \to E_\delta \to k_\lambda \to 0 \quad \text{and} \quad 0 \to U' \to E_{\delta'} \to k_{\lambda'} \to 0.$$

Then $E_\delta \cong E_{\delta'}$ if and only if $\lambda = \lambda'$ and $\delta'(x) = c\delta(x)$ for some nonzero scalar $c \in k$. Observe that the isomorphism f from E_δ to $E_{\delta'}$ yields an isomorphism from U to U'. Therefore, the two s.e.s. are equivalent if and only if $E_\delta \cong E_{\delta'}$. □

Now we can state our main result.

Theorem 2.3. *Suppose* $0 \to U \to E_\delta \to V \to 0$ *is an s.e.s. where* U *and* V *are simple* R*-modules and* E_δ *is associated with the* k*-linear map* δ *in* $\mathrm{Hom}_k(V, U)$. *Let* λ, λ' *be nonzero scalars*:

(i) *If* $\dim(V) = \infty$, *the s.e.s. is always split.*

(ii) *If* $\dim(U) = \infty$ *and* $V = k_\lambda$, *the s.e.s. is nonsplit if and only if* $\delta \neq 0$. *Any such two s.e.s. are equivalent if and only if* $\lambda = \lambda'$ *and the infinite vectors* $\delta(x)$ *and* $\delta'(x)$ *are proportional.*

(iii) *If* $U = k_\lambda$ *and* $V = k_{\lambda'}$ *are both one-dimensional, then the s.e.s. is nonsplit only if* $\delta \neq 0$ *and* $\lambda = \lambda'$. *Any such two nonsplit s.e.s. are equivalent if and only if the submodules* U *are the same.*

Proof. The first two cases are proved in Lemmas 2.1 and 2.2. We only need to consider the case when U and V are both one-dimensional. Suppose the two modules U and V are uniquely determined by nonzero scalars λ and λ'. Let

$$0 \to k_\lambda \to E_\delta \to k_{\lambda'} \to 0$$

be an s.e.s. Then δ is uniquely determined by $\delta(x)$ since $\delta(y) = -(\lambda\lambda')^{-1}\delta(x)$. Moreover, $\rho_\delta(y)$ is the inverse matrix of $\rho_\delta(x)$. Note that the 2×2 matrix $\rho_\delta(x)$ is similar to $\rho_0(x)$ if and only if $\lambda \neq \lambda'$. Hence, the s.e.s. is always split if $\lambda \neq \lambda'$, whether or not $\delta = 0$. Therefore, the nonsplit case occurs when $\delta \neq 0$ and $\lambda = \lambda'$. Consider two nonsplit s.e.s.

$$0 \to k_\lambda \to E_\delta \to k_\lambda \to 0 \quad \text{and} \quad 0 \to k_\gamma \to E_{\delta'} \to k_\gamma \to 0,$$

with nonzero δ and δ'. It is easy to see, by a linear transformation, that the two nonsplit s.e.s. are equivalent if and only if $E_\delta \cong E_{\delta'}$ if and only if the nonzero scalars λ and γ are equal. Thus, there is only one, up to equivalence, nonsplit s.e.s. $0 \to k_\lambda \to E_\delta \to k_\lambda \to 0$ for each one-dimensional simple R-module k_λ. □

3. Closing discussion

Let A be an associative ring. Recall a left (respectively, right) module M over A is called *torsion-free* if for any nonzero element m in M there is some $r \in A$ such that $rm \neq 0$ (respectively, $mr \neq 0$). Two prime ideals P and Q of an associative ring A are *linked*, denoted as $P \rightsquigarrow Q$, if there is an ideal I of A such that $(P \cap Q) > I \geq PQ$ and $(P \cap Q)/I$ is nonzero and torsion-free both as a left A/P-module and a right A/Q-module. The graph of links of A is a directed graph whose vertices are prime ideals of A, with an arrow from P to Q whenever $P \rightsquigarrow Q$. The vertex set of each connected component is called a *clique*.

Jategaonkar's main lemma [1986] states that if M is a (right) module over a noetherian ring A with a nonsplit short exact sequence $0 \to U \to M \to V \to 0$ and corresponding annihilators $Q = \mathrm{ann}_A(U)$ and $P = \mathrm{ann}_A(V)$, then exactly one of the following two alternatives occurs: (i) $P < Q$ and $PM = 0$; (ii) $P \rightsquigarrow Q$.

Now let $0 \to U \to E_\delta \to V \to 0$ be a nonsplit short exact sequence, where U and V are simple R-modules. Suppose $Q = \mathrm{ann}_R(U)$ and $P = \mathrm{ann}_R(V)$ are the affiliated primes. When $\dim U = \infty$ and $V \cong k_\lambda$, we have $Q = (0)$ and $P = \langle 1 - xy, x - \lambda \rangle$. There is no link between P and Q, and $P \not< Q$. When $U \cong V \cong k_\lambda$, we have $Q = P = \langle 1 - xy, x - \lambda \rangle$. There is no link between P and Q, and $P \not< Q$. This suggests that the noetherianess is necessary in the assumptions of Jategaonkar's main lemma.

On the other hand, [Stafford 1987, Corollary 3.13] states that all cliques of prime ideals in any noetherian ring are countable. When k is algebraically closed, the prime ideals of R are (0), $F = \langle 1 - xy \rangle$, and $P_\lambda = \langle 1 - xy, x - \lambda \rangle$, where $\lambda \in k^\times$. One can check that

$$F = F^2 = F \cap P_\lambda = F P_\lambda = P_\lambda F = P_\lambda \cap P_{\lambda'} = P_\lambda P_{\lambda'}$$

whenever $\lambda \neq \lambda'$. Moreover, $P_\lambda / P_\lambda^2 \cong (x - \lambda)/(x - \lambda)^2$ as in $k[x^{\pm 1}]$. Hence the cliques in the graph of links are

$$F, \qquad (0), \qquad \circlearrowright P_\lambda, \qquad \circlearrowright P_{\lambda'}.$$

This suggests that all cliques of R are countable.

Acknowledgements

L. Wang would like to express her gratitude to Professor E. Letzter for his valuable suggestions. Lu was a math major at the University of Pittsburgh who participated in an undergraduate research project that was related to this short article. We are thankful to the math department of the University of Pittsburgh for its support. We also would like to express our gratitude to the referee for careful reading and helpful suggestions.

References

[Bavula 2010] V. V. Bavula, "The algebra of one-sided inverses of a polynomial algebra", *J. Pure Appl. Algebra* **214**:10 (2010), 1874–1897. MR Zbl

[Gerritzen 2000] L. Gerritzen, "Modules over the algebra of the noncommutative equation $yx = 1$", *Arch. Math.* (*Basel*) **75**:2 (2000), 98–112. MR Zbl

[Irving 1979] R. S. Irving, "Prime ideals of Ore extensions over commutative rings, II", *J. Algebra* **58**:2 (1979), 399–423. MR Zbl

[Jacobson 1950] N. Jacobson, "Some remarks on one-sided inverses", *Proc. Amer. Math. Soc.* **1** (1950), 352–355. MR Zbl

[Jategaonkar 1986] A. V. Jategaonkar, *Localization in Noetherian rings*, London Mathematical Society Lecture Note Series **98**, Cambridge University Press, 1986. MR Zbl

[Stafford 1987] J. T. Stafford, "The Goldie rank of a module", pp. 1–20 in *Noetherian rings and their applications* (Oberwolfach, 1983), edited by L. W. Small, Math. Surveys Monogr. **24**, Amer. Math. Soc., Providence, RI, 1987. MR Zbl

Received: 2019-05-08 Revised: 2019-09-08 Accepted: 2019-09-09

zl2965@pitt.edu *Tandon School of Engineering, New York University, Brooklyn, NY, United States*

lhwang@pitt.edu *Department of Mathematics, University of Pittsburgh, Pittsburgh, PA, United States*

xingting.wang@howard.edu *Department of Mathematics, Howard University, Washington, DC, United States*

INVOLVE 12:8 (2019)
dx.doi.org/10.2140/involve.2019.12.1379

Split Grothendieck rings of rooted trees and skew shapes via monoid representations

David Beers and Matt Szczesny

(Communicated by Ravi Vakil)

We study commutative ring structures on the integral span of rooted trees and n-dimensional skew shapes. The multiplication in these rings arises from the smash product operation on monoid representations in pointed sets. We interpret these as Grothendieck rings of indecomposable monoid representations over $\mathbb{F}_1$ — the "field" of one element. We also study the base-change homomorphism from $\langle t \rangle$-modules to $k[t]$-modules for a field k containing all roots of unity, and interpret the result in terms of Jordan decompositions of adjacency matrices of certain graphs.

1. Introduction

In this paper we consider commutative ring structures on the integral spans of rooted trees and n-dimensional skew shapes. The product in these rings arises by first interpreting the corresponding combinatorial structure as a representation of a monoid in pointed sets, and then using the smash product, which defines a symmetric monoidal structure on the category of such representations. We proceed to explain the construction in greater detail.

To a monoid A, one may associate a category $\mathrm{Mod(A)}_{\mathbb{F}_1}$ of "representations of A over the field of one element", whose objects are finite pointed sets with an action of A. The terminology comes from the general yoga of $\mathbb{F}_1$, where pointed sets are viewed as vector spaces over $\mathbb{F}_1$, and monoids are viewed as nonadditive analogues of algebras; see [Chu et al. 2012; Lorscheid 2018]. Given $\mathrm{Mod(A)}_{\mathbb{F}_1}$, their categorical coproduct $M \oplus N$ is given by the wedge sum $M \vee N$ and the product by the Cartesian product $M \times N$ (equipped with diagonal A-action). One may also consider a reduced version of the Cartesian product — the smash product $M \wedge N$, with A-action $a(m \wedge n) = am \wedge an$, which while not a categorical product,

MSC2010: 05E10, 05E15, 16W22, 18F30.
Keywords: field of one element, combinatorics, rooted trees, skew shapes, Grothendieck rings.

defines a symmetric monoidal structure on $\mathrm{Mod(A)}_{\mathbb{F}_1}$. The product $\wedge$ is distributive over $\oplus$; i.e.,

$$M \wedge (K \oplus L) \simeq (M \wedge K) \oplus (M \wedge L).$$

In certain cases, objects of $\mathrm{Mod(A)}_{\mathbb{F}_1}$ have a pleasant interpretation in terms of familiar combinatorial structures. For example, when A is $\langle t \rangle$, the free monoid on one generator t, we may associate to $M \in \mathrm{Mod}(\langle t \rangle)_{\mathbb{F}_1}$ a graph Γ_M which encodes the action of t on M. The vertices of Γ_M correspond to the nonzero elements of M (where the base-point plays the role of zero), and the directed edges join $m \in M$ to $t \cdot m$. The possible connected graphs arising this way, corresponding to indecomposable representations, are easily seen to be of two types — rooted trees and wheels (please note that the term *wheel* is also used in the graph theory literature to describe a different type of graph). See Figure 1.

Given indecomposable $M, N \in \mathrm{Mod}(\langle t \rangle)_{\mathbb{F}_1}$ (corresponding to a tree or wheel), one can ask how $\Gamma_{M \wedge N}$ can be computed from Γ_M and Γ_N. We give the answer in Section 3A, in the form of a simple algorithm, and show that $\Gamma_{M \wedge N}$ corresponds to the tensor product of graphs $\Gamma_M \otimes \Gamma_N$ in the sense of [Weichsel 1962].

In a similar vein, n-dimensional skew shapes can be interpreted as representations of $\langle x_1, \ldots, x_n \rangle$ — the free commutative monoid on n generators $x_1, \ldots, x_n$. We illustrate this for $n = 2$, where the shape S

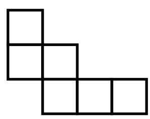

determines a module over the free commutative monoid on two generators $\langle x_1, x_2 \rangle$, whose nonzero elements correspond to the boxes in the diagram. The generator x_1 acts by moving one box to the right, and x_2 by moving one box up, until the edge of the diagram is reached, and by 0 beyond that. Connected skew shapes yield indecomposable representations of $\langle x_1, \ldots, x_n \rangle$, and we may once again ask how to decompose $M_S \wedge M_T$ into $\bigoplus_i M_{U_i}$, where U_i are connected skew shapes. The answer is given in Section 4A, where we prove the following theorem:

Theorem 1.1. *If S_1 and S_2 are n-dimensional skew shapes, then*

$$M_{S_1} \wedge M_{S_2} = \bigoplus_{t \in \mathbb{Z}^n} M_{S_1 \cap (S_2 + t)}.$$

In other words, the U_i are those skew shapes that occur in the intersection of one shape with a translate of the other.

Our results may be phrased in a more structured way as follows. Given a monoid A and a monoidal subcategory $\mathcal{C} \subset (\mathrm{Mod(A)}_{\mathbb{F}_1}, \wedge)$, we may consider the split Grothendieck ring $K^{\mathrm{split}}(\mathcal{C})$. Elements of $K^{\mathrm{split}}(\mathcal{C})$ may be identified with formal integer linear combinations $\sum a_i[M_i]$ of isomorphism classes of $[M_i] \in \mathrm{Iso}(\mathcal{C})$, subject to the relations

$$[M \oplus N] \sim [M] + [N],$$

with multiplication induced by the smash product. In our examples, $K^{\mathrm{split}}(\mathcal{C})$ consists of integer linear combinations of trees/wheels or skew shapes. The results of this paper amount to an explicit combinatorial description of the product in $K^{\mathrm{split}}(\mathcal{C})$.

Structures over $\mathbb{F}_1$ may be base-changed to those over a field (or any commutative ring) k. We denote this functor by $\otimes_{\mathbb{F}_1} k$. Then $\mathrm{A} \otimes_{\mathbb{F}_1} k$ is the monoid algebra $k[\mathrm{A}]$, and for $M \in \mathrm{Mod}(\mathrm{A})_{\mathbb{F}_1}$, $M \otimes_{\mathbb{F}_1} k$ is the $k[\mathrm{A}]$-module spanned over k by elements of M. Since $k[\mathrm{A}]$ is a k-bialgebra, its category of modules monoidal. The functor $\otimes_{\mathbb{F}_1} k$ is monoidal, and so induces a ring homomorphism

$$\Phi_k : \mathrm{K}_0^{\mathrm{sp}}(\mathrm{Mod}(\mathrm{A})_{\mathbb{F}_1}) \to \mathrm{K}_0^{\mathrm{sp}}(\mathrm{Mod}_{k[\mathrm{A}]}).$$

We study this homomorphism in Section 3B in the simple case of the monoid $\mathrm{A} = \langle t \rangle$, in which case generators of $\mathrm{K}_0^{\mathrm{sp}}(\mathrm{Mod}(k[t]))$ can be identified with Jordan blocks. Understanding Φ_k in this case reduces to computing the Jordan form of the adjacency matrices of the trees/wheels above. We show the image of Φ_k is spanned by nilpotent Jordan blocks and cyclotomic diagonal matrices.

1A. ***Outline of paper.*** In Section 2 we recall basic facts regarding monoids and the category $\mathrm{Mod}(\mathrm{A})_{\mathbb{F}_1}$ and define the split Grothendieck ring $\mathrm{K}_0^{\mathrm{sp}}(\mathrm{Mod}(\mathrm{A})_{\mathbb{F}_1})$. In Section 3A we consider the example of $\mathrm{A} = \langle t \rangle$ — the free monoid on one generator, and identify the product in $\mathrm{K}_0^{\mathrm{sp}}(\mathrm{Mod}(\langle t \rangle)_{\mathbb{F}_1})$ with the graph tensor product of trees/wheels. In Section 3B we consider the base-change homomorphism $\Phi_k : \mathrm{K}_0^{\mathrm{sp}}(\mathrm{Mod}(\langle t \rangle)_{\mathbb{F}_1}) \to \mathrm{K}_0^{\mathrm{sp}}(\mathrm{Mod}_{k[t]})$ and describe its image in terms of the Jordan decomposition of the adjacency matrix of the corresponding graph. Section 4A is devoted to the example of $\mathrm{A} = \mathbb{P}_n = \langle x_1, \dots, x_n \rangle$ — the free commutative monoid on n generators, and a certain subcategory of $\mathrm{Mod}(\mathbb{P}_n)_{\mathbb{F}_1}$ corresponding to n-dimensional skew shapes. We give an explicit description of the product in $\mathrm{K}_0^{\mathrm{sp}}(\mathrm{Mod}(\mathbb{P}_n)_{\mathbb{F}_1})$ in terms of intersections of skew shapes.

2. Monoids and their modules

A *monoid* A will be a semigroup with identity 1_A and zero 0_A (i.e., the absorbing element). We require

$$1_A \cdot a = a \cdot 1_A = a, \quad 0_A \cdot a = a \cdot 0_A = 0_A \quad \text{for all } a \in A.$$

Monoid homomorphisms are required to respect the multiplication as well as the special elements $1_A, 0_A$.

Example 2.1. Let $\mathbb{F}_1 = \{0, 1\}$, with

$$0 \cdot 1 = 1 \cdot 0 = 0 \cdot 0 = 0 \quad \text{and} \quad 1 \cdot 1 = 1.$$

We call $\mathbb{F}_1$ *the field with one element.*

Example 2.2. Let

$$\mathbb{P}_n := \langle x_1, \dots, x_n \rangle = \{x_1^{r_1} x_2^{r_2} \cdots x_n^{r_n} \mid r = (r_1, r_2, \dots, r_n) \in \mathbb{Z}^n_{\geq 0}\} \cup \{0\};$$

i.e., $\mathbb{P}_n$ is the set of monomials in $x_1, \dots, x_n$, with the usual multiplication. We will often write elements of $\mathbb{P}_n$ in multi-index notation as x^r, $r \in \mathbb{Z}^n_{\geq 0}$, in which case the multiplication is written as

$$x^r \cdot x^s = x^{r+s}.$$

We identify x^0 with 1. $\mathbb{P}_n$ has a natural $\mathbb{Z}^n_{\geq 0}$-grading obtained by setting $\deg(x_i) = e_i$, where e_i is the i-th standard basis vector in $\mathbb{Z}^n$.

$\mathbb{F}_1$ and $\mathbb{P}_n$ are both commutative monoids.

2A. *The category* $\mathbf{Mod(A)}_{\mathbb{F}_1}$.

Definition 2.3. Let A be a monoid. An A-*module* is a pointed set $(M, 0_M)$ (with $0_M \in M$ denoting the base-point), equipped with an action of A. More explicitly, an A-module structure on $(M, 0_M)$ is given by a map

$$\mathrm{A} \times M \to M, \quad (a, m) \to a \cdot m,$$

satisfying

$$(a \cdot b) \cdot m = a \cdot (b \cdot m), \quad 1 \cdot m = m, \quad 0 \cdot m = 0_M, \quad a \cdot 0_M = 0_M \quad \text{for all } a, b, \in \mathrm{A},\ m \in M.$$

A *morphism* of A-modules is given by a pointed map $f : M \to N$ compatible with the action of A, i.e., $f(a \cdot m) = a \cdot f(m)$. The A-module M is said to be *finite* if M is a finite set, in which case we define its *dimension* to be $\dim(M) = |M| - 1$ (we do not count the base-point, since it is the analogue of 0). We say that $N \subset M$ is an A-*submodule* if it is a (necessarily pointed) subset of M preserved by the action of A. The monoid A always possesses the module $\mathbb{0} := \{0\}$, which will be referred to as the *zero module*. If A has no zero-divisors, it possesses a *trivial module* $\mathbb{1} := \mathbb{F}_1$, on which all nonzero elements of A act by the identity (this arises via the augmentation homomorphism $\mathrm{A} \to \mathbb{F}_1$ sending all nonzero elements to 1).

Note. This structure is called an A-*act* in [Kilp et al. 2000] and an A-*set* in [Chu et al. 2012].

We denote by $\mathrm{Mod(A)}_{\mathbb{F}_1}$ the category of finite A-modules. It is the $\mathbb{F}_1$ analogue of the category of finite-dimensional representations of an algebra. Note that for $M \in \mathrm{Mod(A)}_{\mathbb{F}_1}$, $\mathrm{End}_{\mathrm{Mod(A)}_{\mathbb{F}_1}}(M) := \mathrm{Hom}_{\mathrm{Mod(A)}_{\mathbb{F}_1}}(M, M)$ is a monoid (in general noncommutative). An $\mathbb{F}_1$-module is simply a pointed set, and will be referred to as a vector space over $\mathbb{F}_1$. Thus, an A-module structure on $M \in \mathbb{F}_1$-mod amounts to a monoid homomorphism $A \to \mathrm{End}_{\mathbb{F}_1\text{-mod}}(M)$.

Given a morphism $f : M \to N$ in $\mathrm{Mod(A)}_{\mathbb{F}_1}$, we define the *image* of f to be

$$\mathrm{Im}(f) := \{n \in N \mid \text{there exists } m \in M \text{ such that } f(m) = n\}.$$

For $M \in \mathrm{Mod(A)}_{\mathbb{F}_1}$ and an A-submodule $N \subset M$, the *quotient* of M by N, denoted by M/N, is the A-module

$$M/N := M \backslash N \cup \{0\},$$

i.e., the pointed set obtained by identifying all elements of N with the base-point, equipped with the induced A-action.

We recall some properties of $\mathrm{Mod(A)}_{\mathbb{F}_1}$, following [Kilp et al. 2000; Chu et al. 2012; Szczesny 2014], where we refer the reader for details:

(1) For $M, N \in \mathrm{Mod(A)}_{\mathbb{F}_1}$, we have $|\,\mathrm{Hom}_{\mathrm{Mod(A)}_{\mathbb{F}_1}}(M, N)| < \infty$

(2) The zero A-module $\mathbb{0}$ is an initial, terminal, and hence zero object of $\mathrm{Mod(A)}_{\mathbb{F}_1}$.

(3) Every morphism $f : M \to N$ in C_A has a kernel $\ker(f) := f^{-1}(0_N)$.

(4) Every morphism $f : M \to N$ in C_A has a cokernel $\mathrm{coker}(f) := M/\,\mathrm{Im}(f)$.

(5) The coproduct of a finite collection $\{M_i\},\ i \in I$ in $\mathrm{Mod(A)}_{\mathbb{F}_1}$ exists and is given by the wedge sum

$$\bigvee_{i \in I} M_i = \coprod M_i/\sim,$$

where $\sim$ is the equivalence relation identifying the base-points. We will denote the coproduct of $\{M_i\}$ by

$$\bigoplus_{i \in I} M_i.$$

(6) The product of a finite collection $\{M_i\},\ i \in I$, in $\mathrm{Mod(A)}_{\mathbb{F}_1}$ exists and is given by the Cartesian product $\prod M_i$, equipped with the diagonal A-action. It is clearly associative. It is however not compatible with the coproduct in the sense that $M \times (N \oplus L) \not\simeq M \times N \oplus M \times L$.

(7) The category $\mathrm{Mod(A)}_{\mathbb{F}_1}$ possesses a reduced version $M \wedge N$ of the Cartesian product $M \times N$, called the smash product:

$$M \wedge N := M \times N/M \vee N,$$

where M and N are identified with the A-submodules $\{(m, 0_N)\}$ and $\{(0_M, n)\}$ of $M \times N$ respectively. The smash product inherits the associativity from the Cartesian product, and is compatible with the coproduct — i.e.,

$$M \wedge (N \oplus L) \simeq M \wedge N \oplus M \wedge L.$$

It defines a symmetric monoidal structure on $\mathrm{Mod(A)}_{\mathbb{F}_1}$, with unit $\mathbb{F}_1$ (i.e., $M \wedge \mathbb{F}_1 \simeq M$).

(8) $\mathrm{Mod(A)}_{\mathbb{F}_1}$ possesses small limits and colimits.

(9) Given M in $\mathrm{Mod(A)}_{\mathbb{F}_1}$ and $N \subset M$, there is an inclusion-preserving correspondence between flags $N \subset L \subset M$ in $\mathrm{Mod(A)}_{\mathbb{F}_1}$ and A-submodules of M/N given by sending L to L/N. The inverse correspondence is given by sending $K \subset M/N$ to $\pi^{-1}(K)$, where $\pi : M \to M/N$ is the canonical projection. This correspondence has the property that if $N \subset L \subset L' \subset M$, then $(L'/N)/(L/N) \simeq L'/L$.

These properties suggest that $\mathrm{Mod(A)}_{\mathbb{F}_1}$ has many of the properties of an abelian category, without being additive. It is an example of a *quasiexact* and *belian* category in the sense of [Deitmar 2012] and a *protoabelian* category in the sense of [Dyckerhoff and Kapranov 2012]. Let $\mathrm{Iso}(\mathrm{Mod(A)}_{\mathbb{F}_1})$ denote the set of isomorphism classes in $\mathrm{Mod(A)}_{\mathbb{F}_1}$, and $[M]$ the isomorphism class of $M \in \mathrm{Mod(A)}_{\mathbb{F}_1}$.

We will regard $\mathrm{Mod(A)}_{\mathbb{F}_1}$ as a symmetric monoidal category with respect to $\wedge$ and unit $\mathbb{F}_1$.

Definition 2.4. (1) We say that $M \in \mathrm{Mod(A)}_{\mathbb{F}_1}$ is *indecomposable* if it cannot be written as $M = N \oplus L$ for nonzero $N, L \in \mathrm{Mod(A)}_{\mathbb{F}_1}$.

(2) We say $M \in \mathrm{Mod(A)}_{\mathbb{F}_1}$ is *irreducible* or *simple* if it contains no proper submodules (i.e., those different from 0 and M).

It is clear that every irreducible module is indecomposable. We have the following analogue of the Krull–Schmidt theorem [Szczesny 2014]:

Proposition 2.5. *Every $M \in \mathrm{Mod(A)}_{\mathbb{F}_1}$ can be uniquely decomposed* (*up to reordering*) *as a direct sum of indecomposable* A-*modules.*

Remark 2.6. Suppose $M = \bigoplus_{i=1}^{k} M_i$ is the decomposition of an A-module into indecomposables, and $N \subset M$ is a submodule. It then immediately follows that $N = \bigoplus (N \cap M_i)$.

2B. *Monoid algebras.* We now recall a few facts regarding monoid algebras following [Steinberg 2016]. Let k be a field. The monoid algebra $k[\mathrm{A}]$ consists of linear combinations of nonzero elements of A with coefficients in k; i.e.,

$$k[\mathrm{A}] = \left\{ \sum c_a a \;\middle|\; a \in \mathrm{A},\ a \neq 0,\ c_a \in k \right\},$$

with product induced from the product in A, extended k-linearly. The monoid algebra $k[\mathrm{A}]$ is a bialgebra, with coproduct

$$\Delta : k[\mathrm{A}] \to k[\mathrm{A}] \otimes k[\mathrm{A}]$$

determined by

$$\Delta(a) = a \otimes a, \quad a \in \mathrm{A}.$$

The category $\mathrm{Mod}_{k[\mathrm{A}]}$ of $k[\mathrm{A}]$-modules is therefore symmetric monoidal under the operation of tensoring over k.

There is a base-change functor

$$\otimes_{\mathbb{F}_1} k : \mathrm{Mod}(\mathrm{A})_{\mathbb{F}_1} \to \mathrm{Mod}_{k[\mathrm{A}]} \tag{1}$$

to the category of $k[\mathrm{A}]$-modules defined by setting

$$M \otimes_{\mathbb{F}_1} k := \bigoplus_{m \in M,\, m \neq 0_M} k \cdot m,$$

i.e., setting $M \otimes_{\mathbb{F}_1} k$ to be the free k-module on the nonzero elements of M, with the $k[\mathrm{A}]$-action induced from the A-action on M. It sends $f \in \mathrm{Hom}_{\mathrm{A}}(M, N)$ to its unique k-linear extension in $\mathrm{Hom}_{k[\mathrm{A}]}(M \otimes_{\mathbb{F}_1} k, N \otimes_{\mathbb{F}_1} k)$.

We will find the following elementary observation useful:

Proposition 2.7. *The functor* $\otimes_{\mathbb{F}_1} k : \mathrm{Mod}(\mathrm{A})_{\mathbb{F}_1} \to \mathrm{Mod}_{k[\mathrm{A}]}$ *is monoidal.*

As a consequence, we have that for $M, N \in \mathrm{Mod}(\mathrm{A})_{\mathbb{F}_1}$

$$(M \wedge N) \otimes_{\mathbb{F}_1} k \simeq (M \otimes_{\mathbb{F}_1} k) \otimes_k (N \otimes_{\mathbb{F}_1} k)$$

as $k[\mathrm{A}]$-modules.

2C. *The split Grothendieck ring.*

Definition 2.8. The *split Grothendieck ring* of $\mathrm{Mod}(\mathrm{A})_{\mathbb{F}_1}$, denoted by $\mathrm{K}_0^{\mathrm{sp}}(\mathrm{Mod}(\mathrm{A})_{\mathbb{F}_1})$ is the $\mathbb{Z}$-linear span of isomorphism classes in $\mathrm{Mod}(\mathrm{A})_{\mathbb{F}_1}$ modulo the relation $[M \oplus N] = [M] + [N]$, i.e.,

$$\mathrm{K}_0^{\mathrm{sp}}(\mathrm{Mod}(\mathrm{A})_{\mathbb{F}_1}) = \mathbb{Z}[[M]]/I, \quad [M] \in \mathrm{Iso}(\mathrm{Mod}(\mathrm{A})_{\mathbb{F}_1}),$$

where I is the ideal generated by all differences $[M \oplus N] - [M] - [N]$, with product induced by $\wedge$. Since by Proposition 2.5 every module is a direct sum of indecomposable ones, we can also describe $\mathrm{K}_0^{\mathrm{sp}}\mathrm{Mod}(\mathrm{A})_{\mathbb{F}_1}$ as the $\mathbb{Z}$-linear span of indecomposable A-modules:

$$\mathrm{K}_0^{\mathrm{sp}}(\mathrm{Mod}(\mathrm{A})_{\mathbb{F}_1}) := \left\{ \sum a_i [M_i] \;\middle|\; a_i \in \mathbb{Z},\ [M_i] \in \mathrm{Iso}(\mathrm{Mod}(\mathrm{A})_{\mathbb{F}_1}),\ M_i \text{ is indecomposable} \right\}, \tag{2}$$

with the product of two isomorphism classes $[M], [M']$ of indecomposables given by

$$[M] \cdot [M'] = \sum [N_i] \quad \text{if } M \wedge M' \simeq \bigoplus N_i,\ N_i \text{ indecomposable}.$$

We note that $\mathrm{K}_0^{\mathrm{sp}}(\mathrm{Mod}(\mathrm{A})_{\mathbb{F}_1})$ is a commutative ring. If A has no zero-divisors, the isomorphism class $[\mathbb{F}_1]$ of the trivial A-module is a multiplicative identity in $\mathrm{K}_0^{\mathrm{sp}}(\mathrm{Mod}(\mathrm{A})_{\mathbb{F}_1})$.

More generally, if $\mathcal{C}$ is a subcategory of $\mathrm{Mod}(\mathrm{A})_{\mathbb{F}_1}$ closed under $\oplus$ and $\wedge$, we may consider $\mathrm{K}_0^{\mathrm{sp}}(\mathcal{C})$, where the span in (2) is restricted to the indecomposable modules in $\mathcal{C}$.

The following is an immediate consequence of the of the functor $\otimes_{\mathbb{F}_1} k$ being monoidal:

Proposition 2.9. *There is a ring homomorphism*

$$\Phi_k : \mathrm{K}_0^{\mathrm{sp}}(\mathrm{Mod}(\mathrm{A})_{\mathbb{F}_1}) \to \mathrm{K}_0^{\mathrm{sp}}(\mathrm{Mod}_{k[\mathrm{A}]}).$$

3. Rooted trees, wheels, and the monoid $\langle t \rangle$

We now study the ring $\mathrm{K}_0^{\mathrm{sp}}(\mathrm{Mod}(\mathrm{A})_{\mathbb{F}_1})$ in the case where A is $\langle t \rangle$, the free monoid on one generator, and the corresponding base-change homomorphism

$$\Phi_k : \mathrm{K}_0^{\mathrm{sp}}(\mathrm{Mod}(\mathrm{A})_{\mathbb{F}_1}) \to \mathrm{K}_0^{\mathrm{sp}}(\mathrm{Mod}_{k[t]})$$

for a field k. Recall that finite-dimensional $k[t]$-modules correspond to pairs (V, T), where V is a finite-dimensional vector space over k, and $T \in \mathrm{End}(V)$. The indecomposable $k[t]$-modules thus correspond to Jordan blocks. It follows by analogy that the study of finite $\langle t \rangle$-modules amounts to studying "linear algebra over $\mathbb{F}_1$", and the indecomposable $\langle t \rangle$-modules are the corresponding Jordan blocks over $\mathbb{F}_1$.

Given $M \in \mathrm{Mod}(\langle t \rangle)_{\mathbb{F}_1}$, we may associate to it a graph Γ_M which encodes the action of t on M. The vertices of Γ_M correspond bijectively to the nonzero elements of M, and the directed edges join $m \in M$ to $t \cdot m$. We will make no distinction between $m \in M$ and the corresponding vertex of Γ_M when the context is clear.

Remark 3.1. The data of a function $f : S \mapsto S$ (where S is a set) may be encoded in a directed graph with vertex set S and a directed edge from s to $f(s)$ for every $s \in S$. Γ_M is a special case of this construction where $f : M \mapsto M$ is the map $m \mapsto t \cdot m$.

The possible connected graphs arising as Γ_M, corresponding to indecomposable $\langle t \rangle$-modules, see [Ganyushkin and Mazorchuk 2009; Szczesny 2014], are easily seen to be of two types.

We call the first type a *rooted tree* and the second a *wheel*; see Figure 1. Rooted trees correspond to indecomposable $\langle t \rangle$-modules where t acts nilpotently, in the sense that $t^n \cdot m = 0$ for sufficiently large n. We call such a module *nilpotent*.

We will use the following terminology when discussing the graphs Γ_M:

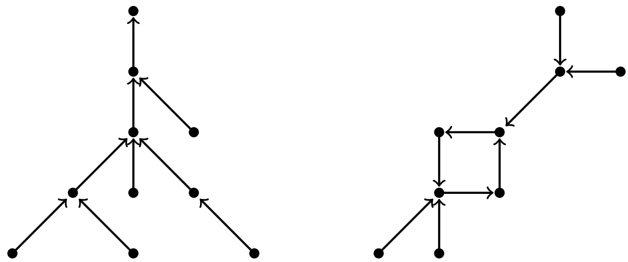

Figure 1. A rooted tree (left) and a wheel (right).

• We call a vertex with no outgoing edges a *root*. It is drawn at the top. A connected Γ_M can have at most one root.

• If M is nilpotent, hence Γ_M a tree, then the *depth* of a vertex $m \neq 0$, denoted by $\operatorname{depth}(m)$, is the number of edges in the unique path connecting m to the root. The only vertex of depth zero is the root. In general, $\operatorname{depth}(m)+1$ is the smallest power of t that annihilates m.

• The *height* of a rooted tree is the maximal depth of any of its vertices. The tree in Figure 1 has height 4.

• A *cycle of length n* is a sequence of distinct elements $Z = \{m_1, \dots, m_n\}$, $m_i \in M$, such that $t \cdot m_i = m_{i+1}$ and $t \cdot m_n = m_1$.

• A *chain of length n* is a sequence of distinct elements $C = \{m_1, m_2, \dots, m_n\}$, $m_i \in M$, such that $t \cdot m_i = m_{i+1}$, $1 \geq i < n$, but $t \cdot m_n \neq m_1$.

Wheels contain a single directed cycle, possibly with trees attached. A wheel is easily seen to arise from a $\langle t \rangle$-module M where $t^r \cdot m = t^{r+n} \cdot m$ for some $r, n \in \mathbb{N}$ for every $m \in M$.

We begin with the problem of computing the product in $\mathrm{K}_0^{\mathrm{sp}}(\mathrm{Mod}(\langle t \rangle)_{\mathbb{F}_1})$ in terms of the graphs above.

3A. ***Products in*** $\mathbf{K_0^{sp}(Mod(\langle t \rangle)_{\mathbb{F}_1})}$**.** Given a $\langle t \rangle$-module M, and $m \in M$, we define

$$\operatorname{pred}(m) = \{m' \in M, t \cdot m' = m\}.$$

At the level of the graph Γ_M, $\operatorname{pred}(m)$, $m \neq 0$, corresponds to the vertices connected to m via directed edge. Recall that for $M, N \in \mathrm{Mod}(\langle t \rangle)_{\mathbb{F}_1}$ and $(m, n) \in M \wedge N$, $t \cdot (m, n) = (t \cdot m, t \cdot n)$. In particular, $t \cdot (m, n) = 0$ if and only if $t \cdot m = 0$ or $t \cdot n = 0$. The following observations are immediate:

Proposition 3.2. *Let* $M, N \in \mathrm{Mod}(\langle t \rangle)_{\mathbb{F}_1}$ *be indecomposable*:

(1) $M \wedge N$ *is nilpotent if and only if at least one of* M, N *is nilpotent.*

(2) *If* M, N *are nilpotent and* $(m,n) \in M \wedge N$, *then*

$$\operatorname{depth}((m,n)) = \min(\operatorname{depth}(m), \operatorname{depth}(n)).$$

(3) *If* M *is nilpotent and* N *is not, then for* $(m,n) \in M \wedge N$,

$$\operatorname{depth}((m,n)) = \operatorname{depth}(m).$$

(4) $\operatorname{pred}(0_M) = \ker(t)$. *We have* $\operatorname{pred}(0_M) \neq \{0_M\}$ *if and only if* M *is nilpotent, in which case this set contains a single nonzero element, corresponding to the root of* Γ_M.

(5) *For* $(m,n) \in M \wedge N$,

$$\operatorname{pred}(m,n) = \{(m', n') \mid m' \in \operatorname{pred}(m), n' \in \operatorname{pred}(n)\},$$

i.e., $\operatorname{pred}(m,n) = \operatorname{pred}(m) \times \operatorname{pred}(n)$.

(6) $\{\operatorname{pred}(0) \subset M \wedge N\} = \big\{\{\operatorname{pred}(0) \subset M\} \times N\} \cup \{M \times \{\operatorname{pred}(0) \subset N\}\big\}$.

We proceed to examine the three cases where each of Γ_M, Γ_N is a rooted tree/wheel.

<u>Case 1</u>: If Γ_M, Γ_N are both rooted trees, $\Gamma_{M\wedge N}$ consists of $\dim(M) + \dim(N) - 1$ rooted trees whose roots correspond to pairs $(m,n) \in M \wedge N$ where at least one of m, n is a root. Each component has height $\leq \min(\operatorname{height}(\Gamma_M), \operatorname{height}(\Gamma_N))$, and at least one component where the inequality is sharp.

<u>Case 2</u>: If Γ_M is a tree and Γ_N is a wheel, $\Gamma_{M\wedge N}$ consists of $\dim(N)$ rooted trees whose roots correspond to pairs (r_M, n) where r_M is the root of Γ_M. Each component has height $\leq \operatorname{height}(\Gamma_M)$.

<u>Case 3</u>: If Γ_M, Γ_N are both wheels containing cycles of length l_M, l_N, then $\ker(t) = 0$ in both M and N, and so $\ker(t) = 0$ on $M \wedge N$. Each connected component of $\Gamma_{M\wedge N}$ is therefore a wheel, and contains a unique cycle. If $(m,n) \in M \wedge N$ is part of a cycle, then

$$t^r \cdot (m,n) = (m,n) \tag{3}$$

for some r, which implies $t^r \cdot m = m$ and $t^r \cdot n = n$. It follows that m (resp. n) is itself part of a cycle in Γ_M (resp. Γ_N). Moreover, r must be a multiple of l_M and l_N. Since the length of the cycle containing (m,n) is the least r such that (3) holds, it follows that $r = \operatorname{lcm}(l_M, l_N)$.

To summarize, have thus shown that each connected component of $\Gamma_{M\wedge N}$ contains a (necessarily unique) cycle of length $\operatorname{lcm}(l_M, l_N)$, and that (m,n) occurs in a cycle if and only if m, n do as well. Since there are $l_M l_N$ such pairs, it follows that $\Gamma_{M\wedge N}$ has $l_M l_N / \operatorname{lcm}(l_M, l_N) = \gcd(l_M, l_N)$ connected components.

We note that each connected component of $\Gamma_{M\wedge N}$ is determined recursively by property (5) above. For instance, if at least one of Γ_M, Γ_N is a rooted tree, we may begin with a vertex (r_M, n) or (m, r_N) corresponding to a root in $\Gamma_{M\wedge N}$ and build the rest of the component using (5). The same approach works if both graphs are wheels, though there is no preferred choice for the starting vertex.

Example 3.3. The two trees Γ_N and Γ_M yield the forest $\Gamma_{N\wedge M}$ pictured below, with six connected components, each of which has height ≤ 1:

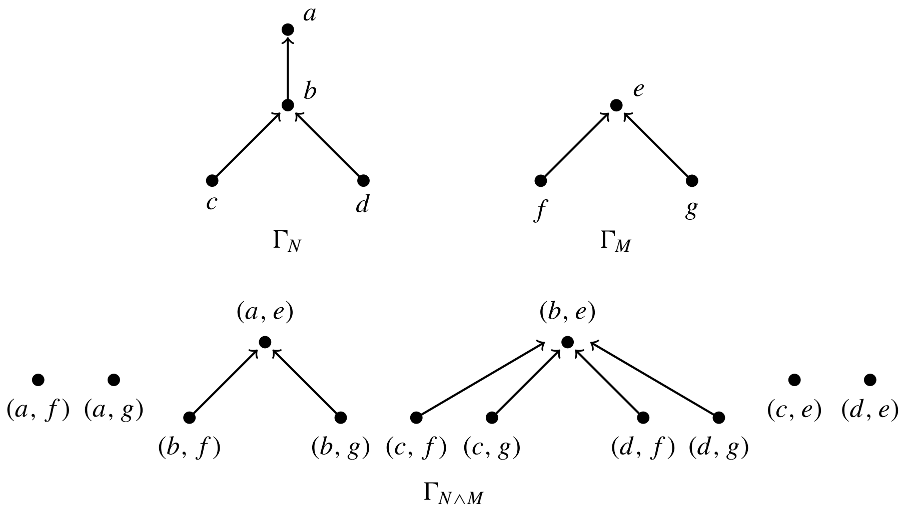

Example 3.4. The tree Γ_N and the wheel Γ_M yield the forest $\Gamma_{N\wedge M}$ pictured below, with three connected components, each of which has height ≤ 2:

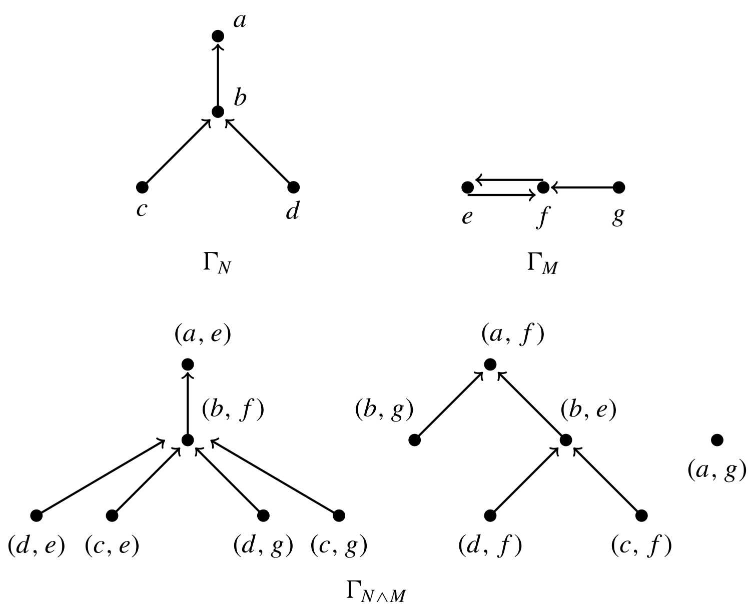

Example 3.5. The two wheels Γ_N and Γ_M yield $\Gamma_{N\wedge M}$ pictured below, with $\gcd(2,2)=2$ wheels, each with a cycle of $\operatorname{lcm}(2,2)=2$ vertices:

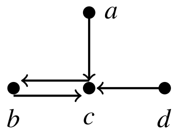

Γ_N

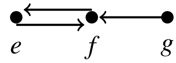

Γ_M

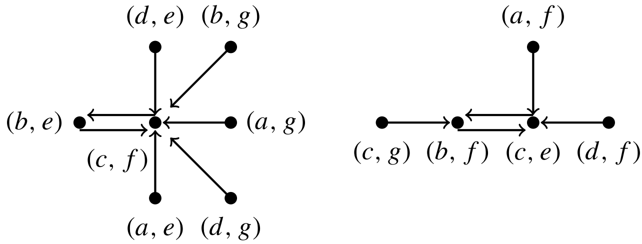

$\Gamma_{N\wedge M}$

Example 3.6. The two wheels Γ_N and Γ_M yield $\Gamma_{N\wedge M}$ pictured below, which consists of a single wheel as $\gcd(3,2)=1$. This wheel contains a cycle of $\operatorname{lcm}(3,2)=6$ vertices:

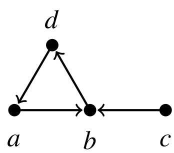

Γ_N

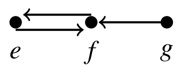

Γ_M

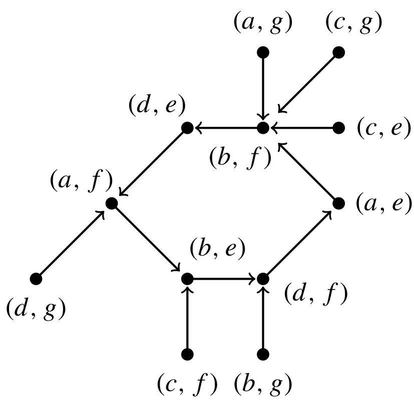

$\Gamma_{N\wedge M}$

We end this section by collecting a couple of observations regarding the structure of $\mathrm{K}_0^{\mathrm{sp}}(\mathrm{Mod}(\langle t\rangle)_{\mathbb{F}_1})$.

(1) The map $K_0^{sp}(\mathrm{Mod}(\langle t\rangle)_{\mathbb{F}_1}) \to \mathbb{Z}$ sending $[M] \to \dim(M)$ is a ring homomorphism.

(2) $N := \left\{\sum_i a_i[M_i] \;\middle|\; M_i \text{ is nilpotent}\right\} \subset K_0^{sp}(\mathrm{Mod}(\langle t\rangle)_{\mathbb{F}_1})$ is an ideal. The quotient

$$K_0^{sp}(\mathrm{Mod}(\langle t\rangle)_{\mathbb{F}_1})/\mathcal{N}$$

can be naturally identified with the integral span of wheels, with product given by $\wedge$.

3B. ***The homomorphism*** $\boldsymbol{\Phi_k}$**.** We now study the ring homomorphism

$$\Phi_k : K_0^{sp}(\mathrm{Mod}(\langle t\rangle)_{\mathbb{F}_1}) \to K_0^{sp}(\mathrm{Mod}_{k[t]}),$$

where k is a field containing all roots of unity. For $[M] \in \mathrm{Iso}(\mathrm{Mod}(\langle t\rangle)_{\mathbb{F}_1})$, we have $\Phi_k([M])$ is the isomorphism class of the $k[t]$-module $M \otimes_{\mathbb{F}_1} k$ with basis $m \in M$, $m \neq 0$, and t-action extended k-linearly from M. In what follows, we will denote $M \otimes_{\mathbb{F}_1} k$ by M_k and the linear transformation $t \in \mathrm{End}(M_k)$ by T_M. Fixing an ordering $m_1, \ldots, m_{\dim(M)}$ of the nonzero elements of M produces a basis for M_k, and the matrix of T_M in this basis is the adjacency matrix $\mathrm{Adj}(\Gamma_M)$ of Γ_M.

The isomorphism classes of indecomposable $k[t]$-modules correspond to $n \times n$ Jordan blocks $J_n(\lambda)$ with eigenvalue λ:

$$\begin{bmatrix} \lambda & 1 & & 0 \\ 0 & \ddots & \ddots & \\ \vdots & \ddots & \ddots & 1 \\ 0 & \cdots & 0 & \lambda \end{bmatrix}.$$

Describing Φ_k thus amounts to decomposing (M_k, T_M), or equivalently the adjacency matrix $\mathrm{Adj}(\Gamma_M)$, into Jordan blocks. It is clearly sufficient to consider the case where Γ_M is connected, that is, when Γ_M is a ladder tree or a simple cycle; see Figure 2.

The Jordan forms of $\mathrm{Adj}(\Gamma_M)$ when M is a ladder tree of height $n-1$ or a simple cycle of length n are easily seen to be the matrices $J_n(0)$ and D_n:

$$J_n(0) = \begin{bmatrix} 0 & 1 & & 0 \\ \vdots & \ddots & \ddots & \\ \vdots & & \ddots & 1 \\ 0 & \cdots & \cdots & 0 \end{bmatrix}, \quad D_n = \begin{bmatrix} \zeta & & 0 \\ & \ddots & \\ 0 & & \zeta^n \end{bmatrix},$$

with $\zeta = e^{2\pi i/n}$

For more general directed graphs arising as Γ_M, this problem is solved in [Cardon and Tuckfield 2011]. We proceed to recall the solution given there, specialized to our setup.

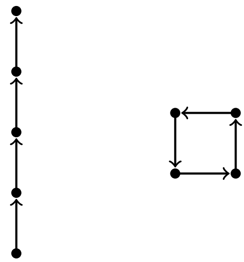

Figure 2. A ladder (left) and a simple cycle (right).

Definition 3.7. A *partition* of Γ_M is a collection $\{C_1, \dots, C_r, Z_1, \dots, Z_s\}$ of disjoint chains $C_1, \dots, C_r$ and cycles $Z_1, \dots, Z_s$ whose union is $M \backslash 0$. A *proper partition* of M is a partition satisfying the following two additional properties:

(1) Each cycle in M is equal to one of $Z_1, \dots, Z_s$.

(2) For each $1 \le i \le r$, if Γ_M^i is the graph obtained from Γ_M by deleting all of the vertices in $Z_1, \dots, Z_s, C_1, \dots, C_i$, then C_{i+1} is a chain of maximal length in Γ_M^i.

It is easy to see that proper partitions of Γ_M exist, and can be obtained as follows. Each connected component of Γ_M has at most one (necessarily unique) cycle — take these to be $Z_1, \dots, Z_s$. Upon deleting the Z_j, $1 \le j \le s$, we are left with a forest of rooted trees. We now look for the longest chain C_1 in this forest, delete it, and repeat, obtaining $C_2, \dots, C_r$.

Example 3.8. In the graph Γ_M given by

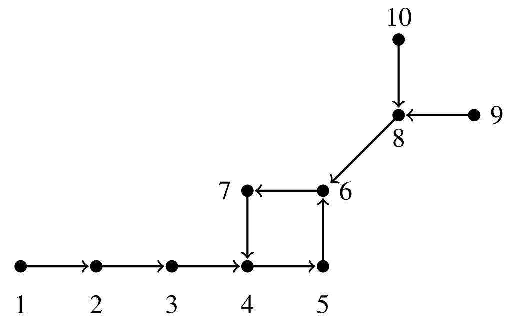

the set $\{C_1, C_2, C_3, Z_1\}$, where $C_1 = \{1, 2, 3\}$, $C_2 = \{9, 8\}$, $C_3 = \{10\}$, and $Z_1 = \{4, 5, 6, 7\}$, is a proper partition.

The following theorem describes the Jordan form of $\mathrm{Adj}(\Gamma_M)$.

Theorem 3.9 [Cardon and Tuckfield 2011]. *Let* $\{C_1, \dots, C_r, Z_1, \dots, Z_s\}$ *be a proper partition of* Γ_M *into chains* C_i *of length* $l(C_i)$ *and cycles* Z_j *of length* $l(Z_j)$.

Then

$$\mathrm{Adj}(\Gamma_M) \simeq \bigoplus_{i=1}^{r} J_{l(C_i)}(0) \oplus \bigoplus_{j=1}^{s} D_n.$$

We are now able to characterize the image of the homomorphism Φ_k:

Theorem 3.10. *The image of* Φ_k *is the subring of* $\mathrm{K}_0^{\mathrm{sp}}(\mathrm{Mod}(\langle t\rangle)_{\mathbb{F}_1})$ *generated by* $[J_n(0)], [D_n],\ n \geq 1$.

We note one final consequence of the fact that Φ_k is monoidal. By the above discussion, $\Phi_k(M)$ may be identified with the adjacency matrix of Γ_M. It follows that

$$\Phi_k(M \wedge N) = \Phi_k(M) \otimes_k \Phi_k(N).$$

In other words, $\mathrm{Adj}(\Gamma_{M\wedge N}) = \mathrm{Adj}(\Gamma_M) \otimes \mathrm{Adj}(\Gamma_N)$, where $\otimes$ on the right denotes the Kronecker product of matrices. This is the defining property of the *tensor product graph* $\Gamma_M \otimes \Gamma_N$; see [Weichsel 1962]. To summarize:

Proposition 3.11. *For* $M, N \in \mathrm{Mod}(\langle t\rangle)_{\mathbb{F}_1}$, *we have* $\Gamma_{M\wedge N} = \Gamma_M \otimes \Gamma_N$.

4. Skew shapes and the monoids $\langle x_1, \dots, x_n\rangle$

We now consider a subcategory $\mathrm{Skew}_n \subset \mathrm{Mod}(\mathbb{P}_n)_{\mathbb{F}_1}$ (originally introduced in [Szczesny 2018]) consisting of n-dimensional skew shapes. Our goal is to give an explicit description of the product in the ring $\mathrm{K}_0^{\mathrm{sp}}(\mathrm{Skew}_n)$.

4A. ***Skew shapes and*** $\mathbb{P}_n$***-modules.*** $\mathbb{Z}^n$ has a natural partial order where for $x = (x_1, \dots, x_n) \in \mathbb{Z}^n$ and $y = (y_1, \dots, y_n) \in \mathbb{Z}^n$, we have

$$x \leq y \iff x_i \leq y_i \quad \text{for } i = 1, \dots, n.$$

Definition 4.1. An *n-dimensional skew shape* is a finite convex subposet $S \subset \mathbb{Z}^n$. S is *connected* if and only if the corresponding poset is. We consider two skew shapes S, S' to be equivalent if and only if they are isomorphic as posets. If S, S' are connected, then they are equivalent if and only if S' is a translation of S, i.e., if there exists $a \in \mathbb{Z}^n$ such that $S' = a + S$.

The condition that S is connected is easily seen to be equivalent to the condition that any two elements of S can be connected via a lattice path lying in S. The name *skew shape* is motivated by the fact that for $n = 2$, a connected skew shape in the above sense corresponds (nonuniquely) to a difference λ/μ of two Young diagrams in French notation (for an explanation of this notation see for instance [Fulton 1997]). For $n = 3$, these correspond to *skew plane partitions*.

Example 4.2. Let $n = 2$ and

$$S \subset \mathbb{Z}^2 = \{(1, 0), (2, 0), (3, 0), (0, 1), (1, 1), (0, 2)\}$$

(up to translation by $a \in \mathbb{Z}^2$). Then S corresponds to the connected skew Young diagram

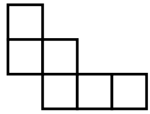

Let $S \subset \mathbb{Z}^n$ be a skew shape. We may attach to S a $\mathbb{P}_n$-module M_S with underlying set

$$M_S = S \sqcup \{0\}$$

and action of $\mathbb{P}_n$ defined by

$$x^e \cdot s = \begin{cases} s+e, & \text{if } s+e \in S, \\ 0 & \text{otherwise}, \end{cases} \qquad e \in \mathbb{Z}^n_{\geq 0},\ s \in S.$$

In particular, $x_i \cdot s = s + e_i$ if $s + e_i \in S$, and equals 0 otherwise, where e_i is the i-th standard basis vector. M_S is a graded $\mathbb{P}_n$-module with respect to its $\mathbb{Z}^n_{\geq 0}$-grading, in which $\deg(x_i) = e_i$.

Example 4.3. Let S be as in Example 4.2. Let x_1 (resp. x_2) act on the $\mathbb{P}_2 = \langle x_1, x_2 \rangle$-module M_S by moving one box to the right (resp. one box up) until reaching the edge of the diagram, and 0 beyond that. A minimal set of generators for M_S is indicated by the black dots:

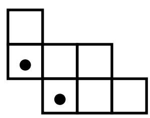

We may consider the subcategory $\text{Skew}_n \subset \mathbb{P}_n$-mod consisting of $\mathbb{P}_n$-modules M satisfying the following two conditions:

(1) M admits a $\mathbb{Z}^n$-grading.

(2) For $a \in \mathbb{P}_n,\ m_1, m_2 \in M$,

$$a \cdot m_1 = a \cdot m_2 \quad \Longleftrightarrow \quad m_1 = m_2 \ \text{ or } \ a \cdot m_1 = a \cdot m_2 = 0.$$

The following proposition follows from results in [Szczesny 2018]:

Proposition 4.4. Skew_n *forms a full monoidal subcategory of* $\text{Mod}(\mathbb{P}_n)_{\mathbb{F}_1}$. *If* $M \in \text{Skew}_n$ *is indecomposable, then* $M \simeq M_S$ *for a connected skew shape* S.

In other words, given connected skew shapes S_1, S_2, the $\mathbb{P}_n$-module $M_{S_1} \wedge M_{S_2}$ is isomorphic to $\oplus M_{U_j}$, where U_j are connected skew shapes.

Lemma 4.5. *If* $S_1, S_2 \in \text{Skew}_n$ *with chosen embeddings in* $\mathbb{Z}^n$, *and* $t \in \mathbb{Z}^n$, *then*

$$S_1 \cap (S_2 + t)$$

is also an n-*dimensional skew shape, possibly empty or disconnected.*

Proof. As S_2 is a skew shape, so is S_2+t. Hence, it suffices to show the intersection of skew shapes is a skew shape, that is, $S_1 \cap S_2$ is a skew shape.

It is immediate that $S_1 \cap S_2$ is a finite poset of $\mathbb{Z}^n$. Further, if $a, b, c \in S_1 \cap S_2$ and $a \le c \le b$, then as both S_1 and S_2 are convex, $c \in S_1 \cap S_2$. Hence, $S_1 \cap S_2$ is convex and therefore a skew shape. □

Theorem 4.6. *If* $S_1, S_2 \in \mathrm{Skew}_n$ *with chosen embeddings in* $\mathbb{Z}^n$ *then*

$$M_{S_1} \wedge M_{S_2} = \bigoplus_{t\in\mathbb{Z}^n} M_{S_1\cap(S_2+t)}.$$

Remark 4.7. Since S_1, S_2 are finite embedded skew shapes, the intersection $S_1 \cap (S_2+t)$ is empty for all but finitely many $t \in \mathbb{Z}^n$. Moreover, by Lemma 4.5, the right-hand side is an object in Skew_n.

Proof. We will use the notation $a_t \in M_{S_1\cap(S_2+t)}$ to denote an element occurring in the t-th summand in $\bigoplus_{t\in\mathbb{Z}^n} M_{S_1\cap(S_2+t)}$. Define

$$\Psi : M_{S_1} \wedge M_{S_2} \to \bigoplus_{t\in\mathbb{Z}^n} M_{S_1\cap(S_2+t)}$$

by

$$\Psi((a, b)) = a_{a-b} \in M_{S_1\cap(S_2+a-b)}.$$

We proceed to show that Ψ is an isomorphism of $\mathbb{P}_n$-modules. Ψ is clearly injective, and sends 0 to 0. Moreover, if $a_t \in M_{S_1\cap(S_2+t)}$ is nonzero, then $a = b+t$ for some nonzero $b \in S_2$; hence $a_t = \Psi((a, b))$. Ψ is therefore a bijection.

It remains to check that Ψ is a morphism of $\mathbb{P}_n$-modules, or equivalently that $\Psi \circ x_i = x_i \circ \Psi$ for $i = 1, \dots, n$.

Suppose (a, b) is a nonzero element in the domain of Ψ. If $x_i((a, b)) = 0$, then either $x_i(a) = 0$ or $x_i(b) = 0$, or equivalently, either $a+e_i \notin S_1$ or $b+e_i \notin S_2$. Thus $a+e_i \notin S_1 \cap (S_2+a-b)$ and so

$$x_i \cdot a_{a-b} = x_i \circ \Psi((a, b)) = 0 = \Psi \circ x_i((a, b)).$$

Otherwise, $x_i((a, b)) = (a+e_i, b+e_i) \in S_1 \times S_2$ and so it follows that

$$\Psi \circ x_i((a, b)) = (a+e_i)_{a-b}.$$

Meanwhile, $\Psi(a, b) = a_{a-b}$. As $a+e_i \in S_1$, $b+e_i \in S_2$, we have $a+e_i \in S_1 \cap (S_2+a-b)$, and so $x_i \cdot a_{a-b} = (a+e_i)_{a-b}$. Hence

$$x_i \circ \Psi((a, b)) = \Psi \circ x_i \cdot (a, b).$$ □

Remark 4.8. The situation can be visualized as follows. For two embedded skew shapes S and T, the connected component of the skew shape in $M_S \wedge M_T$ containing some point (a, b) is the intersection of S with the unique translate of T that makes

a and b coincide. Below is an example of S, T and their intersection in gray for $n = 2$:

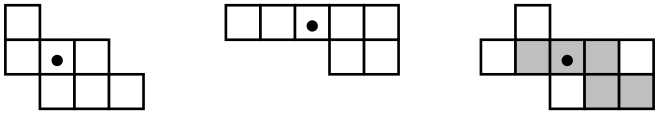

Example 4.9. Suppose the we have the following skew shapes S and T in $n = 2$ dimensions:

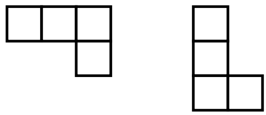

To find the collection of skew shapes occurring in $M_S \wedge M_T$ we observe the nontrivial intersections of S and T under translation are given below with regions of intersection in dark gray, and regions of nonintersection in light gray:

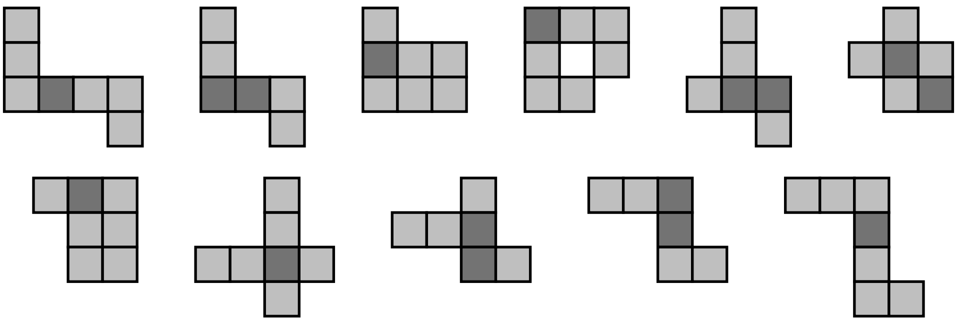

It follows that $M_S \wedge M_T$ decomposes into indecomposable modules corresponding to the following skew shapes with the indicated multiplicities:

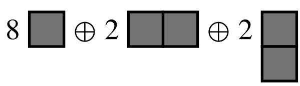

Note that we further decomposed the disconnected skew shape

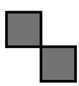

into its connected components.

Acknowledgements

This paper emerged from an undergraduate research project at Boston University completed by Beers with Szczesny as faculty mentor. We gratefully acknowledge the generous support of the BU Undergraduate Research Opportunities Program during the research and writing phase of this project. Szczesny is supported by a Simons Foundation Collaboration Grant.

References

[Cardon and Tuckfield 2011] D. A. Cardon and B. Tuckfield, "The Jordan canonical form for a class of zero-one matrices", *Linear Algebra Appl.* **435**:11 (2011), 2942–2954. MR Zbl

[Chu et al. 2012] C. Chu, O. Lorscheid, and R. Santhanam, "Sheaves and K-theory for $\mathbb{F}_1$-schemes", *Adv. Math.* **229**:4 (2012), 2239–2286. MR Zbl

[Deitmar 2012] A. Deitmar, "Belian categories", *Far East J. Math. Sci.* (*FJMS*) **70**:1 (2012), 1–46. MR Zbl

[Dyckerhoff and Kapranov 2012] T. Dyckerhoff and M. Kapranov, "Higher Segal spaces, I", preprint, 2012. arXiv

[Fulton 1997] W. Fulton, *Young tableaux: with applications to representation theory and geometry*, London Mathematical Society Student Texts **35**, Cambridge University Press, 1997. MR Zbl

[Ganyushkin and Mazorchuk 2009] O. Ganyushkin and V. Mazorchuk, *Classical finite transformation semigroups: an introduction*, Algebra and Applications **9**, Springer, 2009. MR Zbl

[Kilp et al. 2000] M. Kilp, U. Knauer, and A. V. Mikhalev, *Monoids, acts and categories: with applications to wreath products and graphs*, De Gruyter Expositions in Mathematics **29**, Walter de Gruyter, Berlin, 2000. MR Zbl

[Lorscheid 2018] O. Lorscheid, "$\mathbb{F}_1$ for everyone", *Jahresber. Dtsch. Math.-Ver.* **120**:2 (2018), 83–116. MR Zbl

[Steinberg 2016] B. Steinberg, *Representation theory of finite monoids*, Springer, 2016. MR Zbl

[Szczesny 2014] M. Szczesny, "On the Hall algebra of semigroup representations over $\mathbb{F}_1$", *Math. Z.* **276**:1-2 (2014), 371–386. MR Zbl

[Szczesny 2018] M. Szczesny, "The Hopf algebra of skew shapes, torsion sheaves on $\mathbb{A}^n_{/\mathbb{F}_1}$, and ideals in Hall algebras of monoid representations", *Adv. Math.* **331** (2018), 209–238. MR Zbl

[Weichsel 1962] P. M. Weichsel, "The Kronecker product of graphs", *Proc. Amer. Math. Soc.* **13** (1962), 47–52. MR Zbl

Received: 2019-05-09 Revised: 2019-09-18 Accepted: 2019-09-20

dbeers@bu.edu *Department of Mathematics and Statistics, Boston University, Boston, MA, United States*

szczesny@math.bu.edu *Department of Mathematics and Statistics, Boston University, Boston, MA, United States*

INVOLVE 12:8 (2019)
dx.doi.org/10.2140/involve.2019.12.1399

On the classification of Specht modules with one-dimensional summands

Aubrey Piper Collins and Craig J. Dodge

(Communicated by Kenneth S. Berenhaut)

This paper extends a result of James to a combinatorial condition on partitions for the corresponding Specht module to have a summand isomorphic to the unique one-dimensional $F\Sigma$-module over fields of characteristic 2. The work makes use of a recursively defined condition to reprove a result of Murphy and prove a new result for self-conjugate partitions. Finally we present a Python script which utilizes this work to test Specht modules for a one-dimensional summand.

1. Introduction

Specht modules are crucial to understanding the representation theory of the symmetric group; see [James 1978; James and Kerber 1981]. Gwendolen Murphy [1980] classified the decomposable Specht modules which correspond to hook partitions. Dodge and Fayers [2012] produced the first new examples of decomposable Specht modules since Murphy's work. More recently, Donkin and Geranios [2018] used analogous modules for the general linear groups and applied the Schur functor in order to find even broader families of decomposable Specht modules. Further work on the question has been addressed in the Iwahori–Hecke algebra in [Speyer 2014; Speyer and Sutton 2018].

Murphy additionally classified the Specht modules corresponding to hook partitions which have a one-dimensional summand.

Theorem 1.1 [Murphy 1980, Theorem 5.5]. *Let $\lambda = (n-r, 1^r)$ and F be a field of characteristic 2. Then there exists a nonzero $F\Sigma_n$-module M such that $S^\lambda \cong S^{(n)} \oplus M$ if and only if n is odd, r is even, and $\binom{n-1}{r}$ is odd.*

This theorem was a consequence of determining the endomorphism ring of Specht modules corresponding to hook partitions. In this paper we attempt to address the question of one-dimensional summands in the spirit of [Dodge and Fayers 2012] by constructing split exact sequences of $F\Sigma_n$-modules.

MSC2010: 20C20, 20C30.
Keywords: representation theory, group theory, symmetric groups, Specht modules, decomposable.

In Section 2, we present the foundational definitions as well as construct the Specht modules in the style of [James 1978]. In Section 3, we work through the consequences of James's theorem [1978, Theorem 24.4] concerning $\mathrm{Hom}_{F\Sigma_n}(S^{(n)}, S^\lambda)$. Utilizing this work we describe conditions sufficient for the Specht module to decompose as desired (Theorem 3.5). While this final sufficient condition is expressed as a sum of a recursively defined finite sequence, we can use it to provide a new proof of Murphy's result. Additionally in Section 4 we make use of Theorem 3.5 and introduce the notion of the directed graph of a partition in order to prove Specht modules corresponding to self-conjugate partitions cannot have a one-dimensional summand. Finally in Section 5 we present Python [van Rossum 2001] algorithms designed to apply Theorem 3.5 to determine which Specht modules have a one-dimensional summand.

2. Preliminaries and notation

For any positive integer n, let Σ_n denote the symmetric group on n letters, and $F\Sigma_n$ denote the group algebra of Σ_n over F. This paper builds greatly upon the foundations found in [James and Kerber 1981; James 1978], adopting much of the notation and constructions.

2A. ***Compositions, partitions, and Young diagrams.*** We say $\lambda = (\lambda_1, \lambda_2, \lambda_3, \ldots) \in \mathbb{N}_0^{\mathbb{N}}$ is a *partition* of n, and write $\lambda \vdash n$, if $\sum \lambda_i = n$ and for all i, $\lambda_i \geq \lambda_{i+1}$. For a partition λ of n, the *Young diagram* of λ, denoted by $[\lambda]$, is the set

$$[\lambda] := \{(i, j) \in \mathbb{N} \times \mathbb{N} \mid j \leq \lambda_i\}.$$

Each of the elements in the Young diagram is referred to as a *node*. We call the set

$$R_\lambda(i) = \{(i, j) \mid 1 \leq j \leq \lambda_i\} \subseteq [\lambda]$$

the i-th row of $[\lambda]$ and

$$C_\lambda(j) = \{(i, j) \mid 1 \leq i \leq \lambda'_j\}$$

the j-th column of $[\lambda]$. Given a partition $\lambda \vdash n$, we define the *conjugate* of λ, denoted by λ', as the unique partition such that

$$[\lambda'] = \{(i, j) \in \mathbb{N} \times \mathbb{N} \mid (j, i) \in [\lambda]\}.$$

2B. ***Tableau.*** For a partition λ of n, if $t : [\lambda] \to \{1, 2, \ldots, n\}$ is a bijection, we call t a λ-*tableau*. Let $\mathcal{T}(\lambda)$ denote the set of all λ-tableaux. For a partition λ, a λ-tableau t is called *row standard* if for $(i, j), (i, k) \in [\lambda]$ with $j < k$, then $t(i, j) < t(i, k)$. We define *column standard* similarly. Moreover t is *standard* if it is both row standard and column standard and $\mathcal{T}_0(\lambda)$ will denote the set of standard λ-tableaux. We call

$\mathcal{R}_t(i) = t[R_\lambda(i)]$ the set of entries in the i-th row of t. Similarly, $\mathcal{C}_t(j) = t[C_\lambda(j)]$ is the set of entries in the j-th column of t.

Since each element $\sigma \in \Sigma_n$ is a bijection on the set $\{1, 2, 3, \dots, n\}$, there is a Σ_n-action on $\mathcal{T}(\lambda)$ defined by $\sigma t = \sigma \circ t$. From this action, we can define two significant subgroups of Σ_n given a λ-tableau t. Define the *row stabilizer* of t, denoted by R_t, to be the subset of Σ_n which fixes the sets $\mathcal{R}_t(i)$. Similarly define the *column stabilizer* of t, denoted by C_t, to be the subset of Σ_n which fixes the sets $\mathcal{C}_t(j)$. We define an equivalence relation on $\mathcal{T}(\lambda)$ by $t \sim s$ if and only if there exists $\pi \in R_t$ such that $\pi t = s$. We will use $X(\lambda)$ to denote the set of equivalence classes of $\mathcal{T}(\lambda)$ and call an equivalence class $\{t\} \in X(\lambda)$ a λ-*tabloid*. Notice that since there is a well-defined action of Σ_n on $\mathcal{T}(\lambda)$ we can define an action of Σ_n on $X(\lambda)$ by $\sigma\{t\} = \{\sigma t\}$ for all $\sigma \in \Sigma_n$ and $\{t\} \in X(\lambda)$.

Lastly we will make use of a dominance relation on the set of tabloids for a fixed composition λ, using the notation of [James 1978, Definition 3.11]. For $\{t\} \in X(\lambda)$ we let $m_{xy}(t) = |\{t(i, j) \leq x \mid i \leq y\}|$; that is $m_{xy}(t)$ is the number of entries less than or equal to x in the first y rows of $\{t\}$. Using this notation, we define the relation $\lhd$ on $X(\lambda)$ by $\{s\} \lhd \{t\}$ if and only if $m_{xy}(s) \leq m_{xy}(t)$ for all positive integers x, y.

2C. ***Permutation modules and Specht modules.*** Define M^λ to be the free vector space over F generated by the set $X(\lambda)$. Additionally since $X(\lambda)$ is the basis of M^λ, we can define an $F\Sigma_n$-action on M^λ by extending the Σ_n-action on $X(\lambda)$ linearly. We will call M^λ with this module action the *permutation module* associated to λ.

Let $t \in \mathcal{T}(\lambda)$. Then we define $\kappa_t \in F\Sigma_n$ by

$$\kappa_t := \sum_{\sigma \in C_t} (\operatorname{sgn} \sigma)\sigma,$$

where $\operatorname{sgn} : \Sigma_n \to \{1, -1\}$ is the signature function on the symmetric group. So for any $t \in \mathcal{T}(\lambda)$, we can define the element in M^λ called the *polytabloid* of t by $e_t := \kappa_t\{t\}$. Hence we can construct a submodule of M^λ called the *Specht module*, denoted by S^λ, which we define explicitly by

$$S^\lambda := \operatorname{Span}(\{e_t \mid t \in \mathcal{T}(\lambda)\}) \subseteq M^\lambda.$$

The following example describes two Specht modules which can be constructed for any positive integer n and will be a central to the focus of this paper.

Example 2.1. The Specht module $S^{(n)}$ for $F\Sigma_n$ is one-dimensional and for all $v \in S^\lambda$ and $\sigma \in \Sigma$, we have $\sigma v = v$. Alternatively, the Specht module $S^{(1^n)}$ is a one-dimensional $F\Sigma_n$-module, again spanned by any appropriate polytabloid. For all $w \in S^{(1^n)}$ and $\sigma \in \Sigma_n$

$$\sigma w = \begin{cases} w & \text{if } \sigma \text{ is an even permutation,} \\ -w & \text{if } \sigma \text{ is an odd permutation.} \end{cases}$$

For all n, $S^{(n)}$ and $S^{(1^n)}$ form a complete list of the isomorphism classes of the one-dimensional modules of $F\Sigma_n$.

We conclude this section by stating several significant results concerning Specht modules that are relevant to our investigation.

Theorem 2.2. *Let $\lambda \vdash n$.*

(2.2.1) [James 1978, Proposition 4.5] *S^λ is a cyclic $F\Sigma_n$-module generated by every polytabloid.*

(2.2.2) [James 1978, Theorem 8.4] *The set $\{e_t \mid t \in \mathcal{T}_0(\lambda)\}$ is a basis for S^λ.*

(2.2.3) [James 1978, Theorem 8.15] *Let $(S^\lambda)^*$ denote the dual of S^λ. Then $(S^\lambda)^* \cong S^{\lambda'} \otimes S^{(1^n)}$.*

(2.2.4) [James 1978, Corollary 13.18] *Suppose F has characteristic 2. Then S^λ is indecomposable.*

The basis in (2.2.2) is often referred to as the *standard basis* of S^λ. The polytabloids will become very relevant to our discussion, in particular understanding which tabloids appear with nonzero coefficient in certain polytabloids, and so we introduce the following notation. If $s, t \in \mathcal{T}_0(\lambda)$ we say *t produces s* and write $t \to s$ if there exists $\pi \in C_t$ and $\sigma \in R_s$ such that $s = \sigma\pi t$. Note using this definition we see that s appears with nonzero coefficient in e_t if and only if $t \to s$. In order to further understand which standard tableaux produces other standard tableaux, we introduce the following results.

Theorem 2.3. *Let t be a λ-tableau and $s, t \in \mathcal{T}_0(\lambda)$.*

(2.3.1) [James 1978, Lemma 8.13] *If $t \to s$ then $\{s\} \lhd \{t\}$.*

(2.3.2) [James and Kerber 1981, Lemma 1.5.6] *Suppose x, y appear in the same column of t. If $t \to s$ then x and y appear in different rows of s.*

3. $F\Sigma_n$-module homomorphisms

Noting (2.2.4), we will assume F is a field of characteristic 2 for the remainder of the paper, and hence $S^{(n)} \cong S^{(1^n)}$. Therefore there is a unique one-dimensional $F\Sigma_n$-module up to isomorphism, namely $S^{(n)}$. Next we will introduce a theorem of James which will be fundamental to the remaining work of this paper. To this end, for $\lambda \vdash n$, let $l_d(\lambda)$ be the unique integer such that $2^{l_d - 1} \le \lambda_{d+1} < 2^{l_d}$. Using this notation we state the following theorem of James, specifically for the case when $p = 2$.

Theorem 3.1 [James 1978, Theorem 24.4 (p=2)]. *Suppose that F is a field of characteristic 2 and $\lambda = (\lambda_1, \lambda_2, \ldots, \lambda_s)$ is a partition of n. If $\lambda_d \equiv -1 \pmod{2^{l_d(\lambda)}}$ for all $1 \le d < s$, then* $\mathrm{Hom}(S^{(n)}, S^\lambda)$ *is one-dimensional*; *otherwise* $\dim \mathrm{Hom}(S^{(n)}, S^\lambda) = 0$.

Recall that when F is a field of characteristic 2, we have $S^{(n)} \cong S^{(1^n)}$. Moreover we note that for all $F\Sigma_n$-modules M, we have $M \otimes S^{(n)} \cong M$. Thus when F is a field of characteristic 2, (2.2.3) gives us $(S^\lambda)^* \cong S^{\lambda'} \otimes S^{(n)} \cong S^{\lambda'}$. Hence from the previous theorem we have the following corollary.

Corollary 3.2. *Suppose that F is a field of characteristic 2, $\lambda \vdash n$, and $\lambda' = (\lambda'_1, \lambda'_2, \dots, \lambda'_t)$. Then* $\dim \operatorname{Hom}(S^\lambda, S^{(n)}) = 1$ *if and only if* $\lambda'_e \equiv -1 \pmod{2^{l_e(\lambda')}}$ *for all* $1 \le e < t$.

Proof. First note the following isomorphisms of homomorphism spaces:

$$\operatorname{Hom}(S^\lambda, S^{(n)}) \cong \operatorname{Hom}(S^\lambda, S^{(1^n)}) \cong \operatorname{Hom}((S^{(1^n)})^*, (S^\lambda)^*) \cong \operatorname{Hom}(S^{(n)}, S^{\lambda'}).$$

Hence the corollary follows from Theorem 3.1. □

3A. ***Composition of module homomorphisms.*** We can combine Theorem 3.1 and Corollary 3.2 to motivate the following definition about partitions under consideration.

Definition 3.3. Let $\lambda = (\lambda_1, \lambda_2, \dots, \lambda_s)$ and $\lambda' = (\lambda'_1, \lambda'_2, \dots, \lambda'_t)$. We say that λ is *Lucas perfect* if $\lambda_d \equiv -1 \pmod{2^{l_d(\lambda)}}$ for all $1 \le d < s$ and $\lambda'_e \equiv -1 \pmod{2^{l_e(\lambda')}}$ for all $1 \le e < t$.

In order to further our discussion, let us consider an arbitrary Lucas perfect partition of n, λ. We may fix nonzero $F\Sigma_n$-module homomorphisms $i_\lambda : S^{(n)} \to S^\lambda$ and $p_\lambda : S^\lambda \to S^{(n)}$. Our goal will be to understand the composition $p_\lambda \circ i_\lambda : S^{(n)} \to S^{(n)}$. To that end, we first explore the image of i_λ expressed as a linear combination of polytabloids. Let $v \in S^{(n)}$ be nonzero. Since $S^\lambda \subset M^\lambda$, we may fix $a_{\{t\}} \in F$ such that

$$i_\lambda(v) = \sum_{\{t\} \in X(\lambda)} a_{\{t\}}\{t\}.$$

Now let $\sigma \in \Sigma$ be arbitrary. Observe by reindexing the λ-tabloids,

$$\sigma^{-1}\biggl(\sum_{\{t\} \in X(\lambda)} a_{\{t\}}\{t\}\biggr) = \sum_{\{t\} \in X(\lambda)} a_{\{\sigma t\}}\{t\}.$$

Additionally $i_\lambda(v) = i_\lambda(\sigma^{-1}v) = \sigma^{-1} i_\lambda(v)$, so

$$\sum_{\{t\} \in X(\lambda)} a_{\{t\}}\{t\} = \sum_{\{t\} \in X(\lambda)} a_{\{\sigma t\}}\{t\}.$$

Since $X(\lambda)$ is a basis for M^λ it follows that $a_{\{t\}} = a_{\{\sigma t\}}$ for all σ. Moreover since Σ_n acts transitively on $X(t)$, we conclude that

$$i_\lambda(v) = a \sum_{\{t\} \in X(\lambda)} \{t\}.$$

Moreover since $i_\lambda \neq 0$, we know $a \neq 0$. To understand the composition $p_\lambda \circ i_\lambda$, we will be making use of the image of a polytabloid under p_λ. To that end, we will focus on expressing $i_\lambda(v)$ as a linear combination of polytabloids. From our observations of i_λ, we note

$$\sum_{\{t\}\in X(\lambda)} \{t\} \in S^\lambda.$$

Therefore by (2.2.2), we may fix $x_t \in F$ such that

$$\sum_{t\in\mathcal{T}_0(\lambda)} x_t e_t = \sum_{\{s\}\in X(\lambda)} \{s\}. \tag{3-1}$$

Ideally we would be able to determine a closed formula for the coefficients x_t. For now we will settle on developing a recursive formula. To assist with this task, let ρ be the linear transformation defined by

$$\rho(\{s\}) = \begin{cases} \{s\} & \text{if } \{s\} \text{ is standard,} \\ 0 & \text{if } \{s\} \text{ is not standard.} \end{cases}$$

Therefore ρ is a linear projection from M^λ to the span of $\{\{t\} \mid t \in \mathcal{T}_0(\lambda)\}$. We note by (2.3.1) and (2.2.2) that $\{\rho(e_t) \mid t \in \mathcal{T}_0(\lambda)\}$ is linearly independent. By applying ρ to (3-1), we have

$$\sum_{t\in\mathcal{T}_0(\lambda)} x_t \rho(e_t) = \sum_{s\in\mathcal{T}_0(\lambda)} \{s\}. \tag{3-2}$$

Since both $\{e_t \mid t \in \mathcal{T}_0(\lambda)\}$ and $\{\rho(e_t) \mid t \in \mathcal{T}_0(\lambda)\}$ are linearly independent sets, (3-1) and (3-2) have unique solutions and therefore the same solution sets. Using these observations we prove the solution satisfies the following condition.

Lemma 3.4. *If $\lambda \vdash n$ is Lucas perfect and $X_t = \{s \in \mathcal{T}_0(\lambda) \mid s \to t$ and $s \neq t\}$, then*

$$x_t = 1 + \sum_{s\in X_t} x_s$$

is the unique solution to

$$\sum_{t\in\mathcal{T}_0(\lambda)} x_t e_t = \sum_{\{s\}\in X(\lambda)} \{s\}.$$

Proof. It follows from Theorem 3.1 that (3-1) has a unique solution. Thus we complete the proof by demonstrating the solution proposed by the lemma satisfies (3-2). Suppose $t \in \mathcal{T}_0(\lambda)$, and define the sets

$$X_t = \{s \in \mathcal{T}_0(\lambda) \mid s \to t \text{ and } s \neq t\},$$
$$Y_t = \{s \in \mathcal{T}_0(\lambda) \mid t \to s \text{ and } s \neq t\},$$
$$W(\lambda) = \{(u, v) \mid u \in \mathcal{T}_0(\lambda),\ v \in Y_t\} = \{(u, v) \mid v \in \mathcal{T}_0(\lambda),\ u \in X_v\}.$$

Using this notation it follows that $\rho(e_t)=\{t\}+\sum_{s\in Y_t}\{s\}$. Therefore

$$\sum_{t\in\mathcal{T}_0(\lambda)} x_t\rho(e_t)=\sum_{t\in\mathcal{T}_0(\lambda)} x_t\Bigl(\{t\}+\sum_{s\in Y_t}\{s\}\Bigr)=\sum_{t\in\mathcal{T}_0(\lambda)} x_t\{t\}+\sum_{t\in\mathcal{T}_0(\lambda)}\sum_{s\in Y_t} x_t\{s\}.$$

Now observe

$$\sum_{t\in\mathcal{T}_0(\lambda)}\sum_{s\in Y_t} x_t\{s\}=\sum_{(t,s)\in W(\lambda)} x_t\{s\}=\sum_{s\in\mathcal{T}_0(\lambda)}\sum_{t\in X_s} x_t\{s\}.$$

Therefore by reindexing we have

$$\begin{aligned}\sum_{t\in\mathcal{T}_0(\lambda)} x_t\rho(e_t)&=\sum_{s\in\mathcal{T}_0(\lambda)} x_s\{s\}+\sum_{s\in\mathcal{T}_0(\lambda)}\sum_{t\in X_s} x_t\{s\}\\&=\sum_{s\in\mathcal{T}_0(\lambda)}\biggl(\Bigl(1+\sum_{t\in X_s} x_t\Bigr)\{s\}+\sum_{t\in X_s} x_t\{s\}\biggr)=\sum_{s\in\mathcal{T}_0(\lambda)}\{s\}.\end{aligned}$$ □

Now we will use the work thus far to demonstrate how understanding the solution to (3-1) can be used to answer our question of decomposability.

Theorem 3.5. *Let λ be a Lucas perfect partition of n such that $\lambda\neq(n),(1^n)$, and let the coefficients $x_t\in F$ be as in Lemma 3.4. Then there exists a nonzero $F\Sigma_n$-module M such that $S^\lambda\cong S^{(n)}\oplus M$ if and only if $\sum_{t\in\mathcal{T}_0(\lambda)}x_t\neq 0$.*

Proof. Fix nonzero $F\Sigma_n$-module homomorphisms $p_\lambda: S^\lambda\to S^{(n)}$ and $i_\lambda: S^{(n)}\to S^\lambda$. Since $S^{(n)}$ is a simple $F\Sigma_n$-module, p_λ and i_λ span their respective homomorphism spaces, and S^λ is not one-dimensional, S^λ is decomposable with summand isomorphic to $S^{(n)}$ if and only if $p_\lambda\circ i_\lambda\neq 0$. Let $\{r\}$ be the unique tabloid in $M^{(n)}=S^{(n)}$. Notice for all $t,t'\in\mathcal{T}(\lambda)$, we have $p_\lambda(e_t)=p_\lambda(e_{t'})=\alpha\{r\}$ for some $\alpha\neq 0$ since Σ_n acts transitively on the polytabloids and as the identity on $S^{(n)}$. To complete the proof we need only to observe if

$$i_\lambda(\{r\})=\beta\sum_{\{s\}\in X(\lambda)}\{s\}=\beta\sum_{t\in\mathcal{T}_0(\lambda)\}} x_t e_t$$

for some nonzero $\beta\in F$ then

$$p_\lambda\circ i_\lambda(\{r\})=\alpha\beta\Bigl(\sum_{t\in\mathcal{T}_0(\lambda)} x_t\Bigr)\{r\}.$$

Hence $p_\lambda\circ i_\lambda\neq 0$ if and only if $\sum_{t\in\mathcal{T}_0(\lambda)} x_t\neq 0$. □

It is worth noting that this result has a simpler interpretation. Since we know the coefficients of tabloids in polytabloids are either 1 or 0 in characteristic 2, it follows that the x_t are either 0 or 1. The sum of coefficients in Theorem 3.5 is congruent to the number of nonzero coefficients modulo 2. Hence we can say for a Lucas perfect partition, the Specht module is decomposable with a one-dimensional summand if and only if the sum of all tabloids can be expressed as a sum of an odd number of standard polytabloids. In fact we do not need to insist in expressing the sum using standard polytabloids, but rather any polytabloids.

3B. ***New proof of Murphy's result.*** Our work thus far allows us to provide a new proof of the result of Murphy, Theorem 1.1. First we will need a quick lemma concerning hook partitions.

Lemma 3.6. *Let $\lambda = (n-r, 1^r)$ be a hook partition. Then for all $t \in \mathcal{T}_0(\lambda)$,*

$$X_t = \{s \mid s \to t \text{ and } s \neq t\} = \varnothing.$$

Proof. Let t be an arbitrary standard λ-tableau. Assume for contradiction there is a nonidentity element $\pi \in C_t$ such that $\{\pi t\} = \{s\}$ for some $s \in \mathcal{T}_0(\lambda)$. Suppose x is the largest integer not fixed by π. Let $y = \pi^{-1}(x)$ and $z = \pi(x)$, so $y, z < x$ by our assumption of x. Since the first column is the only one with multiple entries, $x, y, z \in \mathcal{C}_t(1)$. We will consider two cases.

<u>Case 1</u>: Suppose $y = 1$. Then 1 is not fixed by π. So $1 \in \mathcal{R}_{\pi t}(j)$ for $j > 1$; thus πt is not row equivalent to a standard tableau. So we have reached a contradiction.

<u>Case 2</u>: Suppose $y \neq 1$. Then $y \in \mathcal{R}_t(i)$ and $x \in \mathcal{R}_t(j)$ with $1 < i < j$. Hence $\pi(y) = x \in \mathcal{R}_{\pi t}(i)$ and $\pi(x) = z \in \mathcal{R}_{\pi t}(j)$ with $1 < i < j$. Hence πt is not row equivalent to a standard tableau and we again have reached a contradiction. □

In order to reproduce Murphy's result suppose $\lambda = (n-r, 1^r)$. First we note that if n is even or r is odd then λ or λ' is not Lucas perfect, so S^λ does not have $S^{(n)}$ as a summand by Theorem 3.5. Now it suffices to consider the case when n is odd, r even, and $0 < r < n$, so λ is Lucas perfect. Notice that a standard tableau is uniquely determined by the choice of r entries not appearing in the first row; thus $|\mathcal{T}_0(\lambda)| = \binom{n-1}{r}$, since the entries can be any subset of $\{2, 3, \dots, n\}$ of size r. Now by Lemmas 3.6 and 3.4 we have a solution to (3-1), $x_t = 1$ for all $t \in \mathcal{T}_0(\lambda)$ since $X_t = \varnothing$. Therefore

$$\sum_{t \in \mathcal{T}_0(\lambda)} x_t = \binom{n-1}{r}.$$

Hence Murphy's result follows from Theorem 3.5.

4. The directed graph of λ

Let Γ_λ be the graph whose vertex set is $\mathcal{T}_0(\lambda)$. The graph Γ_λ has a directed edge from t to s if and only if $t \to s$ and $t \neq s$. To illustrate the definition we will construct the graph $\Gamma_{(4,3)}$ in Figure 1 using the notation of [James 1978, Definition 3.6] to represent a tableau t by a Young diagram where $t(i, j)$ is the (i, j)-node of $[\lambda]$. We will define a *path* γ on Γ_λ to be a sequence $\gamma = (t_1, t_2, \dots, t_l)$, such that $t_i \to t_{i+1}$

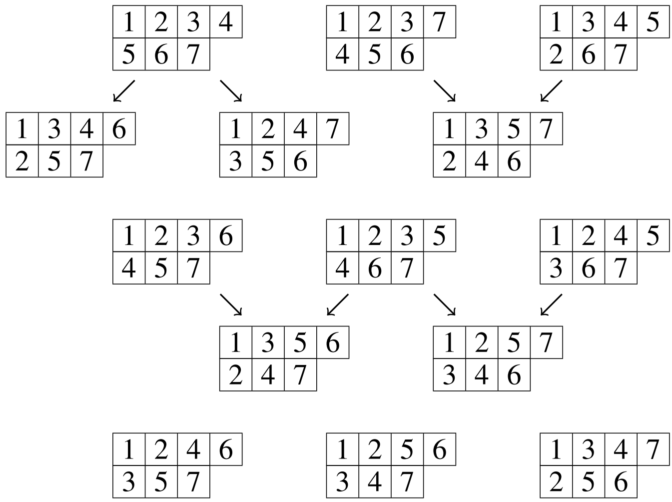

Figure 1. The directed graph of (4, 3).

and $t_i \neq t_{i+1}$ for $1 \leq i < l$. If $\gamma = (t_1, t_2, \ldots, t_l)$ we will say γ has *length* $l-1$ and *terminates* at t_l. We consider $\gamma = (t_1)$ to be a path on Γ_λ of length zero. Let P^λ be the set of all paths on Γ_λ and $\Omega_t = \{\gamma \in P^\lambda \mid \gamma \text{ terminates at } t\}$. We note that $\{\Omega_t \mid t \in \mathcal{T}_0(\lambda)\}$ partitions P^λ. Using this notation we discover that $|\Omega_t|$ satisfies a familiar relationship.

Lemma 4.1. *Let $\lambda \vdash n$ and $X_t = \{s \mid s \to t \text{ and } s \neq t\}$. If*

$$\Omega_t = \{\gamma \in P^\lambda \mid \gamma \text{ terminates at } t\}$$

then

$$|\Omega_t| = 1 + \sum_{s \in X_t} |\Omega_s|.$$

Proof. Let $\gamma = (t_1, t_2, \ldots, t_{l-1}, t) \in \Omega_t - \{(t)\}$. Define $F : \Omega_t - \{(t)\} \to \bigcup_{s \in X_t} \Omega_s$ by $F(\gamma) = (t_1, t_2, \ldots, t_{l-1})$. We will complete the proof by demonstrating that F is a bijection. If $F(\gamma) = (t_1, t_2, \ldots, t_{l-1}) = F(\gamma')$ for $\gamma, \gamma' \in \Omega_t - \{(t)\}$ then $\gamma = (t_1, t_2, \ldots, t_{l-1}, t) = \gamma'$. If $\tau = (t_1, t_2, \ldots, t_{l-1}, t_l)$ for some $t_l \neq t$ such that $t_l \to t$, then $\gamma = (t_1, t_2, \ldots, t_{l-1}, t_l, t) \in \Omega_t$ and $F(\gamma) = \tau$. Therefore F is a bijection. $\square$

Through Lemma 3.4, we establish an important connection between the directed graph of λ and our question of $S^{(n)}$ appearing as a submodule S^λ. We summarize this fact with the following theorem.

Theorem 4.2. *Suppose $\lambda \vdash n$ is Lucas perfect. Then there exists an $F\Sigma_n$-module M such that $S^\lambda \oplus M$ if and only if $|P^\lambda|$ is odd.*

Proof. Observe that $x_t \equiv |\Omega_t| \pmod 2$ is a solution to (3-1) by Lemmas 3.4 and 4.1. Moreover

$$|P^\lambda| = \sum_{\mathcal{T}_0(\lambda)} |\Omega_t| \equiv \sum_{\mathcal{T}_0(\lambda)} x_t \pmod 2.$$

Therefore the result follows immediately from Theorem 3.5. □

4A. ***Self-conjugate partitions.*** We say a partition λ is *self-conjugate* if $\lambda = \lambda'$. For the remainder of the section we will assume that λ is self-conjugate and Lucas perfect. In this circumstance, we are able to define an involution on $\mathcal{T}(\lambda)$. Suppose $t \in \mathcal{T}(\lambda)$, and define $\bar{t} \in \mathcal{T}(\lambda)$ by $\bar{t}(i, j) := t(j, i)$ for all $(i, j) \in [\lambda]$. Since the action of Σ_n is relevant to our discussion we note that $\overline{\sigma t} = \sigma \bar{t}$. From this fact we can conclude the following lemma.

Lemma 4.3. *For $t, s \in \mathcal{T}_0(\lambda)$, if $s \to t$, then $\bar{t} \to \bar{s}$.*

Proof. Suppose there exists $\sigma \in C_s$ and $\pi \in R_{\sigma s} = R_t$ such that $\pi\sigma s = t$. Then $\pi\sigma\bar{s} = \overline{\pi\sigma s} = \bar{t}$. So $\sigma^{-1}\pi^{-1}\bar{t} = \bar{s}$; moreover $\pi^{-1} \in C_{\bar{s}}$ and $\sigma^{-1} \in R_{\bar{t}}$. □

This lemma allows us to induce an involution on P^λ where if $\gamma = (t_1, t_2, \ldots, t_l) \in P^\lambda$ then $\bar{\gamma} = (\bar{t}_l, \bar{t}_{l-1}, \ldots, \bar{t}_1) \in P^\lambda$. Further, we wish to demonstrate that this involution fixes no paths. In order to prove this, we will need the following corollary of (2.3.2).

Corollary 4.4. *Suppose $\lambda \vdash n > 1$ is self-conjugate. Then for all $t \in \mathcal{T}(\lambda)$, we have $t \not\to \bar{t}$.*

Proof. Let $\lambda \vdash n > 1$ be self-conjugate. Then $(2, 1), (1, 2) \in [\lambda]$. Let $a = t(1, 1)$ and $b = t(2, 1)$. Since a, b are in the same column of t, they are in the same row of $\bar{t}$. Thus $t \not\to \bar{t}$ by (2.3.2). □

Now we have the tools needed to prove that the involution on P^λ fixes no elements.

Lemma 4.5. *Suppose $\lambda \vdash n > 1$ is self-conjugate and $\gamma \in P^\lambda$. Then $\gamma \neq \bar{\gamma}$.*

Proof. Let $\gamma = (t_1, t_2, \ldots, t_l)$. Assume for the sake of contradiction that $\gamma = \bar{\gamma}$. We will consider two cases.

Case 1: Assume γ has odd length. Then l is even and $t_{l/2+1} = \bar{t}_{l/2}$; thus $t_{l/2} \to \bar{t}_{l/2}$, which contradicts Corollary 4.4.

Case 2: Assume γ has even length. Then s is odd and $t_{(l+1)/2} = \bar{t}_{(l+1)/2}$, which is impossible. □

Finally we can conclude the following result for self conjugate partitions.

Theorem 4.6. *Suppose $\lambda \vdash n > 1$ is a self-conjugate partition. Then there does not exist a nonzero $F\Sigma_n$-module M such that $S^\lambda \cong S^{(n)} \oplus M$.*

Proof. By Lemma 4.5 there is an involution on the finite set P^λ with no fixed points; hence $|P^\lambda|$ is even. Therefore the theorem follows from Theorem 4.2. □

5. Computing the sum of polytabloid coefficients

In this section, we present an algorithm to compute the sum of the polytabloid coefficients described in Lemma 3.4. For the remainder of the section fix a particular Lucas perfect partition λ of n. For simplicity of notation, we define $m = |\mathcal{T}_0(\lambda)|$ to be the dimension of the Specht module $S^{(\lambda)}$. Let $t_1, \ldots, t_m$ be an enumeration of all standard λ-tableaux which preserves the dominance order, that is, $\{t_j\} \lhd \{t_k\}$ only if $k < j$. Next, for the sake of convenience, we adopt the notation

$$X_j = X_{t_j} = \{s \in \mathcal{T}_0(\lambda) \mid s \to t_j \text{ and } s \neq t_j\}.$$

Additionally for $1 \leq j \leq m$, let $Z_j = \{t_1, t_2, \ldots t_j\}$ be the set of the first j standard tableaux under our chosen ordering, using the convention that $Z_0 = \varnothing$.

Define the $m \times (m+1)$ matrix $\boldsymbol{V} = [\boldsymbol{v}^0, \boldsymbol{v}^1, \boldsymbol{v}^2, \ldots, \boldsymbol{v}^m]$ by

$$\boldsymbol{v}_j^i = 1 + \sum_{s \in X_j \cap Z_i} x_s$$

for all $0 \leq i \leq m$ and $1 \leq j \leq m$. Since $Z_0 = \varnothing$ we have that $v_j^0 = 1$ for all $1 \leq j \leq m$. Also if $t_i \to t_j$ and $i \neq j$ then $t_i \rhd t_j$ and hence $i < j$. So we conclude for $k \geq j$, $X_j \cap Z_k = X_j$. Therefore

$$\boldsymbol{v}_j^m = 1 + \sum_{s \in Z_j} x_s = x_{t_j}.$$

Hence the sum of the coefficients of $\boldsymbol{v}^m$ will be congruent to the sum of polytabloid coefficients from Theorem 3.5. In this final section we develop the algorithm to compute v_j^m for all $1 \leq j \leq m$ in order to compute the sum of those coefficients. To this end, observe if $i = j$ or $t_i \not\to t_j$ then $X_j \cap Z_i = X_j \cap Z_{i-1}$, so $v_j^i = v_j^{i-1}$. Additionally if $i \neq j$ and $t_i \to t_j$, then $i < j$ and $X_j \cap Z_i = (X_j \cap Z_{i-1}) \cup \{t_i\}$. Thus for all $1 \leq i \leq m$,

$$\begin{aligned} \boldsymbol{v}_j^i &= 1 + \sum_{s \in X_j \cap Z_i} x_s = x_{t_i} + 1 + \sum_{s \in X_j \cap Z_{i-1}} x_s \\ &= \left(1 + \sum_{s \in X_i} x_s\right) + \left(1 + \sum_{s \in X_j \cap Z_{i-1}} x_s\right) = \boldsymbol{v}_i^{i-1} + \boldsymbol{v}_j^{i-1} \end{aligned}$$

since $X_i \cap Z_{i-1} = X_i$. We summarize our observations by noting for all $1 \leq i, j \leq m$,

$$\boldsymbol{v}_j^i \equiv \begin{cases} \boldsymbol{v}_i^{i-1} + \boldsymbol{v}_j^{i-1} \pmod 2 & \text{if } t_i \to t_j \text{ and } i \neq j, \\ \boldsymbol{v}_j^{i-1} \pmod 2 & \text{otherwise.} \end{cases}$$

We can now see that in order to develop an algorithm which will compute the desired vectors, it is necessary for our algorithm to determine if $t \to s$ for all $t, s \in \mathcal{T}_0(\lambda)$.

5A. *Algorithm for testing the production of tabloids from polytabloids.* For $\lambda \vdash n$, let $t, s \in \mathcal{T}_0(\lambda)$ be such that $\{s\} \lhd \{t\}$. By definition, $t \to s$ if and only if there exist $\pi \in C_t$ and $\sigma \in R_s$ such that $\sigma\pi t = s$. If such a $\pi \in C_t$ exists, the image of $t(i, j)$ under π is uniquely determined as $t(i_0, j)$, where $t(i, j) \in \mathcal{R}_s(i_0)$. The algorithm defined below will attempt to build the permutation π, defining it by necessity. It is possible that such a function does not exist, depending on the shape of λ. Additionally even if such a function exists, it may not define a bijection. The following algorithm tests to see if a permutation π can be defined.

Python Algorithm 5.1.

```
def produces(t, s):
  is_mapped_to = {}
  for val in t.vals:
  # For each positive integer less than n, attempt to find
  # the necessary image for that integer.
    (i, j), (i0, j0) = t.coords_of(val), s.coords_of(val)
    # Identify the column of t and row of s containing
    # the current value.
    try:
       target = t[i0][j]
       # Identify the necessary image of value by the function.
    except IndexError:
       # Return False since the target node is not in the
       # young diagram, hence the function cannot be defined.
       return False
    if is_mapped_to.get(target):
    # If the target is already an image of a previous value,
    # the function cannot be a bijection, so we return False.
       return False
    is_mapped_to[target] = True
    # After identifying the target for the value, record
    # that the target has been used.
  return True
```

The function produces(t, s) returns True if and only if the desired bijection $\pi \in C_t$ exists, and hence $t \to s$. Now we can use our observations and this function to write an algorithm which will compute the desired sum of polytabloid coefficients.

5B. *Algorithm to sum polytabloid coefficients.* We note that produces(t, s) is computationally demanding. This is not surprising as determining which s are produced from t is inherently tied to generating the coefficients of the polytabloid.

In an effort to be more computationally efficient we note since $v_i^{i-1} + v_j^{i-1} \equiv v_j^{i-1} \equiv v_j^i \pmod 2$ whenever $v_i^{i-1} \equiv 0 \pmod 2$, we have $v^i \equiv v^{i-1} \pmod 2$. Thus it is not necessary to determine if $t_i \to t_j$ for such i. Hence our final algorithm will not evaluate produces(t_i, t_j) in these cases.

Python Algorithm 5.2.

```
def sum_of_coefficients(standard_tableaux):
# standard_tableaux contains a list of all standard tableaux
# for a fixed partition lambda of n, ordered with respect to
# the dominance relation, with the least dominant first.
 standard=standard_tableaux[::-1]
 # this creates a second list of standard tableaux with
 # the order reversed, so most dominant is first.
 v = [1] * len(standard)
 # Define initial vector
 for i, t in enumerate(standard_tableaux):
  if v[i] == 0:
  # Skip the evaluation of produce function since the
  # entry is congruent to 0.  The next vector in the
  # sequence is congruent to the current vector.
    continue
  for j, s in enumerate(standard_tableaux[:i]):
  # Create the next vector in the sequence adjusting
    if produces(t, s):
    # If the corresponding tableau produces the
    # second, adjust the vector entry accordingly,
    # otherwise leave it the same.
     v[j] = (v[j] + 1) % 2
return sum(v) % 2
```

6. Conclusions

Using Python Algorithm 5.2, we are invoking Theorem 3.5 in order to determine if a particular Specht module has a one-dimensional summand. We exhausted the computational power available to us evaluating Lucas perfect partitions up to $n = 19$ excluding the partitions of the form (n) and (1^n). Table 1 records the output of our sum_of_coefficients() function for various partitions. We note in our results that the partitions corresponding to the Specht module having a one-dimensional summand were previously known Specht modules corresponding to hook partitions. Our results again confirm Murphy's result (Theorem 1.1) for these partitions.

n	λ	Σ
5	(3,1,1)	0
7	(3,1,1,1,1)	1
7	(5,1,1)	1
8	**(3,3,2)**	0
9	(3,1,1,1,1,1,1)	0
9	(5,1,1,1,1)	0
9	(7,1,1)	0
9	**(3,3,3)**	0
11	(3,1,1,1,1,1,1,1,1)	1
11	(5,1,1,1,1,1,1)	0
11	(7,1,1,1,1)	0
11	(9,1,1)	1
13	(3,1,1,1,1,1,1,1,1,1,1)	0
13	(5,1,1,1,1,1,1,1,1)	1
13	(7,1,1,1,1,1,1)	0
13	**(3,3,3,1,1,1,1)**	0
13	(9,1,1,1,1)	1
13	(11,1,1)	0
13	**(7,3,3)**	0
15	(3,1,1,1,1,1,1,1,1,1,1,1,1)	1
15	(5,1,1,1,1,1,1,1,1,1,1)	1
15	(7,1,1,1,1,1,1,1,1)	1
15	(9,1,1,1,1,1,1)	1
15	(11,1,1,1,1)	1
15	(13,1,1)	1
17	**(3,3,3,1,1,1,1,1,1,1,1)**	0
17	**(11,3,3)**	0
17	(9,1,1,1,1,1,1,1,1)	0
17	(11,1,1,1,1,1,1)	0
17	(7,1,1,1,1,1,1,1,1,1,1)	0
17	**(7,3,3,1,1,1,1)**	0
17	(13,1,1,1,1)	0
17	(5,1,1,1,1,1,1,1,1,1,1,1,1)	0
17	(15,1,1)	0
17	(3,1,1,1,1,1,1,1,1,1,1,1,1,1,1)	0
19	(3,1,1,1,1,1,1,1,1,1,1,1,1,1,1,1,1)	1
19	(17,1,1)	1
19	(5,1,1,1,1,1,1,1,1,1,1,1,1,1,1)	0
19	(15,1,1,1,1)	0
19	(7,1,1,1,1,1,1,1,1,1,1,1,1)	0
19	(13,1,1,1,1,1,1)	0
19	(9,1,1,1,1,1,1,1,1,1,1)	0
19	(11,1,1,1,1,1,1,1,1)	0

Table 1. The partitions which are not hook partitions are noted in bold.

We see that in the collection of partitions within our computational limits, there are very few such nonhook partitions. Moreover a handful of these partitions are self-conjugate, so based on Theorem 4.6, we know these partitions would not have a one-dimensional summand. Perhaps with additional computational power or a more refined algorithm, we may discover a nonhook Specht module with a one-dimensional summand. It is worth noting that such an example would be the first decomposable Specht module associated to a partition that is not 2-quotient separated (see [James and Mathas 1996, Section 2] and [Dodge and Fayers 2012, Section 8.2]) ever discovered.

Acknowledgements

The authors would like to thank Harald Ellers and Gregory Kapfhammer of Allegheny College for their consultation during this project. Additionally, much of the work would not have been possible without James Lombardi, Jr. and the Allegheny College Physics Department's computing resources. This work was supported in part by funding through the John B. Frick and Deborah K. Watson, Ph.D. Student-Faculty Research Fund. Finally we would like to thank the referee for their suggestions following the original submission of this paper.

References

[Dodge and Fayers 2012] C. J. Dodge and M. Fayers, "Some new decomposable Specht modules", *J. Algebra* **357** (2012), 235–262. MR Zbl

[Donkin and Geranios 2018] S. Donkin and H. Geranios, "Decompositions of some Specht modules, I", preprint, 2018. arXiv

[James 1978] G. D. James, *The representation theory of the symmetric groups*, Lecture Notes in Mathematics **682**, Springer, 1978. MR Zbl

[James and Kerber 1981] G. James and A. Kerber, *The representation theory of the symmetric group*, Encyclopedia of Mathematics and its Applications **16**, Addison-Wesley, Reading, MA, 1981. MR Zbl

[James and Mathas 1996] G. James and A. Mathas, "Hecke algebras of type **A** with $q = -1$", *J. Algebra* **184**:1 (1996), 102–158. MR Zbl

[Murphy 1980] G. Murphy, "On decomposability of some Specht modules for symmetric groups", *J. Algebra* **66**:1 (1980), 156–168. MR Zbl

[van Rossum 2001] G. van Rossum, "Python reference manual", online reference, 2001, available at https://docs.python.org/2.0/ref/ref.html.

[Speyer 2014] L. Speyer, "Decomposable Specht modules for the Iwahori–Hecke algebra $\mathcal{H}_{\mathbb{F},-1}(\mathfrak{S}_n)$", *J. Algebra* **418** (2014), 227–264. MR Zbl

[Speyer and Sutton 2018] L. Speyer and L. Sutton, "Decomposable specht modules indexed by bihooks", preprint, 2018. arXiv

Received: 2019-05-20 Revised: 2019-07-29 Accepted: 2019-08-29

collinsa@allegheny.edu *Department of Mathematics, Allegheny College, Meadville, PA, United States*

cdodge2@allegheny.edu *Department of Mathematics, Allegheny College, Meadville, PA, United States*

INVOLVE 12:8 (2019)
dx.doi.org/10.2140/involve.2019.12.1415

The monochromatic column problem with a prime number of colors

Loran Crowell and Steve Szabo

(Communicated by Kenneth S. Berenhaut)

Let $p_1, \dots, p_n$ be a sequence of n pairwise coprime positive integers, $P = p_1 \cdots p_n$, and $0, \dots, m-1$ be a sequence of m different colors. Let A be an $n \times mP$ matrix of colors in which row i consists of blocks of p_i consecutive entries of the same color with colors 0 through $m-1$ repeated cyclically. The monochromatic column problem is to determine the number of columns of A in which every entry is the same color. The solution for a prime number of colors is provided.

1. Introduction

Let m be a positive integer. The colors for m are represented by the integers $0, 1, \dots, m-1$. An $n \times s$ *m-color matrix* is an $n \times s$ matrix $A = (a_{ij})$ in which every entry is one of the m colors. Column j of A is *monochromatic* if $a_{ij} = a_{1j}$ for $1 \le i \le n$. For a positive integer p, row i of A is p-blocked with initial color ρ if $p \mid s$ and, for $1 \le j \le s$,

$$a_{ij} = \left(\left\lfloor \frac{j-1}{p} + \rho \right\rfloor \right) \bmod m.$$

For $D = \{(p_i, \rho_i)\}_{i=1}^{n}$, where $p_1, \dots, p_n$ are pairwise coprime positive integers and $\rho_i \in \{0, \dots, m-1\}$, an $n \times mp_1 \cdots p_n$ m-color matrix A is the (m, D)*-color matrix* if for every i satisfying $1 \le i \le n$, row i of A is p_i-blocked with initial color ρ_i. For instance, the layout of the $(5, \{(2,1), (3,4)\})$-color matrix is

$$\begin{pmatrix} 1&1&2&2&3&3&4&4&0&0&1&1&2&2&3&3&4&4&0&0&1&1&2&2&3&3&4&4&0&0 \\ 4&4&4&0&0&0&1&1&1&2&2&2&3&3&3&4&4&4&0&0&0&1&1&1&2&2&2&3&3&3 \end{pmatrix}.$$

MSC2010: 05A15, 11A07.

Keywords: monochromatic column problem, Chinese remainder theorem, multiple sequence alignment problem.

The *monochromatic column problem* (*MCP*) is to determine the number of monochromatic columns in the (m, D)-color matrix, which is denoted by $N(m, D)$. Note, $N(5, \{(2, 1), (3, 4)\}) = 6$.

The MCP was originally posed in [Nagpaul and Jain 2002]. Their stated motivation is captured in the following from their paper:

> The motivation for studying this problem arose from a question asked by a biomathematician working on the multiple sequence problem that deals with finding, for given k sequences of characters from a fixed alphabet, an alignment with optimal score according to a given scoring scheme.

The multiple sequence alignment problem is a well-studied problem in molecular biology. It is of crucial importance according to [Jiang et al. 1999]. Independently of its tenuous connections to the multiple sequence alignment problem, the MCP is an interesting combinatorial problem in its own right.

The solution of the MCP for two colors is given in [Nagpaul and Jain 2002] and for three colors is given in [Srivastava and Szabo 2008]. The technique developed by Srivastava and Szabo for three colors is generalized here to give the solution for a prime number colors. A partial solution for the prime color case was the topic of [Crowell 2016].

Section 2 contains the complete solution to the prime color problem. In Section 3, the three color solution is restated, correcting a small issue in the solution in [Srivastava and Szabo 2008].

2. The monochromatic column problem: a prime number of colors

Throughout this section, let n be a positive integer, q a prime, $D = \{(p_i, \rho_i)\}_{i=1}^{n}$, where $p_1, \ldots, p_n$ are pairwise coprime positive integers and $\rho_i \in \{0, \ldots, q-1\}$, and $A = (a_{ij})$ be the (q, D)-color matrix. To solve the prime color problem, three cases are considered which exhaust the possibilities. First, in Proposition 1, it is assumed that $p_1, \ldots, p_n$ are congruent to one another modulo q. Then in Proposition 2, it is assumed that $p_1, \ldots, p_n$ may not all be congruent to one another but none are divisible by q. Finally, in Proposition 3, it is assumed that $q \mid p_n$. In the statements of the propositions, an ordering of $p_1, \ldots, p_n$ is assumed, but of course this ordering does not affect the number of monochromatic columns.

Proposition 1. *Let* $s \in \{1, \ldots, q-1\}$. *Assume* $p_i \equiv s \pmod q$ *for* $i \in \{1, \ldots, n\}$. *Then*

$$N(q, D) = q \sum_{\beta=1}^{\min\{p_1, q\}} \prod_{i=1}^{n} \frac{p_i - s}{q} + \left\lfloor \frac{s - (\beta + s(\rho_i - \rho_1) - 1) \bmod q - 1}{q} \right\rfloor + 1.$$

Proof. Let $P = p_1 p_2 \cdots p_n$. Note

$$a_{ij} = \left(\left\lfloor \frac{j-1}{p_i} \right\rfloor + \rho_i \right) \bmod q$$

since $\lfloor (j-1)/p_i \rfloor$ calculates the number of complete blocks that the element is away from the beginning of the row. This number of blocks is added to the starting color of the row, ρ_i, and then taking this modulo q gives the color. We will first show that if column j is monochromatic, then a column some multiple of P away is also monochromatic.

Let $1 \le x, y \le n,\ 1 \le j \le P$, and $0 \le \alpha \le q-1$. Since $p_x \equiv p_y \pmod q$,

$$\begin{aligned} \frac{\alpha P}{p_x} &\equiv \frac{\alpha P}{p_y} \pmod q \\ \left\lfloor \frac{j-1}{p_x} \right\rfloor - \frac{\alpha P}{p_x} - \left\lfloor \frac{j-1}{p_x} \right\rfloor &\equiv \left\lfloor \frac{j-1}{p_y} \right\rfloor - \frac{\alpha P}{p_y} - \left\lfloor \frac{j-1}{p_y} \right\rfloor \pmod q \\ \left\lfloor \frac{j-1}{p_x} \right\rfloor - \left\lfloor \frac{\alpha P + j - 1}{p_x} \right\rfloor &\equiv \left\lfloor \frac{j-1}{p_y} \right\rfloor - \left\lfloor \frac{\alpha P + j - 1}{p_y} \right\rfloor \pmod q \\ a_{x,j} - a_{x,\alpha P + j} &\equiv a_{y,j} - a_{y,\alpha P + j} \pmod q. \end{aligned} \tag{1}$$

This shows that if column j is monochromatic, then so is column $\alpha P + j$. Hence, it suffices to count the number of monochromatic columns in the first P columns of A and multiply by q.

Let

$$k_{ij} = j - \left\lfloor \frac{j-1}{p_i} \right\rfloor p_i.$$

This is the count into the $\lfloor (j-1)/p_i \rfloor$-th monocolored block in the i-th row.

Since $p_1, \ldots, p_n$ are pairwise coprime integers and $1 \le k_{ij} \le p_i$, the Chinese remainder theorem guarantees that $|\{(k_{1j}, \ldots, k_{nj})\}_{j=1}^{P}| = P$. Therefore, by counting the n-tuples that map to a monochromatic column, the number of monochromatic columns in the first P columns of A can be determined. For $1 \le i \le n$ and $1 \le j \le P$,

$$a_{ij} = \left(\left\lfloor \frac{j-1}{p_i} \right\rfloor + \rho_i \right) \bmod q = \left(\frac{j - k_{ij}}{p_i} + \rho_i \right) \bmod q.$$

Since $p_i \equiv s \pmod q$, we have $a_{ij} = a_{1j}$ if and only if $k_{ij} \equiv k_{1j} + s(\rho_i - \rho_1) \pmod q$. So, column j is monochromatic if and only if $k_{ij} \equiv k_{1j} + \rho_i s \pmod q$ for all $i \in \{1, \ldots, n\}$. Hence, the number of monochromatic columns in the first P columns of A is the product of the number of integer solutions to

$$1 \le q x_i + (k_{1j} + s(\rho_i - \rho_1)) \bmod q \le p_i$$

for each $i \in \{1, \dots, n\}$; equivalently,

$$\frac{1-(k_{1j}+s(\rho_i-\rho_1)) \bmod q}{q} \le x_i \le \frac{p_i-(k_{1j}+s(\rho_i-\rho_1)) \bmod q}{q}.$$

The number of integer solutions for a given i is

$$\begin{aligned}
&\left\lfloor \frac{p_i-(k_{1j}+s(\rho_i-\rho_1)) \bmod q}{q} \right\rfloor - \left\lceil \frac{1-(k_{1j}+s(\rho_i-\rho_1)) \bmod q}{q} \right\rceil + 1 \\
&= \frac{p_i-s}{q} + \left\lfloor \frac{s-(k_{1j}+s(\rho_i-\rho_1)) \bmod q}{q} \right\rfloor + \left\lfloor \frac{(k_{1j}+s(\rho_i-\rho_1)) \bmod q - 1}{q} \right\rfloor + 1 \\
&= \frac{p_i-s}{q} + \left\lfloor \frac{s-(k_{1j}+s(\rho_i-\rho_1)-1) \bmod q - 1}{q} \right\rfloor + 1.
\end{aligned}$$

The possible values of $[(k_{1j}+s(\rho_i-\rho_1))-1] \bmod q$ are given by

$$\{(\beta+s(\rho_i-\rho_1)-1) \bmod q \mid \beta \in \{1, \dots, \min\{p_1, q\}\}.$$

Summing over these possibilities for k_{1j}, multiplying the number of solutions for each row, and multiplying the sum by q, we find that the number of monochromatic columns in A is

$$N(q, D) = q \sum_{\beta=1}^{\min\{p_1,q\}} \prod_{i=1}^{n} \frac{p_i-s}{q} + \left\lfloor \frac{s-(\beta+s(\rho_i-\rho_1)-1) \bmod q - 1}{q} \right\rfloor + 1. \quad \square$$

Proposition 2. *Let $S = \{p_i \bmod q \mid i \in I\}$, $r = |S|$ and $s_1, \dots, s_r \in S$ be the distinct elements of S. Assume $q \nmid p_i$ for $i \in I$ and $r > 1$. Let $i_0, i_1, \dots, i_r$ be such that $i_0 = 0$, $i_r = n$, and $p_i \equiv s_l$ for $i_{l-1} < i \le i_l$. Let*

$$B = \big\{(\beta_1, \dots, \beta_r) \mid \beta_l \in \{1, \dots, \min\{p_{i_l}, q\}\}\big\}, \tag{2}$$

where

$$\beta_l = \frac{\beta_1(s_l-s_2)+\beta_2(s_l-s_1)+s_l(s_2-s_1)(\rho_{i_l}-\rho_{i_1})+s_2(s_l-s_1)(\rho_{i_1}-\rho_{i_2})}{s_2-s_1}.$$

Then

$$N(q, D) = \sum_{(\beta_1,\dots,\beta_r)\in B} \prod_{l=1}^{r} \prod_{i=i_{l-1}+1}^{i_l} \frac{p_i-s_l}{q} + \left\lfloor \frac{s_l-(\beta_l+s_l(\rho_i-\rho_{i_l})-1) \bmod q - 1}{q} \right\rfloor + 1.$$

Proof. Let $P = p_1 \cdots p_n$. From the proof of Proposition 1, the following can be deduced. The number of columns in the first P columns of A such that the color vector of the column, $(c_1, \dots, c_n)$, has the property that $c_i = c_{i_l}$ for $i_{l-1} < i \le i_l$ (i.e., is a column where the colors are identical if the associated p_i's are congruent) is

$$\sum_{(\beta_1,\ldots,\beta_r)\in B'} \prod_{l=1}^{r} \prod_{i=i_{l-1}+1}^{i_l} \frac{p_i - s_l}{q} + \left\lfloor \frac{s_l - (\beta_l + s_l(\rho_i - \rho_{i_l}) - 1) \bmod q - 1}{q} \right\rfloor + 1,$$

where

$$B' = \left\{(\beta_1, \ldots, \beta_r) \mid \beta_l \in \{1, \ldots, \min\{p_{i_l}, q\}\}\right\}.$$

Such columns will be called r-chromatic columns. First, it is shown that for $1 \le \alpha \le q-1$ and $1 \le j \le P$, column j is r-chromatic if and only if column $j+\alpha P$ is r-chromatic. Fix l and let $i_l - 1 \le x, y \le i_l$, $1 \le j \le P$, and $0 \le \alpha \le q-1$. Since $p_x \equiv p_y \pmod q$, the computations of (1) hold and we have

$$a_{x,j} - a_{x,\alpha P+j} \equiv a_{y,j} - a_{y,\alpha P+j} \pmod q.$$

This shows that column j is r-chromatic if and only if column $\alpha P + j$ is r-chromatic. Next, the conditions on an r-chromatic column, j, that guarantee that one and only one of the set of columns $\{j, j+P, \ldots, (q-1)P\}$ is monochromatic is developed. Let $j \in \{1, \ldots, P\}$ and assume column j is r-chromatic. Denote by the r-tuple $(c_1, \ldots, c_r)$ the entries of an r-chromatic column where $a_{ij} = c_l$ for all $i \in \{i_1, \ldots, i_l\}$. Of the noted columns, the only ones that may be monochromatic will have the property that

$$c_1 + \frac{\alpha P}{s_1} \equiv c_2 + \frac{\alpha P}{s_2} \pmod q$$

for some $\alpha \in \{0, \ldots, q-1\}$. So,

$$\alpha = (c_2 - c_1)\left(\frac{P}{s_1} - \frac{P}{s_2}\right)^{q-2} \bmod q.$$

This then shows that the only possible column that may be monochromatic is $\alpha P + j$. Furthermore, for such a column to be monochromatic, working over $\mathbb{Z}_p$, for $l \in \{3, \ldots, q\}$,

$$\frac{c_l - c_1}{1/s_1 - 1/s_l} = \frac{c_2 - c_1}{1/s_1 - 1/s_2}$$

$$\frac{s_1 s_l}{s_l - s_1}(c_l - c_1) = \frac{s_1 s_2}{s_2 - s_1}(c_2 - c_1)$$

$$\left(\frac{j - k_{i_l j}}{s_l} + \rho_{i_l} - \left(\frac{j - k_{i_1 j}}{s_1} + \rho_{i_1}\right)\right) = \frac{s_2(s_l - s_1)}{s_l(s_2 - s_1)}\left(\frac{j - k_{i_2 j}}{s_2} + \rho_{i_2} - \left(\frac{j - k_{i_1 j}}{s_1} + \rho_{i_1}\right)\right)$$

and thus

$$k_{i_l j} = \frac{k_{i_1 j}(s_l - s_2) + k_{i_2 j}(s_l - s_1)}{s_2 - s_1} + s_l(\rho_{i_l} - \rho_{i_1}) + \frac{s_2(s_l - s_1)(\rho_{i_1} - \rho_{i_2})}{s_2 - s_1}.$$

This shows which elements of B' correspond to a monochromatic column. Recall the set B given in (2). Hence, the number of monochromatic columns is

$$N(q,D) = \sum_{(\beta_1,\dots,\beta_r)\in B} \prod_{l=1}^{r} \prod_{i=i_{l-1}+1}^{i_l} \frac{p_i - s_l}{q} + \left\lfloor \frac{s_l-(\beta_l+s_l(\rho_i-\rho_{i_l})-1) \bmod q-1}{q} \right\rfloor + 1. \square$$

Proposition 3. *Assume $n > 1$ and $q \mid p_n$. Let $D' = D \setminus \{(p_n, \rho_n)\}$. Then*

$$N(q,D) = \frac{p_n}{q} N(q,D').$$

Proof. Let $P = p_1 p_2 \cdots p_n$. Note,

$$a_{ij} = \left(\left\lfloor \frac{j-1}{p_i} \right\rfloor + \rho_i \right) \bmod q$$

since $\lfloor (j-1)/p_i \rfloor$ calculates the number of complete blocks that the element is away from the beginning of the row. This number of blocks is added to the starting color of the row, ρ_i, and then taking this modulo q gives the color.

Let $1 \le x, y \le n-1$, $1 \le j \le P$, and $0 \le \alpha \le q-1$. Since $q \mid (P/p_x)$ and $q \mid (P/p_y)$, again the computations of (1) hold and we have

$$a_{x,j} - a_{x,\alpha P+j} \equiv a_{y,j} - a_{y,\alpha P+j} \pmod q.$$

This shows that if the first $n-1$ entries of column j are the same color then the first $n-1$ entries of column $j+\alpha P$ are the same color. Next, it is shown that $|\{a_{nj}, a_{n,P+j}, \dots, a_{n,(q-1)P+j}\}| = q$. Note that $(P/p_n) \not\equiv 0 \pmod q$. Now,

$$\begin{aligned} a_{nj} - a_{n,\alpha P+j} &\equiv \left\lfloor \frac{j-1}{p_n} \right\rfloor - \left\lfloor \frac{\alpha P + j - 1}{p_n} \right\rfloor \pmod q \\ &\equiv \left\lfloor \frac{j-1}{p_n} \right\rfloor - \left\lfloor \frac{j-1}{p_n} \right\rfloor + \frac{\alpha P}{p_n} \pmod q \\ &\equiv \frac{\alpha P}{p_n} \pmod q. \end{aligned}$$

Since q is prime, every color is represented in the set

$$\{a_{nj}, a_{n,P+j}, \dots, a_{n,(q-1)P+j}\}.$$

Therefore, $N(q,D) = (p_n/q)N(q,D')$. $\square$

3. Monochromatic column in three colors

In [Srivastava and Szabo 2008], there is a small issue in the results when 2 is one of the coprimes. The issue is that there is a possibility that β may only need to run up to 2 instead of 3. This can be seen in the general results of the previous section. We make the corrections while also restating the results with our simplified notation. Throughout this section, let n be a positive integer, $D = \{(p_i, \rho_i)\}_{i=1}^n$, where $p_1, \ldots, p_n$ are pairwise coprime positive integers and $\rho_i \in \{0, 1, 2\}$, and $A = (a_{ij})$ be the $(3, D)$-color matrix. The first result is a direct application of Proposition 1 for $q = 3$.

Proposition 4 [Srivastava and Szabo 2008, Lemma 1]. *Let* $s \in \{1, 2\}$. *Assume* $p_i \equiv s \pmod 3$ *for* $i \in \{1, \ldots, n\}$. *Then*

$$N(3, D) = q \sum_{\beta=1}^{\min\{p_1,3\}} \prod_{i=1}^{n} \frac{p_i - s}{3} + \left\lfloor \frac{s - (\beta + s(\rho_i - \rho_1) - 1) \bmod 3 - 1}{3} \right\rfloor + 1.$$

Proposition 5 [Srivastava and Szabo 2008, Lemma 2]. *Assume*

$$\{p_i \bmod 3 \mid i \in I\} = \{1, 2\}.$$

Let $i_0 = 0$, $i_2 = n$, *and* i_1*be such that, for* $i \in I$, *we have* $p_i \equiv l$ *for* $i_{l-1} < i \le i_l$. *Then*

$$N(3, D) = \sum_{\beta_1=1}^{3} \sum_{\beta_2=1}^{\min\{p_n,3\}} \prod_{l=1}^{2} \prod_{i=i_{l-1}+1}^{i_l} \frac{p_i - l}{q} + \left\lfloor \frac{l - (\beta_l + l(\rho_i - \rho_{i_l}) - 1) \bmod q - 1}{q} \right\rfloor + 1.$$

Proof. In Proposition 2, if $r = 2$ then $B = B'$. Furthermore, when $p_i \equiv 1 \pmod 3$, we have $p_i > 3$. This result then follows. □

For completeness, the following result is included as well.

Proposition 6 [Srivastava and Szabo 2008, Lemma 3]. *Assume* $n > 1$ *and* $3 \mid p_n$. *Let* $D' = D \setminus \{(p_n, \rho_n)\}$ *and* $A' = (3, D')$. *Then*

$$N(3, D) = \frac{p_n}{3} N(3, D').$$

References

[Crowell 2016] L. Crowell, *The monochromatic column problem: the prime case*, master's thesis, Easter Kentucky University, 2016, available at https://encompass.eku.edu/etd/356/.

[Jiang et al. 1999] T. Jiang, P. Kearney, and M. Li, "Open problems in computational molecular biology", *ACM SIGACT News* **30**:3 (1999), 43–49.

[Nagpaul and Jain 2002] S. R. Nagpaul and S. K. Jain, "Columns of uniform color in a rectangular array with rows having cyclically repeated color patterns", *Discrete Math.* **254**:1-3 (2002), 371–392. MR Zbl

[Srivastava and Szabo 2008] A. K. Srivastava and S. Szabo, "The monochromatic column problem", *Discrete Math.* **308**:17 (2008), 3906–3916. MR Zbl

Received: 2019-07-05 Revised: 2019-08-06 Accepted: 2019-08-12

loran.crowell@gmail.com *Eastern Kentucky University, Richmond, KY, United States*

steve.szabo@eku.edu *Eastern Kentucky University, Richmond, KY, United States*

INVOLVE 12:8 (2019)
dx.doi.org/10.2140/involve.2019.12.1423

Total Roman domination edge-critical graphs

Chloe Lampman, Kieka (C. M.) Mynhardt and Shannon Ogden

(Communicated by Anant Godbole)

A total Roman dominating function on a graph G is a function $f : V(G) \to \{0, 1, 2\}$ such that every vertex v with $f(v) = 0$ is adjacent to some vertex u with $f(u) = 2$, and the subgraph of G induced by the set of all vertices w such that $f(w) > 0$ has no isolated vertices. The weight of f is $\sum_{v \in V(G)} f(v)$. The total Roman domination number $\gamma_{tR}(G)$ is the minimum weight of a total Roman dominating function on G. A graph G is k-γ_{tR}-edge-critical if $\gamma_{tR}(G+e) < \gamma_{tR}(G) = k$ for every edge $e \in E(\overline{G}) \neq \varnothing$, and k-γ_{tR}-edge-supercritical if it is k-γ_{tR}-edge-critical and $\gamma_{tR}(G+e) = \gamma_{tR}(G) - 2$ for every edge $e \in E(\overline{G}) \neq \varnothing$. We present some basic results on γ_{tR}-edge-critical graphs and characterize certain classes of γ_{tR}-edge-critical graphs. In addition, we show that, when k is small, there is a connection between k-γ_{tR}-edge-critical graphs and graphs which are critical with respect to the domination and total domination numbers.

1. Introduction

We consider the behaviour of the total Roman domination number of a graph G upon the addition of edges to G. A *dominating set* S in a graph G is a set of vertices such that every vertex in $V(G) - S$ is adjacent to at least one vertex in S. The *domination number* $\gamma(G)$ is the cardinality of a minimum dominating set in G. A *total dominating set* S (abbreviated by *TD-set*) in a graph G with no isolated vertices is a set of vertices such that every vertex in $V(G)$ is adjacent to at least one vertex in S. The *total domination number* $\gamma_t(G)$ (abbreviated by *TD-number*) is the cardinality of a minimum total dominating set in G. For $S \subseteq V(G)$ and a function $f : S \to \mathbb{R}$, define $f(S) = \sum_{s \in S} f(s)$. A *Roman dominating function* (abbreviated by *RD-function*) on a graph G is a function $f : V(G) \to \{0, 1, 2\}$ such that every

MSC2010: 05C69.
Keywords: Roman domination, total Roman domination, total Roman domination edge-critical graphs.
Lampman was supported by an Undergraduate Student Research Award from the Natural Sciences and Engineering Research Council of Canada. Mynhardt was supported by a Discovery Grant from the Natural Sciences and Engineering Research Council of Canada. Ogden was supported by a Science Undergraduate Research Award from the University of Victoria.

vertex v with $f(v)=0$ is adjacent to some vertex u with $f(u)=2$. The *weight* of f, denoted by $\omega(f)$, is defined as $f(V(G))$. The *Roman domination number* $\gamma_R(G)$ (abbreviated by *RD-number*) is defined as $\min\{\omega(f) : f$ is an RD-function on $G\}$. For an RD-function f, let $V_f^i=\{v\in V(G) : f(v)=i\}$ and $V_f^+=V_f^1\cup V_f^2$. Thus, we can uniquely express an RD-function f as $f=(V_f^0, V_f^1, V_f^2)$.

As defined by Ahangar, Henning, Samodivkin and Yero [2016], a *total Roman dominating function* (abbreviated by *TRD-function*) on a graph G with no isolated vertices is a Roman dominating function with the additional condition that $G[V_f^+]$ has no isolated vertices. The *total Roman domination number* $\gamma_{tR}(G)$ (abbreviated by *TRD-number*) is the minimum weight of a TRD-function on G; that is, $\gamma_{tR}(G)=\min\{\omega(f) : f$ is a TRD-function on $G\}$. A TRD-function f such that $\omega(f)=\gamma_{tR}(G)$ is called a *$\gamma_{tR}(G)$-function*, or a *γ_{tR}-function* if the graph G is clear from the context; *γ_R-functions* are defined analogously.

The addition of an edge to a graph has the potential to change its total domination or Roman domination number. Van der Merwe, Mynhardt and Haynes [1998b] studied *γ_t-edge-critical graphs*, that is, graphs G for which $\gamma_t(G+e)<\gamma_t(G)$ for each $e\in E(\overline{G})$ and $E(\overline{G})\neq\varnothing$. We consider the same concept for total Roman domination. A graph G is *total Roman domination edge-critical*, or simply *γ_{tR}-edge-critical*, if $\gamma_{tR}(G+e)<\gamma_{tR}(G)$ for every edge $e\in E(\overline{G})$ and $E(\overline{G})\neq\varnothing$. We say that G is *k-γ_{tR}-edge-critical* if $\gamma_{tR}(G)=k$ and G is γ_{tR}-edge-critical. If $\gamma_{tR}(G+e)\le\gamma_{tR}(G)-2$ for every edge $e\in E(\overline{G})$ and $E(\overline{G})\neq\varnothing$, we say that G is *γ_{tR}-edge-supercritical*. If $\gamma_{tR}(G+e)=\gamma_{tR}(G)$ for all $e\in E(\overline{G})$, or $E(\overline{G})=\varnothing$, we say that G is *stable*.

Pushpam and Padmapriea [2017] established bounds on the total Roman domination number of a graph in terms of its order and girth. Total Roman domination in trees was studied by Amjadi, Nazari-Moghaddam, Sheikholeslami and Volkmann [2017], as well as by Amjadi, Sheikholeslami and Soroudi [2019]. Amjadi, Sheikholeslami, and Soroudi [2018] also studied Nordhaus–Gaddum bounds for total Roman domination. Campanelli and Kuziak [2019] considered total Roman domination in the lexicographic product of graphs. We refer the reader to the well-known books [Chartrand and Lesniak 2016; Haynes, Hedetniemi, and Slater 1998] for graph theory concepts not defined here. Frequently used or lesser known concepts are defined where needed.

We begin with some general results regarding the addition of an edge $e\in E(\overline{G})$ to a graph G in Section 2. In Section 3, we characterize n-γ_{tR}-edge-critical graphs of order n. We characterize 4-γ_{tR}-edge-critical graphs in Section 4, and, after investigating γ_{tR}-edge-supercritical graphs in Section 5, we present a necessary condition for 5-γ_{tR}-edge-critical graphs in Section 6. In Section 7, we determine the total Roman domination number of spiders and characterize γ_{tR}-edge-critical spiders. As can be expected, every graph G with $\gamma_{tR}(G)=k\ge 4$ is a spanning subgraph of a k-$\gamma_{tR}(G)$-edge-critical graph; a short proof is given in Section 8, where we also show that for any $k \geq 4$, there exists a k-γ_{tR}-edge-critical graph of diameter 2. We conclude in Section 9 with ideas for future research.

2. Adding an edge

We begin with a result from [Van der Merwe, Mynhardt, and Haynes 1998a] which bounds the effect the addition of an edge can have on the total domination number of a graph and show that the same bounds hold with respect to the total Roman domination number.

Proposition 2.1 [Van der Merwe, Mynhardt, and Haynes 1998a]. *For a graph G with no isolated vertices, if $uv \in E(\overline{G})$, then $\gamma_t(G) - 2 \leq \gamma_t(G + uv) \leq \gamma_t(G)$.*

An edge $uv \in E(\overline{G})$ is *critical* if $\gamma_{tR}(G+uv) < \gamma_{tR}(G)$. The following proposition restricts the possible values assigned to the vertices of a critical edge uv by a $\gamma_{tR}(G+uv)$-function f, which will be useful in proving subsequent results. For a graph G and a vertex $v \in V(G)$, the *open neighbourhood* of v in G is $N_G(v) = \{u \in V(G) : uv \in E(G)\}$, and the *closed neighbourhood* of v in G is $N_G[v] = N_G(v) \cup \{v\}$. When $G \neq K_2$, the unique neighbour of an end-vertex of G is called a *support vertex*.

Proposition 2.2. *Given a graph G with no isolated vertices, if $uv \in E(\overline{G})$ is a critical edge and f is a $\gamma_{tR}(G+uv)$-function, then*

$$\{f(u), f(v)\} \in \{\{2, 2\}, \{2, 1\}, \{2, 0\}, \{1, 1\}\}.$$

If, in addition, $\deg(u) = \deg(v) = 1$, *then there exists a $\gamma_{tR}(G+uv)$-function f such that $f(u) = f(v) = 1$.*

Proof. Let G be a graph with no isolated vertices, $uv \in E(\overline{G})$ such that $\gamma_{tR}(G+uv) < \gamma_{tR}(G)$, and f a γ_{tR}-function on $G + uv$. Suppose for a contradiction that $\{f(u), f(v)\} \notin \{\{2, 2\}, \{2, 1\}, \{2, 0\}, \{1, 1\}\}$. Then $\{f(u), f(v)\} \in \{\{0, 0\}, \{0, 1\}\}$. Note that, in either case, the edge uv cannot affect whether u and v are dominated or whether, in the case where (say) $f(v) = 1$, v is isolated. Hence f is a TRD-function of G, contradicting $\gamma_{tR}(G + uv) < \gamma_{tR}(G)$. Therefore $\{f(u), f(v)\} \in \{\{2, 2\}, \{2, 1\}, \{2, 0\}, \{1, 1\}\}$.

Now, suppose in addition that $\deg(u) = \deg(v) = 1$, and let f be a $\gamma_{tR}(G+uv)$-function such that $|V_f^2|$ is as small as possible. Let w and x be the unique neighbours of u and v, respectively, noting that possibly $w = x$. Suppose for a contradiction that $f(u) = 2$ (without loss of generality). If $f(v) = 0$, then $f(w) > 0$, otherwise u would be isolated in $G[V_f^+]$. Thus, regardless of whether $w = x$ or not, consider the function $f' : V(G) \to \{0, 1, 2\}$ defined by $f'(u) = f'(v) = 1$ and $f'(y) = f(y)$ for all other $y \in V(G)$. Otherwise, if $f(v) \geq 1$, then clearly $f(w) = 0$. Thus, regardless of whether $w = x$ or not, consider the function $f' : V(G) \to \{0, 1, 2\}$ defined by $f'(u) = f'(w) = 1$ and $f'(y) = f(y)$ for all other $y \in V(G)$. In either case, f' is a γ_{tR}-function on $G + uv$. However, $|V^2_{f'}| < |V^2_f|$, contradicting $|V^2_f|$ being as small as possible. Hence $f(u) \neq 2$, and thus $f(u) = f(v) = 1$. □

Proposition 2.3. *Given a graph G with no isolated vertices, if $uv \in E(\overline{G})$, then $\gamma_{tR}(G) - 2 \leq \gamma_{tR}(G + uv) \leq \gamma_{tR}(G)$.*

Proof. Let G be a graph with no isolated vertices. Clearly, adding an edge cannot increase the total Roman domination number; hence the upper bound holds. Now, let $uv \in E(\overline{G})$. Note that when $\gamma_{tR}(G + uv) = \gamma_{tR}(G)$, the lower bound clearly holds. So assume $\gamma_{tR}(G + uv) < \gamma_{tR}(G)$ and let f be a $\gamma_{tR}(G+uv)$-function. By Proposition 2.2, $\{f(u), f(v)\} \in \{\{2, 2\}, \{2, 1\}, \{2, 0\}, \{1, 1\}\}$.

First assume $\{f(u), f(v)\} \in \{\{2, 2\}, \{2, 1\}, \{1, 1\}\}$. Then f is an RD-function of G, and the only possible isolated vertices in $G[V^+_f]$ are u and v. Consider the function $f' : V(G) \to \{0, 1, 2\}$ defined as follows: If u is isolated in $G[V^+_f]$, choose $u' \in N_G(u)$ and let $f'(u') = 1$. Similarly, if v is isolated in $G[V^+_f]$, choose $v' \in N_G(v)$ and let $f'(v') = 1$. Let $f'(x) = f(x)$ for all other $x \in V(G)$. Now, assume instead that $f(u) = 2$ and $f(v) = 0$ (without loss of generality). Since u is not isolated in $G[V^+_f]$, f is a TRD-function of $G - v$. Consider the function $f' : V(G) \to \{0, 1, 2\}$ defined as follows: Let $f'(v) = 1$. Then, if v is isolated in $G[V^+_{f'}]$, choose $v' \in N_G(v)$ and let $f'(v') = 1$. Let $f'(x) = f(x)$ for all other $x \in V(G)$. In either case, f' is a TRD-function of G and $\omega(f') \leq \gamma_{tR}(G + uv) + 2$. Thus $\gamma_{tR}(G) \leq \gamma_{tR}(G + uv) + 2$, and hence the lower bound holds. □

3. γ_{tR}-edge-critical graphs with large TRD-numbers

We now investigate the γ_{tR}-edge-critical graphs G which have the largest TRD-number, namely $|V(G)|$. A *subdivided star* is a tree obtained from a star on at least three vertices by subdividing each edge exactly once. A *double star* is a tree obtained from two disjoint nontrivial stars by joining the two central vertices (choosing either central vertex in the case of K_2). The *corona* $\mathrm{cor}(G)$ (sometimes denoted by $G \circ K_1$) of G is obtained by joining each vertex of G to a new end-vertex.

Connected graphs G for which $\gamma_{tR}(G) = |V(G)|$ were characterized in [Ahangar, Henning, Samodivkin, and Yero 2016]. There $\mathcal{G}$ was defined as the family of connected graphs obtained from a 4-cycle v_1, v_2, v_3, v_4, v_1 by adding $k_1 + k_2 \geq 1$ vertex-disjoint paths P_2, and joining v_i to the end of k_i such paths for $i \in \{1, 2\}$. Note that possibly $k_1 = 0$ or $k_2 = 0$. Furthermore, they defined $\mathcal{H}$ to be the family of graphs obtained from a double star by subdividing each pendant edge once and the nonpendant edge $r \geq 0$ times. For $r \geq 0$, we define $\mathcal{H}_r \subseteq \mathcal{H}$ as the family of graphs in $\mathcal{H}$ where the nonpendant edge was subdivided r times.

Proposition 3.1 [Ahangar, Henning, Samodivkin, and Yero 2016]. *If G is a connected graph of order $n \geq 2$, then $\gamma_{tR}(G) = n$ if and only if one of the following holds*:

(i) *G is a path or a cycle.*

(ii) *G is the corona of a graph.*

(iii) *G is a subdivided star.*

(iv) *$G \in \mathcal{G} \cup \mathcal{H}$.*

Using Proposition 3.1, we characterize connected n-γ_{tR}-edge-critical graphs as follows.

Theorem 3.2. *A connected graph G of order $n \geq 4$ is n-γ_{tR}-edge-critical if and only if G is one of the following graphs*:

(i) C_n, $n \geq 4$.

(ii) $\mathrm{cor}(K_r)$, $r \geq 3$.

(iii) *a subdivided star of order $n \geq 7$.*

(iv) $G \in \mathcal{G}$.

(v) $G \in \mathcal{H} - \mathcal{H}_0 - \mathcal{H}_2$.

Proof. Let G be a connected graph of order $n \geq 4$ with $\gamma_{tR}(G) = n$. First, suppose G is any of the graphs listed in (i)–(v) above. Then, for any $e \in E(\overline{G})$, $G + e$ is not one of the graphs listed in Proposition 3.1. Therefore $\gamma_{tR}(G + e) < n$ for all $e \in E(\overline{G})$, and thus G is γ_{tR}-edge-critical.

Otherwise, suppose G is not one of the graphs listed in (i)–(v) above. Note that since $\gamma_{tR}(G) = n$, G is still listed in Proposition 3.1(i)–(iv). If $G \cong P_n : v_1, \dots, v_n$, $n \geq 4$, then $G + v_1 v_n \cong C_n$ and $\gamma_{tR}(G) = \gamma_{tR}(C_n) = n$. If $G \cong \mathrm{cor}(F)$, where F is not a complete graph of order at least 3, then $\gamma_{tR}(G) = \gamma_{tR}(G + uv)$ for any $uv \in E(\overline{F})$. If G is a subdivided star of order less than 7, then $G = P_5$. In each of these cases, G is clearly not γ_{tR}-edge-critical.

Now consider $G \in \mathcal{H}$. Let $w_1, \dots, w_k$ be the leaves of G, $u_1, \dots, u_k$ be their respective support vertices, and $v_1, \dots, v_m$ be the path such that v_1 and v_m are the two support vertices in the original double star S, labelled so that w_1 is adjacent, in S, to v_1. Note that $m = r + 2$, and therefore $m \geq 2$. If $G \in \mathcal{H}_0$, consider the graph $G + v_2 w_1$, and note that $G + v_2 w_1 \in \mathcal{G}$. Therefore, by Proposition 3.1, $\gamma_{tR}(G + v_2 w_1) = n$, and thus G is not γ_{tR}-edge-critical. Similarly, if $G \in \mathcal{H}_2$, consider the graph $G + v_1 v_4$, and note that $G + v_1 v_4 \in \mathcal{G}$. Therefore, by Proposition 3.1, $\gamma_{tR}(G + v_1 v_4) = n$, and again G is not γ_{tR}-edge-critical. □

4. 4-γ_{tR}-edge-critical graphs

Before we characterize the graphs G such that $\gamma_{tR}(G) = 4$ and $\gamma_{tR}(G+e) = 3$ for any $e \in E(\overline{G})$ (that is, the graphs which are 4-γ_{tR}-edge-critical), we present the following result from [Pushpam and Padmapriea 2017] which characterizes the graphs with a total Roman domination number of 3, the smallest possible TRD-number. Note that while the authors required that G has girth 3, the result actually holds in general for any graph G on at least three vertices, as we now show. A *universal vertex* of G is a vertex that is adjacent to all other vertices of G.

Proposition 4.1. *For a graph G of order $n \geq 3$ with no isolated vertices, $\gamma_{tR}(G) = 3$ if and only if $\Delta(G) = n-1$, that is, G has a universal vertex.*

Proof. Suppose $\gamma_{tR}(G) = 3$ and let $f = (V_f^0, V_f^1, V_f^2)$ be a $\gamma_{tR}(G)$-function. If $V_f^2 = \varnothing$, then $|V_f^1| = 3$, and thus $n = 3$. Since G has no isolated vertices, this implies that $G = K_3$ or P_3, both of which have a universal vertex. Otherwise, assume $|V_f^2| = 1$ and $|V_f^1| = 1$. Pick $u, v \in V(G)$ so that $f(u) = 1$ and $f(v) = 2$. Since $G[V_f^+]$ has no isolated vertices, $uv \in E(G)$. Furthermore, since $\gamma_{tR}(G) = 3$, $f(x) = 0$ for all other $x \in V(G)$. Therefore $N_G[v] = V(G)$, and thus v is a universal vertex.

Conversely, suppose G has a universal vertex v, and take any $u \in N_G(v)$. Consider the TRD-function $f : V(G) \to \{0, 1, 2\}$ defined by $f(v) = 2$, $f(u) = 1$, and $f(x) = 0$ for all other $x \in V(G)$. Since G has at least three vertices, $\gamma_{tR}(G) > 2$. Therefore, since $\omega(f) = 3$, we conclude that $\gamma_{tR}(G) = 3$. □

A *galaxy* is defined as the disjoint union of two or more nontrivial stars. The characterization of 4-γ_{tR}-edge-critical graphs follows; note that this class of graphs is exactly the class of 2-γ-edge-critical graphs, as characterized in [Sumner and Blitch 1983].

Theorem 4.2. *A graph G with no isolated vertices is 4-γ_{tR}-edge-critical if and only if $\overline{G}$ is a galaxy.*

Proof. Let G be a graph of order n with no isolated vertices. Suppose first that G is 4-γ_{tR}-edge-critical. Then for any $e \in E(\overline{G})$, we have $\gamma_{tR}(G+e) = 3$, and thus Proposition 4.1 implies that the addition of any edge to G creates a universal vertex. Therefore, for each edge $uv \in E(\overline{G})$, one of u and v has degree $n-2$ in G; that is, one of u and v is a leaf in $\overline{G}$. Since each edge of $\overline{G}$ connects a leaf to either a support vertex or another leaf, the components of $\overline{G}$ are nontrivial stars. Moreover, $\overline{G}$ has at least two components, otherwise G has an isolated vertex.

Conversely, suppose $\overline{G}$ is a galaxy. Since $\overline{G}$ has no isolated vertices, G has no universal vertices, and thus, by Proposition 4.1, $\gamma_{tR}(G) > 3$. Let u and v be vertices in different components of $\overline{G}$, and define $f : V(G) \to \{0, 1, 2\}$ by $f(u) = f(v) = 2$ and $f(x) = 0$ for all other $x \in V(G)$. Clearly f is a TRD-function on G, and hence

$\gamma_{tR}(G) = 4$. Since the deletion of any edge in $\overline{G}$ produces an isolated vertex, the addition of any edge to G creates a universal vertex. Therefore, by Proposition 4.1, $\gamma_{tR}(G+e) = 3$ for all $e \in E(\overline{G})$, and hence G is 4-γ_{tR}-edge-critical. □

Corollary 4.3. *If G is a connected $(n-2)$-regular graph, then G is 4-γ_{tR}-edge-critical.*

Having characterized 4-γ_{tR}-edge-critical graphs, our next result demonstrates the existence of stable graphs with total Roman domination number 4.

Proposition 4.4. *If G is an $(n-3)$-regular graph of order $n \geq 6$, then $\gamma_{tR}(G) = 4$. Moreover, G is stable.*

Proof. We prove that $\gamma(G) = 2$. Since G is $(n-3)$-regular, its complement $\overline{G}$ is 2-regular. If $\overline{G}$ is disconnected, let u and v be vertices in different components of $\overline{G}$. Otherwise, if $\overline{G}$ is connected, then $\overline{G} \cong C_n$, $n \geq 6$, and thus we can choose $u, v \in V(\overline{G})$ such that $d_{\overline{G}}(u, v) \geq 3$. In either case, $N_{\overline{G}}[u] \cap N_{\overline{G}}[v] = \varnothing$. In G, u dominates all vertices in $G - N_{\overline{G}}(u)$ and v dominates all vertices in $G - N_{\overline{G}}(v)$. Therefore $\{u, v\}$ dominates G, and thus, since G has no universal vertex, $\gamma(G) = 2$.

Now, define $f : V(G) \to \{0, 1, 2\}$ by $f(u) = f(v) = 2$ and $f(y) = 0$ for all other $y \in V(G)$. Since $uv \in E(G)$, f is a TRD-function on G and $\omega(f) = 4$, so $\gamma_{tR}(G) \leq 4$. Since G has no universal vertex, $\gamma_{tR}(G) > 3$ by Proposition 4.1, and thus $\gamma_{tR}(G) = 4$, as required. Furthermore, since the addition of any edge to G does not create a universal vertex, it follows from Proposition 4.1 that $\gamma_{tR}(G+e) = \gamma_{tR}(G)$ for all $e \in E(\overline{G})$. Therefore G is stable. □

5. γ_{tR}-edge-supercritical graphs

We now consider the graphs G which attain the lower bound in Proposition 2.3 for all $e \in E(\overline{G})$, that is, γ_{tR}-edge-supercritical graphs. An edge $uv \in E(\overline{G})$ is *supercritical* if $\gamma_{tR}(G+uv) = \gamma_{tR}(G) - 2$. Van der Merwe, Mynhardt, and Haynes [1998a] defined a graph G to be *γ_t-edge-supercritical* if $\gamma_t(G+e) = \gamma_t(G) - 2$ for all $e \in E(\overline{G})$. We begin with their characterization of γ_t-edge-supercritical graphs.

Proposition 5.1 [Van der Merwe, Mynhardt, and Haynes 1998a]. *A graph G is γ_t-edge-supercritical if and only if G is the union of two or more nontrivial complete graphs.*

The proof of the previous result relies on the fact that, if u and v are vertices of a graph G with $d(u, v) = 2$, then $\gamma_t(G) - 1 \leq \gamma_t(G+uv)$. However, the analogous result does not hold with respect to the total Roman domination number, as we now show. Consider the graph $G = \mathrm{cor}(K_3)$. By Proposition 3.1, $\gamma_{tR}(G) = 6$. Consider any two nonadjacent vertices u and v in G such that $\deg(u) = 1$ and $\deg(v) = 3$. Clearly uv is a supercritical edge with $d(u, v) = 2$, and thus $d(u, v) = 2$ does not always imply that $\gamma_{tR}(G) - 1 \leq \gamma_{tR}(G+uv)$.

As a result, the classification of γ_{tR}-edge-supercritical graphs will be less straightforward than that of γ_t-edge-supercritical graphs. However, it is easy to see that there are no 5-γ_{tR}-edge-supercritical graphs, where 5 is the smallest possible TRD-number of a γ_{tR}-edge-supercritical graph, and that the disjoint union of two or more complete graphs of order at least 3 is γ_{tR}-edge-supercritical.

Proposition 5.2. (i) *There are no 5-γ_{tR}-edge-supercritical graphs.*

(ii) *If G is the disjoint union of $k \geq 2$ complete graphs, each of order at least 3, then G is $3k$-γ_{tR}-edge-supercritical.*

Proof. (i) Suppose for a contradiction that G is a 5-γ_{tR}-edge-supercritical graph. Then $\gamma_{tR}(G+uv) = 3$ for any edge $uv \in E(\overline{G})$. However, as in the proof of Theorem 4.2, this implies that $\overline{G}$ is a galaxy, that is, G is 4-γ_{tR}-edge-critical, a contradiction.

(ii) It follows from Proposition 4.1 that $\gamma_{tR}(G) = 3k$. Moreover, joining any two vertices in different components of G results in a graph with TRD-number $3k-2$. □

6. 5-γ_{tR}-edge-critical graphs

We now investigate the graphs which are 5-γ_{tR}-edge-critical. We begin with the following results, which bound $\gamma_{tR}(G)$ in terms of $\gamma_t(G)$.

Proposition 6.1 [Ahangar, Henning, Samodivkin, and Yero 2016]. *If G is a graph with no isolated vertices, then $\gamma_t(G) \leq \gamma_{tR}(G) \leq 2\gamma_t(G)$. Furthermore, $\gamma_{tR}(G) = \gamma_t(G)$ if and only if G is the disjoint union of copies of K_2.*

Note that Amjadi, Nazari-Moghaddam, Sheikholeslami, and Volkmann [2017] characterized the trees which attain the upper bound in Proposition 6.1.

Proposition 6.2 [Ahangar, Henning, Samodivkin, and Yero 2016]. *Let G be a connected graph of order $n \geq 3$. Then $\gamma_{tR}(G) = \gamma_t(G)+1$ if and only if $\Delta(G) = n-1$, that is, G has a universal vertex.*

By Proposition 4.1, Proposition 6.2 implies that, if G is a connected graph of order $n \geq 3$, then $\gamma_{tR}(G) = \gamma_t(G)+1$ if and only if $\gamma_{tR}(G) = 3$. These results lead to the following observation.

Observation 6.3. If G is a connected graph of order $n \geq 3$ such that $\Delta(G) \leq n-2$, then $\gamma_t(G)+2 \leq \gamma_{tR}(G) \leq 2\gamma_t(G)$.

We now provide a result characterizing graphs with $\gamma_{tR} \in \{3, 4\}$ in terms of their domination and total domination numbers that will be useful in describing 5-γ_{tR}-edge-critical graphs.

Proposition 6.4. *If G is a connected graph of order $n \geq 3$, then $\gamma_{tR}(G) \in \{3, 4\}$ if and only if $\gamma_t(G) = 2$. Moreover, $\gamma(G) = 1$ when $\gamma_{tR}(G) = 3$, and $\gamma(G) = 2$ when $\gamma_{tR}(G) = 4$.*

Proof. Suppose first that $\gamma_t(G) = 2$. By Proposition 6.1, $2 \le \gamma_{tR}(G) \le 4$. Clearly $\gamma_{tR}(G) \ne 2$, since $n \ge 3$. Therefore $\gamma_{tR}(G) \in \{3, 4\}$.

Conversely, suppose $\gamma_{tR}(G) \in \{3, 4\}$. First, if $\gamma_{tR}(G) = 3$, then Proposition 4.1 implies that G has a universal vertex. Therefore $\gamma_t(G) = 2$ and $\gamma(G) = 1$. Otherwise, if $\gamma_{tR}(G) = 4$, then Proposition 4.1 implies that G has no universal vertex. Therefore, by Observation 6.3, $\gamma_t(G) + 2 \le 4$, and thus $\gamma_t(G) = 2$. Furthermore, since $\gamma(G) \le \gamma_t(G)$ and G has no universal vertex, $\gamma(G) = 2$. □

Proposition 6.5. *For any graph G, if G is 5-γ_{tR}-edge-critical, then G is either 3-γ_t-edge-critical or $G = K_2 \cup K_n$ for $n \ge 3$, in which case G is 4-γ_t-edge-supercritical.*

Proof. Suppose G is 5-γ_{tR}-edge-critical. By Proposition 6.4, $\gamma_t(G) > 2$ and $\gamma_t(G + e) = 2$ for any $e \in E(\overline{G})$. Therefore, by Proposition 2.1, G is either 3-γ_t-edge-critical or 4-γ_t-edge-supercritical. If G is 4-γ_t-edge-supercritical, then by Proposition 5.1, G is the union of two or more nontrivial complete graphs. Since $\gamma_{tR}(G) = 5$, this implies that $G = K_2 \cup K_n$ for $n \ge 3$. □

Note that if we add the condition that G is not 6-γ_{tR}-edge-supercritical, then the above becomes a necessary and sufficient condition. Clearly $G = K_2 \cup K_n$ is 5-γ_{tR}-edge-critical for any $n \ge 3$. Otherwise, if G is 3-γ_t-edge-critical, then by Proposition 6.4, $\gamma_{tR}(G) > 4$ and $\gamma_{tR}(G + e) \in \{3, 4\}$ for any $e \in E(\overline{G})$. By Proposition 6.1, $\gamma_{tR}(G) \le 6$, and thus, since G is not 6-γ_{tR}-edge-supercritical, $\gamma_{tR}(G) = 5$. Hence G is 5-γ_{tR}-edge-critical, as required.

7. γ_{tR}-edge-critical spiders

A (*generalized*) *spider* $\mathrm{Sp}(l_1, \dots, l_k)$, $l_i \ge 1$, $k \ge 2$, is a tree obtained from the star $K_{1,k}$ with centre u and leaves $v_1, \dots, v_k$ by subdividing the edge uv_i exactly $l_i - 1$ times, $i = 1, \dots, k$. Thus, a spider $\mathrm{Sp}(2, \dots, 2)$ is a subdivided star. The $u - v_i$ paths (of length l_i) are called the *legs* of the spider, while u is its *head*. We now investigate the spiders which are γ_{tR}-edge-critical. Note that when $k = 2$, $\mathrm{Sp}(l_1, \dots, l_k) \cong P_n$ for $n \ge 3$, which, by Theorem 3.2, is not γ_{tR}-edge-critical. We begin with two propositions restricting γ_{tR}-edge-criticality in general graphs, which will be useful in classifying γ_{tR}-edge-critical spiders.

Proposition 7.1. *For a graph G with no isolated vertices, if G has an end-vertex w with support vertex x such that $G[N(x) - \{w\}]$ is not complete, then G is not γ_{tR}-edge-critical.*

Proof. Suppose $u, v \in N_G(x) - \{w\}$ such that $uv \in E(\overline{G})$. We claim $\gamma_{tR}(G + uv) = \gamma_{tR}(G)$. Suppose for a contradiction that $\gamma_{tR}(G + uv) < \gamma_{tR}(G)$, and consider a γ_{tR}-function $f = (V_f^0, V_f^1, V_f^2)$ on $G + uv$. Note that, since w is an end-vertex, $f(x) > 0$. By Proposition 2.2, $\{f(u), f(v)\} \in \{\{2, 2\}, \{2, 1\}, \{2, 0\}, \{1, 1\}\}$. Since $ux, vx \in E(G)$ and at least one of $f(u)$ and $f(v)$ is positive, we can assume without loss of generality that $f(x) = 2$. In any case, f is also a TRD-function on G, contradicting $\gamma_{tR}(G+uv) < \gamma_{tR}(G)$. Therefore $\gamma_{tR}(G+uv) = \gamma_{tR}(G)$ and G is not γ_{tR}-edge-critical. □

In a tree, the support vertex of a leaf is called a *stem*. A stem is called *weak* if it is adjacent to exactly one leaf, and *strong* if it is adjacent to two or more leaves. A vertex b of a tree such that $\deg(b) \geq 3$ is called a *branch vertex*. An *endpath* in a tree is a path from a branch vertex to a leaf, where all of the internal vertices of the path have degree 2. The next result follows immediately from Proposition 7.1.

Corollary 7.2. *If T is a γ_{tR}-edge-critical tree, then T contains no stems of degree at least* 3, *and hence no strong stems.*

Proposition 7.3. *For a graph G with no isolated vertices, if G has two endpaths $v_0, v_1, \dots, v_k$ and $u_0, u_1, \dots, u_m$, where $k, m \geq 3$ and v_k and u_m are leaves, then G is not γ_{tR}-edge-critical.*

Proof. We claim that $\gamma_{tR}(G + v_k u_m) = \gamma_{tR}(G)$. Suppose for a contradiction that $\gamma_{tR}(G + v_k u_m) < \gamma_{tR}(G)$, and let f be a γ_{tR}-function on $G + v_k u_m$. Then, by Proposition 2.2, we may assume $f(u_m) = f(v_k) = 1$. Define $f' : V(G) \to \{0, 1, 2\}$ as follows: If $f(v_{k-1}) = 0$, then clearly $f(v_{k-2}) = 2$ and $f(v_{k-3}) \geq 1$, so let $f'(v_{k-1}) = f'(v_{k-2}) = 1$. Otherwise, let $f'(v_{k-1}) = f(v_{k-1})$ and $f'(v_{k-2}) = f(v_{k-2})$. Similarly, if $f(u_{m-1}) = 0$, then clearly $f(u_{m-2}) = 2$ and $f(u_{m-3}) \geq 1$, so let $f'(u_{m-1}) = f'(u_{m-2}) = 1$. Otherwise, let $f'(u_{m-1}) = f(u_{m-1})$ and $f'(u_{m-2}) = f(u_{m-2})$. Finally, let $f'(y) = f(y)$ for all other $y \in V(G)$. Clearly f' is a TRD-function on G and $\omega(f') = \omega(f)$, contradicting $\gamma_{tR}(G + v_k u_m) < \gamma_{tR}(G)$. Therefore $\gamma_{tR}(G + v_k u_m) = \gamma_{tR}(G)$, and thus G is not γ_{tR}-edge-critical. □

Let S be a spider with $k \geq 3$ legs. In what follows, let c be the head of S, and let the k legs be labelled $c, v_{i1}, v_{i2}, \dots, v_{im_i}$, where $i \in \{1, 2, \dots, k\}$, in order of increasing length. Let $m = m_k$; that is, m is the length of a longest leg of S. We begin by determining the TRD-number of spiders.

Proposition 7.4. *If S is a spider of order n with $k \geq 3$ legs such that S has y legs of length* 2, *then*

$$\gamma_{tR}(S) = \begin{cases} n & \text{if } y \geq k-1, \\ n-k+y+1 & \text{if } 1 \leq y < k-1, \\ n-k+2 & \text{if } y = 0. \end{cases}$$

Proof. Suppose S has x legs of length 1, and consider a γ_{tR}-function f on S such that $|V_f^2|$ is as small as possible. First, suppose $y \geq k-1$. If $y = k$, then S is a subdivided star. Otherwise, if $y = k-1$, then S has exactly one leg that is not of length 2, and thus either $x = 1$ or $x = 0$. If $x = 1$, then S is the corona of a graph (specifically, $S = \mathrm{cor}(K_{1,k-1})$). Otherwise, if $x = 0$, then $m = m_k \geq 3$, and $S \in \mathcal{H}_r$, where $r = m - 3$. In any case, by Proposition 3.1, $\gamma_{tR}(S) = n$.

Assume therefore that $y < k - 1$. Then S has at least two legs that are not of length 2. Therefore S is not one of the graphs listed in Proposition 3.1, and thus $\gamma_{tR}(S) < n$. Hence there is some vertex $u \in V(S)$ such that $f(u) = 2$ and $f(w) = 0$ for at least two vertices w adjacent to u. Furthermore, since f is a TRD-function, such a vertex u is not isolated in $S[V_f^+]$, and thus $\deg(u) \geq 3$. Since c is the only vertex in S with degree at least 3, $f(c) = 2$. Therefore c Roman dominates each v_{i1}, and we need $f(v_{i1})$ to be positive for at least one i to ensure that $S[V_f^+]$ has no isolated vertices.

Consider an arbitrary leg $c, v_{i1}, v_{i2}, \ldots, v_{im_i}$ of S. If $m_i = 1$, then $f(v_{i1}) \in \{0, 1\}$ in order for f to totally Roman dominate c and v_{i1}. If $m_i = 2$, a total weight of 2 on v_{i1} and v_{i2} is required in order for f to total Roman dominate $\{v_{i1}, v_{i2}\}$. Since $|V_f^2|$ is as small as possible, $f(v_{i1}) = f(v_{i2}) = 1$. Finally, if $m_i > 2$, by Proposition 3.1 and since $f(c) = 2$, a total weight of at least $m_i - 1$ on $v_{i1}, \ldots, v_{im_i}$ is required in order for f to totally Roman dominate c and $\{v_{i1}, \ldots, v_{im_i}\}$. Moreover, by the choice of f, $f(v_{i1}) \in \{0, 1\}$ and $f(v_{i2}) = \cdots = f(v_{im}) = 1$. Therefore $\omega(f) \geq n - k + y + 1$.

Now, if $y > 0$, where (say) $m_j = 2$, then $f(v_{j1}) = 1$. By minimality and since c is adjacent to v_{j1}, $f(v_{i1}) = 0$ for each i such that $m_i \neq 2$. Then $\gamma_{tR}(S) = \omega(f) = n - k + y + 1$, as required. Otherwise, if $y = 0$, then $f(v_{i1}) = 1$ for some i to ensure that c is not isolated in $S[V_f^+]$. By minimality, $f(v_{j1}) = 0$ for each $j \neq i$. Therefore $\gamma_{tR}(S) = \omega(f) = n - k + 2$. □

The characterization of γ_{tR}-edge-critical spiders follows. Our result also shows that a spider of order n is γ_{tR}-edge-critical if and only if it is n-γ_{tR}-edge-critical.

Theorem 7.5. *A spider $S = \mathrm{Sp}(l_1, \ldots, l_k)$, $k \geq 3$, is γ_{tR}-edge-critical if and only if $l_i = 2$ for each i, $1 \leq i \leq k - 1$, and $l_k \in \{2, m\}$, where $m = 4$ or $m \geq 6$.*

Proof. Suppose S has order n. If $l_i = 2$ for each $i = 1, \ldots, k$, then S is a subdivided star and, by Theorem 3.2, S is n-γ_{tR}-edge-critical. Now, suppose S has exactly one leg of length $m \neq 2$. If $m = 1$, then by Proposition 7.1, S is not γ_{tR}-edge-critical. If $m = 3$ or $m = 5$, then $S \in \mathcal{H}_r$ with $r = 0$ or 2, respectively, and thus, by Theorem 3.2, S is not γ_{tR}-edge-critical. If $m = 4$ or $m \geq 6$, then $S \in \mathcal{H}_r$ with $r = m - 3$, and therefore, by Theorem 3.2, S is n-γ_{tR}-edge-critical. Finally, suppose S has at least two legs that are not of length 2. Again, by Proposition 7.1, if S has a leg of length 1, S is not γ_{tR}-edge-critical. Otherwise, assume S has at least two legs of length at least 3. Then, by Proposition 7.3, S is not γ_{tR}-edge-critical. □

8. k-γ_{tR}-edge-critical graphs with minimum diameter

We now consider the minimum diameter possible in a k-γ_{tR}-edge-critical graph for $k \geq 4$. There are no γ_{tR}-edge-critical graphs with diameter 1, as the only graphs with diameter 1 are nontrivial complete graphs, which are clearly not γ_{tR}-edge-critical since $E(\overline{G}) = \varnothing$. Therefore, the minimum possible diameter for a γ_{tR}-edge-critical graph is 2. Asplund, Loizeaux and Van der Merwe [2018] constructed families of 3-γ_t-edge-critical graphs with diameter 2. We will show that, for any $k \geq 4$, there exists a k-γ_{tR}-edge-critical graph of diameter 2. We first present the following proposition which shows that every graph G without a dominating vertex is a spanning subgraph of a $\gamma_{tR}(G)$-edge-critical graph with the same total Roman domination number, which will be useful in proving our result.

Proposition 8.1. *For a graph G with no isolated vertices, if $\gamma_{tR}(G) = k \geq 4$, then G is a spanning subgraph of a k-$\gamma_{tR}(G)$-edge-critical graph.*

Proof. Suppose $\gamma_{tR}(G) = k \geq 4$. If G is k-$\gamma_{tR}(G)$-edge-critical, then we are done. Otherwise, there is, by definition, some edge $e_1 \in E(\overline{G})$ such that $\gamma_{tR}(G + e_1) = \gamma_{tR}(G)$. Let $G_1 = G + e_1$. If G_1 is k-$\gamma_{tR}(G)$-edge-critical, then we are done. Otherwise, there is some edge $e_2 \in E(\overline{G}_1)$ such that $\gamma_{tR}(G_1 + e_2) = \gamma_{tR}(G_1)$. Let $G_2 = G_1 + e_2$. Continuing in this way, we eventually obtain a graph G_i such that for all $e \in E(\overline{G}_i)$, $\gamma_{tR}(G_i + e) < \gamma_{tR}(G_i)$ and $\gamma_{tR}(G_i) = \gamma_{tR}(G_{i-1}) = \cdots = \gamma_{tR}(G_1) = \gamma_{tR}(G)$. Since $k \geq 4$, G_i is not complete and thus $E(G_i) \neq \varnothing$. Therefore, G_i is a k-$\gamma_{tR}(G)$-edge-critical graph, of which G is a spanning subgraph. □

Before demonstrating the existence of k-γ_{tR}-edge-critical graphs of diameter 2 for any $k \geq 4$, we determine the TRD-number of $K_n \square K_m$, where $n, m \geq 2$. Consider the vertices of $K_n \square K_m$ as an $n \times m$ matrix, where vertices v_{ij} and v_{st} are adjacent if and only if $i = s$ or $j = t$. The rows and columns of the matrix form disjoint copies of K_m and K_n, respectively. If v_{ij} and v_{st} are nonadjacent, then v_{sj} is adjacent to both v_{ij} and v_{st}, and hence $\operatorname{diam}(K_n \square K_m) = 2$.

Proposition 8.2. *If m and n are integers such that $m \geq n \geq 2$, then $\gamma_{tR}(K_n \square K_m) = 2n$.*

Proof. Let $G = K_n \square K_m$. To see that $\gamma_{tR}(G) \leq 2n$, consider the TRD-function $g = (V_g^0, V_g^1, V_g^2)$ on G where $V_g^1 = \varnothing$ and $V_g^2 = \{v_{i1} : 1 \leq i \leq n\}$.

Now, suppose for a contradiction that $\gamma_{tR}(G) \leq 2n - 1$ and consider a TRD-function $f = (V_f^0, V_f^1, V_f^2)$ on G with $\omega(f) = 2n - 1$. Each vertex v dominates one row and one column of G, so if $|V_f^2| = x$ (note that $x \leq n - 1$), then at most x rows and at most x columns are dominated by elements of V_f^2. Let S be the set of vertices undominated by V_f^2. Then $|S| \geq (n - x)(m - x) \geq (n - x)^2$. Moreover, $|V_f^1| = (2n - 1) - 2x$ since $\omega(f) = 2n - 1$ and $|V_f^2| = x$.

If $x = n - 1$, then $|V_f^1| = 1$. Since f is a TRD-function and $|S| \geq (n - x)^2$, we have $|S| = 1$; say $S = \{w\}$. Hence $V_f^1 = \{w\}$. However, V_f^2 does not dominate w, and thus w is isolated in $G[V_f^+]$, which is a contradiction. Therefore, there is no TRD-function on G with weight $2n - 1$ when $x = n - 1$.

Otherwise, if $x < n-1$, then

$$\begin{aligned} |S| - |V_f^1| &\geq (n-x)^2 - (2n-1-2x) \\ &= x^2 - 2(n-1)x + (n-1)^2 \\ &= (n-1-x)^2 > 0. \end{aligned}$$

Therefore, the number of vertices undominated by V_f^2 is greater than $|V_f^1|$, contradicting f being a TRD-function. Thus there is no TRD-function on G with weight $2n-1$ when $x < n-1$. We conclude that $\gamma_{tR}(G) = 2n$. □

Theorem 8.3. *If $k \geq 4$, then there exists a k-γ_{tR}-edge-critical graph of diameter* 2.

Proof. First, assume that k is even; say $k = 2l$ for some $l \geq 2$. Let $G_l = K_l \,\square\, K_l$. By Proposition 8.2, $\gamma_{tR}(G_l) = 2l$, and, by Proposition 8.1, G_l is a spanning subgraph of a k-γ_{tR}-edge-critical graph G_l'. Since $k > 3$, Proposition 4.1 implies that G_l' has no dominating vertex, and hence $2 \leq \operatorname{diam}(G_l') \leq \operatorname{diam}(G_l) = 2$.

Now, consider the case where k is odd; say $k = 2l+1$ for some $l \geq 2$. Let G_l^d be the graph formed by taking $K_{l+1} \,\square\, K_{l+1}$ and deleting the vertices in the set $\{v_{j1} : \lfloor \frac{l}{2} \rfloor + 2 \leq j \leq l+1\}$. Similarly to G_l, $\operatorname{diam}(G_l^d) = 2$. See Figure 1.

We claim that $\gamma_{tR}(G_l^d) = 2l+1$. To see that $\gamma_{tR}(G_l^d) \leq 2l+1$, consider the following TRD-function on G_l^d: If l is even, place two 2's in each of the first $\frac{l}{2}-1$ rows, and one 2 in each of rows $\frac{l}{2}$ and $\frac{l}{2}+1$, such that they span columns 2 through $l+1$. At this point, every vertex in G_l^d is dominated. However, the 2's in rows $\frac{l}{2}$ and $\frac{l}{2}+1$ are isolated, so place a 1 in row $\frac{l}{2}$ such that it shares a column with the 2 in row $\frac{l}{2}+1$. Otherwise, if l is odd, place two 2's in each of the first $\frac{l-1}{2}$ rows, and one 2 in row $\frac{l+1}{2}$, such that they span columns 2 through $l+1$. Similarly to the even case, every vertex in G_l^d is now dominated. However, the 2 in row $\frac{l+1}{2}$ is isolated, so place a 1 in row $\frac{l-1}{2}$ such that it shares a column with that 2. In either case, we have a TRD-function on G_l^d with weight $2l+1$; hence $\gamma_{tR}(G_l^d) \leq 2l+1$.

Now, suppose for a contradiction that $\gamma_{tR}(G_l^d) < 2l+1$, and consider a TRD-function $f = (V_f^0, V_f^1, V_f^2)$ on G_l^d with $\omega(f) = 2l$. We claim that $f(v_{j1}) = 0$ for all $1 \leq j \leq \lfloor \frac{l}{2} \rfloor + 1$. If $f(v_{j1}) = 2$ for $x \geq 1$ vertices in column 1, the undominated vertices in columns 2 through $l+1$ form the graph $K_l \,\square\, K_{l+1-x}$. By Proposition 8.2, a TRD-function on $K_l \square K_{l+1-x}$ requires a weight of $2\min\{l, l+1-x\} = 2(l+1-x)$. However, since $2x + 2(l+1-x) > 2l$, this is impossible. Therefore $f(v_{j1}) \neq 2$ for all $1 \leq j \leq \lfloor \frac{l}{2} \rfloor + 1$. If $f(v_{j1}) = 1$ for $x \geq 1$ vertices in column 1, the undominated vertices in columns 2 through $l+1$ (that is, those for which f could be assigned a 2) form the graph $K_l \,\square\, K_{l+1}$. Again by Proposition 8.2, a TRD-function on $K_l \,\square\, K_{l+1}$ requires a weight of $2\min\{l, l+1\} = 2l$. However, $x + 2l > 2l$ for $x \geq 1$, so this is also not possible. Therefore, $f(v_{j1}) = 0$ for all $1 \leq j \leq \lfloor \frac{l}{2} \rfloor + 1$.

As a result, in order to totally Roman dominate the first column, there must be a 2 in each of the first $\lfloor \frac{l}{2} \rfloor + 1$ rows, none of which can be in the first column. That

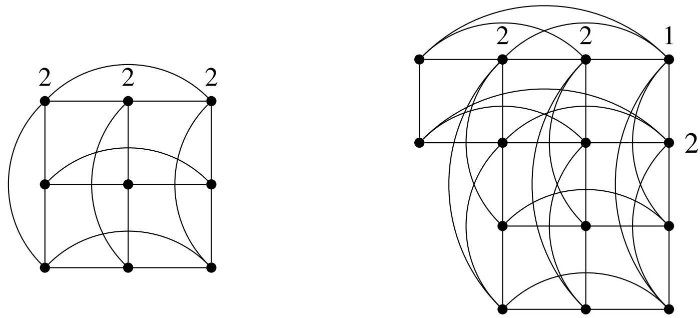

Figure 1. The graphs G_3 and G_3^d with a γ_{tR}-function.

is, for each $1 \le s \le \lfloor \frac{l}{2} \rfloor + 1$, $f(v_{st}) = 2$ for some $2 \le t \le l+1$. Let S be the set of these vertices. Note that, thus far, we have accounted for a total weight of

$$2\left(\left\lfloor \tfrac{l}{2} \right\rfloor + 1\right) = \begin{cases} l+2 & \text{if } l \text{ is even,} \\ l+1 & \text{if } l \text{ is odd,} \end{cases}$$

which leaves a weight of $l-2$ if l is even and $l-1$ if l is odd to be assigned. That is, a weight of $2\left(\left\lceil \frac{l}{2} \right\rceil - 1\right)$ remains to be accounted for. We now claim that no two vertices in S can be in the same column. If the vertices in S span fewer than $\lfloor \frac{l}{2} \rfloor + 1$ columns, then the vertices which are undominated by S induce a graph containing $K_{\lceil l/2 \rceil} \square K_{\lceil l/2 \rceil}$ as subgraph. If $l = 2$, then no weight remains to dominate this vertex, as $2\left(\left\lceil \frac{l}{2} \right\rceil - 1\right) = 0$. Otherwise, if $l > 2$, Proposition 8.2 implies that $\gamma_{tR}(K_{\lceil l/2 \rceil} \square K_{\lceil l/2 \rceil}) = 2\left(\left\lceil \frac{l}{2} \right\rceil\right)$. However, $2\left(\left\lceil \frac{l}{2} \right\rceil\right) > 2\left(\left\lceil \frac{l}{2} \right\rceil - 1\right)$. In either case, this contradicts f being a TRD-function, and thus no vertices of S share a column.

Therefore, the vertices left undominated by S induce a graph $T \cong K_{\lceil l/2 \rceil} \square K_{\lceil l/2 \rceil - 1}$, with $\left\lceil \frac{l}{2} \right\rceil$ rows and $\left\lceil \frac{l}{2} \right\rceil - 1$ columns. Moreover, the vertices in S are all isolated, as none share a row or column. By Proposition 8.2, $\gamma_{tR}(T) = 2\left(\left\lceil \frac{l}{2} \right\rceil - 1\right)$. Thus the entire remaining weight is required in order to dominate T; necessarily, the vertices in $V_f^+ - S$ belong to rows and columns that do not contain vertices in S. However, this still leaves the vertices in S isolated, which contradicts f being a TRD-function on G_l^d. Therefore $\gamma_{tR}(G_l^d) \ge 2l+1$ and we conclude that $\gamma_{tR}(G_l^d) = 2l+1$. As in the case where k is even, G_l^d is a spanning subgraph of a k-γ_{tR}-edge-critical graph with diameter 2. □

9. Future work

We showed in Section 5 that the disjoint union of two or more complete graphs, each having order at least 3, is γ_{tR}-edge-supercritical. We also explained that a proof similar to that of Proposition 5.1 does not work for total Roman domination. Hence we pose the following question.

Question 1. *Are the disjoint unions of two or more complete graphs, each having order at least* 3, *the only* γ_{tR}*-edge-supercritical graphs*?

Note that if this is the case, Proposition 6.5 automatically becomes a necessary and sufficient condition for a graph to be 5-γ_{tR}-edge-critical.

Now consider, for a moment, Roman dominating functions, and suppose a graph G has nonadjacent vertices u and v such that $f(u) = f(v) = 0$ for every γ_R-function f on G. We claim that $\gamma_R(G+uv) = \gamma_R(G)$. Suppose $\gamma_R(G+uv) < \gamma_R(G)$ and let f be a γ_R-function on $G+uv$. Similar to Proposition 2.2, we may assume without loss of generality that $f(u) = 2$ and $f(v) = 0$, otherwise f is an RD-function on G such that $\omega(f) < \gamma_R(G)$. However, the function f' defined by $f'(v) = 1$ and $f'(y) = f(y)$ for all other $y \in V(G)$ is a γ_R-function on G such that $f'(v) > 0$, contrary to our assumption. The situation for total Roman domination is different.

For a graph G, we define $u \in V(G)$ to be a *dead vertex* if every γ_{tR}-function f on G has $f(u) = 0$. Not only do there exist graphs G containing nonadjacent dead vertices u and v such that $\gamma_{tR}(G+uv) < \gamma_{tR}(G)$, but it is possible to find such a graph G with $\gamma_{tR}(G+uw) < \gamma_{tR}(G)$ for every edge $uw \in E(\overline{G})$; that is, every edge in $E(\overline{G})$ incident with the dead vertex u is critical. We define the graph D_n below and show that D_n is such a graph.

Let D_n be the graph composed of $n \geq 2$ copies of $K_4 - e$ sharing a single central vertex as follows: let c be the central vertex, $w_1, \ldots, w_n$ be the degree-2 vertices, and $u_1, \ldots, u_n$ and $v_1, \ldots, v_n$ be the remaining vertices (where u_i and v_i are adjacent for each i) such that c, u_i, w_i, v_i, c is a 4-cycle in D_n for each $1 \leq i \leq n$. See Figure 2.

Proposition 9.1. *If* $n \geq 2$, *then* $\gamma_{tR}(D_n) = 2n+1$. *Moreover*, w_i *is a dead vertex for each* $1 \leq i \leq n$.

Proof. To see that $\gamma_{tR}(D_n) \leq 2n+1$, consider the TRD-function $g : V(D_n) \to \{0, 1, 2\}$ on D_n defined by $g(c) = 1$, $g(u_i) = 2$ for $1 \leq i \leq n$, and $g(y) = 0$ for all other $y \in V(D_n)$.

We claim that, if f is a TRD-function on D_n with $\omega(f) \leq 2n+1$, then $f(c) = 1$. If $f(c) = 2$, then the only vertices that remain undominated in D_n are w_i for $1 \leq i \leq n$. However, since $d(w_i, w_j) = 4$ for all $i \neq j$, a weight of $2n$ is required in order to totally Roman dominate these vertices, contradicting $\omega(f) \leq 2n+1$. If $f(c) = 0$, then since $D_n - c$ is the disjoint union of n triangles, Proposition 3.1 implies that a weight of $3n$ is required to totally Roman dominate the remaining vertices, contradicting $\omega(f) \leq 2n+1$. Therefore $f(c) = 1$. Since a weight of at least $2n$ is required to totally Roman dominate the remaining disjoint union of n triangles, we conclude that $\gamma_{tR}(D_n) = 2n+1$.

Now, let f be any γ_{tR}-function on D_n. Then $\omega(f) = 2n+1$ and $f(c) = 1$. To dominate each triangle of $D_n - c$ with a weight of 2, $\{f(u_i), f(v_i)\} = \{0, 2\}$ and $f(w_i) = 0$ for each $1 \leq i \leq n$. Hence each w_i is a dead vertex. □

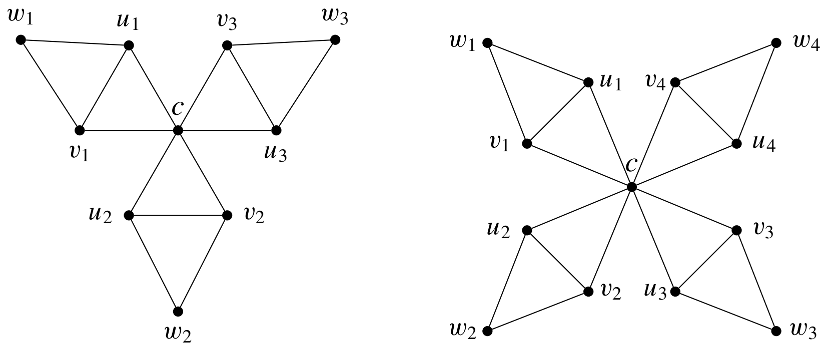

Figure 2. The graphs D_3 and D_4.

The following result shows that, for $n \geq 3$, every edge in $E(\overline{D}_n)$ incident with w_i is critical.

Proposition 9.2. *If* $n \geq 3$, $i \in \{1, \ldots, n\}$, *and* $w_i v \in E(\overline{D}_n)$, *then* $\gamma_{tR}(D_n + w_i v) < \gamma_{tR}(D_n)$.

Proof. Without loss of generality, consider an edge $w_1 v \in E(\overline{D}_n)$. Then (without loss of generality) $v \in \{w_2, u_2, c\}$. If $v = w_2$, define $f : V(D_n + w_1 v) \to \{0, 1, 2\}$ by $f(w_1) = f(w_2) = 1$, $f(c) = f(u_3) = \cdots = f(u_n) = 2$, and $f(y) = 0$ for all other $y \in V(D_n)$. Otherwise, if $v \in \{u_2, c\}$, define $f : V(D_n + w_1 v) \to \{0, 1, 2\}$ by $f(c) = f(u_2) = f(u_3) = \cdots = f(u_n) = 2$ and $f(y) = 0$ for all other $y \in V(D_n)$. In either case, f is a TRD-function on $D_n + w_1 v$ and $\omega(f) = 2n$. Therefore, by Proposition 9.1, every edge $w_i v \in E(\overline{D}_n)$ is critical. □

However, for $n \geq 3$, the graph D_n is not γ_{tR}-edge-critical since (for example) $\gamma_{tR}(D_n + u_1 u_2) = 2n + 1$. Furthermore, the graph D_2 is not γ_{tR}-edge-critical since (for example) $\gamma_{tR}(D_2 + w_1 w_2) = 5$. However, adding edges to D_n until a $(2n{+}1)$-γ_{tR}-edge-critical graph D_n' is obtained results in D_n' having no dead vertices. Hence we pose the following question.

Question 2. *Do there exist* γ_{tR}*-edge-critical graphs containing dead vertices*?

We characterized γ_{tR}-edge-critical spiders in Theorem 7.5. Finding other classes of γ_{tR}-edge-critical trees and, indeed, characterizing γ_{tR}-edge-critical trees, remain open problems.

References

[Ahangar, Henning, Samodivkin, and Yero 2016] H. A. Ahangar, M. A. Henning, V. Samodivkin, and I. G. Yero, "Total Roman domination in graphs", *Appl. Anal. Discrete Math.* **10**:2 (2016), 501–517. MR Zbl

[Amjadi, Nazari-Moghaddam, Sheikholeslami, and Volkmann 2017] J. Amjadi, S. Nazari-Moghaddam, S. M. Sheikholeslami, and L. Volkmann, "Total Roman domination number of trees", *Australas. J. Combin.* **69** (2017), 271–285. MR Zbl

[Amjadi, Sheikholeslami, and Soroudi 2018] J. Amjadi, S. M. Sheikholeslami, and M. Soroudi, "Nordhaus–Gaddum bounds for total Roman domination", *J. Comb. Optim.* **35**:1 (2018), 126–133. MR Zbl

[Amjadi, Sheikholeslami, and Soroudi 2019] J. Amjadi, S. M. Sheikholeslami, and M. Soroudi, "On the total Roman domination in trees", *Discuss. Math. Graph Theory* **39**:2 (2019), 519–532. MR Zbl

[Asplund, Loizeaux, and Van der Merwe 2018] J. Asplund, M. Loizeaux, and L. van der Merwe, "A note on total domination edge critical graphs", *J. Combin. Math. Combin. Comput.* **104** (2018), 245–260. MR Zbl

[Campanelli and Kuziak 2019] N. Campanelli and D. Kuziak, "Total Roman domination in the lexicographic product of graphs", *Discrete Appl. Math.* **263** (2019), 88–95. MR Zbl

[Chartrand and Lesniak 2016] G. Chartrand and L. Lesniak, *Graphs & digraphs*, 6th ed., Chapman & Hall/CRC, Boca Raton, FL, 2016.

[Haynes, Hedetniemi, and Slater 1998] T. W. Haynes, S. T. Hedetniemi, and P. J. Slater, *Fundamentals of domination in graphs*, Monographs and Textbooks in Pure and Applied Mathematics **208**, Marcel Dekker, New York, 1998. MR Zbl

[Pushpam and Padmapriea 2017] P. R. L. Pushpam and S. Padmapriea, "On total Roman domination in graphs", pp. 326–331 in *Theoretical computer science and discrete mathematics*, edited by S. Arumugam et al., Lecture Notes in Comput. Sci. **10398**, Springer, 2017. MR Zbl

[Sumner and Blitch 1983] D. P. Sumner and P. Blitch, "Domination critical graphs", *J. Combin. Theory Ser. B* **34**:1 (1983), 65–76. MR Zbl

[Van der Merwe, Mynhardt, and Haynes 1998a] L. C. van der Merwe, C. M. Mynhardt, and T. W. Haynes, "Criticality index of total domination", pp. 67–73 in *Proceedings of the Twenty-ninth Southeastern International Conference on Combinatorics, Graph Theory and Computing* (Boca Raton, FL, 1998), Congressus Numerantium **131**, Utilitas Math., Winnipeg, MB, 1998. MR Zbl

[Van der Merwe, Mynhardt, and Haynes 1998b] L. C. van der Merwe, C. M. Mynhardt, and T. W. Haynes, "Total domination edge critical graphs", *Util. Math.* **54** (1998), 229–240. MR Zbl

Received: 2019-07-23 Accepted: 2019-09-26

chloe.lampman3@gmail.com *Department of Mathematics and Statistics, University of Victoria, Victoria, BC, Canada*

kieka@uvic.ca *Department of Mathematics and Statistics, University of Victoria, Victoria, BC, Canada*

sogden@uvic.ca *Department of Mathematics and Statistics, University of Victoria, Victoria, BC, Canada*

Guidelines for Authors

Submissions in all mathematical areas are encouraged. All manuscripts accepted for publication in *Involve* are considered publishable in quality journals in their respective fields, and include a minimum of one-third student authorship. Submissions should include substantial faculty input; faculty co-authorship is strongly encouraged. Authors may submit manuscripts in PDF format on-line at the Submission page at the Involve website.

Originality. Submission of a manuscript acknowledges that the manuscript is original and and is not, in whole or in part, published or under consideration for publication elsewhere. It is understood also that the manuscript will not be submitted elsewhere while under consideration for publication in this journal.

Language. Articles in *Involve* are usually in English, but articles written in other languages are welcome.

Required items. A brief abstract of about 150 words or less must be included. It should be self-contained and not make any reference to the bibliography. If the article is not in English, two versions of the abstract must be included, one in the language of the article and one in English. Also required are keywords and subject classifications for the article, and, for each author, postal address, affiliation (if appropriate), and email address.

Format. Authors are encouraged to use LaTeX but submissions in other varieties of TeX, and exceptionally in other formats, are acceptable. Initial uploads should be in PDF format; after the refereeing process we will ask you to submit all source material.

References. Bibliographical references should be complete, including article titles and page ranges. All references in the bibliography should be cited in the text. The use of BibTeX is preferred but not required. Tags will be converted to the house format, however, for submission you may use the format of your choice. Links will be provided to all literature with known web locations and authors are encouraged to provide their own links in addition to those supplied in the editorial process.

Figures. Figures must be of publication quality. After acceptance, you will need to submit the original source files in vector graphics format for all diagrams in your manuscript: vector EPS or vector PDF files are the most useful.

Most drawing and graphing packages (Mathematica, Adobe Illustrator, MATLAB, etc.) allow the user to save files in one of these formats. Make sure that what you are saving is vector graphics and not a bitmap. If you need help, please write to graphics@msp.org with details about how your graphics were generated.

White space. Forced line breaks or page breaks should not be inserted in the document. There is no point in your trying to optimize line and page breaks in the original manuscript. The manuscript will be reformatted to use the journal's preferred fonts and layout.

Proofs. Page proofs will be made available to authors (or to the designated corresponding author) at a Web site in PDF format. Failure to acknowledge the receipt of proofs or to return corrections within the requested deadline may cause publication to be postponed.

involve

2019 vol. 12 no. 8